1

NON-METALLIC INCLUSION MODIFICATION AND ITS EFFECT ON THE

FINAL PROPERTIES OF A LINEPIPE STEEL.

NEIL JOHN KEEGAN

DOCTOR OF PHILOSOPHY

THE UNIVERSITY OF ASTON IN BIRMINGHAM.

AUGUST 1987

THE UNIVERSITY OF ASTON IN BIRMINGHAM.

TITLE: NONMETALLIC INCLUSION MODIFICATION AND ITS EFFECT ON THE

FINAL PROPERTIES OF A LINEPIPE STEEL

NEIL JOHN KEEGAN

PhD.

1987

SUMMARY

Five linepipe type steels were produced in order to study the effect of calcium and magnesium injection on their final properties. Two of these steels were at the extremes of the sulphide range ie. 0.003 and 0.017% sulphur with no injection attempted; thereby, providing standards to compare with the injected steels. The oxygen level varied from 21 to 63 p.p.m. The cast ingots were controlled-rolled and isothermally rolled in order to study the deformation characteristics of the residual non-metallic inclusions.

The structure and cleanliness of these steels was evaluated metallographically using the light microscope, SEM, and image analysis and the results related to their Charpy toughness and HIC resistance.

Increasing sulphur levels decreased final properties of the steel. In the untreated state, with as little as 0.003% sulphur, test orientation was highly influential. Modification of sulphur bearing steels was achieved with low modifying element to sulphur ratios provided that the oxygen content was very low. Injection of calcium into steel caused interaction with oxide and sulphide inclusions which was biased towards oxide reduction relative to sulphur removal. Magnesium again reduced oxides and appeared to be linked with alumina containing inclusions in the final product. It produced improved toughness values relative to a similar sulphur containing calcium treated steel.

The results of this work could be extended to establish the mechanism of inclusion modification with magnesium additions to sulphur bearing steels.

Key Words: linepipe, calcium, magnesium, inclusions, toughness, cleanliness.

DEDICATION

.

Mum and Dad.

.

ACKNOWLEDGEMENTS

CONTENTS

LIST OF TABLES

.

9

LIST OF FIGURES

1. INTRODUCTION

In recent years increasing demands have been placed on the steelmaker to produce steels with improved cleanliness for use as linepipe and ancillary pipe fittings. This has been primarily due to the diverse and stringent property requirements associated with the discovery and exploitation of oil and natural gas from some of the World's most difficult and hostile climatic environments.

Over the last fifteen years the tendency has been to lay larger diameter, thicker walled pipelines that can be operated at high pressures in an attempt to maximise transportation efficiency. In addition the fluid media being transported is often of leaner quality which has led to problems with sour gas and associated corrosive elements. This has resulted in the development of very clean, low sulphur steels of a specification previously unavailable on a commercial scale.

Obviously, the material properties required for a pipeline system can vary depending on its geographical and physical location. The pipe diameter and wall thickness of a land based transmission system is controlled mainly by the operating pressure, which is determined to be that which is most economical for the requisite flow rate and transportation distance. A number of large,land based transmission systems are in operation today e.g. the Alaskan Natural Gas Transportation System has 6,400 km. of 1066 mm-1422 mm diameter X70 (480MPa Min.Y.S.) grade linepipe and in Europe pipes from the Yamal Peninsula in northern Russia to West Germany and Austria use 5,800 km. of 1422 mm. diameter pipeline [1]. Operating pressures are generally in the range 6-7000 KPa. Apart from requiring the strength to support its own weight and that of the fluid being

transported, the pipe must be able to support ancillary pipe fittings and subsidiary networks which run off it. Further, steels for oil and natural gas transmission must possess excellent low temperature toughness properties in order to guarantee their integrity at operating temperatures as low as -65°C (Alaskan and Arctic regions of Siberia) [2]. In Arctic regions pipe is supported at intervals along its length to prevent sinking into the permafrost. Thus, there must be the ability to withstand bending stresses generated by the weight of the pipe and its fluid between these supports.

In addition to the above property requirements, submarine systems need to possess corrosion and buckling resistance. These material demands have been intensified in recent years with the extraction of resources from greater marine depths which vary from 30m. in the North sea to 500m. in the Sicilean channel [3]. The technical problems associated with submarine systems can most easily be appreciated by taking two fields in the North sea as an example. Firstly, West Sole on the United Kingdom Continental Shelf is a gas reservoir lying nearly 3000 m. below the seabed which is at 28m. water depth. A 40 cm. diameter concrete-coated steel pipeline is laid at this depth over a length of 70km. The BP Forties field comprises of 170km of 81cm diameter pipe which is in 130m depth of water. The pipes were laid by two laybarges working towards each other prior to joining of the pipe at the surface before lowering to the seabed [4]. Buckling of the empty as-laid (coated) pipeline is thus a matter of real concern and designers have had to consider what problems may arise at these depths if the phenomenon of a "propagating buckle" were to develop. Further, problems arise from wave motion in rough seas, water temperature and distance.

The four most important property requirements of a linepipe steel are therefore :

(1) strength

(2) toughness

(3) weldability and

(4) corrosion resistance.

The use of high strength material can be justified in terms of economy and safety. Its use ensures the pipeline remains within operational safety limits, whilst also allowing the wall thickness to be reduced, thereby lowering the total tonnage requirements of the line. Significant cost savings can be made as a result of reduced handling costs and more rapid welding. These savings normally more than outweigh the extra processing costs involved in the production of the higher strength original plate material [5]. A disadvantage of lowering the wall thickness to diameter ratio is that it makes the pipe more susceptible to denting. The designer needs to consider the effect of mechanical damage defects on high strength material that may arise as a result of external impact loads (for example from an excavator).

A pipeline steel needs to be tough enough to ensure that if fracture initiation occurs, propagation will be restricted to a predictable and acceptable level. It is essential to contain a running fracture to a small section of the pipeline. If this can be achieved the amount of environmental damage can be limited, along with the financial loss associated with a major failure.

Ferrite-pearlite steels are favoured for linepipe because of their strength and toughness. Strengthening parameters include carbon content, solid solution strengthening,

precipitation hardening and grain refinement. It is essential that a correct balance is found if the pipeline is to be tough, strong and weldable. Carbon ,whilst providing srength, is extremely detrimental to impact toughness and weldability. The recent trend of reduced carbon contents and lower carbon equivalents has seen a spectacular improvement in the weldability of these steels. Grain refinement is the only parameter that is strongly beneficial to the strength and toughness whilst not impairing weldability [6].

Strength is developed in low carbon steels by controlled rolling which is designed to develop a uniform fine grained microstructure. Careful control of microalloying elements such as niobium and vanadium along with ingot preheating and rolling temperatures is required to achieve this grain refinement. A disadvantage of controlled rolling can be the development of a banded and textured microstructure which contributes to anisotropy of the rolled product (the segregation of alloying elements such as manganese is particularly deleterious in this respect). One way to eliminate anisotropy has been the use of ultra low carbon,bainitic (ULCB) steels to alter the microstructure from one of ferrite and pearlite to a bainitic structure by compositional adjustment.

The high quality of today's steels has only been achieved through considerable research and development work and an important consideration was the correlation of material, melting and fabrication variables with structure-property relationships. Similarly, the development of deoxidation and desulphurisation technology and its effect on the reaction mechanisms is an area requiring continual review.

2. LITERATURE REVIEW

2.1 INTRODUCTION

The final properties of a linepipe steel are affected by a number of variables including composition, thermomechanical treatment and microstructure. Composition embraces carbon and alloy content,together with so called residual elements such as oxygen, phosphorus and sulphur. During solidification.secondary inclusions of oxides and sulphides are formed. It is, therefore, necessary to study the origin of these products, their removal and/or modification during steelmaking, behaviour during major forming operations such as hot rolling, and their effect on the final physical properties of the steel such as toughness and hydrogen induced cracking resistance (H.I.C.). A review of the literature relevant to these subjects is given below.

2.2 FORMATION AND REMOVAL OF NON-METALLIC INCLUSIONS.

Oxygen and sulphur are introduced into steel during its production either by design, as in the case of oxygen, or as an impurity (sulphur from coke in the blast furnace and in scrap additions made to the vessel). These elements have a lower solubility in solid iron than in liquid steel, so that during solidification, they are precipitated in the form of non-metallic inclusions as oxides, sulphides or oxysulphides. In an unalloyed cast steel the sulphur would be precipitated as iron sulphide, which forms a eutectic with

iron at a melting point of 980°C - the cause of hot shortness during hot working [7]. The addition of manganese can overcome this problem since it has a greater affinity for sulphur than iron, and during solidification forms manganese sulphide which has a higher melting point eutectic with iron of 1492°C. The classic categorization of manganese sulphide inclusions into three morphological types was reported in 1938 by Sims and Dahle [8]. This work was later clarified by Fredriksson and Hillert [9] and Baker and Charles [10]. The original classification of manganese sulphides defined type I as round, type II as chain-like 'eutectic', and type III as angular. Since then, the second class has been further subdivided to give a fourth inclusion type i.e. platelike or lamellar manganese sulphide [11,12]. The distinct morphologies present within a steel are determined by its composition, and degree of deoxidation. In a steel with a high concentration of oxygen, typically in excess of 0.01%, type I manganese sulphides are formed. These are spherical because they are precipitated (over a wide temperature range) as liquid globules rich in oxygen and sulphur during solidification [10,12]. Primary inclusions contain the highest oxygen concentration and thus appear duplex - the manganese sulphide being associated with large proportions of a MnO-MnS eutectic phase. Concave cavities are often evident in type I inclusions because of contraction of the sulphide during cooling. In low oxygen, conventional steels, the type I morphology is replaced by type II sulphides which form three dimensional networks in between solidified dendrite arms. The resultant rod-like sulphides are present as parallel 'fences' or 'chains'. Originally, type II inclusions were thought to be formed as a eutectic between

iron and manganese sulphide. It is now accepted to be the result of a co-operative monotectic, where manganese sulphide precipitates as a liquid phase together with a solid iron-rich phase, due to the melting point of the sulphide being depressed by the presence of iron and other elements in solution [9,11,12]. The presence of carbon, aluminium, silicon and phosphorus, in a fully killed steel results in the formation of angular type III manganese sulphides. These sulphides can appear as perfect octahedra due to their precipitation as a solid from the molten steel. They are considered to be formed by a degenerate eutectic due to the lowering of the freezing point of the steel, by the alloying elements, such that it becomes less than that of the manganese sulphide. Lamellar type IV are also crystalline in nature and are considered to be formed as a result of a co-operative eutectic reaction with the solid iron rich-phase [11].

It can be seen, therefore, that all manganese sulphides and oxysulphides are precipitated in the solute enriched interdendritic regions of a steel during the latter stages of solidification. Turkdogan and Grange [13] suggest that for a sulphur content of 0.01%, there is not enough sulphur in the system to form a continuous network of interdendritic sulphides. However, as a result of macrosegregation during solidification, solute enrichment causes localised precipitation of relatively large manganese sulphides in a steel with as little as 0.002% sulphur. Upon reaustenitizing during heat treatment or hot working, these regions become the grain boundaries of the steel. The sulphides and oxysulphides are readily deformed resulting in poor transverse mechanical properties. This can be remedied by the addition of a sulphide former which has a greater affinity for

sulphur than manganese and forms higher melting point sulphides. These sulphides

precipitate out earlier during cooling prior to solidification,converting a large proportion

of the sulphur to sulphides which are evenly distributed throughout the steel as opposed

to being interdendritically accumulated. The resultant mechanical properties of the steel

are thus more isotropic.

A variety of oxide inclusions can be formed within a steel,dependent on the

deoxidation practice. Steels are deoxidised to varying degrees depending on quality and

processing requirements. Linepipe steels are normally 'killed', i.e. they are deoxidised to

low oxygen levels (10-30 p.p.m.) in order to suppress gaseous (CO) evolution during

solidification. The fundamental requirement of a deoxidiser is that it has an affinity for

oxygen and is soluble in steel. In addition to this, its reaction products must be insoluble

and capable of rapid separation from the melt, whilst any residuals must not have a

deleterious effect on final steel properties. This has led to the replacement of a single

deoxidiser by a complex deoxidation practice, where improved deoxidation is achieved as

a result of alloying or consecutive additions with other elements. Simultaneous

deoxidation with a silicomanganese alloy results in a lower residual oxygen in solution

because the activity of silica is reduced by the presence of manganese oxide [14-18]. This

deoxidation alloy combination is now used primarily in the production of rimmed and

capped steels. Aluminium-silicon-manganese deoxidation is used for semi-killed steels

resulting in deoxidation products ranging from liquid alumino-silicates to the more

complex inclusions of galaxite, corundum, or mullite depending on the concentration of

the deoxidant in solution [14]. It is important to be able to predict the likely composition since these crystalline inclusions are non-deformable and can lead to crack initiation and propagation during hotworking. Ekerot [19], for example, showed that inclusions of spessartite ($3MnO.Al_2O_3$ $3SiO_2$) have a high deformability index and a low transition temperature and are, therefore, preferred in steels deoxidised with aluminium, silicon and manganese. The residual oxygen content of an aluminium-killed steel is reduced to a very low level when deoxidation is accompanied by the addition of burnt lime. The resultant calcium aluminates separate more readily from the melt than unmodified alumina inclusions.

Steel deoxidation has been extensively reviewed over the years by a number of authors [14,17,18,20,21] and can be divided into two fundamental areas. Firstly, the dissolution and subsequent nucleation of the products within the melt and secondly, their growth and flotation from the melt. The oxidation reaction is initially limited by the rate of solute and oxygen diffusion to the oxide particles dispersed in the melt. Oxide layers on the surface of solid deoxidisers also act as nucleation sites allowing spontaneous deoxidation to occur. In most steelmaking practices the diffusion controlled rate of the deoxidation reaction occurs relatively quickly. The rate controlling step is flotation of small primary oxide inclusions (<20μm) from the melt [14]. Primary indigenous inclusions are formed whilst the steel is molten and often escape by flotation due to specific gravity differences between themselves and the steel. The flotation rate of a particle from a

quiescent bath can be predicted by Stokes' law. This assumes that the steady state

velocity at which an inclusion of fixed size rises in a homogeneous fluid medium is equal

to :

$$\upsilon = 2\,g\,r^2\,\Delta_p\,/\,9\,\mu$$

where υ = velocity

           g = acceleration due to gravity

           r = inclusion radius

           Δ_p = difference in densities of liquid steel and the inclusion

           μ = viscosity of the metal

Coalescence and growth of inclusions caused by collisions resulting from random

movements within a melt, flotational interactions or as a result of stirring or turbulence

obviously enhance inclusion removal rate. However, the rate of removal and eventual

elimination is not determined by Stokes' law alone. A number of other factors such as

inclusion viscosity, wettability and interfacial tension have a significant effect. In

aluminium-killed steel small alumina particles readily coalesce to form large clusters

which float rapidly from the melt. Entrapment of molten steel within the arms of these

clusters giving them the characteristics of a sphere with a large effective radius, is one

explanation for the enhanced removal rate of this inclusion type from molten steel [22].

Cluster formation has been linked to the morphology of an assemblage since the dendritic nature of alumina promotes the development of three dimensional networks [23].

The coalescence of inclusions is promoted by the interfacial tension between the particle and the metal [21,25]. The form of a liquid metal droplet resting on a solid oxide surface is determined by the relative values of the interfacial energies. Figure (1) gives the vector relationships between interface energies.

i) No Wetting   ii) Wetting Tendency

FIGURE 1. Form of a droplet of metal resting on a solid oxide support.[25].

where γ_m = surface tension of molten metal

γ_s = surface tension of substances forming solid inclusions

γ_{sm} = metal-inclusion interfacial tension

The equilibrium of the surface forces involved can be written as

$$\gamma_s - \gamma_m \cos \theta - \gamma_{sm} = 0$$

In order to measure the attraction between different materials, the work of adhesion can be calculated directly from experimental data using

$$W_{ad} = (\gamma_m + \gamma_s) - \gamma_{sm}$$

This work represents the decrease in energy in bringing together a unit area of liquid surface and a unit area of solid surface to form a unit area of interface. Considering the vector relationship above it can be seen that as the interfacial energy between the inclusion and the metal decreases the degree of wettability increases. When considered in terms of inclusion flotation, a high inclusion interfacial tension indicates a small attractive force between the steel and the oxide and hence a small dragging force opposing the motion of the particle. A low interfacial tension should cause a large dragging force and a slower rate of separation. This was substantiated by the work of Lindon and Billington [16] who showed inclusion separation rates decreased according to product type in the order alumina, silica, calcium alumino-silicate. They conclude that separation rates for products in a quiescent bath increase as the interfacial tension between particles and the melt increases. Their results confirm those of Plockinger et al[26] and are in agreement with those of Torssell and Olette [23], supporting the theory that low interfacial tensions cause wetting of the particles by liquid iron hindering their flotation to the melt surface. More recently Riboud and Gatellier [27] stated that for solid inclusions

the wetting angle was all important and that it should be larger than 90 ° to make coalescence possible. Alumina has a contact angle of 140 ° in liquid iron compared with 115 ° for silica and, therefore, alumina should cluster more readily than silica in the solid state.

Following the establishment of primary contact between inclusions a further reaction mechanism comes into effect helping to maintain the cluster formation. This is the drainage of the metal film from the space separating neighbouring inclusions after their initial point contact. This leads to the development of a metal-'vacuum' which is believed to be essential for the maintenance of stable agglomerates [28]. Kozakevitch and Olette [25] consider that the formation of a convex meniscus is required for the removal of the metal and believe it can be only spontaneous for wetting angles that exceed 90 °.

In order for an inclusion to be finally removed from the steel it is not sufficient for it to be transferred to the surface of the bath, it must also have the capacity to break the metal and/or slag surface or be fixed in the slag. A number of papers have considered the phenomenon of emergence [20,25,27], again concluding that the wetting angle is of paramount importance. The influence of this contact angle is shown in Figure (2) where it can be seen that the angle should be as large as possible in order to increase the emergent part of the cluster.

INCLUSION

METAL

θ

METAL

θ_1

θ_2

$\theta_1 < \theta_2$
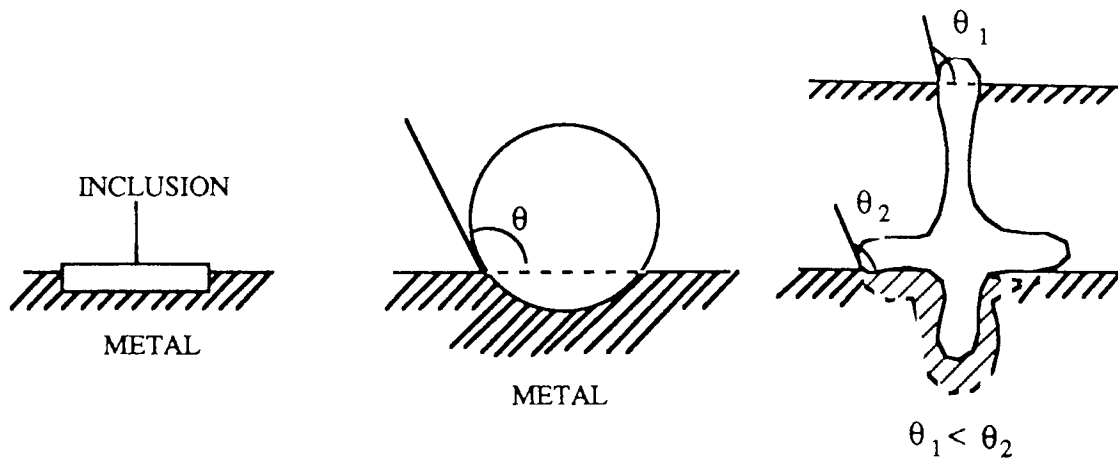
STABLE POSITION = FUNCTION OF θ

FIGURE 2. Stable position of emersion for solid inclusions : influence of contact angle for different shapes[27].

Any stirring or turbulence within a melt must obviously enhance the rate of inclusion removal since it increases the number of collisions between particles and causes others to be thrown onto the ladle wall. Work by Myashita et al [29] has shown that the rise rate is considerably faster in stirred melts than in quiescent baths. Studies by Lindskog and Sandberg [30] on deoxidation mechanisms in a stirred steel bath using radioactive isotopes showed inclusions to be separated out by adsorption onto the crucible linings. With stirring, a cluster has even more chance of removal since it is sufficient for a single inclusion in the cluster to adhere to the refractory walls, or emerge at the melt surface in order for the whole cluster to remain there [25]. Unfortunately, secondary indigenous inclusions formed during the latter stages of solidification, have a very poor chance of escape because of the time available for flotation and, therefore, they become an integral part of the final steel product.

To improve the desulphurisation of a steel the oxygen level needs to be controlled to a very low level. Desulphurisation occurs by an electrochemical exchange reaction between the sulphur in the steel and the oxygen in the slag.

$$\underline{S} + [\,O''\,] \longrightarrow [\,S''\,] + \underline{O}$$

$$2\,\underline{Al} + 3\,\underline{O} \longrightarrow [\,Al_2\,O_3\,] \qquad \underline{Mn} + \underline{O} \longrightarrow [\,MnO\,] \qquad \underline{Si} + 2\,\underline{O} \longrightarrow [\,Si\,O_2\,]$$
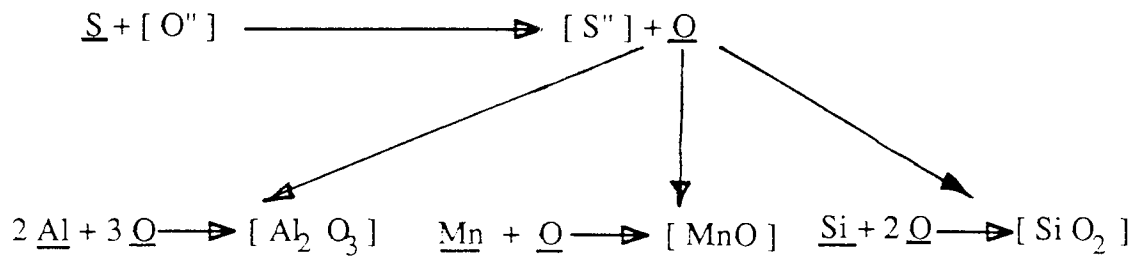
The free basic oxygen ions in the slag donate two electrons to the sulphur thereby facilitating transfer of the sulphur ion to the slag phase. Atomic oxygen is transferred to the steel, where it reacts with the deoxidiser. Since the oxygen activity in the steel is controlled by the deoxidising element, its significance with regard to desulphurisation can be understood. For this reason a number of researchers recommended minimum aluminium contents for effective desulpurisation [22,32,33]. For example, Shalimov et al [33] found during industrial trials that the sulphur distribution was dependent on the aluminium content of the steel. By varying the aluminium level from 0.025% to 0.06% it was possible to reduce the final sulphur level from 0.006% to 0.003%.

Desulphurisation obviously depends on the degree of mass transfer between slag and metal. The limiting factor for melt desulphurisation, is the supersaturation level of sulphur in the slag. The largest values to date, have been achieved using highly basic slags and reducing conditions [22,34]. Low basicity slags have resulted in poor sulphur

removal [22]. Frohberg et al [35] found that the mass transfer of sulphur from the metal to the slag occurred more readily with increasing basicity and temperature, as well as a low oxygen content of the melt. Avoidance of reoxidation of the bath is also important in the desulphurisation process if the best results are to be achieved.

Since the mid-1970's there has been a revolution in the production of high quality steels for use in the pipeline industry. The increased demands for stronger, tougher and cleaner steels require lower oxygen, sulphur and phosphorus contents in the final products. Subsequently, the overall industrial recession led to the need for rationalisation of the steel industry in order to optimize its economic viability. A vital step in this reorganisation was the introduction of an additional stage in the steel processing called secondary steelmaking, i.e. refining in the ladle. This released the primary steelmaking unit for processing hot metal and scrap to produce steel of intermediate quality. Refining and alloying was completed in the ladle leaving the primary unit for processing the next heat thereby increasing production rates. Similarly, the introduction of ladle refining treatments and ancillary processing plants reduced the chemical load on the steelmaking vessel. More importantly, however, the new stage enabled a much closer control over the final steel composition together with homogenisation of temperature which facilitated its integration with a concast plant (an important growth area of the last few decades). Improved steel quality has been due to advances made in the field of secondary steelmaking.

2.3 SECONDARY STEELMAKING

In addition to homogenisation of temperature and composition, Secondary Steelmaking results in improved yields, increased reaction rates, and a greater degree of reproducibility. It also offers the facilities for enhanced removal of nonmetallic inclusions, inclusion shape modification, alloying element adjustment and gas purging to remove hydrogen and nitrogen [22,36-39]. A major advantage of ladle refining is the possible use and production of gases in the processing. All reactions where one component is a gas are affected by the partial pressure of that gas [36]. Kinetically it is advantageous to lower the partial pressure of that phase, which can be done in one of two ways. Firstly, by lowering the total pressure of the system by vacuum treatment or secondly, by dilution with another gas i.e. gas flushing. A discussion of vacuum treatments will not be undertaken here as it is not relevant to this work.

In ladle metallurgy reactions primarily take place between a top slag and the melt, making it essential therefore, that a liquid reactive slag is formed and thus a high degree of mass transfer occurs between the slag and the metal. A reducing synthetic slag based on the $CaO-Al_2O_3-SiO_2$ system is the one which is most often used during desulphurisation in the ladle [39-41]. In some practices fluorspar is substituted for the silica[42]. In others a slag based purely on lime and fluorspar is used [43,44]. Herrera and Sussman [39], report that the use of fluorspar has been discontinued during steel processing at Armco because of its erosive nature on lance and ladle refractories.

In order to produce low sulphur steels (< 0.005%S) carry over of slag from the primary melting vessel must be a minimum so that the FeO and MnO content of the ladle slag can be minimised. Maximum sulphur capacity of the slag is dependent upon basicity and its oxygen potential. A concensus of opinion believes that the greatest sulphur partition ratio between the slag and metal is obtained with a slag composition of $60\%CaO, 30\%Al_2O_3, 10\%SiO_2$[39-41]. Argon stirring of the melt greatly enhances desulphurisation efficiency, since it creates intimate mixing of the slag and metal phase and a large interaction surface area. Slag bulk also has a pronounced effect on sulphur removal.

Haastert et al [45] conducted industrially based desulphurisation trials using a synthetic slag and deep lance argon injection to assist in the transfer of reaction products to this top slag. For a given amount of argon supply, the greater the slag bulk the greater was the degree of desulphurisation. This is shown in Figure (3) . It can be taken to be representative of the sulphur loading of the slag, obviously an increased slag volume will result in a greater sulphur capacity. However, large slag volumes can lead to handling problems and difficulties with metal compositional adjustments when adding low density alloy additions.
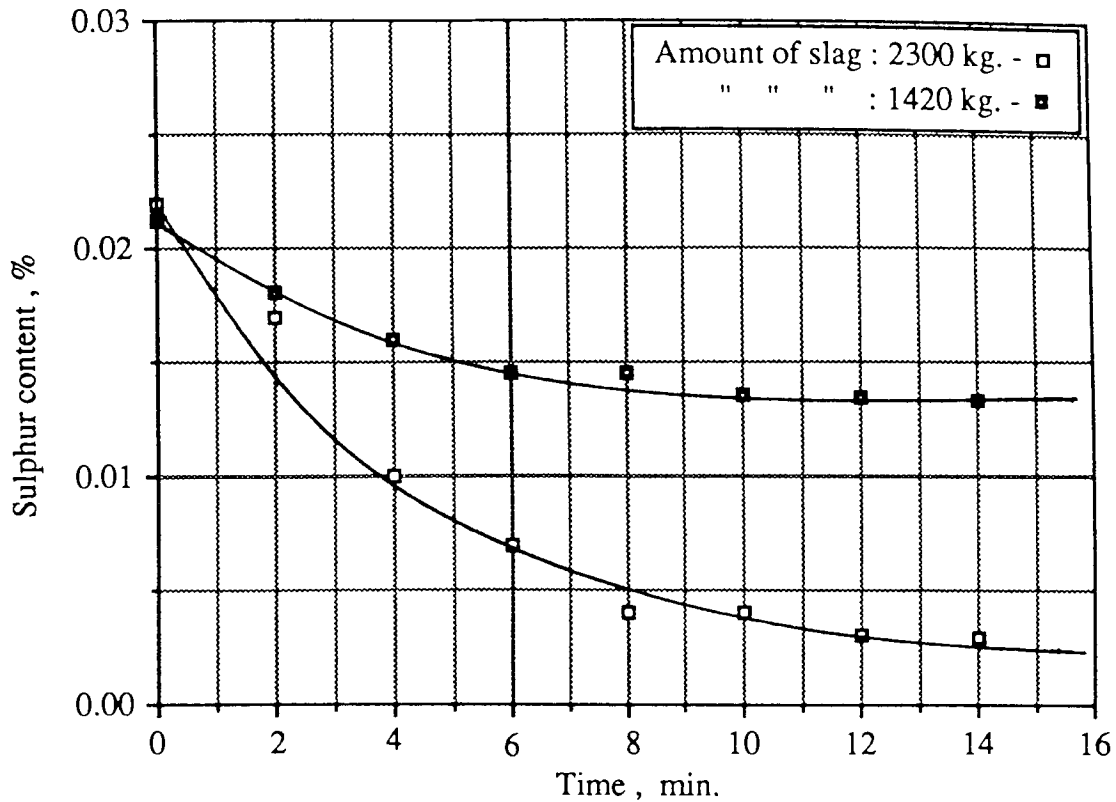
FIGURE 3. Process of desulphurisation on 120-t melts under slag by stirring with argon and the influence of the amount of slag (dolomite ladle)[45]

Injection metallurgy can be considered as a natural extension of ladle metallurgy. Its main benefit being rapid and efficient desulphurisation and reproducible inclusion modification by effective introduction of desulphurising elements with high vapour pressures into molten steel. The injected material reacts with the steel during upwards movement through the bath. The greater the injection depth the longer the contact time between material and steel giving a greater transfer of sulphur to the rising inclusions. Further, stirring intensity increases with depth of injection resulting in an extended reaction zone within the melt and improved inclusion removal. Treatment is generally conducted in one of two ways ; by powder injection via an inert carrier gas, or by the

introduction of sheathed material into the melt using a wire-feed system. Both practices are now well established. However, powder injection is the more widely used for the production of very low sulphur steels. Additional benefits include enhanced rates of inclusion removal, with modification of those inclusions left in the melt together with a homogenisation of temperature and composition of the steel bath.

Wire-feed systems are now primarily used for inclusion modification treatments at the tundish where they have proved convenient and reproducible whilst, at the same time, requiring only relatively low capital cost equipment [42,45-47]. When a sheathed material is introduced into molten steel, time is required to achieve the dissolution of the desulphurising material in the melt and, therefore, the depth of the treatment is determined by the thickness of the sheath and the speed of wire-feed. Whilst it may be possible to introduce greater amounts of a volatile reactant into molten steel at any one time using this technique, powder injection still has the great advantage of the additional turbulence provided by the carrier gas.

A physical reaction model for powder injection illustrating the importance of stirring intensity and circulation contour has been described by Lehner [48] and is shown in Figure(4) .

Ohman and Lehner [36] report that the finely dispersed gas bubbles in the mammoth 'pump-zone' have a great flotation potential, and that 90% of the total oxygen content in a bath can be removed in this zone.
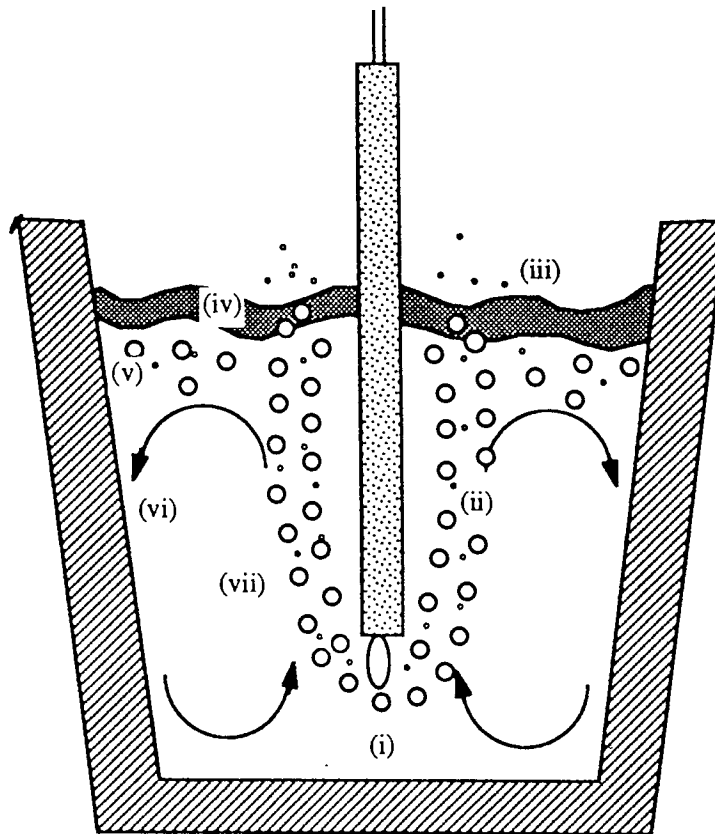
FIGURE 4. Reactor model for ladle injection according to Lehner [48].

(i) jet zone, in front of the lance outlet

(ii) major pump zone (bubble zone) formed by the rising gas bubbles and injected material.

(iii) breakthrough zone, where gas bubbles emerge through the slag into the atmosphere.

(iv) slag zone.

(v) dispersion zone, where injected gas and slag and even top slag can be dispersed.

(vi) lining zone, where metal is in contact with lining.

(vii) intermediate zone, with lowest stirring intensity.

A similar reaction model has been developed for desulphurisation under a top slag, and is given in Figure (5). A powder injectant can reach sulphur saturation level by reaction with molten steel during its upward flotation through the melt. Fresh high sulphur capacity material is introduced into the melt and desulphurisation can proceed much further providing the floating slag is removed from the system after its reaction.
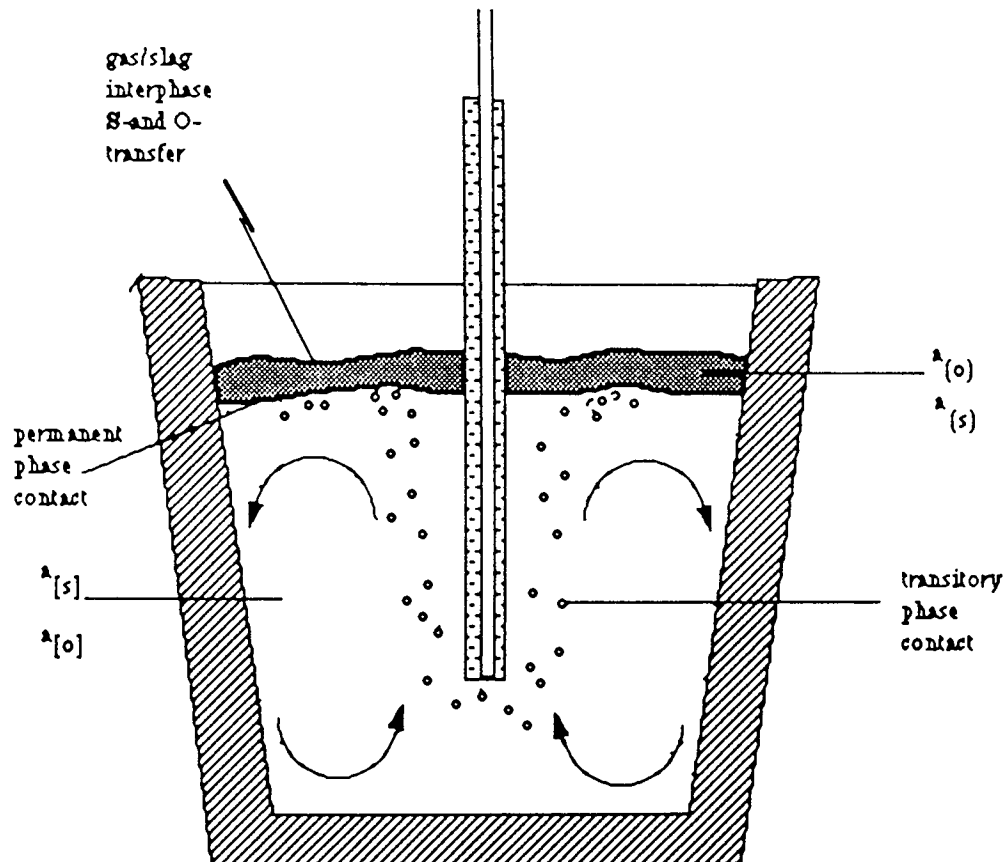
FIGURE 5. Desulphurisation model for ladle injection under top slag [22].

This does not generally occur in industrial practice, so that ladle injection is best considered as a combination of the two reaction mechanisms [22].

Now, the pipeline and constructional steel industry not only expects the cleanliness associated with ≤30 p.p.m. oxygen and sulphur but also requires shape control of the residual nonmetallic inclusions. Otherwise, these nonmetallics elongate during working and lead to a reduced ductility and toughness in the transverse and through thickness directions of rolled plate. Manganese sulphides are particularly deleterious in this respect. In order to prevent this a number of modification treatments have been developed based on the introduction of elements which have large affinities for sulphur and form high melting point sulphides that precipitate before those of manganese sulphide during solidification.

2.4 INCLUSION SHAPE MODIFICATION TREATMENTS

Rare earths were added initially because they were soluble in liquid steel, had limited solubility in the solid state but more importantly because they had significantly lower vapour pressures than the alkaline earth metals, e.g. at steelmaking temperatures of 1600°C the vapour pressure of cerium is 0.002 bar, compared with 1.8 bar for calcium and 17.8 bar for magnesium [49]. This naturally made the addition of rare earth metal much easier to achieve than the alkaline earths. Considerable interest was shown in these additions to HSLA steels during the late 1970's particularly in the United States of America.

Wilson [50] in his studies on rare earth treated aluminium killed steel considered three levels of addition to be important. Residual rare earth contents of between 0.008% and 0.02% were reported to replace alumina inclusions with a type of rare earth/alumina

oxide, the composition of which varied from the stoichiometric $REAl_2O_3$ to the more prevalent inclusions of $REAl_{11}O_{18}$. In addition to discrete particles of these rare earth aluminium oxides which were distributed throughout the solidified steel, they were often found associated with manganese sulphide. When rare earth contents were in the range 0.02-0.07% the inclusions were commonly found to have an oxysulphide core, or to comprise of rare earth oxysulphides surrounded by rare earth sulphides of varying stoichiometry. Discrete rare earth sulphides only appeared when rare earth contents were greater than 0.07%. A large number of investigations into sulphide shape control using rare earths conclude that it is achieved when the RE/S ratio is ≈ 3 [51-58]. Problems were encountered, however, when excess additions of rare earths were found to result in subsurface entrapment of inclusions and heavy accumulations of rare earth sulphides in the bottom cone of an ingot [39,51,59]. In addition to this, residual rare earth elements were found to segregate to as-cast grain boundary regions where they formed low melting point eutectics, which subsequently resulted in hot shortness [59]. This segregation of sulphur leading to inadequate shape control led to early criticisms of inclusion modification. Further problems with rare earth treatments were experienced with nozzle blockage during teeming [61], which was attributed to the fact that the lanthanides formed by reaction with oxygen were solid and had physical and mechanical properties similar to those of alumina [54,59,62]. For this reason the protection of the pouring stream by inert gas shrouding proved to be essential if reoxidation was to be prevented.

A number of elements have been investigated in order to find more suitable

inclusion shape modifiers than rare earths. Of the elements possessing a high chemical activity in molten steel, calcium seemed an obvious choice since thermodynamically it was one of the strongest oxide and sulphide forming agents available to the steelmaker. The use of calcium as a modifier, however, was restricted by its low solublity in liquid steel. The solubility of calcium in liquid steeel at 1600°C has been shown to be 0.016%[49,56] at atmospheric pressure,although this solubility is increased slightly in the presence of certain alloying elements such as carbon, silicon, aluminium, and nickel [47,49]. This low concentration is rarely attained in practice due to the low boiling point (1492°C) and high vapour pressure at 1600°C (1.8 bar) of calcium which has led to technical difficulties with its introduction and solution in molten steel. As a result of the violence and general inefficiency of the reaction, solid calcium is rarely added directly into molten steel. Thus, it is generally injected under controlled conditions where the rate of release of calcium is closely regulated by its mixture with a large volume of inert carrier gas. Further improvements in the efficiency of the calcium addition have been achieved by adding it either as a chemical compound which dissociates at steelmaking temperatures or as an alloy with an element which is itself soluble in iron [63]. The earliest investigations into calcium treatment of steel were conducted around the turn of the century [64,65] but little work of any merit was produced until 1938 when Sims and Dahle [8] studied the effects of deoxidising steel with calcium-silicon additives. Their work was one of the first to attempt to study the effect microscopically. Significantly, it concluded

that calcium-silicon had little effect as a deoxidiser or as a method of inclusion control. Ironically, this same paper categorised the effect of aluminium in steel and defined the classical type I, II and III manganese sulphide inclusions noted earlier in this review. This work, like many preceding it, failed to notice the beneficial effects of calcium additives mainly because of inadequate addition techniques, and the limited equipment available for inclusion detection and classification. In contrast to this, later work showed that calcium minimised deleterious type II sulphide and alumina inclusions[66]. More importantly, subsequent research has clearly demonstrated that calcium treatments modify inclusions by introducing it as a component of the inclusion [67,68]. A good review of early work with calcium and the mechanisms of inclusion modification has been presented by Hilty and Popp [69]. Once the credibility of calcium as a modifier had been established, further investigations using injection trials were undertaken.

Gatellier and Olette [70] found that an excess of calcium resulted in an increase in the rate of removal of alumina inclusions. Experimental melts showed that it took 8 minutes to reduce total oxygen from 0.05% to 0.007% by aluminium deoxidation, and only 5 minutes if primary aluminium deoxidation was followed by a 2 minute calcium-silicide treatment. They attributed this acceleration in oxide separation kinetics to the transformation from dendritic alumina inclusions into globular liquid lime aluminates, stating that the resultant decrease in inclusion surface/volume ratio caused an increased rate of flotation according to Stoke's law. Unfortunately in this work, the experimental conditions for the addition of the aluminium and calcium silicide have to be deduced. It is

43

probable that Stokes' law is applicable to the removal of inclusions following the

aluminium, or aluminium-silicon deoxidation additions and for the removal of inclusions

after the calcium silicide injection period. However, their Figure 10 reproduced in

Figure (6) shows very clearly that the removal of oxygen (oxide inclusions) is at a

maximum during the injection of calcium silicide (note between 2- 4 minutes). It is

inappropriate to imply that Stokes' law is responsible for the removal of oxides during

this period and the discussion based on Stokes law is therefore irrelevant. What their

results do show is the powerful effect of calcium injection in the intermediate period of

oxide removal.
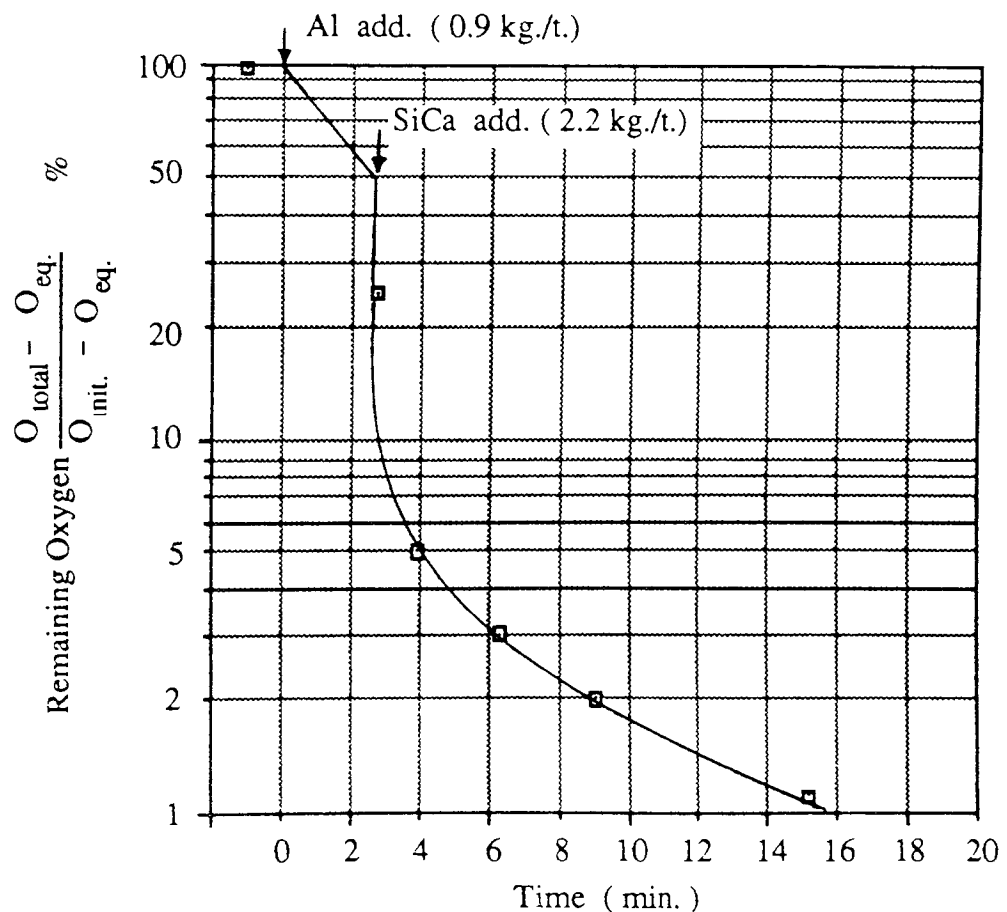
FIGURE 6. Deoxidation by successive additions of aluminium and calcium-silicon alloy[70]

Further, shape is important when considering liquid versus solid inclusion removal. A larger dragging force would be exerted on a dendritic inclusion with a large surface to volume ratio and it would, therefore, have a slower rate of separation. The transformation of alumina inclusions into globular lime aluminates by a calcium addition can be understood by reference to the $CaO\text{-}Al_2O_3$ phase diagram, shown in Figure (7).

Aston University

Illustration has been removed for copyright restrictions

Fig. 7. —System $CaO\text{-}Al_2O_3$. C = CaO; A = Al_2O_3
F. M. Lea and C. H. Desch, The Chemistry of Cement and Concrete, 2d ed., p. 52. Edward Arnold & Co., London, 1956.

From this it can be seen that the presence of between 40-60% CaO in a lime aluminate inclusion ensures that it would be liquid at steelmaking temperatures. These inclusions are formed almost immediately after a calcium addition (after ≈ 10 seconds) [46,71] and are low in density. The fact that these liquid inclusions readily coalesce and increase in size, accounts for their enhanced rate of removal in accordance with Stokes law [46,47,56,69,72].

A relationship has also been established between the calcium content and aluminium content of a killed steel, necessary to obtain spheroidisation of alumina inclusions. This is given in Figure (8). The flotation capacity of lime aluminate inclusions does not remain constant. A short time after a calcium addition, the flotation rate of these inclusions decreases and stabilises, since after 2 or 3 minutes the lime content of the inclusions has generally fallen to 15-20% [46,71]. These inclusions are solid at 1600°C and have a relatively slow rate of separation. It is now accepted that the continuation of steady argon bubbling through a melt after the completion of a calcium addition, greatly assists in the floating-out of the smaller residual inclusions [13,14,46,47,71]. Subsequent research [56] has also noted that the effectiveness of alumina transformation depends on the degree of calcium addition. Too little is considered to result in the formation of solid inclusion clusters with a composition between pure alumina and lime aluminate ($6Al_2O_3CaO$) and these are generally regarded as being more deleterious than those of the original alumina inclusions.
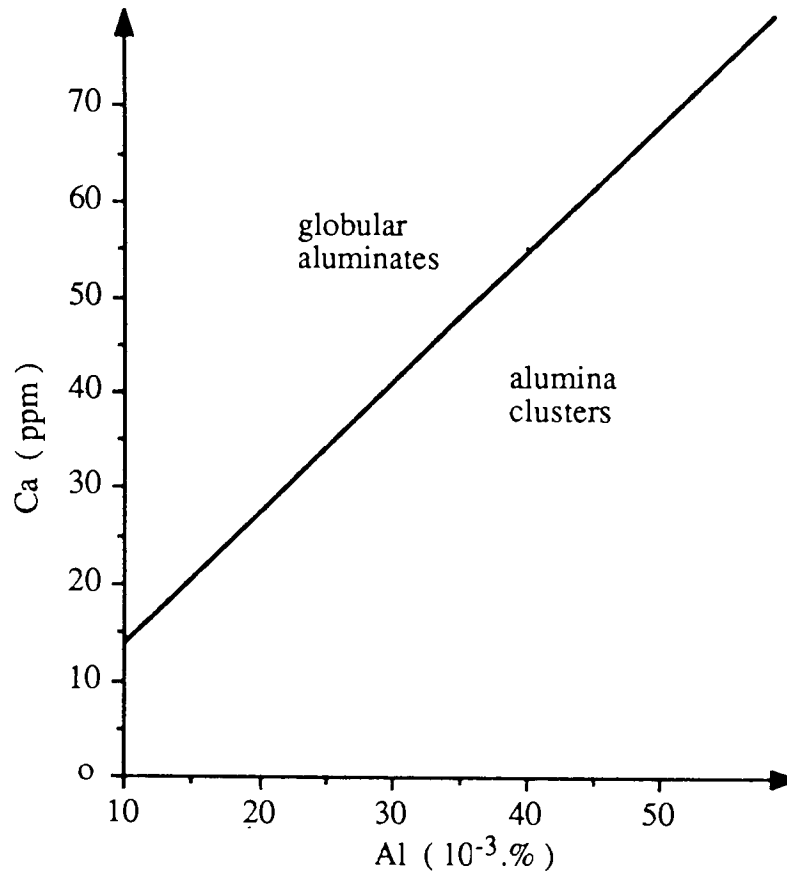
FIGURE 8. Relationship between calcium content and aluminium content in a killed steel to obtain spheroidisation of alumina clusters [73].

Lime aluminates and the level of calcium treatment have also been found to be important in the control of sulphide morphology. A number of workers [47,74-77] have noted that CaS or Ca-Mn-S rims form on or around lime aluminates after calcium treatment. Nashiwa et al [74] reported that with an increasing amount of calcium in steel, the percentage of lime in the inner phase of duplex lime aluminates became greater, whilst the amount of manganese in the Ca-Mn-S rim decreased and the inclusion eventually transformed to a single phase globular $CaO-Al_2 O_3-CaS$. In contrast to this, Kawawa et al [76], noted that with large calcium additions samples taken from a 250 tonne

ladle contained inclusions of CaO-Al$_2$O$_3$ combined with CaS as a heterogeneous phase.

Similarly Narita et al [77] also reported that CaO(10-40%)-Al$_2$O$_3$(5-60%)-CaS(10-60%)

were formed within several minutes of the onset of calcium injection. The primary

inclusions contained CaS as CaO-Al$_2$O$_3$-CaS but later in the injection period calcium

sulphide or calcium oxysulphide inclusions formed with a degree of clustering . This

modification of inclusions by calcium treatment has been schematically represented by

Tahtinen et al [78], and is shown in Figure(9).
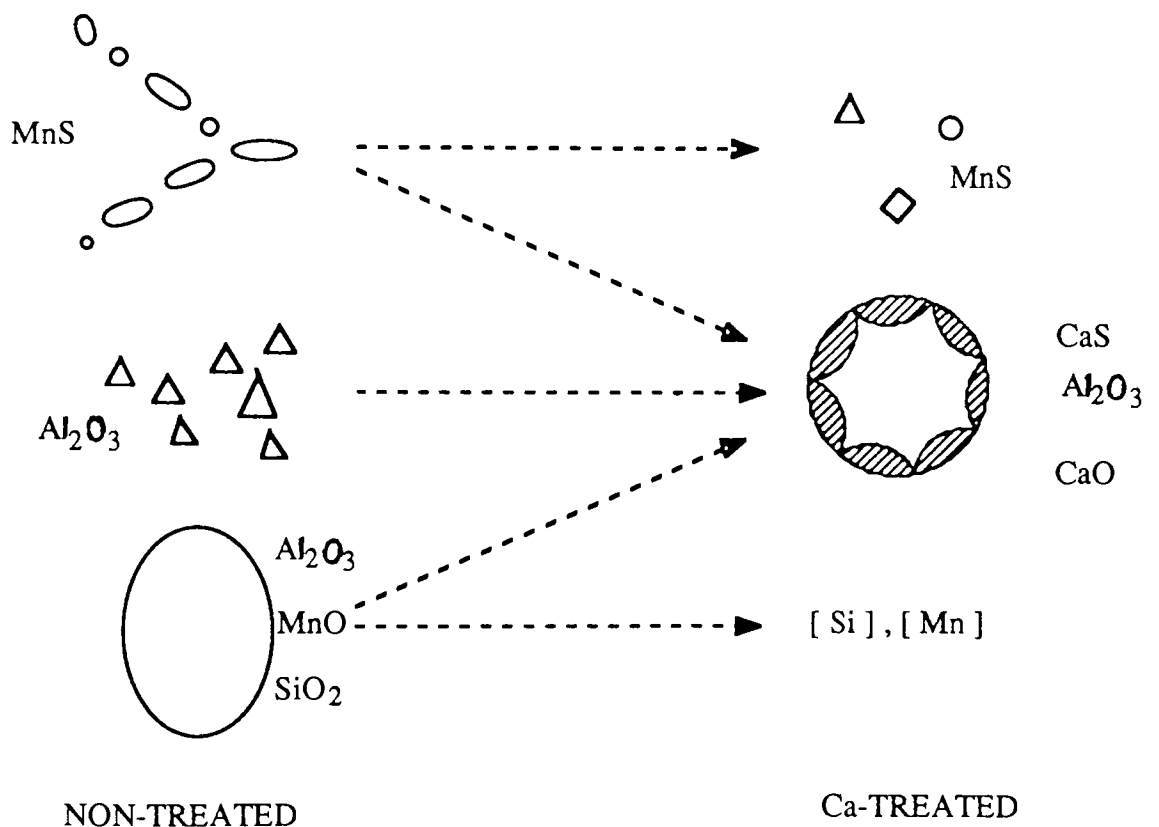
FIGURE 9. Schematic presentation showing modification of inclusions with calcium treatment [78].

The significance of these treatments was that segregation of sulphur within the steel was minimized by dispersion to widely distributed spheroidal calcium aluminates. Manganese sulphide inclusions were unlikely to be present due to the low sulphur concentrations anywhere within the steel.

The other way in which sulphide shape control is brought about is by the substitution of calcium for manganese within the manganese sulphide lattice [47]. Calcium sulphide has a similar crystal structure to that of manganese sulphide [69] and it is widely accepted that calcium can partly or wholly replace manganese in manganese sulphide inclusions [47,56,69]. Leung and Van Vlack [79] have demonstrated that even relatively low concentrations of calcium sulphide (as little as 10%) in manganese sulphide raises the melting point of the sulphide phase. The accompanying increase in hardness helps to reduce stringer formation.

The advantage of calcium compared with rare earths is that lower concentrations can be used because of its smaller atomic weight [51] (calcium has an atomic weight, 3.5 times less than that of rare earths). Evidence to support this came from Hilty and Popp [69] who found in laboratory trials that only a quarter of the quantity of rare earth was required for calcium to achieve the same result. Further, CaS inclusions are more easily removed from a melt than RES, since CaS has a lower density (1.5 times less dense than RES) which results in an enhanced flotation rate although the added beneficial effects of stirring associated with a calcium addition cannot be overstated.

Calcium silicide is now almost universally accepted as the refining agent for inclusion control of fine grained aluminium killed steels. However, the gradual lowering of permissible silicon levels in linepipe and constructional steel has resulted in some steelmakers finding difficulty in achieving the specification level and at the same time bringing about complete inclusion shape control [80,81]. An interest was generated, therefore, in alternative elements that would be able to fulfil this role in these steels. Magnesium has been considered because of its strong affinity for oxygen and sulphur and its chemical similarity to calcium. However, because its vapour pressure is considerably higher, its effective introduction into molten steel is much more difficult, although its solubility in steel is very similar to that of calcium, being marginally higher at 0.023% [49,56]. Whilst this is limited, it is not considered to be so low as to preclude its dissolution into steel during treatment [63]. More importantly, a wealth of experience exists with the desulphurisation of molten pig iron using magnesium. In this, the injection of chloride salt-coated granulated magnesium has resulted in greatly improved magnesium yields and desulphurisation abilities [34,82-85]. It is also claimed that the salt prevents nozzle blockage from metal 'blow-back' by removing the volatile reaction zone from around the nozzle exit [84]. A study has been made by Irons and Guthrie [86,87] on the kinetics of magnesium desulphurisation of iron. They consider that 90% of the desulphurisation occurs away from the bubble surface. Magnesium and sulphur dissolve in the iron and precipitate as MgS on existing nuclei such as inclusions or MgS particles

which have been stripped from the rising gas bubbles of magnesium vapour, in a heterogeneous reaction. Further, magnesium is also essential in the production of ductile cast irons. It can be seen, therefore, that its potential as a refining agent in steel should not be discounted on the grounds of technical or processing difficulties. Widely differing opinions exist over the refining of steel with magnesium. The views of those that consider that magnesium cannot be used reliably to modify manganese sulphide inclusions are typified by Olette and Gatellier [56] who consider that, although magnesium has proved an excellent desulphurising agent for iron, it cannot play the same role in steel. They state that even if the reaction of magnesium with oxygen was non-existent a steel would have to be saturated with magnesium to reduce the sulphur content to about 0.01%. Interestingly, however, they consider that magnesium may have an indirect effect on desulphurisation since it reduces certain oxides in the slag (e.g. FeO,MnO) to form MgO which leads to an increase in basicity and produces a lower oxygen potential in the bath throughout treatment. Further, work by Ritakallio [88] has demonstrated, experimentally, the desulphurising ability of magnesium in low alloy steel. The benefits of a magnesium injection are shown in Figures (10), and (11) which compare the performance of calcium silicide with a magnesium bearing calcium-silicide addition. It can be seen that the rate of sulphur removal is greater for the injected powders containing magnesium than for the treatment with calcium silicide. One reason for the noted beneficial effects of magnesium could be due to the fact that it was alloyed with calcium, which may have acted as a 'moderator' effectively reducing its vapour pressure and thereby increasing its residence time in the melt.
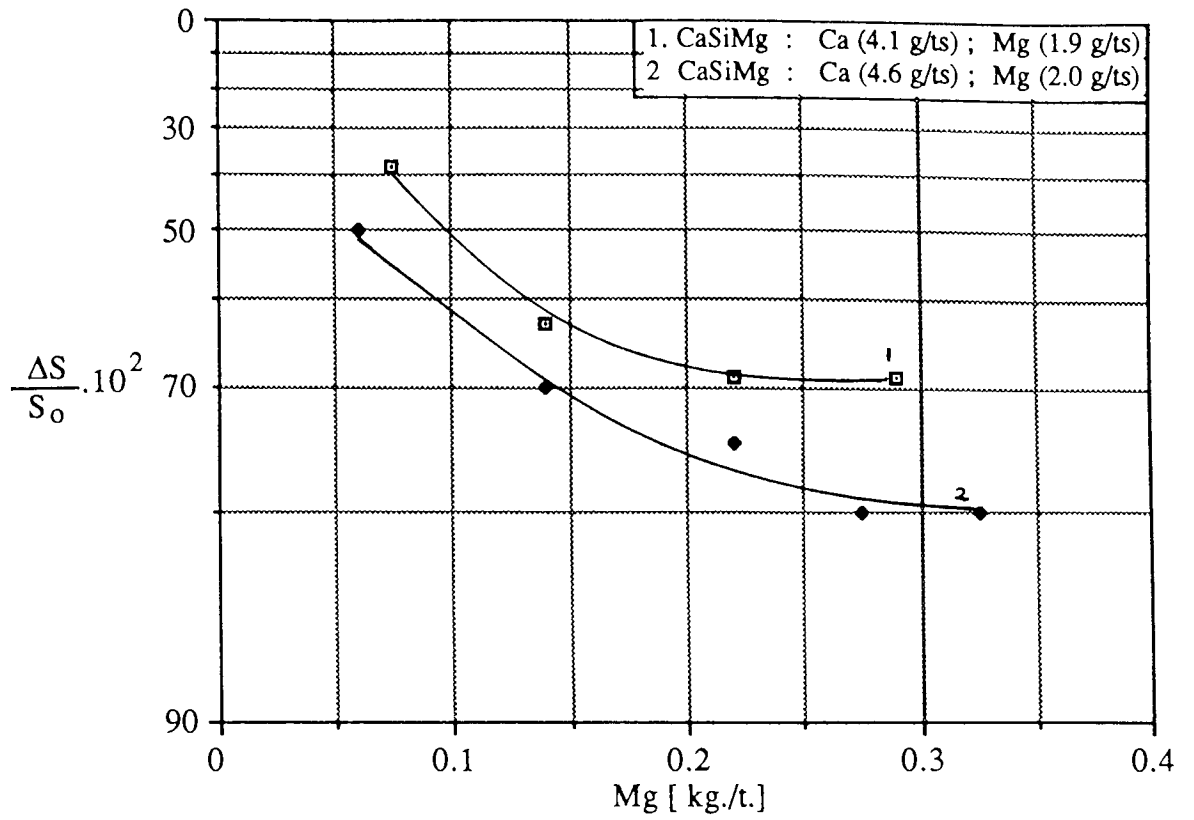
FIGURE 10. Desulphurising by magnesium injection [88]
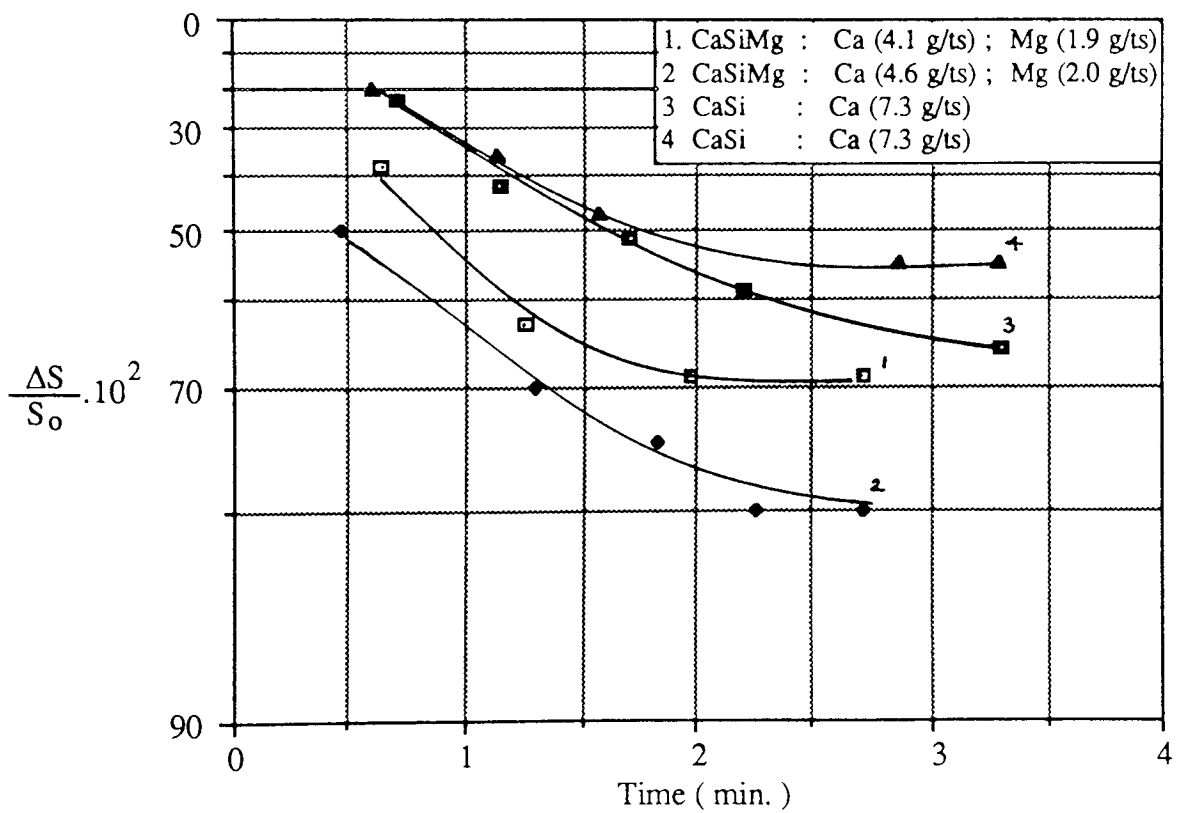
FIGURE 11. Desulphurising by Ca- and Mg- injection as a function of injection time [88]

Thermodynamic data for the calcium-magnesium system is known to show that calcium has a strong negative effect on magnesium activity [63,89]. The Figures (10) and (11) clearly show that after a given time or powder addition, the desulphurising ability does not appear to improve. In Figure (11) the time needed to reach this levelling off of sulphur removal with calcium silicide is three minutes or more. When the calcium is replaced partly by magnesium, desulphurisation is not only accelerated but quasi-equilibrium is achieved after approximately 2 minutes. The rate of reaction for the magnesium containing powder (as indicated by the gradient of the curves at the initial stages) is roughly twice that for the calcium silicide addition. Of course, the higher vapour pressures of the Ca-Si-Mg containing injectants will cause stronger stirring currents and thus mass transfer will increase with beneficial effects on sulphur removal.

Work by Saxena [90,91] using magnesium and magnesium containing slag powders has confirmed, on both an experimental and industrial scale, the beneficial effects of a magnesium addition to steel. In the initial work, magnesium additions were plunged into a slag free, aluminium killed steel. Evidence for the interaction of magnesium with the melt was provided initially by the association of MgO with clustered aluminium oxides. Higher concentrations of dissolved magnesium in the bath led to the formation of small randomly dispersed spinel type inclusions of $MgOAl_2O_3$. Small and complex sulphides containing MgS together with manganese sulphide were present, but no isolated inclusions of MgS were found. The author concludes that the high interfacial energy of these inclusions means they float quickly from the bath. However, some inclusions

containing pure MgS together with the spinel oxide did appear in the melt. The presence of these spinel oxides and complex sulphides was taken to indicate that magnesium like calcium modifies the morphology, distribution and composition of inclusions in aluminium killed steel. Saxena suggested that aluminium level controlled the dissolved oxygen in the melt enabling the magnesium to take part primarily in desulphurisation. This would appear to be debatable as the inclusions in the experimental series and those of a subsequent industrial trial in which a magnesium bearing slag powder was injected into a 10 tonne melt, seemed to be essentially oxide based. In the latter study, calcium was associated with some oxides of the $CaO-Al_2O_3-MgO$ type but more significantly with sulphur as CaS rims around $MgOAl_2O_3$. It would appear, therefore, that the small randomly dispersed spinel inclusions act as nuclei for sulphide precipitation.

Whilst this work is important in demonstrating that magnesium can be found as an integral part of an inclusion, and there is no doubt that injection treatment reduces the final sulphur level, further work would appear to be necessary to link it conclusively with the desulphurising ability of magnesium.

In an attempt to produce the highest quality linepipe steel, the secondary steelmaker has aimed to reduce the sulphur and oxygen contents of the cast product to a minimum whilst at the same time removing as many oxide and sulphide inclusions as economically feasible. Complete removal is impractical remembering that 1 tonne of steel containing only 1 p.p.m. of oxygen and sulphur will contain 10^{12} inclusions of 1 micron size [92]. It is, therefore, necessary to consider the effect of deformation on these

residual inclusions. In order to be able to fully understand the effect of inclusions in the steel it is also necessary to have a clear understanding of the effect of processing variables and microalloying elements on the property of the steel matrix. Consequently, a study of the correlation of fabrication variables with structure property relationships follows.

2.5 STEEL FABRICATION

The optimisation of properties through controlled rolling is a complex science and as such has received considerable attention in recent years [93-100]. A discussion of the more fundamental aspects will be undertaken here. Grain refinement is critical in the production of linepipe steels because it has a major effect on the strength and toughness of the steel whilst not impairing its weldability [94,95]. Carefully designed rolling schedules ensure that the desired structure and hence, requisite final properties are developed. This is achieved in the main by matching the deformation temperatures to those at which certain alloy (Ti, Al, Mo, Nb and V) carbides and nitrides are in existence, and it is their precipitates which are important in optimising properties through grain size control. Precipitate size and the temperature range over which these carbides/nitrides exist in relation to the hot working temperature, determines their influence rather than their morphology or composition [93]. Precipitate growth can in turn be regulated by controlled cooling, or the presence of alloying elements such as Cr, Cu, and Mo in solid solution, which tend to limit precipitation and, therefore, refine the precipitates. This control of precipitate size is necessary for them to fulfil the function of grain refinement. The

rolling schedules necessary to achieve these structural properties are elaborated overleaf.

Soaking temperatures have a profound effect on toughness because a fine ferrite grain size can be produced after rolling consequent upon a fine austenite grain size at the onset of rolling. The Japanese[94], in particular, consider that regulation of soaking temperature is crucial and as such have adopted very low soaking temperatures (850-950°C) in the production of high toughness linepipe. They report that fracture appearance transition temperature (F.A.T.T.) declines by 40°C for every 100°C decline in the reheating temperature [96]. This practice has not been widely adopted, however, and 1150°C appears to be the lowest generally accepted soaking temperature. Grain growth during reheating is prevented by TiN precipitates at normal reheating temperatures or by NbCN at lower reheating temperatures. It has been suggested that to achieve a relatively fine austenite grain size at the onset of rolling TiN particles should be less than 0.02μm. and the TiN content should not be less than 0.004% [94]. During high temperature rolling the main aim is recrystallisation and grain refinement. Rolling is carried out at a critical deformation rate so as to ensure complete austenite recrystallisation. If not inhibited by precipitates the recrystallised grains would grow at temperatures in excess of 900°C. TiC, TiN, NbCN, AlN, or NbC are the most important compounds which are used to ensure a fine austenite grain size at the end of the first stage of rolling. During the intermediate rolling stage deformation of the recrystallised austenite grains is carried out in a temperature range where further recrystallisation is not possible. Fine precipitates

1.SOAKING Precipitates

NORMAL TEMPERATURE TiN
(1250°C)

LOW TEMPERATURE REHEATING NbC
(1150°C) Nb(CN)

} Precipitates inhibit grain growth and ensure a relatively fine grain size at the onset of rolling.

2. HIGH TEMPERATURE ROLLING
(1200°C)

At a critical deformation rate to ensure complete austenite recrystallisation.

Main aim :
Reduction and Grain Refinement

3. COOLING TO 900°C

4. INTERMEDIATE ROLLING (VC)
(880-900°C)

Rolling of recrystallised austenite in a temperature range where further recrystallisation is not possible.

Recrystallisation and growth prevented by NbCN (or VC) to produce fine elongated, deformed austenite grains. (Pancake grains with a large aspect ratio).

Without further work transforms to

5.COOLING TO 700°C (VC)
(V(CN))

Fine grained equiaxed ferrite.

6. LOW TEMPERATURE ROLLING (VC)
(700°C) (V(CN))

Where no recrystallisation occurs producing further grain flattening, finally transforming to polygonal ferrite grains.

7. COOLING

VCN (or to a lesser extent NbCN) causes precipitation hardening of ferrite on cooling. Increased strength is gained at the expense of toughness.

forming late in the first stage of rolling or at the start of intermediate rolling prevent

recrystallisation. NbCN is the major compound affecting austenite in this way, with

sufficient precipitation occurring with a niobium addition of 0.03% [93]. The main aim at

this stage is the production of uniformly elongated 'pancake' austenite grains with many

deformation bands. Without further work these transform to fine equiaxed ferrite grains -

the finer the austenite,the finer the ferrite. If rolling is carried out at lower temperatures

no recrystallisation occurs resulting in further austenite grain elongation. An interesting

development in recent years has been to employ microalloy additions in tandem, for

example, Nb-V, or Ti-V. The more stable, less soluble phase prevents grain growth

whilst the more soluble phase can be used to precipitation strengthen during the

austenite-ferrite transformation or, subsequently, in the ferrite.

The aim of controlled rolling is to maximise the sites available for ferrite

nucleation. Most of the sites have been identified as austenite grain and twin boundaries,

recovered sub-boundaries and undissolved carbides or nitrides [97]. Ferrite nucleation

occurs primarily at the austenite grain boundaries, growing inwards producing fine

equiaxed ferrite grains with a diameter of less than half the minor axis of the austenite

grain. This highlights the need for the production of not only a fine austenite grain size

but one with a large surface area (e.g. pancake shape). The finishing temperature in

controlled rolled steel has also been shown to greatly influence the toughness and

strength of linepipe steel [102] where a high reduction rate in a low temperature range

produced high strength with a low F.A.T.T. Similarly, the recently developed Sumitomo

process [3] uses a low finishing temperature for production of its low temperature toughness linepipe. One disadvantage of using a relatively low finishing temperature has recently been highlighted [97], whilst the optimum matrix properties are produced with respect to strength and toughness there is a problem with the elongation of manganese sulphide inclusions. The relative plasticity of manganese sulphide increases with decreasing rolling temperature causing manganese sulphide elongation which can lead to poor through thickness toughness, lamellar tearing or longitudinal cracking in bending. The solution to these problems was the development of inclusion shape control treatments essentially based on calcium.

2.6 THE INFLUENCE OF NONMETALLIC INCLUSIONS ON THE MATERIAL PROPERTIES OF STEEL.

This effect is very complex and to understand it, it is necessary to follow the genesis of inclusions within the final steel. The physical properties of the matrix and subsequent modification of these properties in the vicinity of the inclusion is of fundamental importance with respect to material performance . The constraint that the inclusion places on the matrix depends on its formation temperature. If the inclusion is liquid at steel solidification temperatures (i.e. surrounded by a solid steel matrix) a compressive residual stress system will be generated thus ensuring coherency between the inclusion and the matrix. Coherence would also be ensured by virtue of the fact that a liquid would fill the contraction cavity formed within the steel. If on the other hand the

inclusion is solid whilst being surrounded by a solid steel matrix, any stress development will depend on the differences in thermal contraction between the steel and the inclusion. When an inclusion contracts to a lesser degree than the matrix a compressive residual stress develops within the inclusion and a resultant tensile stress develops in the matrix around the inclusion. Conversely, if the inclusion contracts faster than the matrix then tensile residual stresses will be generated in the inclusion followed ultimately by void formation between it and the matrix. Brooksbanks and Andrews [106-108] determined the mean linear coefficients of thermal expansion of a variety of inclusion compounds in order to predict the likely stress development within the surrounding iron matrix. They concluded that the most damaging inclusion types were Cordierite ($2MnO.2Al_2O_3.5SiO_2$), calcium aluminates and alumina since these had low coefficients of contraction relative to iron, and thus were responsible for the development of high 'tesselated' stresses which could cause matrix yielding and crack initiation. Iron oxide, MnO and calcium sulphide inclusions were found to have little effect since they had a similar coefficient of contraction to iron. Manganese sulphides, however, were considered to be beneficial, especially when duplexed with oxide inclusions, since their coefficient of thermal contraction led to the development of residual compressive stresses within the matrix. Sulphide envelopes were, therefore, considered to be beneficial since they acted as a 'stress-buffer' between the oxide inclusion and the matrix. The authors' inclusion ranking system has been substantiated by fatigue results [108,109] and photoelasticity measurements[110].

Kiessling and Nordberg [111] further developed these stress calculations by taking into account the elastic modulus of the matrix around inclusions. They concluded that for inclusions with a lower thermal contraction than the matrix, the effect of elastic modulus of the matrix on the tesselated stress and any stress concentration generated by an applied stress tended to cancel each other out. What they considered to be important, was not whether the inclusion could lead to cracking of the matrix, but whether the inclusion itself cracked. If a surface defect of a critical size existed within an inclusion it could be considered to be equivalent to a crack. This postulation was supported by their studies of inclusions which revealed that those with a low thermal coefficient of contraction were found to contain surface cracks, whilst those of sulphides showed no border cracks.

The type of void formed as a result of the inclusion shrinking away from the matrix can be significant in another respect. These voids have been reported to account for 10-20% of the total void volume in a 0.01% sulphur steel [106]. They can, therefore, be important with respect to hydrogen crack initiation. This would depend on the size and distribution of these voids. A large number of small voids would result in low individual hydrogen entrapment and, consequently, the pressure build up would be unlikely to lead to rupture of the steel. The worst case would obviously be when high hydrogen pressures are developed around large voids causing premature failure as a result.

Voids which are formed around hard particles during plastic deformation are quite distinct to those above, being larger in size and consequently, more deleterious.

Decohesion is intimately linked with the bond strength between the inclusion and the matrix and the plasticity of that inclusion. Rudnik [112] suggests deformation of inclusions occurs because of a frictional interaction between the inclusion and the flowing steel. He considers the making or breaking of inclusion/matrix interfacial bonds determines whether or not discontinuities are formed in the steel. Inclusions will obviously lengthen if the interfacial bond is strong and remains unbroken during hot working. Under such conditions discontinuities do not occur. The plasticity of the inclusion relative to the matrix at the deformation temperature will determine whether the interfacial bonds are broken, and hence the deformation characteristics of the inclusion. This has led to the development of a deformability index, υ , which characterises the plasticity of the inclusion relative to the matrix. Maunder and Charles [113] have modified the original relationship predicted by Malkiewicz and Rudnik [114], to a more generally accepted form which assumes plain strain deformation during rolling and the inclusions to be initially spherical, subsequently deforming to ellipsoids, such that :

$$\upsilon \ = \ \frac{\ln a/b}{2 \ln h_o / h}$$

where 'a' and 'b' are the major and minor axes of the deformed inclusions respectively and 'h$_o$' and 'h' are the initial and final thicknesses of the rolled steel plate.

Undeformable inclusions which have a low plasticity relative to the matrix do not participate in the flow of the steel phase and discontinuities can be formed as a result. The plasticity of an inclusion is linked to its composition and slight variations are known to dramatically affect their deformation-transition temperature [14,19]. Inclusions which are undeformable or crystalline at the hot working temperature such as galaxite ($MnO.Al_2O_3$) or corundum (Al_2O_3) are undesirable since they can lead to crack initiation and propagation. For this reason, the deformable inclusions of spessartite have been shown to be the most desirable reaction products produced during Mn-Si-Al deoxidation practice [19]. On the other hand inclusions which are liquid during hot working operations are highly detrimental since they readily deform into thin films and hot tearing results[7,115]. The plasticity of an inclusion is important, therefore, in determining its final shape within the steel. This in turn has been shown to be important with regard to its local stress-raising potential, a criterion considered to be particularly influential with respect to material properties, especially fatigue strength [116]. A useful study by Edmonds and Beevers [117], using photoelasticity techniques afforded an immediate demonstration of the existence of stress concentrations at inclusions. In this work they demonstrated severe stress build-up around hard inclusions during tensile loading. Also they showed that the stress intensification depended on the elastic modulus, shape and orientation of the inclusion. It has been suggested that in the case of fatigue, round inclusions are the most deleterious [116]. This does not explain the discrepancies reported in the literature [110,115] that round undeformed inclusions of FeO or CeS were found to have little effect on

fatigue properties. The plasticity of these inclusion types obviously has a more profound effect on the material properties than the shape factor in these cases. This is borne out by the general concensus of opinion that the most detrimental inclusion types are the undeformable calcium aluminates, single phase alumina, or spinel type inclusions[110,111,115,118]. That plasticity cannot be considered in isolation, is emphasised by the fact that the parameter is not sensitive enough to distinguish the more deleterious calcium aluminate inclusions from those of alumina, as they both have zero deformability. Inclusions with an intermediate relative plasticity ($v = 0.03\text{-}0.3$) [112] have been found to lead to problems with another defect. The flow of metal round the inclusion tends to extend its surface layers relative to the more rigid centre and finally, causes separation of its extremeties from the matrix as shown in Figure (12) [note the 'fish-tail'shape].
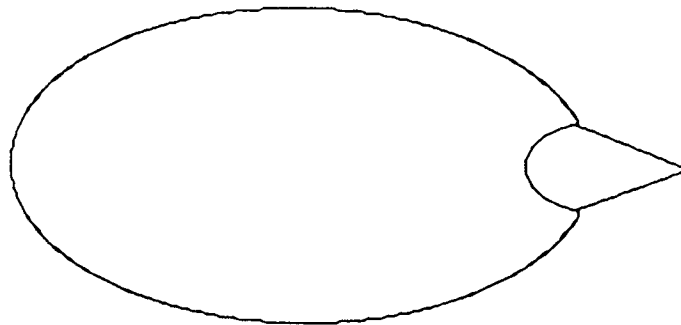
FIGURE 12. Fishtail with crack

Thus, it becomes obvious that there is an optimum degree of plasticity required for an inclusion. It needs to be high enough to prevent crack formation but not so great as to result in the inclusion being extensively elongated in the working direction causing a reduction in mechanical properties in the transverse and through thickness directions. The work of Rudnik [112] suggests that the most preferable relative plasticity index is in the range $\upsilon = 0.5\text{-}1.0$.

It can be understood, therefore, that the complex interactions between inclusion size, shape, composition, relative plasticity, orientation with respect to applied stress, and distribution within a steel, all influence the final material properties of a steel.

In order for an inclusion to cause crack propagation, either decohesion between the inclusion and the matrix must occur, or the inclusion must fracture. Ductile fracture in steel can be brought about by the creation of voids around nonmetallic inclusions as a result of an applied stress. This can only happen when the stress normal to the inclusion

interface is large enough to overcome the adhesive force between the inclusion and the matrix. This normal stress is a summation of the applied stress, stresses generated as a result of differences in thermal contraction between the inclusion and the steel, and those resulting from matrix elastic modulus effects. Ductility can therefore be improved by increasing the inclusion/matrix bond strength. Easterling [119] noted that changes in matrix composition affected the interfacial strength and hence the void nucleation strain. It has been reported that the plastic strain required to nucleate voids at sulphide, oxide or silicate inclusions can be very small [120]. As stated previously, for manganese sulphide it can be non-existent since void formation often occurs as a result of the inclusion shrinking away from the steel interface during cooling.

Ductile fracture at room temperature is usually caused by void growth at particles. Fracture can be described by a sequence of events : void nucleation, void growth, void coalescence and fracture propagation [113,119,121,122]. In a recent review Leslie [120] clearly outlines the importance of inclusions in this process. He reports that in steel, because the interfacial bond strength of cementite is much stronger than for inclusions, voids form first around the largest inclusions, generally manganese sulphide and then, with increasing strain around smaller oxide or silicate inclusions and finally, around very small carbides. The spacing between inclusions has been shown to be of particular importance during the void growth stage, since the linking together of adjacent voids leads to eventual failure [123-125]. In a review of the effects of inclusions on fracture, Lagneborg [121] suggests that the three most important inclusion parameters affecting ductile fracture are

size, volume fraction and interparticle spacing.

Elongated inclusions are known to be the major causes of reduced toughness levels, poor

mechanical properties and anisotropy in steel. Whilst stringered manganese sulphide

inclusions are the predominant inclusion type affecting toughness and through thickness

properties, silicates and oxides have also been shown to be deleterious when strung out or

clustered together [22,56]. The effect of a calcium treatment on impact toughness is shown

below.
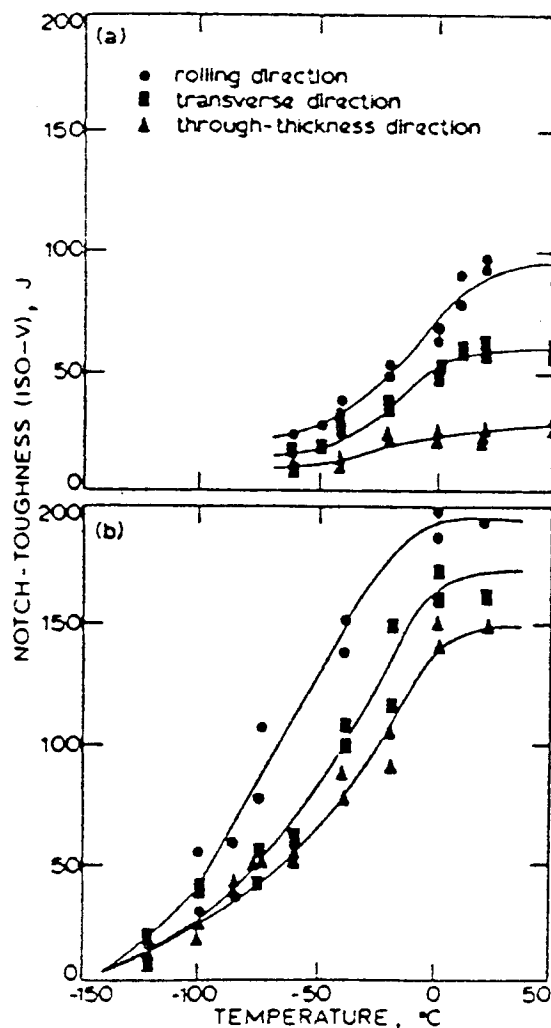
Figure 12a.

Influence of Ca injection on notch toughness of 50 mm plate of FG 36 steel.
(a) conventional steelmaking practice; (b) desulphurization with CaSI injection to 0.004% S.

Desulphurisation to a low sulphur level (0.004%S) using a calcium silicide treatment can be seen to significantly improve toughness values down to approximately -100°C . The transverse and through thickness values are also improved by the calcium treatment.

The level of toughness and ductility of a steel can be assessed by the area reduction during tensile testing. The through thickness ductility is used as a measure of the resistance of the steel plate to tearing during and after welding. This is a particularly important quality in the case of offshore linepipe steels. Deformed oxides and sulphides are again the main cause of poor mechanical properties. Lamellar tearing is of interest since generally it has been detected during fabrication. Although it has led rarely to in-service failures, it has caused a number of expensive repair operations. As such, the phenomenon of lamellar tearing is another justification for the use of inclusion shape modification during steel melting practices. The dramatic effect of calcium treatment on the through thickness reduction properties are shown clearly below, where improvements of up to 60% have been obtained.
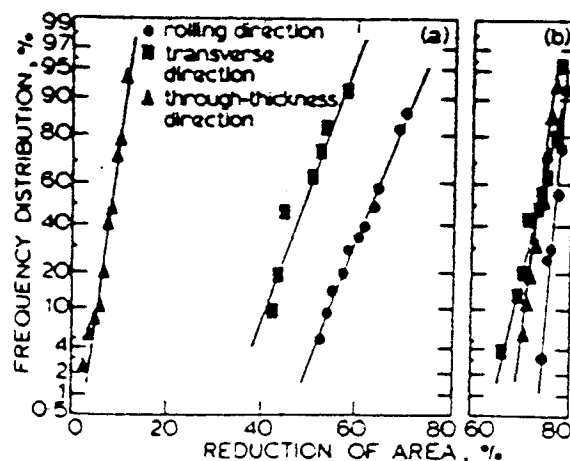
Figure 12 b
Influence of Ca injection
on ductility of 50 mm
plate of FG 36 steel
(a) conventional steelmaking
practice; (b) desulphurization
with Ca Si injection to
0.004% S

Lamellar tearing is a form of cracking that occurs in the base metal of welded steel,due to the combined effects of the anisotropic characteristics of hot rolled steel plate and high stresses generated by weld thermal contraction acting perpendicular to the rolling plane. A lamellar tear is characterised by terrace fracture surfaces parallel to the rolling plane of the plate, joined in a step-like manner by shear wall fractures perpendicular to the rolling plane. Terrace fracture surfaces have been shown to be associated with closely linked elongated or aligned inclusions, a material characteristic which also causes poor short transverse mechanical properties [126] . This work demonstrated the fact that lamellar tearing is a surface or subsurface phenomenon since there was a wide variation in ductility with through thickness location of the fracture. The plates tested had a high susceptibility to lamellar tearing when taken from the quarterline section of the plate, whereas those taken from the centreline proved significantly better.

Ludwigson [127] agrees that lamellar tearing is initiated by weld thermal contraction strain. He goes on to point out, however, that since lamellar tearing proceeds by microvoid growth and coalescence into terraces and finally by shear between terraces, that a critical factor in the latter stages is matrix strength and toughness. It was found that through thickness reduction in area fell with higher strength, lower toughness and increased inclusion concentration. Wilson and other workers [123,126,128] have noted that the single most important factor controlling the lamellar tearing resistance is the form of the nonmetallic inclusions. Silicates and sulphides flattened by rolling were the most damaging. The importance of Kaufmann et al's [128] work is not so much that it agrees

with previous work but that it highlights another problem in the area of lamellar tearing and inclusion studies in general, that of the adverse effect of hydrogen. During the examination of weld variables they found that increases in hydrogen potential led to a sharp fall in lamellar tearing resistance.

An important property of plate for use as linepipe or oil refining materials is that it should have good hydrogen induced cracking (H.I.C.) resistance, since the operational environments are rich in moisture and hydrogen sulphide[22]. The problem of hydrogen in steel has been extensively reviewed by Interrante[129]. Hydrogen is considered to be deleterious because it is highly mobile as an atom or ion, and can diffuse through the lattice or be transported by the movement of dislocations. The migration of hydrogen in steel is restricted to its atomic form since the smaller atoms can readily diffuse through the lattice unlike the relatively larger hydrogen molecules. It is known to diffuse towards elastic stress fields which are tensile in nature[129]. Stress concentrations around inclusions can thus provide the driving force for diffusion. It is generally accepted that type II manganese sulphides or elongated alumina inclusions are the most detrimental with respect to HIC[130-133]. Steelmaking practice can, therefore, have a direct influence on the susceptibility of a steel to this type of failure since it ultimately dictates the type of residual inclusion present within the final product. Type I manganese sulphides are considered to be less deleterious than type II because they are initially globular and do not deform readily[130]. A series of carefully designed experiments on hydrogen occlusivity by Chan, Madrid and Charles[134] has shown quite clearly that the larger the

sulphide/matrix interface the greater the amount of hydrogen that can be trapped. HIC is brought about by a combination of factors. Atomic hydrogen diffuses through the steel and is 'trapped' at incoherent inclusion/matrix interfaces where it reassociates to form molecular hydrogen. The resultant internal pressure builds up to cause an expansion of the void space around the inclusion which acts as a crack front that stresses the matrix locally [129]. This stress intensification is generally associated with high concentrations of dissolved hydrogen which cause embrittlement of the immediately surrounding matrix. Cracks can propagate as a result of this embrittlement if the inter-inclusion spacing is low or a banded microstructure exists as a result of segregation. Venkatasubramanian and Baker [135] report the quasi-cleavage fracture mode evident in a number of failed linepipes to be indicative of the pressurisation and embrittlement mechanisms within HIC. It has been shown that HIC resistance can be significantly improved by sulphide shape control, a limitation of hydrogen penetration into steel, and reduced amounts of segregation within the matrix [136,137].

It can be seen, therefore, that oxygen and sulphur in molten steel should be reduced to as low a level as possible. The latest 'Clean-Steel' conference in Hungary [138] concentrated on inclusion removal rather than modification. However, the linepipe steel user not only expects the associated high levels of cleanliness but also shape modification of the residual nonmetallics. 'Modified steels' also fulfil an important market for use in less demanding applications. Calcium silicide has established itself almost universely in

this role, generally being introduced by injection treatment. The obvious question is whether there is any commercially viable alternative. Magnesium has been proposed as an inclusion modifier and has been identified as an integral part of nonmetallic inclusions, namely magnesium aluminates and complex sulphides. Work was needed, therefore, to confirm these findings and to investigate whether its presence in a nonmetallic inclusion leads to improvements in material properties. At present there is no published work which compares a calcium treated steel with a magnesium treated steel. The following project has investigated this area. An attempt was made to produce treated steels of a similar matrix and to compare them metallographically and materially.

3. EXPERIMENTAL PROCEDURE

3.1 INTRODUCTION

To study the effect of calcium and magnesium injection on the final properties of a linepipe steel it was decided to produce two linepipe steels at the extremes of the sulphide range, i.e. 0.003 and 0.017%S with no injection attempted. These were to act as standards with which to compare the calcium and magnesium treated steels. The very low sulphur standard contained 30 p.p.m. sulphur and 21 p.p.m oxygen, whereas the other unmodified high sulphur metal contained 170 p.p.m. sulphur and 56 p.p.m. oxygen. Calcium and magnesium injected steels were intermediate to these values.

3.2 MELTING

Each of the five steels was produced by melting an 18 kg. charge under an argon atmosphere in a medium frequency (3.5KHz) induction furnace. The charge for the low sulphur steel standard was scrap X52 plate provided by British Steel Hartlepool, the analysis of which is given in Table 1 (steel A, P137). The high sulphur steel standard was produced by melting down 18 kg. of low carbon mild steel scrap of the composition given in Table 1 (steel B). Finally, the three injection treated steels with intermediate sulphur levels were produced by melting down Armco iron of the analysis shown in Table 1 (iron C).

Once the charge had been weighed it was loaded into a 30 kg. capacity alumina crucible which had an internal diameter of 13.6 cm. and was 30.5 cm. in depth. This crucible had been positioned in the furnace by ramming a standard commercial alumina

based lining material around it. A specially constructed refractory lined steel lid was then positioned over the crucible, sealed to the main furnace body and kept in place throughout the melting programme. The furnace spout was similarly sealed from the atmosphere using firebrick and a standard sealing compound. Finally, a graphite plug was sited over the central hole of the furnace lid and an argon shielding system introduced. The experimental melting unit is shown in Figure (13).
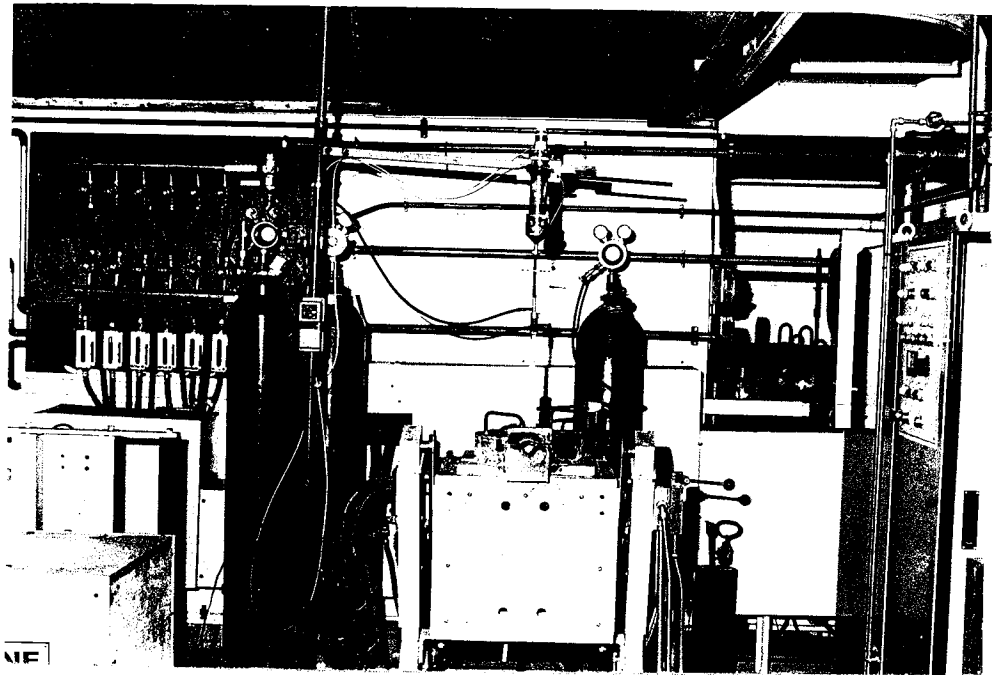
FIGURE 13 a EXPERIMENTAL MELTING UNIT.
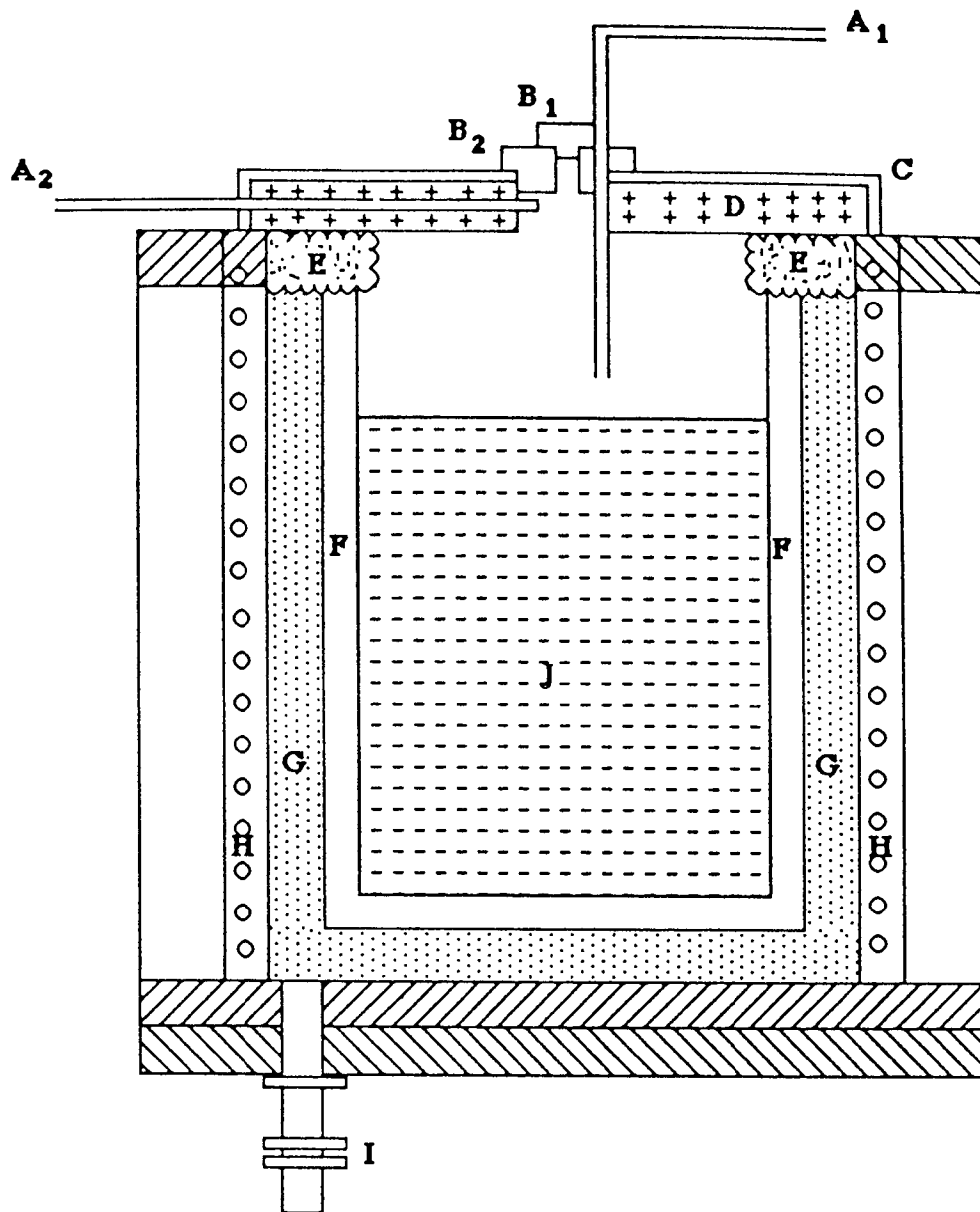
FIGURE 13 b. Section through the experimental melting unit.

A_1	ARGON SHROUD	E.	SPLASH PROTECTION
A_2	ARGON SHROUD	F.	ALUMINA CRUCIBLE
B_I	GRAPHITE PLUG	G.	RAMMED LINING
B_2	GRAPHITE PLUG	H.	INDUCTION COILS
C.	STEEL LID	I.	EARTH LEAKAGE SPIDER
D.	REFRACTORY LINING	J.	LIQUID STEEL MELT

Charge manipulation and melt control during deoxidation and microalloying was facilitated by removal of the graphite plug. The original charge in the crucible was heated to a temperature of 1600ºC (+/-10ºC), before deoxidising with a Mn-Si-Al addition contained in steel shim. Deoxidation and microalloy adjustment was carried out in a series of stages. In the case of the high sulphur untreated steel, three minutes were allowed for primary oxide removal, followed by a further four minutes for final deoxidation. During this time, final compositional adjustment was achieved by a further shim addition containing carbon, nickel, copper, and niobium. The steel was then cast into a coated, pre-heated cast iron ingot mould (76 x 76 x 254 mm.) with an argon atmosphere around the pouring stream. A standard exothermic hot-top was applied to prevent piping in the solidifying ingot. A total time of eight minutes elapsed from completion of the first shim addition to final casting. A slight variation in this procedure ocurred during the production of the low sulphur untreated steel. Rationalisation of the second and third shim additions allowed three minutes for primary deoxidation prior to final deoxidation and microalloy adjustment with a final shim addition. In this case seven minutes elapsed from primary deoxidation through to casting.

3.3 INJECTION

The technical difficulties associated with the injection of powders containing volatile constituents into molten steel are varied and have been discussed in the literature[22,34,36,139]. In this work in an attempt to safely and effectively transfer calcium

and magnesium bearing powder into liquid steel a purpose built injection system was developed. Some of the practical problems experienced in the development of this system have been published in a previous paper [140].

For the alkaline earth treated steels, an injection unit was put into place and powder blowing was achieved over a 2.5 minute period subsequent to the last shim addition. Primary deoxidation was again for three minutes prior to final deoxidation and microalloy adjustment. The injection treatment was started 1.5 minutes after this shim addition. The injection system used in this work is shown in Figure (14).
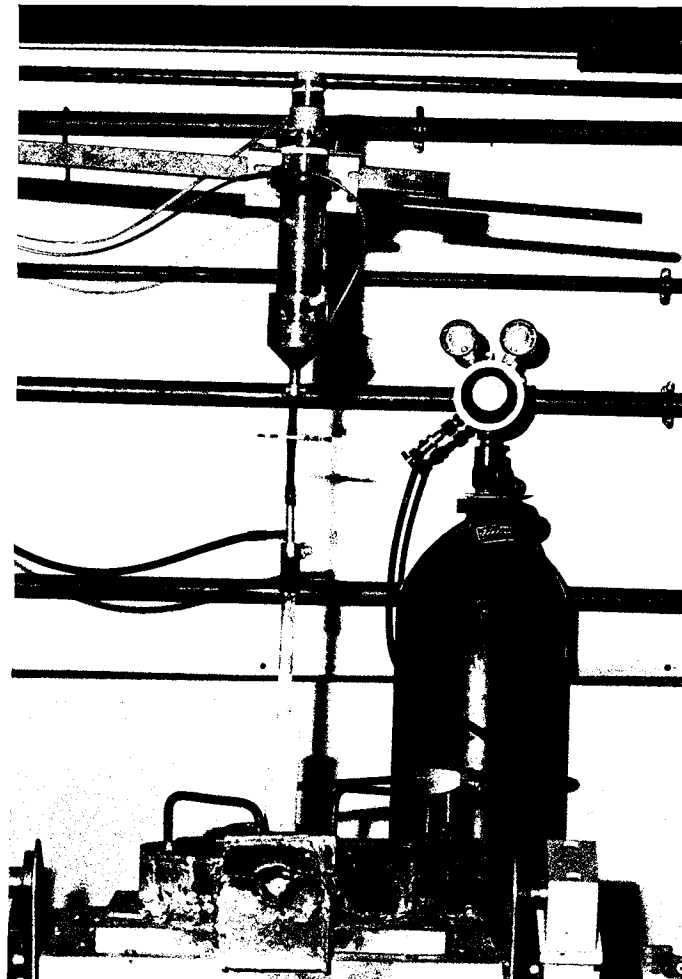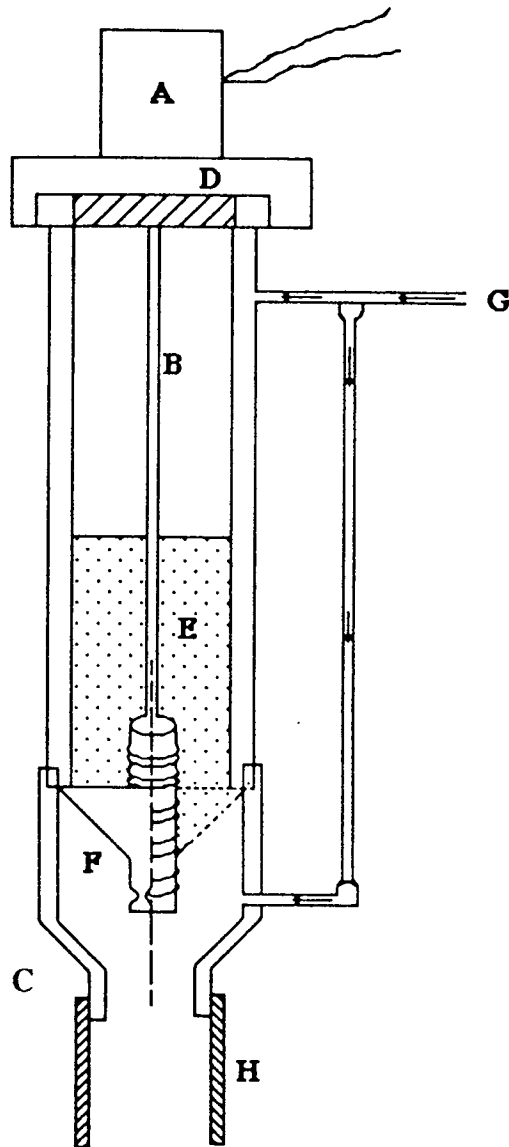
A . WORM FEEDER MOTOR

B . WORM DRIVE

C . WORM SCREW

D . FIBRE WASHER

E . POWDER

F . FEED OUTLET

G . ARGON CARRIER GAS INLET

H . FLEXIBLE HOSING

FIGURE 14 b.   Section through the powder injection unit

It can be seen that powder was moved through a storage silo by a screw conveyor into four feed outlets and transported by an argon gas stream through flexible hosing and a refractory lance into the molten steel. During the injection process a decreased furnace power input was sufficient to keep the bath temperature constant. The magnesium addition was achieved by the injection of 85 grams of a magnesium-bearing ferrosilicon powder containing 45% silicon, 9% magnesium, 0.2% aluminium and balance iron. For calcium silicide powder injection, 60 grams of a 70% silicon, 30% calcium alloy was used instead of the magnesium bearing ferrosilicon powder. A more detailed description of the injection assembly and its usage giving subsequent yields and metalloid recoveries is given in the published paper [140].

On completion of the injection treatments the steel was cast into cast iron ingot moulds, as before. Once again a total time of eight minutes elapsed from completion of the first shim addition through to final casting.

A sample of the solidified steel was sent away for independent chemical analysis. The final steel compositions are given in Table (2) and details of the sectioning procedure for each ingot is shown in Figure (15).

DISCARD

ISOTHERMALLY ROLLED FOR
DEFORMATION STUDIES.

CHEMICAL ANALYSIS

CONTROLLED HOT ROLLED FOR
CHARPY TOUGHNESS AND H.I.C.
SPECIMENS.
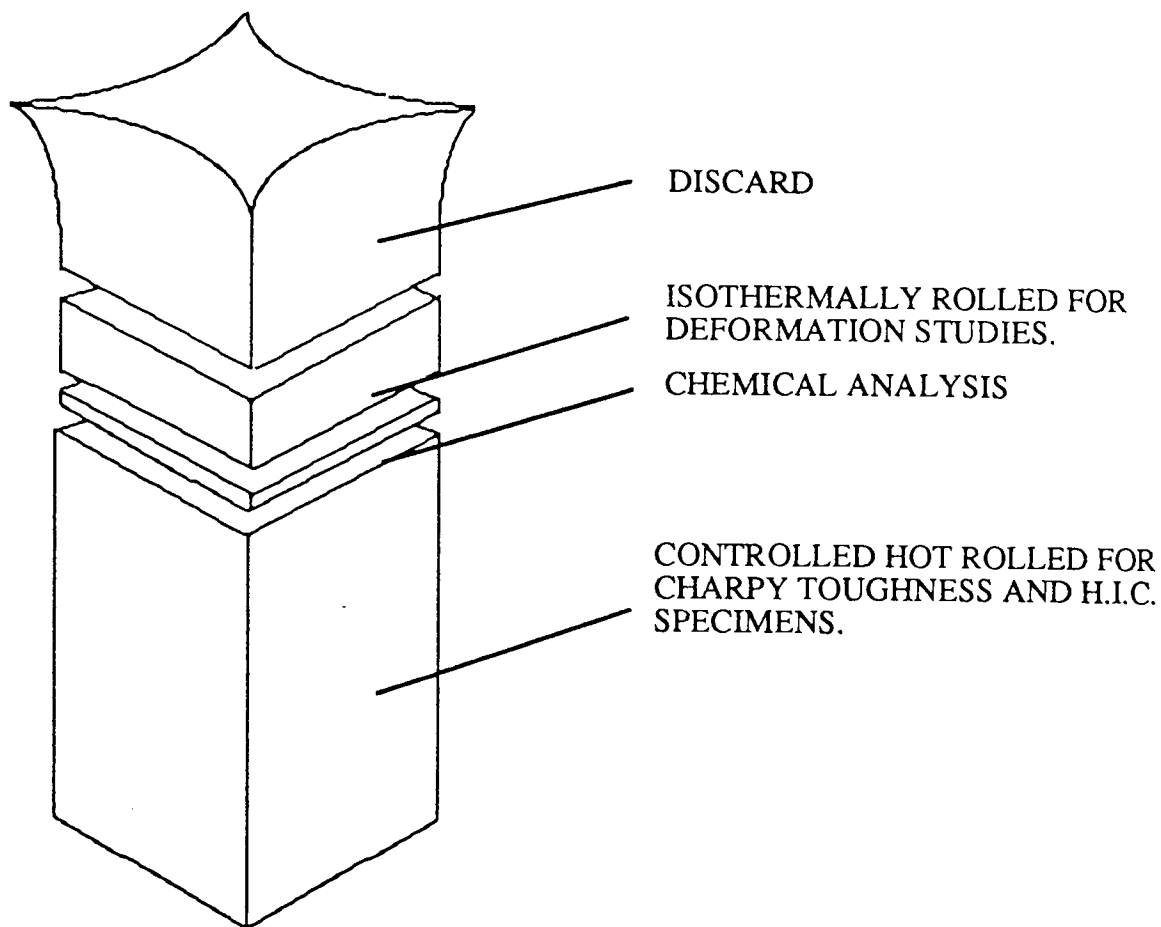
FIGURE 15. Sectioning procedure for the 'as-cast' ingot

3.4 ROLLING

The bulk of the solidified ingot was hot rolled by a controlled rolled sequence starting at 1200°C and finishing at 820°C to complete a total reduction of 76% (see Appendix 1). Three of the steels were isothermally rolled at temperatures of 800, 1000, and 1200°C for relative plasticity determinations. These samples were rolled down to 3 mm. to give an 88% reduction. Each steel was reheated to the original temperature between each pass in a controlled atmosphere ($90\%N_2 10\%H_2$) to prevent excessive oxidation. The deformation behaviour of the inclusions was examined for each sample parallel to the rolling direction.

3.5 RELATIVE PLASTICITY DETERMINATIONS

To determine the amount of deformation the inclusions had undergone in comparison with the matrix, the relative plasticity index, υ, was determined using the formula developed by Maunder and Charles [113]. This assumes plane strain deformation during rolling and the inclusions to be initially spherical, subsequently deforming to ellipsoids, and is defined as :

$$\upsilon = \frac{\ln a/b}{2 \ln h_o/h}$$

where 'a' and 'b' are the major and minor axes of the deformed inclusions respectively, and 'h_o' and 'h' are the initial and final thicknesses of the rolled steel plate.

In this work the dimensions of up to 450 deformed inclusions per sample were individually measured at a magnification of X 3000 on a Cambridge AMS image analysis

instrument. The index of deformability was then plotted against $\sqrt{ab}$, which was taken as representative of the original dimension of the inclusion, in order to study the deformation trends of the inclusions.

3.6 STEEL TOUGHNESS MEASUREMENTS.

This property was determined by Charpy V notch tests made on a minimum of three samples per test temperature conducted over the temperature range $-196^{o}C$ to $+80^{o}C$, on specimens taken from the transverse and longitudinal directions of the rolled plate. The resultant Ductile Brittle Transition Temperature curves are plotted in Figures (25) and (26). A cryostat was specially constructed to enable the specimens to be accurately held at the lower temperatures. The solvent media used during this work was n-pentane. A thermostatically controlled water bath was used for the higher temperatures of the testing programme. The Upper Shelf Energies (U.S.E.) in joules, transition temperatures in ^{o}C, and anisotropy ratios were then determined and are listed in Table (15) (P 147).

3.7 EVALUATION OF RESISTANCE TO HYDROGEN INDUCED CRACKING.

A purpose built test vessel, shown in Figure (16), was used for this assessment series in accordance with the most recent NACE standard[141]. Two test coupons of 40mm. +/-1 mm. length, and 20 mm.+/-1mm. width, were sectioned with their long axis parallel to the rolling direction of the plate, for each of the five steels. The specimens were dry ground and taken to a 320 grit finish. They were then ultrasonically cleaned, degreased in acetone, dried, and placed in the test vessel. Subsequently, a typical NACE

solution (consisting of 0.5% acetic acid and 5% sodium chloride solution) was poured

gently onto the samples for complete immersion, the pH was noted, and the box made as

airtight as possible. 10% sodium hydroxide solution was used as a trap on the exit side of

the H_2S flow.
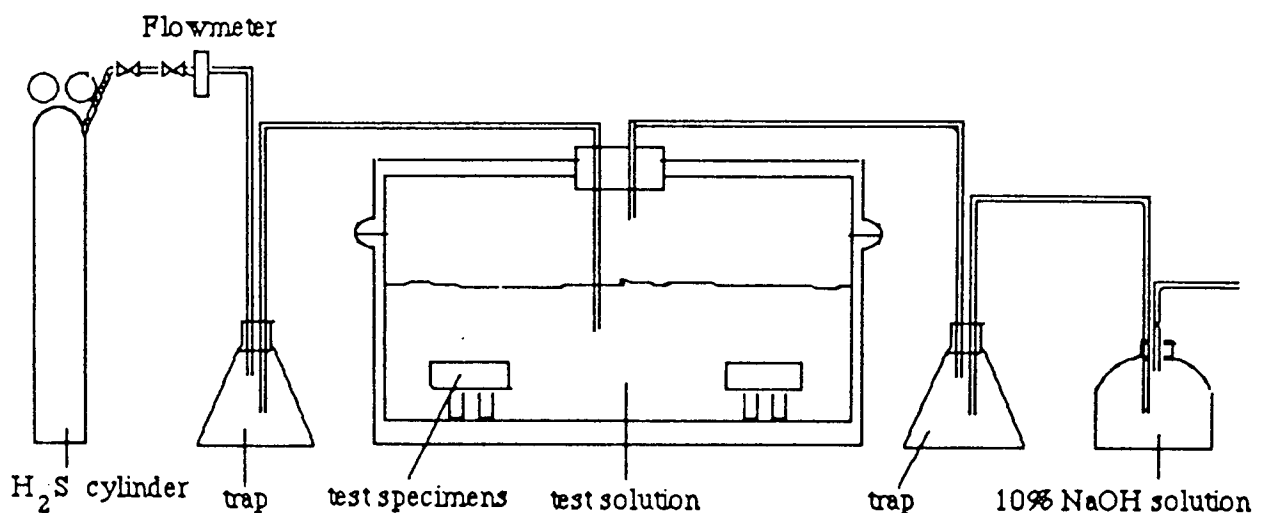
FIGURE 16. Schematic diagram of H.I.C. test assembly.

Deaeration of the solution was commenced immediately with nitrogen purging at

an optimum pressure of 3 p.s.i. (20.7MPa) for over an hour, consistent with the

specification [141] . Saturation was achieved by bubbling H_2S through the deaerated

solution at the rate of 45 c.c./min / litre for the first hour, and 17 c.c. / min / litre for

96 hours. At the end of the 96 hours the test was stopped and the pH noted. A summary

of the experimental conditions are shown in Table (3).

After exposure, the samples were cleaned in detergent before being dried and stored in a dessicator. The coupons were then sectioned transverse to the steel rolling direction, mounted and hand polished using standard metallographic techniques. It was necessary to give each sample a light etch in between final polishing in order to prevent fine cracks being closed over. Each coupon was initially examined at low magnification, (x 2 and x 5) on a Polyvar light microscope. Photographs were then taken of each crack colony over a range of magnifications in order to facilitate accurate crack length assessment. A graticule was similarly photographed at each magnification for calibration purposes. These were used to ensure standardization of print size. The amount and orientation of stepwise cracking was assessed in terms of the crack length ratio, the crack thickness ratio, and the crack sensitivity ratio, see Figure (17), and the test results given in Table (22) (P 153)
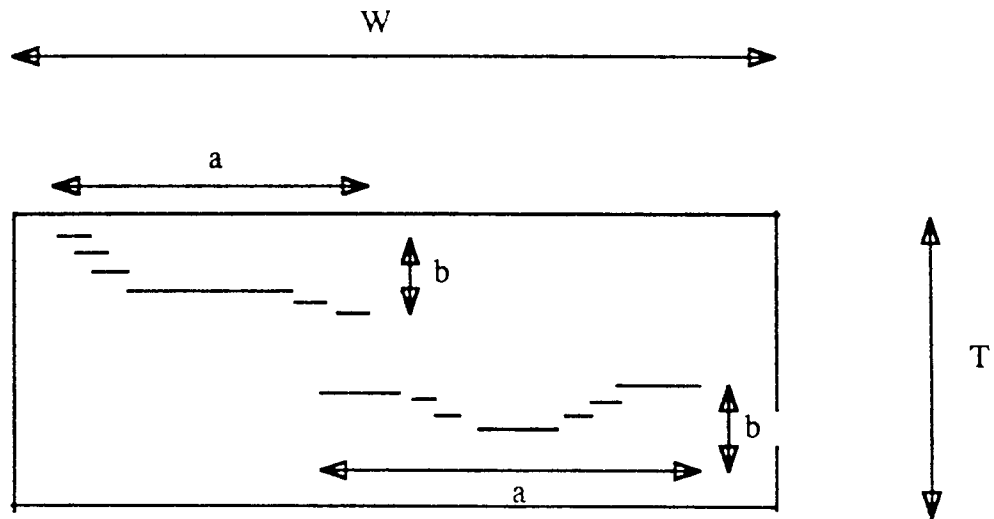
$$\text{Crack Sensitivity Ratio (CSR)} = \frac{\sum a \cdot b}{W \cdot T} \cdot 100\%$$

$$\text{Crack Length Ratio (CLR)} = \frac{\sum a}{WT} \cdot 100\%$$

$$\text{Crack Thickness Ratio (CTR)} = \frac{\sum b}{WT} \cdot 100\%$$

FIGURE 17. Method used for the quantitative evaluation of S.W.C.
in metallographic sections.

3.8 IMAGE ANALYSIS

Samples were taken from the Charpy test stubs for image analysis assessment. They were taken as close to the fracture surface as possible, with the plane of examination parallel to the fracture and mounted and polished using standard metallographic techniques. A Cambridge AMS image analysis machine was used for this purpose. The parameters measured included inclusion area fraction, mean inclusion

length, and inclusion number per unit area. The inclusion projected length was subsequently calculated from this data. Size distribution analysis was also carried out on three of the as-cast steels. Inclusions were measured by scanning 100 fields at random using a magnification of x950.

The detection capabilities of image analysis systems are contrast controlled and the machine requires flat specimens to be viewed under very even illumination. Prior to the onset of image analysis the field of view was calibrated by graticule. The detection limits were calibrated according to a standard procedure; a field of view was selected containing 'n' inclusions, the contrast limit was adjusted to detect the same number of inclusions as were observed optically. The variation in reflectivity both within an inclusion and between inclusions, required a balance to be obtained in the setting of the threshold level. If the threshold was set too high, false readings could be obtained by detecting areas of the metal with low reflectivity due,for example,to staining. Too low a threshold resulted in underestimation of the size of the inclusion. Inspection and counting over a range of magnifications and a large number of fields enabled an optimum setting to be determined, and all readings were taken under these conditions, in order that all results were comparable.

3.9 SCANNING ELECTRON MICROSCOPE NON-METALLIC INCLUSION COMPOSITIONAL ANALYSIS.

The samples which had been examined on the image analysis machine were repolished and carbon coated for examination under the scanning electron microscope

(SEM). Individual inclusions were analysed using a Link Energy Dispersive Analysis system (L.E.D.A.). Inclusion analysis was carried out at an appropriate magnification using the spot mode. The E.D.A. system uses calculations based on standard spectra (normally pure element standards) obtained from spot analyses. Fifty non-metallic inclusions were analysed for each steel sample. The shape and size of each inclusion was recorded along with its elemental analysis.

3.10 PHOTOGRAPHIC ANALYSIS.

Photographic assessment of the steels was carried out in order to further substantiate the inclusion characteristics of each steel as determined by image analysis. The same samples were repolished and 50 random fields photographed on the Polyvar light microscope, so as to produce photographs of approximately x450 magnification. The length and width of each inclusion was measured manually using a x8 graticule eyepiece. The mean inclusion length and width were determined for a total of 600 inclusions. The average number of inclusions per field and the deformablity index, υ, were also determined for each steel. A comparison of the image analysis results and the photographic assessment data is given in Table (8) (P 140).

4. RESULTS

4.1 Compositional Analysis Of Steel Ingots.

The composition of the steels as independently analysed are listed in Table 2. The basic linepipe steel specification aimed for was in accordance with that of 'special toughness steels' as reported by Mitchell and Barr of British Steel Plates, Motherwell[142]. It can be seen that whilst close control has been achieved in carbon, silicon, copper, nickel and niobium, a variability exists with the final aluminium contents of these steels. This has had a direct bearing on the final oxygen contents, generally a high residual aluminium content has resulted in a low total oxygen in the ingot although the maximum oxygen is only 63 p.p.m. compared with the minimum of 21 p.p.m. Steels 1 and 2 were used to assess the effect of a low level calcium treatment on an intermediate sulphur steel while steels 2 and 3, both calcium injected, provided a comparison to enable the assessment of the effectiveness of an increase in the calcium:sulphur ratio but were also affected by the increase in residual aluminium of the former. Steels 3 and 4 provided a very interesting comparison between a calcium and a magnesium injected steel at similar levels of treatment. It can be seen that the calcium:sulphur ratio of 0.38 is at the lower limit recommended for sulphide/oxide inclusion modification [74,143]. However, the magnesium containing steel has a ratio of 0.31 and should be directly comparable with a calcium containing steel.

Assessment of the relative merits of the individual ingots can be made by reference to the standard steel 1, containing 30 p.p.m. sulphur and 21 p.p.m. oxygen.

4.2 Size Range Classification Of As-Cast Inclusions.

A size range classification of the as-cast inclusions present within steels 3, 4 and 5 are

presented in Tables 4-6. This data shows that the calcium and magnesium treated steels

have a similar distribution of inclusion sizes within a fixed sample. Note the effect on

volume % of the very small number of large inclusions. Although these may seem

insignificant in 2000 inclusions their influence on fracture properties could be

disastrous. Again, the higher sulphur untreated steel has a greater proportion of

inclusions in the larger size ranges.

4.3 Field Area Image Analysis Results.

The results of the field area image analysis for each of the five steels are given in Table 7

(P140) and the specimen orientation and plane of examination with respect to the rolling

direction are shown in Fig.18 (P158). The mean length of inclusions in the longitudinal

direction is greater than that in the transverse direction for all five steels. A definite trend

is seen to exist with regard to the mean size of inclusions moving from the 0.003%

sulphur steel through to the 0.017% sulphur steel. An increase in mean length in this

longitudinal direction from 1.9 μm. to 4.2 μm. is shown. The data suggests that greater

elongation of inclusions in the rolling direction has occurred with increasing sulphur

content. The difference between the calcium and magnesium treated steels is very small.

It can be seen that there is a significant rise in the inclusion area fraction

(approximately quadrupled) between the 0.003% sulphur and 0.017% sulphur steel.

Both the calcium containing steels have increased area fractions of inclusions compared

with the low sulphur standard steel. The area remaining in the magnesium treated steel

was only double that in the standard steel compared with a much higher area in the 0.012% sulphur (calcium containing) steel.

The projected length of the inclusions increases progressively as the sulphur content increases but as would be expected the nearest neighbour (inclusion) distance is inversely related to the sulphur.

4.4 Comparison Of Field Area Image Analysis With Photographic Analysis Data.

A comparison of the results from these two measuring techniques is given in Table 8. It can be seen that they have produced very similar results. The inclusion characteristics revealed by photographic assessment follow the same trend of increasing mean inclusion length (in the longitudinal direction) with increasing sulphur content. The magnesium containing steel is again the exception to this. Note also there is a discrepancy between the average number of inclusions per field recorded for the magnesium treated steel.

During routine metallographic analysis and photographic assessment a number of observations were made. Firstly, the inclusions in the low sulphur (0.003%) steel were relatively difficult to find. In comparison, the inclusion population in the 0.009% sulphur calcium containing steel were much easier to locate. A striking feature of this sample was the existence of a large number of rounded inclusions along with the more general deformed inclusion type. This was very much the case for the 0.012% sulphur calcium treated steel where the rounded inclusions were even more evident. The inclusion population of this sample was distinctly mixed, since apart from these round inclusions, stringer colonies were also present. The 0.013% sulphur magnesium treated

steel contained a large number of inclusions of a similar deformability, ie. elongated in form. Round inclusions or extensively stringered colonies were not apparent in this sample. The inclusion population of the high sulphur untreated steel were mostly stringered together with a number of large elongated 'stringer' colonies.

4.5   Quantitative Inclusion Assessment Based On Inclusion Length Distribution.

The disproportionate effect of large inclusions on ductile fracture is well known[120,122,144-146]. DeArdo, Ratz and Wilson [147] proposed a simple method of rating inclusion content based on the characterisation of inclusion length distribution. This quantitative method of inclusion assessment has been repeated in this work. During photographic assessment the lengths of 600 inclusions were measured at X 450 on a 10 mm 2 sample for each of the five steels. The thirty (5% of the total) largest inclusions from each sample were measured (Table 9) and their lengths plotted on arithmetic probability paper (Fig.19,P155). From this it can be seen that 90% of these inclusions in the 0.003% sulphur steel were less than 13.5 μm. The next in order was the 0.013% sulphur magnesium containing steel with 90% less than 16μm, followed by the 0.009% sulphur calcium treated steel with 90% less than 20μm. Naturally, the two worst steels in this inclusion assessment were the 0.012% sulphur calcium treated and the 0.017% sulphur untreated steel. 90% of their inclusion lengths were less than 31.5 and 35μm respectively.

4.6 S.E.M. Compositional Analysis Of Inclusions

The results of the SEM inclusion compositional analysis for each of the five steels are listed in Tables 10-14. These are elemental analyses apart from the oxygen which has been calculated by difference. Due to the small size of inclusions or the small width and thickness of inclusion stringers, a very high iron content has been obtained for the majority of the inclusions. It can be assumed that a substantial amount of this is as a result of beam penetration into the surrounding steel matrix.

A better understanding of the inclusion types present within each of the five steels can be gained by relating their composition to inclusion shape. The basic shape categorisation for each of the inclusions analysed are given in Figures 20-24.(Pp156-160). The number appearing in front of an inclusion refers to the number of inclusions of this type and is not part of a chemical formula. The primary constituent of any complex inclusion is listed first followed by the rest of the inclusion phase.

Figure 20 shows that 74 % of the inclusions analysed in the low sulphur standard steel were alumina based. The sulphide inclusions measured were almost all manganese sulphide stringers.

Figure 21 gives the inclusion breakdown for the 0.009% sulphur calcium treated steel. It can be seen that a fairly even compositional distribution was found for this sample. 36% of the inclusions were calcium aluminate based, 34% manganese sulphide based and 30% calcium sulphide based. The shape categorisation reflects the metallographic observations of the presence of a large number of round inclusions in this

sample. Of these, the predominant composition was fairly evenly split between calcium aluminate and calcium sulphide based inclusions.

The shape categorisation for the other calcium treated steel is given in Figure 22. Once again a large number of round inclusions were obtained. However, in this sample they were found to be predominantly calcium aluminate based. No round calcium sulphide inclusions were recorded. It is notable that only one calcium sulphide based inclusion was analysed in this sample, as compared with fifteen for the other calcium treated steel. Of the inclusions analysed in this sample, 76% were found to be calcium aluminate based and 20% manganese sulphide based.

Figure 23 shows the categorisation of the analysed inclusions from the magnesium treated steel. 86% of the inclusions were found to be manganese sulphide based with 12% magnesia-alumina based. Magnesium was, however, readily found as a constituent of the inclusions in this sample. In each case it was associated with a similar amount of aluminium.

The inclusion classification for the high sulphur untreated steel is given in Figure 24. It can be seen that manganese sulphide stringered inclusions are the predominant type (88% were manganese sulphide based).

4.7   Charpy V Notch Properties Of The Steels.

The results of the Charpy V notch tests are plotted in Figures 25 and 26 over the temperature range $+80^0C$ to -196^0C. From these graphs the Upper Shelf Energies (USE) in joules, Transition Temperatures in ^0C and the Anisotropy Ratios are given in Table 15 (P147) It is well known that hot rolled steels exhibit anisotropy with respect to

mechanical properties, especially for high sulphur containing steels, and the results

presented show that the very low sulphur, 0.009% sulphur calcium containing and

0.013% sulphur magnesium treated steels have the closest approach to isotropic

properties.

The graphs of impact energy absorbtion against temperature illustrate   the

expected decrease in the steels' toughness with increasing sulphur content. It can be

noted that the magnesium containing steel was very much closer to the 0.009% sulphur

steel than the higher sulphur (0.012%) calcium alloy. It can be calculated that the upper

shelf energies of the magnesium treated steel are approximately 20% less than the

standard steel (0.003% sulphur) values compared with a 40-50% decrease for the

calcium bearing alloy with 0.012% sulphur.

4.8   Relative Plasticity Determinations Of Steel/Inclusions.

Figures 27 to 35 show the inclusion deformation trends obtained in the 0.012%

sulphur calcium treated, 0.013% sulphur magnesium treated   and 0.017% sulphur

untreated steels respectively after isothermal rolling at 800^0C, 1000^0C and 1200^0C for

an overall 88% reduction. The mean diameter of each individual inclusion is plotted

against the relative plasticity index. The overall means of the relative plasticities are

shown against the rolling temperature in Figure 36.

For the calcium treated 0.012% sulphur steel (Figures 27--29) the inclusions

appeared to separate into two groups a) small,essentially undeformed particles and b)

larger deformed inclusions. This is especially evident at the 800^0 C and 1000^0 C rolling

temperatures. In contrast to this the deformation trend of the inclusions rolled at 1200 ^{0} C seemed to be much more even. A number of lower deformability inclusions are still present but the more extensively deformed inclusion types (relative plasticity index > 1) are missing, giving the appearance of a downward shift in the overall deformability of the inclusion population.

The deformability of the inclusions in the magnesium treated steel (Figures 30-32) showed a mixed deformability. In contrast to those of the calcium treated steel, they seemed to be more evenly spread over the plasticity range. Again a marked downward trend in overall deformability was apparent at the higher rolling temperature (Figure 32).

Data for the 0.017% sulphur untreated steel (Figures 33-35) indicated that there were very few undeformed inclusions but their deformability increased with size. It can be noted that there was a marked absence of inclusions with a low deformability index for the steels rolled at 800^0C and 1000^0C.

Figure 36 illustrates the high relative plasticities of the 0.017% sulphur steel compared with the lower values of the modified steels and also, the significant decrease in mean relative plasticity with increasing rolling temperature. The magnesium containing steel seemed to have more deformable inclusions at temperatures of 800 and 1000^0C but they were less deformable at 1200^0C than inclusions in the calcium bearing steel. It is interesting to note that the mean lengths of the deformed inclusions in the longitudinal direction, as measured at higher magnification in the image analysis for individual inclusions was greatest at all three temperatures for the 0.017% sulphur

untreated steel and least for the magnesium steel, with the calcium 0.012% sulphur steel in between. These measurements confirm the trends obtained from the field area analysis listed in Table 7. Figures 37 to 41 give the deformation characteristics of the inclusions present within the controlled rolled steels. The relative plasticity index has been calculated from the photographic assessment data.

The low sulphur steel (Figure 37) shows an increasing deformability with size but in general the majority of inclusions have a low deformability, in the range υ = 0.05-0.25.

The 0.009% sulphur calcium containing steel (Figure 38) again exhibited the two-fold deformation characteristics which were revealed in the isothermal tests for the 0.012% sulphur calcium treated steel. There is a preponderence of inclusions with a very low deformability index (υ = 0.0-0.2) but a second group had an increasing deformability with size.

In contrast, the inclusions in the 0.012% sulphur calcium treated steel (Figure 39) did not exhibit any distinct categorisation of inclusion deformability. A number of lower deformability inclusions are apparent along with those of increasing deformability with size.

The deformation characteristics of the inclusions in the magnesium containing steel (Figure 40) show virtually the same trend as that obtained in the isothermal rolling treatments. This is particularly the case for the steels rolled at 1000^0C and 800^0C (Figures 31 and 30 respectively). The inclusions seem to be evenly spread over the

deformability range. It must be remembered that the controlled rolled samples should show a summation of the isothermally rolled specimens and this is borne out by these diagrams.

Figure 41 shows the increasing deformability with size of the inclusions present within the 0.017% sulphur untreated steel. The trend is similar to that of the isothermally rolled steels and, again, the deformability range covered by the inclusions in this sample appears to combine the results of the former. The deformability of the inclusions extends from those which are relatively undeformed through to highly deformed nonmetallic inclusion types .

The mean relative plasticities for the controlled rolled steels are plotted against steel type in Figure 42. Table 16 (P147) compares these mean relative plasticities with those of the isothermally rolled steels.

4.9 Hydrogen Induced Crack Evaluation.

The results obtained during NACE testing are listed in Table 22 (P153) and the method of determination of the crack length ratio (CLR), crack thickness ratio (CTR) and crack sensitivity ratio (CSR) is given in Figure 17 (P85). From Table 22 it can be seen that the mean CLR, CTR, and CSR of the steel increases with increasing sulphur content, with the exception of the magnesium containing steel (steel 4). No cracking at all was observed at a sulphur level of 0.003%. A typical example of hydrogen induced cracking showing its characteristic 'stepwise' form is shown in Figure 104 (taken from the 0.017% sulphur untreated steel). Figure 105 gives an indication that hydrogen

induced crack formation is assisted by the presence of inclusions. It shows that

inclusions could be likely sites for crack initiation since the stepwise crack appears to

have originated at two large adjacent particles.

5. DISCUSSION OF RESULTS

This work naturally divides into three sections for discussion :

(1)   physical properties of inclusions

(2)   their chemical properties and

(3)   the toughness and chemical properties of the final steel product.

5.1   Physical Properties Of Inclusions

These were measured using the AMS image analysis system. However, it was thought important that a separate assessment of inclusion size should be made by another technique to test the accuracy and reproducibility of the AMS work. As described in section 3.10, the length and width of 600 inclusions per sample were measured manually using a x8 graticule eyepiece on photographs at x450 magnification. The graph of mean inclusion length (in the longitudinal direction) against inclusion number, Figure (43), shows that after approximately 350 inclusions there is no significant variation in the overall mean length values. This trend was verified by plotting the 95 and 99% confidence intervals for the mean lengths as shown in Figures (44-48). It was, therefore, considered that a sample size of 600 could be taken to be representative of the inclusion population as a whole.

A comparison of the mean lengths of inclusions in the longitudinal direction and the average number of inclusions per field for the image analysis and photographic data

is given in Table 8 (P140). The overall reproducibility of mean length measurement for all the steels was $^{+}_{-}15$ %. However, four of the steels are within $^{+}_{-}$ 6.5% and, as is discussed below, there is a specific problem associated with steel 3.

The discrepancy in the results of the photographic analysis for the mean length for steel 3 could be explained by the fact that very mixed inclusions were present within this steel ie. stringered and round inclusions. Further, the variation in contrast, as witnessed metallographically would mean it would be difficult to totally 'fill-in' all inclusions using a fixed contrast setting on the image analysis machine. It is possible that the full length of some of the bigger inclusions was not recorded which would result, therefore, in a lower overall mean length when averaged over the inclusions per field. This trend is repeated for the other higher sulphur bearing steels (which contain naturally a wider range of inclusion sizes).

The difficulty in relating steel cleanliness as determined by routine metallographic preparation and inclusion counting to material performance has long been understood by the steelmaker. Kiessling [92], in particular, has constantly argued that it is more important to be able to relate steel quality to the probability of finding an inclusion of a critical size in a critical location. The disproportionate effect of large or highly deformed inclusions on material properties is taken into consideration in the simple method of assessing inclusion contents based on their length distribution proposed by DeArdo, Ratz and Wilson [147], see Fig.(19) (P155) and Table (9). Whilst this method is simplistic it could prove to be realistic as a method of comparison between steels. For the present

work the results for steels 1 and 5 confirm the expected differences in inclusion lengths between low and high sulphur containing steels. similarly, steels 2 and 3 reflect the difference in sulphur levels on mean inclusion length. However, steels 3 and 4 containing similar sulphur contents show significant differences in the inclusion length distribution and reflect the differences in properties obtained for these steels.

The relationship between the mean length of inclusions (as determined by image analysis) and sulphur content of the steel is shown in Figure (49) (P184). A straight line has been drawn for reference purposes between the values for the two untreated steels and an abscissa of 1, since this represents the limit of resolution of the AMS optical system. The mean length of inclusions measured in the longitudinal direction increases with increasing sulphur content. The graph shows the effect of increasing sulphur from 0.003% to 0.017% is quite dramatic. The mean length has increased from 1.9 to 4.2μm. This trend is in agreement with the results of Spitzig[148-150] for inclusion studies conducted on a similar series of experimental steels (it is interesting to note that the results of Spitzig and the present work lie on two parallel lines). The variation in the mean lengths and the shift in the two lines can be explained by compositional differences and variations in rolling temperature and total reduction.

In this study there was no facility for simultaneous inclusion analysis and measurement on the AMS so that it was impossible to accurately determine the compositional breakdown of the inclusion population of each steel. However, an indication of the general inclusion types present within the steels was afforded by the

SEM compositional assessment which folowed the image analysis. Differences in inclusion populations could account for some variation between the results of this and other work. The high aluminium content of the 0.003% sulphur steel resulting in the large number of alumina and alumina rich inclusions observed during the SEM compositional analysis would cause a lowering of the mean length of inclusions since alumina is known to deform to a very much smaller extent than manganese sulphide. It is important to stress, however, that the results of this work follow the same trend and are as significant as those where aluminium and oxygen was not a variable [149].

Figure (50) shows the cumulative inclusion probability data determined for the total inclusion populations measured during the photographic assessment of all five steels. The curved form of the data indicates that the inclusion length distributions as would be expected do not follow a normal distribution. It can be seen that there is a significant difference in the overall size range of inclusions present within the low and high sulphur steels. This is shown more clearly in Figure (51) where the cumulative inclusion distribution data is plotted on logarithmic probability paper. On this scale the linear relationship of the inclusion length distributions of the steels again indicates that they obey a log normal distribution. In the 0.003 % sulphur steel 99% of the inclusions were less than 10 µm in size compared with 99% less than 25 µm in size for the 0.017% sulphur steel. Table (9) (P141) listing the thirty largest inclusions measured during the photographic assessment clearly demonstrates the differential inclusion size ranges of these two steels. The large particles vary from 17 to 71 µm for the 0.017% sulphur steel and from 4 to 17 µm for the 0.003% sulphur steel. The greater elongation of inclusions

in the higher sulphur steel is due to a preponderance of manganese sulphide inclusions as indicated by the SEM compositional analysis (Fig.24,P160). The mean aspect ratio of inclusions in the 0.017% sulphur steel was 6.4 compared with a value of 2.0 for the low sulphur steel. A plot of the mean length of the inclusions in the longitudinal direction against mean length in the transverse direction taken from the AMS results confirms these trends. The higher sulphur steel inclusions are much more highly deformed in the direction of rolling.

A further disadvantage in an increase in sulphur from 0.003% to 0.017% is the significant rise in inclusion area fraction, which has approximately quadrupled for the higher sulphur steel. A plot of area fraction against sulphur for allthe steels examined is given in Figure (52) (P187). Whilst the relationship obtained agrees with previous work the effect appears to be more pronounced in this study, particularly for the higher sulphur steels. The area fractions recorded on the AMS image analysis are consistently higher than those reported in previous work and also that which might be predicted theoretically. In Appendix (2) the area fraction of sulphides has been calculated for each steel assuming all the sulphur is converted to manganese sulphide. The volume fraction attributed to oxides has been calculated in two ways, firstly assuming all the oxygen was taken up in the form of alumina and secondly, assuming it to be split evenly between alumina, silica and manganese oxide. Theoretically, it can be predicted that the volume fraction (equivalent to the area fraction) of inclusions in the high sulphur steel should be four times that of the low sulphur steel. This in agreement with the results obtained in

practice which justifies confidence in the predicted trends since the steels are all being compared on an equal basis. Examination of Table 7 (P140) reveals the number of inclusions in the 0.017% sulphur steel is approximately two and a half times that for the 0.003% sulphur steel. The projected length of the inclusions calculated from the product of the number of inclusions per unit area on a longitudinal section and the mean inclusion length in that direction, naturally reflects these differences in the high and low sulphur steels. From Table 7 it can be seen that both the calcium treated steels have increased area fraction of inclusions compared with the low sulphur standard steel. The mean length of inclusions have also increased to 2.41 and 3.05 μm respectively. Considering first the 0.009% sulphur,calcium containing steel, it is important to remember that the calcium /sulphur ratio of 0.21 is less than the minimum recommended by other workers for inclusion modification [69,143]. The mean length of inclusions in the longitudinal direction suggests the inclusions in this steel are only slightly more deformed than those in the standard steel. This is confirmed by the fact that the mean aspect ratio of inclusions measured from the photographic assessment was 1.9 for the 0.009% sulphur steel compared with 2.0 for the standard steel. However, the graph of mean length against sulphur would seem to indicate that the calcium treatment has had little effect (maybe within experimental error). A clearer indication of the effect of the calcium treatment can only be gained by studying the size distribution of inclusions as a whole along with their chemical analysis.

The more important overall inclusion length distributions as shown in

Figures (50) and (51) (Pp 185-186) show the low sulphur calcium treated steel is much closer to the standard steel than the higher sulphur calcium treated steel or the 0.017% sulphur untreated steel. 99% of the inclusions in the 0.009% sulphur calcium containing steel were less than 13 μm compared with 99% less than 10 μm for the standard steel. The SEM compositional analysis for the low sulphur calcium containing steel showed that calcium was a constituent of 66% of the inclusions sampled. 30% were calcium sulphide based which suggests that even at this low level of calcium to sulphur ratio, sulphide modification had occurred resulting in a reduction in stringered inclusion formation.

From Table 7 (P140) there is a distinct increase in the number of inclusions recorded for the two calcium treated steels. The great rise in inclusions may have been due to an increase in oxides and the break up of dendritic oxide inclusions eg. Al_2O_3 in the turbulent stream of the melt during injection without a commensurate elimination at the melt surface. This is substantiated by the inclusion compositions in the 0.009% sulphur steel which showed 36% of the inclusions sampled to be calcium aluminate based. These predominantly round inclusions were noted as a distinctive feature in earlier metallographic observations (Section 4.4). The increase in area fraction of inclusions is in agreement with that predicted theoretically for the total oxide and sulphide inclusions.

The increase in area fraction is even more dramatic for the 0.012% sulphur calcium treated steel. The SEM compositional analysis confirms the existence of a large

number of calcium aluminate inclusions within this sample (Figure 22) (P158). The fact that the calcium would have appeared to react preferentially with oxygen would account for the mixed inclusion grouping present within this steel. This trend is also apparent in the relative plasticity determinations given in Figures (27) and (28) (Pp162-163). Examination of the cumulative length distribution data given in Figures (50) and (51) shows the greatly increased range of inclusion lengths present within this steel compared with those of the 0.009% sulphur, calcium containing steel and that of the 0.003% sulphur, standard steel. Also the inclusion distribution is much closer to that of the 0.017% sulphur steel than those of the lower sulphur steels. 99% of the inclusions were less than 22 μm compared with 99% less than 13 μm for the 0.009% sulphur calcium containing steel and 10 μm for the 0.003% sulphur standard steel.

The beneficial effects of an increased calcium/sulphur ratio, which at 0.38 represents the lower limit for reported inclusion modification, would therefore appear to have been lost due to the higher oxygen content (63 p.p.m.) of the finished steel which has resulted in a marked increase in calcium aluminate inclusions at the expense of calcium sulphides (see Figures 21 and 22). Elongation of unmodified manganese sulphides will account for the larger inclusion size range present within this sample. These results confirm the claims of other workers that to achieve adequate modification for higher sulphur bearing steels the calcium/sulphur ratio should be greater than that used for low sulphur metal and a very low oxygen content is essential.

Magnesium injection was attempted only on the 0.013% sulphur containing melt and produced a magnesium/sulphur ratio of 0.31 in the final steel. However, it can be

seen from the composition of the steels listed in Table 2 that for constant sulphur and comparable calcium/sulphur and magnesium/sulphur ratios, the inclusion parameters of steel 3 and 4 can be fairly compared and contrasted although the oxygen in the latter steel was 35% less at 40 p.p.m. than in the calcium bearing material. The mean length of inclusions in the longitudinal direction as determined by image analysis can be seen to be marginally lower for the magnesium containing steel at 2.80 μm compared with 3.05 μm for the calcium containing steel, but this is not considered to be significant. A greater difference was recorded from the photographic assessment (2.99 μm compared with 3.86μm for the calcium treated steel). Further, the cumulative length distribution data shown in the Figures (50) and (51) highlights a dramatic difference in inclusion size range between the two steels. 99% of the inclusions in the magnesium containing steel were less than 13 μm compared with 99% less than 22 μm for the calcium containing steel. Thus, it is seen that the magnesium treated steel is comparable with the 0.009% sulphur calcium containing steel. Even more dramatic is the size range of the thirty largest inclusions measured during photographic assessment which showed 7.8 to 21.7 μm for the magnesium treated steel and 10.9 to 37.8 μm for the calcium treated steel.

From Table 7 it can be seen that another important difference between the two steels is that the area fraction of inclusions remaining in the magnesium treated steel was significantly lower than that of the calcium containing steel (0.11 compared with 0.19%). This is reflected in the greater number of inclusions present within the calcium treated steel, a trend which was verified by the average number of inclusions per field measured in the photographic assessment. Whilst this confirmed the difference between

the two injected steels it was not as low as that earlier recorded during image analysis. The projected length of the inclusions in the magnesium treated steel is very much lower than that of the calcium treated steel as a consequence of the influence of the inclusion number per unit area on its calculation.

In order to explain the differences in inclusion size ranges between the two steels (the absence of larger sized inclusions in the magnesium treated steel) and the discrepancies in recorded inclusion numbers, it is useful to consider the load bearing capacity of a bubble of magnesium vapour compared with one of calcium as it travels through the melt. With magnesium, for the same weight of powder per unit time injected at the same pressure, the final emerging bubble will be larger because of the magnesium's greater vapour pressure. The larger bubble will be able, therefore, to carry a larger inclusion burden which should make it possible to remove more nonmetallic inclusions using magnesium. Further, magnesium seems to preferentially form oxide rather than sulphide inclusions in this steel. According to the SEM compositional analysis, it enters the inclusion as $MgOAl_2O_3$. Although calcium appears to exist as sulphide and aluminate in the 0.009% sulphur steel, it is preferentially as an oxide former in the higher sulphur containing material similar to the magnesium reaction in the 0.013% sulphur steel. However, there was a marked difference in oxygen content in these latter steels (63 p.p.m. in the calcium bearing steel and 40 p.p.m. in the magnesium steel) and consequently, a higher proportion of calcium would be taken up in the production of oxide leaving a much lower weight available for sulphide formation. In the case of

magnesium the much lower tendency to form sulphide would cause the majority of the injected metal reacting to give oxide. The differences in surface tension between calcium and magnesium oxides/sulphides could be a further contributary factor to their relative rates of removal. However, the turbulence for magnesium is very much greater than for calcium and is likely to far outweigh any slight differences in surface tension.

5.2 Chemical Properties Of Inclusions

To rationalize the SEM analyses of the inclusions they have been recalculated to 100% omitting the (background) iron content, and relisted in Tables (17-21) (Pp148-152). In all subsequent diagrams this data has been plotted against inclusion size and shape. Initially, only inclusions containing 1% minimum sulphur are considered which for steels 2,3,4 and 5 represents over 92% of the total inclusion population but for the 0.003% sulphur standard steel it only represents 48%.

A plot of inclusion size (in the longitudinal direction) against sulphur content is given in Figure 53 for the 0.003% sulphur untreated steel. 88% of the inclusion population (sulphur containing) is less than 5 μm in size. The remaining three large sized inclusions had a sulphur content of approximately 25%. Sulphur appears to be constant with sizes greater than 5μm (only for a sample of three). This trend is repeated for the higher sulphur (0.017%) untreated steel as shown in Figure 57 but is approximately 30% in this example.

Figure 54 gives the plot of sulphur content versus inclusion size for the 0.009% sulphur calcium treated steel. Over 90% of the inclusions are less than 4 μm in size and

their sulphur content is very variable. Again there are a number of higher sulphur containing inclusions but these are predominantly in the small size ranges. The larger sized ones and in particular the 20 μm particle (stringered inclusion) would seem to confirm the trend that large inclusions have a sulphur content which is between 25-30%. However, there are three inclusions with more than 37% sulphur and these may contain calcium sulphide as indicated by the presence of calcium in the analysis (the relationships between manganese, calcium and sulphur will be examined in detail later). It should be noted that 80% of the small inclusions were undeformed despite some containing significant quantities of sulphur. This was due probably to the rotation of small inclusions (1-4μm) during rolling with little or no deformation [151].

Figure 55 depicts sulphur against size for the 0.012% sulphur calcium treated steel. It is possible to split these inclusions into two groups. The first group has a high sulphur content typically above 20%, similar to those found in Figures 53 and 54, whilst the other consists of a concentration of small sized (4μm and less) inclusions with a low sulphur content, typically 2-8%. The large ones have high sulphur contents but there is a greater spread of sulphur levels within the small inclusions.

The plot of size against sulphur content for the 0.013% sulphur magnesium treated steel is given in Figure 56. A mixed overall sulphur distribution is evident. The higher sulphur containing inclusions (20% and above) can be conveniently grouped together and as such show a similar trend to that displayed in the two untreated sulphur steels. The low sulphur group is distinct from that displayed in the two calcium treated steels in that the sulphur level is constant with size at approximately 10%. The large

inclusions are generally high in sulphur, but there are two low sulphur inclusions which are larger than in the other steels.

Figure 57 shows the plot of size versus sulphur content for the 0.017% sulphur untreated steel. A far greater number of large nonmetallic inclusions are present in this sample (25% were greater than 10 μm). The average sulphur content of this group is approximately 30%, although there are some which contain 35% or more. A small isolated group of low sulphur containing inclusions were again present in this steel. Once again it can be seen that large ones are generally rich in sulphur (in this sample those that were over 5 μm in size had a sulphur content between 25 and 35%).

The shape of each nonmetallic inclusion analysed were also noted along with its size. They were categorised simply as either round, slightly deformed, eyeshaped or tailed, or stringered (shapes 1-4 in the diagrams). These characteristics are plotted against sulphur content for each of the steels in Figures 58 through to 62.

Figure 58 for the 0.003% sulphur untreated steel shows that most of the sulphur bearing inclusions are deformed (58% were in the last two shape categories). None of these inclusions were round and will be discussed later. The higher sulphur containing ones were predominantly stringered, 50% of the sulphur containing inclusions were in this category. This is very interesting since there is very little sulphur in the steel.

Figure 59 for the 0.009% sulphur calcium treated steel was in complete contrast to the above. The inclusions present were predominantly round (78% of the population) even when they contained 20-40% sulphur. It would appear that calcium has

had a major effect on the deformation characteristics.

Figure 60 for the 0.012% sulphur steel shows the inclusions were more deformed than those in the 0.009% sulphur steel along with a significant shift to lower sulphur contents.

Figure 61 for the magnesium treated steel shows a much more uniform inclusion deformability. 18% were in the round and slightly deformed categories, and a similar 22% in the eyeshaped or tailed class. However, the greatest number of inclusions (41%) were stringered. This may not be immediately apparent from the diagram but can be confirmed from Table (20) (the apparent error is due to duplication of plotted analyses). This steel is, therefore, distinct from the two calcium treated steels. It contained many more undeformed inclusions than the 0.003% and 0.017% sulphur untreated steels. It should be noted here that Figure 58 may be misleading in that only sulphur bearing inclusions are shown and the 0.003% sulphur steel does contain many more undeformed inclusions than are shown. Therefore, it is very unlikely that the magnesium treated steel had a less deformable population which may be erroneously deduced by comparing Figures 58 and 61.

Figure 62 for the 0.017% sulphur untreated steel shows a skew towards the strongly deformed inclusion type. 82% of the population were stringered, the vast majority of which had high sulphur contents ranging from approximately 23-38%. It is interesting to compare the deformation trends of this sample with that of the 0.013% sulphur magnesium treated steel. 41% of the inclusions were stringered in the latter

compared with 82% for the high sulphur steel. On this evidence it would appear that magnesium could have been beneficial in producing inclusions resistant to deformation. The untreated steels had the greater deformability, calcium definitely reduced this whilst magnesium appeared to be intermediate.

The manganese/sulphur ratio for the inclusions present within the 0.003% sulphur steel are plotted against size in Figure 63. There are no inclusions with a Mn/S ratio below 1.7 and, therefore, it would seem that the sulphur present, even at very low levels, is present as manganese sulphide and it is this which either on its own or in conjunction with other oxides (alumina, manganese oxide etc.), which has caused deformation. Of course, most of the inclusions have Mn/S ratios >1.7 and this will be discussed later. This is most significant in the less than 2 μm sizes where it would be expected that round inclusions would have been obtained due to the 'rotational effect' during rolling [151]. These trends are confirmed in Figure 67 for the 0.017% sulphur untreated steel where it can be seen that all the inclusions have a Mn/S ratio > 1.6. The deformation (from Figure 62) is weighted towards larger sized particles and only 10-15% are slightly deformed. The skew seen in the 0.003% sulphur steel is thus confirmed but is more definitive here.

The Mn/S ratio of the inclusions in the 0.009% sulphur calcium treated steel is shown in Figure 64 and shows manganese sulphide types (20% of the total population) together with a larger grouping of inclusions with reduced Mn/S ratios. Of the manganese sulphide containing inclusions (>1.7 Mn/S ratio), 60% were strongly

deformed , the remaining being generally round. The large number of inclusions (with>1.7 Mn/S) emphasises even more the high Mn/S ratio of all the inclusions (>1.7) in the 0.003% sulphur steel. The reason for the decreased manganese/sulphur ratio of these particles is the presence of calcium where it has replaced the manganese in association with sulphur.

The graph for the Mn/S ratio of the 0.012% sulphur calcium treated steel shown in Figure 65 again shows a wide range of Mn/S containing particles. There is a group containing sulphides with high Mn/S ratios (>1.7) but also a number with a low Mn/S ratio (<0.7). This mixed grouping agrees with the deformation trends displayed in Figure 60, and earlier metallographic observations (4.4). It is important to remember that there were 14 inclusions which did not contain manganese and, therefore, are not shown in Figure 65.

The first thing to note about Figure 66 is that the average Mn/S ratio for the magnesium treated steel was less than that of the untreated sulphur steels (Figures 63 and 67). Nevertheless, it is significantly greater than for the calcium steels suggesting that much of the sulphur is present as manganese sulphide. This will lead to a mixed inclusion deformability and this is shown in Figure 61. Most of the deformed particles (groups 3 and 4) had high Mn/S ratios (see Table 20). The manganese /sulphur ratio is high for all nonmetallic inclusions in the two untreated steels, and has been significantly reduced in both calcium and magnesium treated steels, but the reduction is not as marked for magnesium.

Manganese sulphide should be reduced by calcium and magnesium in these steels (see Appendix 3). However, the evidence from Figures 64 and 65 suggests that calcium has reduced manganese ie. the Mn/S ratio is reduced below 1.6 and even to less than 0.2, but the data shown in Figure 66 (magnesium treated) is much less definitive although many inclusions ($\approx$ 40%) do show a reduction in Mn/S ratio down to 1. This is to be expected from thermodynamic data where calcium is shown to be a very much stronger reductant of manganese sulphide (10^4x) than magnesium and when associated with the kinetics (dynamic problems of calcium and magnesium dissolving in the liquid steel from the rapidly rising bubbles) it is not surprising that magnesium reduction of manganese sulphide is very much less conclusive. Nevertheless, the evidence would certainly seem to indicate that some reduction has occurred even with magnesium.

Calcium content compared with size for the 0.009% sulphur steel is shown in Figure 68. 90% of the calcium containing inclusions (88% of the total population) were less than 4μm in size and their calcium contents were very variable. The inclusions (again 88% of the total population) in the 0.012% sulphur calcium treated steel (Figure 69) show a similar variability, but have only four inclusions with high calcium contents (20% and above) compared with the eleven in the 0.009% sulphur steel. Table (18) and Figures 70 and 71 show that 86% of the calcium containing inclusions in the 0.009% sulphur steel were round compared with 77% in the 0.012% sulphur steel.

Figure 72 shows that the magnesium content of the inclusions in steel 4 is much more evenly distributed with size and it can be seen from Figure 73 that these inclusions

are very evenly distributed within each deformation category with a significant number of stringered ones. Calcium and magnesium containing inclusion deformation characteristics reflect their size distributions.

Figure 74 shows the plot of inclusion aluminium content against size for the 0.003% sulphur steel. There is a wide range of aluminium (alumina) contents portrayed (80% of the population ranging from 20-80% Al) due to the high supersaturation of aluminium in this steel (0.09%) causing many sites to be active for Al_2O_3 nucleation and growth. However, the lower aluminium containing inclusions suggest that the Al_2O_3 particles were also active sites for the subsequent precipitation of manganese sulphide. Figure 75 for the 0.009% sulphur calcium treated steel shows a downward shift in the aluminium content of the inclusion population, over 90% are in the range 2-55%. This is probably due to the higher sulphur content of these inclusions and interactions of calcium with aluminium (discussed later). Figure 76 for the 0.012% sulphur calcium treated steel shows that there is a narrower range of aluminium contents within the inclusions (over 90% in the range 22-58%) and that the overall value is intermediate to that of the 0.009% calcium containing steel and the 0.003% sulphur untreated steel. The graph for the magnesium treated steel (Figure 77) is again distinctive in that the aluminium content is much lower and more evenly dispersed over the size range. The 0.017% sulphur steel (Figure 78) contained very few alumina inclusions (only 14% of the total population). Not surprisingly, they showed a similar trend to those of the 0.012 % sulphur calcium treated steel which was also low in final aluminium

(0.03 compared with 0.01 in the untreated steel) and had a similar oxygen content.

Figure 79 shows the aluminium content against shape for the 0.003% sulphur steel. There is no obvious tendency for the Al_2O_3 rich inclusions to be undeformed although there is a slight preponderance of them in the first two deformable categories. However, it must be remembered that most of the inclusions are less than 4 μm in size and would naturally remain undeformed. The graph for the 0.009% sulphur steel in Figure 80 shows that the lower aluminium content coincides with a marked shift towards the undeformed category (74% of the inclusions were round). A similar trend was displayed for the 0.012% sulphur calcium treated steel as can be seen in Figure 81. 81% of the inclusions were round and as will be shown later were calcium aluminate based. The plot of aluminium content against shape for the 0.013% sulphur magnesium treated steel Figure 82 shows a very even inclusion deformability. It is interesting to note that the trend demonstrated is identical to that for the sulphur content versus shape given in Figure 61. This would have been expected since examination of the inclusion analysis reveals that the magnesium and aluminium were always associated with manganese sulphide based inclusion types. Both the sulphide or oxide phases could influence, therefore, the inclusion deformability. It would be logical to assume that the predominance of manganese sulphide would lead to its overriding influence. This will be shown later not to be completely true and will be further discussed. Figure 83 for the 0.017% sulphur steel shows that the few aluminium inclusions that were present occupied the slightly deformed or eyeshaped/tailed categories. Few conclusions can be

drawn, however, from such a small number of results.

Whilst it is relevent to consider the individual chemical components of an inclusion it is more important to have an understanding of their combined effects if their influence on final material performance is to be predicted. To this end it is useful to review the series of compositional graphs as a whole. This is acceptable for steels 2,3 and 4 where 90, 84 and 76% respectively of the total population contained both aluminium and sulphur, but in steel 1 only 36% contained significant quantities of both elements, whilst in steel 5 the population consisted essentially of manganese sulphide particles.

The sulphide inclusions in steel 2 (0.009% sulphur calcium treated steel) had an average sulphur content of 20% and it can be seen (Figures 54 and 55) that this is considerably higher than the sulphur contents of steel 3 at 10%. Conversely, the aluminium contents of the inclusions in steel 2 were significantly lower than those of steel 3 (an average content of 26% compared with 35%). This is an indication that the inclusions in steel 2 were essentially sulphide rich and they must have been present in the form of manganese or calcium sulphide. If this was manganese sulphide it would make the inclusion deformable and as noted previously in steel 2, 78% of its sulphur bearing inclusions were round even at the higher sulphur contents of between 20 and 40% and only 10% of the sulphides were stringered. In steel 3, 65% of the inclusions were round with 17% being stringered. However, the mean calcium contents of the inclusions was the same for both steels and it is reasonable to assume, therefore, that more sulphur was associated with calcium in steel 2 than in steel 3. Figure 84 gives the

plot of calcium versus sulphur for all Ca/S inclusions analysed in steel 2 which represent 88% of those sampled. A reference line indicating the Ca/S stoichiometric ratio (5:4) has been drawn on this diagram. Whilst it is possible to suggest that a relationship exists between calcium and sulphur (the general trend being for calcium to increase with increasing sulphur) it is not statistically significant. The true relationship may be masked by including particles which, although containing small amounts of calcium and sulphur, were not calcium sulphide based. When those that are manganese sulphide rich (group of five with $\approx$5% calcium and between 25-33% sulphur with an average Mn/S ratio of 1.72) and those with an intermediate composition (Mn/S ratio between 1.0 and 1.5) are removed to leave those with a ratio of Mn/S less than 1, a much stronger relationship can be seen to exist (Figure 85). This graph is indicative that calcium has replaced the manganese in association with the sulphur in a number of inclusions. Finally, those with >10% manganese are omitted in Figure 86 ie. all the remaining inclusions contain significantly greater amounts of calcium than manganese and, as would be anticipated, a good agreement with the stoichiometric ratio exists for these calcium sulphide rich inclusions.

The same trend does not hold for steel 3 as shown in Figure 87, where it can be seen that a large majority of the inclusions are high in calcium but have a very low sulphur content. Figure 88 gives the plot of calcium against sulphur for those inclusions in steel 3 which had a Mn/S ratio less than 0.8, and whose calcium content was significantly greater than that of manganese. Thus, it can be seen that this group show a

similar trend (although not as definitive) to that of the 0.009% sulphur steel (Figure 86) indicating that some of the calcium had been involved in a sulphide reaction. More importantly, reference to Table (19) shows that the majority of inclusions in steel 3 which were rich in calcium and low in sulphur were calcium-aluminium rich, and as shown in Figure 89 a strong relationship exists between these two elements assuming the following interaction occurred

$$3Ca_v + Al_2O_3 = 3CaO + 2Al$$
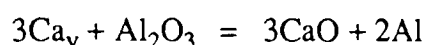
It is interesting to note that, as expected, the opposite is the case for steel 2 as shown in Figure 90 where no relationship between calcium and aluminium is apparent. A plot of magnesium versus sulphur for all magnesium and sulphur bearing inclusions in steel 4 is shown in Figure 91 and there is no obvious relationship. The majority are high in sulphur and low in magnesium. This is not surprising as a greater proportion of these high sulphur inclusions contained high manganese and were probably manganese sulphide based. Possible evidence that magnesium has been involved in a sulphide reaction can be seen in Figure 92 where only those particles that had a significant amount of magnesium present (ie. >10%) are plotted. Figure 93 assumes the reduction of alumina by magnesium according to the following reaction:

$$3Mg_v + Al_2O_3 = 3MgO + 2Al$$
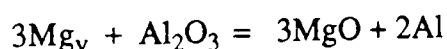
It can be seen that a possible relationship exists but this is not as strong as the oxide relationship shown in Figure 89 for the 0.012% sulphur calcium treated steel.

Finally, Figure 94 shows an overall plot between manganese and sulphur for the

sulphur containing inclusions in all five steels. A good relationship exists between the sulphur and manganese for steels 1,3 and 4 , note the gradient is approximately 1.7 Mn/S. The high sulphur untreated steel was distinct in that an accumulation of inclusions occurred at approximately 60% manganese and between 25 and 40% sulphur (Figure 95). If those inclusions which were high in aluminium are removed it is shown that only the grouped inclusions remain (Figure 96) but with an average Mn/S ratio much greater than 1.7. This can be explained if the manganese were associated with another element of lower atomic weight eg. oxygen. It should be remembered that the aluminium content of this steel was very low (0.01%) and ,consequently, a high oxygen was obtained which would be associated with silicon and/or manganese. It would seem, therefore, that some MnO has been formed. This graph reinforces the concept that to obtain good desulphurisation a low final oxygen in the steel is imperative.

Steel 2 also seems to be an exception to the other steels in that it shows a lower Mn/S ratio in the inclusions. This has been explained in Figures 85 and 86 where a relationship between calcium and sulphur was proven.

A further complicating factor in the calcium-manganese-sulphur interaction is the presence of differing oxygen contents before calcium injection ie. it was controlled by deoxidation by Al-Si-Mn. In steel 2 the aluminum content was 0.1% with a final overall oxygen content of 49 p.p.m., whilst in steel 3 63 p.p.m. oxygen was associated with 0.03% aluminium. During the injection of the calcium alloy, it is suggested that steel 3 required a significant quantity of calcium to reduce the oxygen to achieve the same

starting level as that in steel 2 with 0.1% aluminium present. Consequently, the remaining calcium for sulphide formation would be considerably reduced and, therefore, in steel 2 a high proportion of calcium sulphide was found compared with calcium aluminates, whereas in steel 3 the reverse was true. Further, a lower calcium/sulphur ratio was used in steel 2 (below the minimum recommended for inclusion modification) but it would seem that when the oxygen is low enough calcium can be very effective as a modifier in pipeline steels. However, too much aluminium detracts from the castability of the steel and thus higher calcium/sulphur ratios are recommended to control the oxygen and the sulphur.

It has been shown earlier (Section 2.6) that the effectiveness of any inclusion modification treatment or steelmaking practice can only be established by relating the residual nonmetallic inclusion behaviour during processing and fabrication to the final material properties of the steel. This has led to a number of studies on the deformability of the more common inclusion types, eg. sulphides, oxides, silicates etc. Those of particular relevance relate the deformation behaviour of the inclusion to that of its surrounding matrix using a relative plasticity index. The extent of the deformation of the inclusion in its matrix can be estimated by comparing the inclusion strain with matrix strain. The former is normally found by measuring the aspect ratio of individual inclusions. A criticism that could be levelled at relative plasticity studies is that they are time consuming and can be subject to operator bias. In order to try to limit this in this work, a large number of inclusions (over 350 per sample) were selected at random over a wide range of fields. It is felt that, as indicated by the earlier comparisons of mean

length measurements from image analysis and photographic assessment (Section 4.4), this number is large enough to allow a relevant comparison between each of the steels. On the other hand the advantage of conducting individual inspections of a large number of inclusions per sample is that it can provide an indication of the likely genesis and inherent characteristics of the general inclusion population eg. whether the particles are essentially stringered or there has been a tendency to form duplex inclusions etc.

Relative plasticity is known to be affected by a number of variables such as the temperature of working, degree of deformation, matrix constraint and inclusion size and composition [152-154]. In this study steels 3,4 and 5 were isothermally rolled for a total reduction of 88% at 800,1000 and 1200^0C, and the relative plasticity index of each inclusion was determined (in the longitudinal direction). Figures 27-35 show how the plot of relative plasticity is influenced by size. The square root of the deformed particle major and minor axes was taken as a measure of the original inclusion size. It must be remembered that these indexes represent all types, no discrimination was made between sulphides or oxides etc.

The plotting of relative plasticity index versus $\sqrt{ab}$ results in a series of curves dependent upon the magnitude of the major and minor axes. This occurs because both terms contain both 'a' and 'b'. It is reasonable to expect that a family of curves would be obtained since it is inevitable that a number of inclusions with the same major and minor axes would be encountered. The general deformation trend exhibited in each of the steels was one of increasing deformability with size. This was especially pronounced for the

high sulphur untreated steel (Figures 33-35). This is in agreement with the findings of a number of workers [153,155-157] who found a variation of inclusion plasticity with size.

Considering first the inclusion deformation behaviour for the 0.017% sulphur untreated steel rolled at 800, 1000 and 1200^{0}C (Figures 33-35), it can be seen that there is a rapid increase in relative plasticity with size up to approximately 6 μm. This is particularly pronounced at the lower rolling temperature of 800^{0}C, where even the smallest inclusions (<3μm) exhibit a degree of deformability. A marked decrease in mean relative plasticity is evident with increasing rolling temperature. This was to be expected since the SEM analysis for this steel showed the predominant inclusion type to be manganese sulphide. These results confirm that manganese sulphide becomes progressively more deformable at lower temperatures [113,152] and are also in agreement with those reported by Maunder and Charles [113] during relative plasticity studies of manganese sulphide inclusions (see Figure 97).

The results for the 0.012% sulphur calcium treated steel showed that the inclusions appeared to separate into two groups a) small essentially undeformed inclusions and b) larger deformed particles. This latter group showed a sharp increase in relative plasticity with size similar to those of the high sulphur untreated steel. Their relative plasticity index also appeared to decrease with increasing rolling temperature suggesting this group was again mainly manganese sulphide based. Initial metallographic examination of this steel revealed a preponderance of round inclusions. SEM analysis (Figure 22) subsequently showed that 94% of the analysed round

inclusionswere calcium aluminate based. It was assumed, therefore, that the undeformed inclusion grouping was made up of these inclusions. Further, the distinction between the two inclusion groupings was not as marked in the sample rollled at 1200°C. These results confirm the earlier postulation that a significant quantity of the injected calcium preferentially reacted with oxygen to leave a high proportion of calcium aluminates and reduce the amount of calcium available for manganese sulphide modification.

The relative plasticity data for the 0.013% sulphur magnesium treated steel shows a more mixed inclusion deformability. An increasing deformability with size is once again evident as is a decrease in mean relative plasticity with increasing rolling temperature. Although the SEM analysis revealed the majority of inclusions to be rich in manganese and sulphur, Figures 30-32 display a deformability which is quite distinct from that of the high sulphur untreated steel (see Figure 33-35). A large number of inclusions occupy a range of low relative plasticity indices. This apparent change in deformability can be explained in one of two ways. Firstly, by the removal of the larger more deformable nonmetallic inclusions due to the increased load bearing capacity of the magnesium bubbles, or secondly, if as a result of the presence of MgO and Al_2O_3 (which were found to be present in over 70% of the inclusions analysed) the deformability of manganese sulphide is reduced.

The deformation behaviour of the controlled rolled steels calculated from the photographic data appears to be slightly contradictory. The 0.012% sulphur calcium treated steel (Figure 39) does not look significantly different to that of the 0.017%

sulphur steel (Figure 41), both exhibiting a sharp increase in deformability with size up to approximately 5 μm and the same number of inclusions per unit area (Table 15). Whilst the deformation of inclusions within the calcium treated steel does not break down into two distinct groups as was the case following isothermal rolling, it can be noted that there are significantly more inclusions which have remained relatively undeformed ($\upsilon < 0.25$) compared with those of the higher sulphur steel. This is reflected in the mean relative plasticity index as shown in Figure 42. The deformation characteristics of the inclusions in the magnesium treated steel are again intermediate to those of steel 3 and steel 5 with the steel again showing a mixed inclusion deformability. Further, it can be noted that this steel in contrast to steel 3 and 5 contained very few inclusions with a relative plasticity greater than 1, but at the same time contained significantly more at $\upsilon < 0.25$, resulting in a lower mean relative plasticity index (Figure 42). This would again suggest that either the larger inclusions have been removed from this sample or the deformability of the general inclusion population has been reduced by the treatment with magnesium.

Figures 37 and 38 show the deformation characteristics of the inclusions within the 0.003% sulphur and 0.009% sulphur calcium treated steel, respectively. Steel 1 shows an overall increasing deformability with size up to approximately 4 μm, but it can be noted that a large number of inclusions have a low relative plasticity index ($\upsilon <$ 0.25). The earlier SEM analysis suggested that the larger inclusions were manganese sulphide rich whilst the smaller ones were aluminium rich (Al_2O_3). It must be remembered that the plasticity of the inclusions and the matrix will alter over the rolling

temperature range. The inclusion behaviour is, therefore, likely to be a summation of that evidenced in the isothermal studies. The lower inclusion deformability range must therefore consist of manganese sulphides which are relatively less plastic at higher rolling temperatures and oxide inclusions which are relatively more plastic with respect to the matrix. It can be seen that (Figure 39) whilst the 0.009% sulphur steel contains a greater number of inclusions displaying increasing deformability with size the preponderence of inclusions have a relative plasticity < 0.2.

5.3 The Toughness And Chemical Properties Of The Final Steel Product.

One of the causes of anisotropy in wrought steel products is the presence of deformed inclusions within the alloy structure [120,155]. In this section it is aimed to relate the properties of inclusions discussed in section 5.1 with toughness, as measured by the Charpy Impact test. Toughness is a major property requirement of international specifications especially for linepipe steels, even though the energy absorbtion values cannot be directly related to structural design parameters. The required energy absorbtion value is selected on the basis of practical experience. Transition temperature studies have been favoured for material selection and quality control of linepipe steels because of their relative simplicity, low cost, and small specimen size.

Figures 25 and 26 show the Ductile Brittle Transition Temperature (DBTT) curves for each of the five steels over the temperature range $+80^0C$ to -196^0C. The Upper Shelf Energies (USE), transition temperatures, and anisotropy ratios are listed in Table 15. The upper shelf energy in the transverse and through thickness directions is

known to be affected by second phase particles [120,122,144-146] and the deleterious effect

of elongated manganese sulphides has been well established. Toughness is dependent on

both the content and shape of inclusions. Figures 25 and 26 show that the USE

increases with decreasing sulphur content for the untreated steels. A more important

disadvantage is the reduction in USE values obtained when the direction of testing is

changed from longitudinal to transverse for the 0.003 and 0.017% sulphur steels (40%

and 65% respectively). Further, there is an increase in the anisotropic ratio from 1.25 to

over 2.0. It should be noted that even at 0.003% sulphur the USE is dependent on the

orientation of the test specimen which is in agreement with the earlier work of

Paxton[156].

Since the benefits of inclusion shape modification treatments are more clearly

reflected in improvements in transverse properties, the transverse upper shelf energy

(TUSE) of the five steels have been correlated with the relevant inclusion parameters.

Figures 98 and 99 plot the TUSE against total oxygen and sulphur. These values can be

taken to be related to the number or volume fraction of inclusions present within each

steel (as shown in Figure 52). In these diagrams a straight line has been drawn for

reference purposes only between the two USE values for the untreated steels. From

Figure 98 it can be seen that steel 2 (0.009%S) appears to have a high USE for its total

oxygen content. Oxygen cannot, therefore, be predominant in this case. It is suggested

that the modification of sulphides with calcium as proven in section 5.2 has led to the

improvements in TUSE and are not relatable on this graph. Comparison of the two steels

with similar sulphur contents (steels 3 and 4) show steel 3 to have a significantly poorer upper shelf energy as a result of the increased level of oxygen. Figure 99 reemphasises these observations. The marked decrease in properties between the 0.017% sulphur and the 0.003% sulphur steel is due to a significant rise in inclusion area fraction (approximately quadrupled) and an increase in the mean inclusion length (from 1.9μm to 4.2μm). Figures 100 and 101 show the relationship between TUSE and area fraction and TUSE and mean length respectively. It can be seen that the toughness relationship is particularly strong for the inclusion mean length parameter. Returning to Figure 99, the 0.012% sulphur steel has a lower TUSE than would be expected from the comparison with the two untreated steels. This decrease in toughness is as a result of the increased number of oxide inclusions introduced into this steel during injection treatment (remembering the final oxygen is 0.0063%). This fact is again reflected in the correlation with inclusion lengths (Figure 101). Steel 3 is distinct in that it has a lower shelf energy than would have been predicted for its mean inclusion size. It can be suggested, therefore, that this is due to the production of undeformable oxide inclusions (calcium aluminates) during injection.

Figure 99 indicates that the 0.009% sulphur "Ca" steel and the 0.013% sulphur "Mg" steel have slightly higher shelf energies than would have been anticipated from the results of the untreated steel standards. This again suggests that sulphide modification has resulted in an improvement in toughness.

From the results listed in Table 15 and shown in Figures 25 and 26 it can be seen that the 0.009% sulphur steel with as little as 0.0019% calcium has a USE approximately 90% of the 0.003% sulphur standard steel. In contrast to this the USE's of the 0.012% sulphur steel with 0.0046% calcium were reduced by 62% in the longitudinal direction and 47% in the transverse directions compared with the standard steel. These results confirm the claims by other workers that to achieve adequate modification of higher sulphur steels the calcium/sulphur ratio should be greater than that used for lower sulphur metal. In the latter steel an anisotropic ratio of 1.29 was obtained which compares favourably with that of the standard steel, but for the 0.012% sulphur material this ratio was 1.65.

Magnesium injection was attempted only on a 0.013% sulphur containing melt using a magnesium/sulphur ratio of 0.31. The USE was approximately 80% of the standard steel (longitudinal 88% and transverse 78%) with an anisotropic ratio of 1.32 compared with 1.25. These results may be compared with those of Spitzig et al [148-150] on a similar linepipe type steel using a 0.004% sulphur steel standard and a 0.013% sulphur steel treated with rare earths to give a ratio of 2.5 RE:1 sulphur. In that work, the toughness values were 84% of the standard steel values. It is also interesting to note that his 0.004% sulphur steel was reported to be isotropic in contrast to this and earlier work where even at low sulphurs, test orientation was found to be important [120,156,157]. Further, Spitzig's TUSE of a 0.013% sulphur untreated steel was found to be 57% of that of the 0.004% sulphur steel standard. Recent work by Saxena [90,91] on magnesium injection of production scale melts also confirms that magnesium injection has a

beneficial effect on impact properties. From Table 15 the area fraction of inclusions remaining in the magnesium injected steel was only double that of the 0.003% sulphur standard steel compared with a very much higher area fraction of inclusions in the 0.012% sulphur (calcium containing) steel. Therefore, it would appear that the higher vapour pressure of magnesium compared with that of calcium at 1600^0C was instrumental in removing most of the extra inclusions produced by magnesium deoxidation and the break up of dendritic inclusions.

Comparing the data for calcium and magnesium injected steels of similar sulphur contents, the USE values were increased by 34% in the longitudinal direction and 67% in the transverse in favour of the magnesium treatment. This appeared to have been achieved by the significant decrease in area fraction in the magnesium containing steel. Also the remaining inclusions would seem to have been modified to a greater extent than with the calcium treatment.

In section 5.1 the disproportionate effect of large inclusions on ductile fracture was considered. For this reason the inclusion length distributions were assessed quantitatively using a method proposed by DeArdo, Ratz and Wilson [147]. The 95% length probability for each of the steels is plotted against TUSE in Figure 102. A reasonable relationship holds for these thirty largest inclusions where it can be seen in steel 5, for example, that 95% of the inclusions were less than 42 μm compared with 95% less than 15 μm for steel 1. An even stronger relationship exists when the cumulative length distributions for all 600 inclusions measured during the photographic

assessment are plotted against TUSE (Figure 103). This toughness ranking bears out the comments made earlier that it is the large inclusions (in a critical location) which controls the final toughness of a steel. Thus, it is suggested that this may form the basis of a quality control test of use to the steelmaker.

Each of the five steels can also be ranked on the basis of their susceptibility to hydrogen induced cracking as determined by the NACE test (see Table 22). It is interesting to note that the order of ranking is exactly the same as that predicted by inclusion assessment and Charpy toughness testing. The mean crack length ratio (CLR), crack thickness ratio (CTR) and crack sensitivity ratio (CSR) increase with increasing sulphur content which is in agreement with the findings of a number of workers [130,131,137,158]. However, in this work the magnesium containing steel appeared to be an exception. It is quite significant that no cracking was observed in the 0.003% sulphur steel which is in agreement with similar studies [159,160] and the recommendation that sulphur should be lowered to below 0.005% in steels for sour gas service [131]. In contrast to this, the performance of the 0.017% sulphur steel (noting in particular the CLR which is representative of the amount of cracking in the rolling plane) was very much worse. It can be suggested that this was due to the preponderance of elongated manganese sulphide inclusions present within this steel, one of which is shown in Figure (105) associated with HIC. This would support the widely accepted view that inclusions with sharp edges, and large surfaces act as preferential sites for the initiation of hydrogen induced cracking [158,161,162]. The slight improvement in

the HIC resistance of the magnesium treated steel (mean CSR 1.6) as compared with that of the similar sulphur calcium containing steel (mean CSR 2.0) could also be attributed, therefore, to its reduced inclusion area fraction and mean inclusion length.

It is quite widely considered that the addition of small amounts of nickel (0.26%) and copper (0.35%) to a steel can markedly improve its HIC resistance, particularly in BPtest solutions. From the limited amount of results presented here it would appear that the presence of these elements does not guarantee HIC resistance in the more agressive environment of the NACE test solution.

6 CONCLUSIONS.

1. Increasing sulphur decreases the toughness and HIC resistance of steel.

2. In untreated steels containing as little as 0.003% sulphur, test orientation does influence final toughness properties.

3. Modification of sulphur bearing steels can be achieved with low modifying element to sulphur ratios provided that the oxygen content is kept very low.

4. Injection of calcium into steel causes interaction with oxide and sulphide inclusions which is biased toward oxide reduction relative to sulphur removal.

5. Magnesium again reduces oxides and appears to be linked with alumina containing inclusions in the final product. Its interaction with sulphur is debatable in this work.

6. Inclusion size is decreased most notably by magnesium which has been related to its increased bubble size and load carrying capacity.

7. Magnesium produces improved toughness values relative to the similar sulphur calcium containing steel. This was due to the improved shape control of the residual non-metallic inclusions.

8. Calcium and magnesium changed the relative deformability characteristics of the inclusions due to modification of the sulphides and oxides.

9. The crack length ratio (CLR), crack thickness ratio (CTR) and crack sensitivity ratio (CSR) of the steel increases with increasing sulphur.

10. Even with the recommended levels of copper and nickel within the steel HIC is not totally eliminated in NACE solution.

7. SUGGESTIONS FOR FURTHER WORK

The results of this work should be extended to establish the mechanism of inclusion modification with magnesium additions to sulphur bearing steels. A series of unalloyed steels should be produced with a range of Mg/S ratio's in the final steel. A comparison with calcium treated steels of similar sulphur level and injectant /sulphur ratio's is required also. It is important to control critically the final oxygen and sulphur of these steels and this would be best achieved by vacuum melting. An in depth metallurgical study should follow in order to assess the performance and commercial viability of magnesium versus calcium ie. any improvements in assessed cleanness values and/or inclusion compositional modification must be reflected in significant material property improvements with economic advantages. To this end a more extensive range of mechanical testing in different test orientations (longitudinal, transverse, and through thickness) need to be undertaken. Large scale trials could then follow in order to establish the industrial reproducibility of these results.

Table1 : CHARGE COMPOSITIONAL ANALYSIS

		C	Mn	Si	S	Al	Nb	V	Ca	Mg
A.	BRITISH STEEL X52 SCRAP	0.07	1.36	0.29	0.002	0.04	0.04	0.004	0.0028	---
B.	MILD STEEL SCRAP	0.06	0.39	0.05	0.018	0.001	---	---	0.0002	---
C.	ARMCO IRON	0.01	0.17	0.03	0.010	0.02	0.001	---	0.0004	0.0002

TABLE 2 : INGOT STEEL ANALYSIS

STEEL	C	Mn	Si	S	Al	Cu	Ni	Nb	Ca	Mg	O
1	0.10	1.20	0.23	0.003	0.09	0.34	0.26	0.04	0.0005	---	0.0021
2	0.10	1.22	0.27	0.009	0.10	0.35	0.27	0.04	0.0019	---	0.0049
3	0.11	1.32	0.30	0.012	0.03	0.32	0.28	0.04	0.0046	0.0002	0.0063
4	0.09	1.26	0.31	0.013	0.06	0.34	0.26	0.04	0.0007	0.0040	0.0040
5	0.10	1.36	0.27	0.017	0.01	0.35	0.25	0.05	0.0004	0.0003	0.0056

TABLE 3. HIC TEST CONDITIONS.

NACE TEST CONDITIONS FOR HIC TESTING.	
Solution	5% NaCl $sol^{\underline{n}}$
H_2S Concentration (p.p.m.)	134 000
H_2S flow rate after saturation	17/min/litre.
Initial pH of solution	2.40
Final pH of solution	3.20
pH controlling agent	CH_3COOH (0.5%)
Specific volume (cc/cm)	7.0
Loading stress	none
Temperature (^{o}C)	16-18 ^{o}C
Duration (hours)	96

TABLE 4 : AS-CAST INCLUSION ASSESSMENT FOR STEEL 3.

SIZE RANGE (MICRONS)	COUNT	CUMULATIVE COUNT %	VOLUME %
0.0 - 2.0	966	47.9	2.3
2.0 - 4.0	1002	97.6	64.6
4.0 - 6.0	38	99.5	11.3
6.0 - 8.0	5	99.7	4.1
8.0 - 10.0	1	0	1.7
10.0 - 12.0	5	99.9	15.9
12.0 - 14.0	0	0	0

TABLE 5 : AS-CAST INCLUSION ASSESSMENT FOR STEEL 4

SIZE RANGE (MICRONS)	COUNT	CUMULATIVE COUNT %	VOLUME %
0.0 - 2.0	985	49.1	2.6
2.0 - 4.0	962	97.1	67.6
4.0 - 6.0	45	99.3	14.6
6.0 - 8.0	11	99.8	9.8
8.0 - 10.0	1	0	1.9
10.0 - 12.0	1	0	3.5
12.0 - 14.0	0	0	0

TABLE 6 : AS-CAST INCLUSION ASSESSMENT FOR STEEL 5

SIZE RANGE (MICRONS)	COUNT	CUMULATIVE COUNT %	VOLUME %
0.0 - 2.0	742	36.4	1.3
2.0 - 4.0	1170	93.9	55.8
4.0 - 6.0	100	98.8	22.1
6.0 - 8.0	18	99.7	10.9
8.0 - 10.0	4	99.9	5.2
10.0 - 12.0	2	100	4.7
12.0 - 14.0	0	0	0

Table 7 : FIELD AREA IMAGE ANALYSIS DATA

STEEL	PLANE OF EXAMINATION	AREA FRACTION %	MEAN LENGTH μ m	PROJECTED LENGTH cm/cm^2	MEAN NEAREST NEIGHBOUR DISTANCE μ m
1	L-S	0.046	1.88	3.39	37.3
	T-S	0.056	1.87		35.1
2	L-S	0.125	2.41	7.32	28.7
	T-S	0.150	1.88		24.4
3	L-S	0.199	3.05	10.88	26.5
	T-S	0.183	2.17		22.5
4	L-S	0.102	2.80	6.01	34.1
	T-S	0.109	2.48		31.3
5	L-S	0.227	4.23	14.58	26.9
	T-S	0.191	2.50		22.5

TABLE 8 : COMPARISON OF FIELD AREA IMAGE ANALYSIS WITH PHOTOGRAPHIC ANALYSIS DATA.

STEEL NUMBER	IMAGE ANALYSIS DATA		PHOTOGRAPHIC ANALYSIS DATA		
	MEAN LENGTH (MICRONS)	AVERAGE NUMBER OF INCLUSIONS PER FIELD	MEAN LENGTH (MICRONS)	AVERAGE NUMBER OF INCLUSIONS PER FIELD	LARGEST INCLUSION MEASURED (MICRONS)
1	1.88	7	1.65	8	17.39
2	2.41	12	2.47	12	24.35
3	3.05	14	3.86	15	37.83
4	2.80	9	2.99	12	21.74
5	4.23	14	4.82	13	71.74

LENGTHS OF THIRTY LARGEST INCLUSIONS (MICRONS)				
STEEL 1	STEEL 2	STEEL 3	STEEL 4	STEEL 5
4.3	8.9	10.8	7.8	16.7
4.3	9.3	11.3	8.2	17.3
4.8	9.3	11.9	8.2	17.3
5.2	9.3	12.3	8.4	17.3
5.2	9.5	13.0	8.6	17.3
5.4	9.7	13.0	8.6	17.3
5.4	9.7	13.0	8.6	17.3
5.4	10.0	13.6	8.6	17.3
5.7	10.2	14.1	8.6	17.3
5.9	10.4	14.1	8.6	17.8
5.9	10.8	15.2	8.6	17.8
5.9	11.3	15.2	8.6	18.4
6.5	11.5	17.3	9.1	18.6
7.6	11.7	17.3	9.3	19.5
7.6	11.7	17.8	9.3	19.5
7.6	11.9	18.4	9.5	20.2
7.6	12.3	18.4	9.7	21.0
7.8	12.6	19.5	10.2	21.3
8.3	12.6	19.5	10.2	21.7
8.7	13.0	19.5	10.6	21.7
9.3	13.0	20.2	10.8	23.9
9.8	13.0	20.6	11.9	23.9
9.8	13.4	21.0	11.9	25.0
10.9	13.6	21.7	12.3	26.0
10.9	13.9	22.8	12.6	27.1
12.0	15.6	23.9	12.6	28.6
12.0	15.6	26.0	14.5	29.3
13.9	19.5	32.1	18.0	41.3
17.0	21.7	34.7	20.0	43.4
17.4	24.3	37.8	21.7	71.7

TABLE 10 : SEM COMPOSITIONAL ANALYSIS OF INCLUSIONS IN STEEL 1

NMI STEEL1	SIZE μm	O	FE	Mn	S	Si	Al	Mg	Ca
P434	2	25.6	38.1	1.9	0.6	0.0	33.3	0.1	0.0
P435	2	31.6	29.9	0.4	0.0	0.1	37.4	0.2	0.3
P436	1	19.4	55.4	3.1	0.7	0.1	19.9	0.4	0.1
P437	1	49.6	21.5	0.4	0.1	0.2	27.9	0.2	0.0
P438	6	5.3	43.7	33.6	14.7	0.3	1.7	0.0	0.0
P440	3	40.0	31.5	0.4	0.0	0.2	27.3	0.1	0.1
P441	16	6.1	43.1	33.1	14.9	0.2	0.0	0.2	0.0
P442	1	36.9	33.8	2.9	1.0	0.1	19.1	0.0	0.4
P443	2	1.2	64.7	17.5	9.0	0.2	4.7	0.1	0.0
P445	1	3.1	73.8	0.9	0.0	0.3	21.2	0.1	0.0
P447	2	3.4	65.4	2.8	0.7	0.3	24.7	0.1	0.1
P448	2	7.8	61.9	15.4	8.1	0.2	1.8	0.0	0.0
P449	1	11.6	70.3	2.9	1.2	0.1	12.8	0.0	0.0
P450	1	9.3	59.8	11.4	6.3	0.2	10.4	0.2	0.2
P453	8	24.2	16.2	0.1	0.1	59.0	0.2	0.1	0.0
P454	2	8.4	50.3	6.3	3.0	0.1	30.8	0.0	0.4
P455	3	16.5	66.4	0.8	0.0	0.2	15.4	0.0	0.0
P456	2	48.6	22.3	0.3	0.1	0.0	27.9	0.0	0.3
P458	5	6.4	62.3	1.3	0.2	0.2	28.9	0.1	0.1
P461	1.5	7.2	65.6	0.7	0.2	0.1	25.7	0.2	0.0
P462	1	0.7	71.6	13.1	7.1	0.1	5.2	0.2	0.1
P463	2	20.6	61.5	0.8	0.1	0.1	16.2	0.2	0.0
P464	4	22.4	51.0	5.0	1.9	0.0	17.4	0.1	1.5
P465	1	12.3	68.8	0.6	0.0	0.1	17.8	0.1	0.1
P468	1	20.4	48.8	3.1	1.4	0.1	24.5	0.3	0.0
P469	3	2.0	53.0	25.1	14.1	0.3	0.3	0.0	0.1
P470	2	0.4	75.3	13.2	7.7	0.3	0.4	0.0	0.1
P471	1	20.5	50.5	4.1	2.2	0.1	21.9	0.0	0.0
P472	2	4.2	69.5	0.9	0.0	0.1	24.7	0.1	0.0
P475	2	1.5	67.2	2.7	1.3	0.1	29.9	0.1	0.0
P476	4	2.7	62.7	18.4	10.5	0.4	3.9	0.1	0.1
P478	2	51.4	17.9	2.2	0.5	0.0	27.7	0.1	0.0
P479	4	4.2	67.1	19.4	10.3	0.3	0.1	0.0	0.1
P480	1	10.3	65.3	1.1	0.2	0.2	22.1	0.0	0.1
P481	2	11.6	48.7	1.2	0.4	0.1	37.0	0.1	0.3
P482	1	18.5	53.9	0.6	0.0	0.2	26.1	0.0	0.0
P484	1	34.2	45.2	0.6	0.1	0.2	18.8	0.1	0.2
P485	2	16.0	59.9	0.8	0.0	0.1	22.8	0.0	0.0
P490	2	17.7	50.0	0.9	0.2	0.2	29.8	0.7	0.0
P491	1	38.8	33.0	1.0	0.2	0.1	26.3	0.3	0.2
P492	1	20.3	43.5	2.5	1.1	0.1	32.1	0.1	0.0
P498	1.5	32.6	43.0	1.2	0.5	0.1	21.5	0.1	0.1
P499	1	9.5	65.7	1.0	0.1	0.2	22.7	0.2	0.1
P500	3	10.9	58.0	5.7	2.2	0.0	20.3	0.1	1.7
P501	2	4.1	78.6	13.8	8.1	0.3	0.4	0.0	0.1
P502	2	13.4	65.2	0.6	0.1	0.1	20.1	0.0	0.0
P503	1	28.8	35.1	10.1	2.7	0.0	22.2	0.0	0.0
P504	1	4.7	72.0	2.6	1.1	0.3	18.6	0.1	0.2
P505	10.0	4.1	54.5	27.7	11.7	0.2	0.0	0.0	0.0
P506	1	36.0	34.2	3.0	1.0	0.1	19.3	0.0	0.4

TABLE 11 : SEM COMPOSITIONAL ANALYSIS OF INCLUSIONS IN STEEL 2

NMI STEEL2	SIZE μm	O	FE	Mn	S	Si	Al	Mg	Ca
K366	2	3.0	46.8	8.7	11.1	0.3	25.0	0.3	10.3
K367	1	9.6	66.4	7.4	8.7	0.4	19.2	0.3	6.4
K368	2	2.4	58.1	11.3	16.7	0.1	2.0	0.1	13.1
K369	1	1.7	59.5	10.1	8.6	0.2	14.1	0.3	4.5
K370	1.5	2.4	76.1	11.9	6.5	0.2	4.3	0.0	1.9
K372	2	13.1	31.4	8.3	9.2	0.2	25.1	0.4	11.7
K373	20	0.7	84.3	7.4	4.7	0.5	0.0	0.0	0.1
K374	2	3.6	48.5	14.2	13.2	0.2	11.3	0.1	7.4
K376	5	7.1	9.0	47.4	26.9	0.1	2.9	0.0	5.8
K377	8	2.7	85.5	9.8	5.7	0.3	0.0	0.1	0.1
K378	2	4.1	46.9	10.2	12.8	0.2	15.5	0.2	9.1
K381	2	39.1	14.6	2.5	3.2	0.3	31.3	0.2	8.6
K382	1	0.2	77.8	6.9	6.3	0.3	3.9	0.1	3.3
K383	2	6.2	40.7	10.8	15.3	0.3	11.3	0.0	14.5
K384	7	11.5	26.1	38.2	18.3	0.2	4.1	0.1	0.6
K385	2	0.9	64.2	10.8	13.8	0.2	0.2	0.3	9.2
K387	2	11.0	26.5	8.0	19.3	0.2	11.2	0.0	23.1
K388	1	10.8	55.5	10.1	5.7	0.2	14.1	0.2	2.9
K389	2	9.2	54.1	1.8	4.4	0.2	22.8	0.0	6.5
K391	1.5	9.0	64.3	2.8	2.1	0.4	19.1	0.2	1.2
K392	2	2.2	62.1	3.7	12.8	0.3	3.5	0.2	14.4
K394	2	27.0	32.8	1.1	4.2	0.2	24.5	0.2	10.0
K395	3	22.8	21.3	2.2	10.6	0.2	26.4	0.1	15.3
K396	2	19.1	39.0	2.9	5.0	0.2	24.9	0.2	8.4
K398	1.5	11.9	59.2	6.1	8.8	0.1	4.8	0.1	7.8
K399	4	5.1	42.5	32.4	17.5	0.1	0.0	0.1	0.4
K400	1	1.4	81.0	6.3	3.4	0.3	3.5	0.1	0.6
K403	4	2.0	24.8	31.3	20.8	0.2	15.7	0.1	4.5
K404	3	21.3	26.6	1.4	8.7	0.1	21.7	0.0	19.6
K405	2	36.8	24.1	0.5	1.1	0.1	25.8	0.1	11.3
K406	2	47.4	13.7	0.4	3.4	0.2	19.4	0.3	15.1
K409	1	1.3	41.2	19.8	16.6	0.3	10.3	0.3	9.8
K410	1.5	8.1	37.0	26.1	17.7	0.1	0.7	0.2	9.6
K411	2	8.1	34.2	21.1	18.1	0.1	6.0	0.1	11.8
K412	2	1.9	22.5	44.9	26.0	0.2	1.5	0.0	2.2
K414	2	23.3	40.2	1.1	1.0	0.3	30.4	0.2	3.1
K415	1	13.6	48.7	4.8	8.0	0.2	14.6	0.3	9.0
K416	1	18.2	37.6	9.8	15.2	0.2	2.7	0.0	16.0
K418	1	14.5	50.7	3.6	5.6	0.3	17.4	0.4	6.4
K419	1	9.6	57.3	8.2	8.0	0.2	9.5	0.3	5.8
K421	3	34.6	8.8	5.6	12.0	0.1	21.2	0.2	16.9
K422	2	18.2	46.1	1.5	2.0	0.2	28.4	0.2	2.6
K423	3	25.9	10.3	5.0	14.8	0.1	23.9	0.3	19.5
K424	5	4.5	26.1	41.3	22.2	0.1	4.0	0.2	0.7
K426	3	12.9	33.3	7.5	11.5	0.2	20.1	0.1	13.9
K427	3	31.7	20.9	3.6	12.8	0.1	14.3	0.1	15.8
K428	3	12.9	36.6	5.0	10.8	0.2	21.0	0.2	12.9
K429	1	4.0	50.2	22.9	12.6	0.2	6.5	0.0	2.3
K430	2	19.2	35.6	1.8	5.9	0.4	27.3	0.0	9.1
K432	2	20.9	31.6	12.0	14.2	0.3	8.8	0.0	11.4

TABLE 12 : SEM COMPOSITIONAL ANALYSIS OF INCLUSIONS IN STEEL 3.

NMI STEEL3	SIZE μm	O	FE	Mn	S	Si	Al	Mg	Ca
L170	2	38.5	10.2	1.4	2.8	1.1	29.1	0.2	16.5
L177	2	28.5	27.0	14.8	11.0	0.2	11.0	0.2	6.9
L178	2	22.7	39.7	5.5	3.5	0.3	22.8	0.0	5.4
L179	2	31.8	27.7	5.4	3.8	0.3	23.6	0.3	6.9
L180	1	37.3	24.6	9.5	6.3	0.4	14.8	0.0	7.0
L183	2	15.1	35.0	1.5	3.8	0.8	32.0	0.4	11.2
L184	3	30.9	16.7	1.3	2.5	1.0	31.5	0.1	15.7
L185	2	26.4	22.0	2.0	3.0	1.1	29.2	0.4	15.5
L188	2	10.6	56.9	2.2	1.9	0.3	24.1	0.3	3.1
L192	2	2.4	63.6	7.2	6.0	0.2	16.6	0.2	3.1
L193	4	2.5	66.8	16.2	8.7	0.4	0.1	0.2	0.0
L195	12	2.0	29.0	42.8	23.6	0.2	0.1	0.0	0.1
L196	12	6.0	41.6	27.0	13.2	0.2	0.0	0.1	0.0
L197	1.5	2.6	55.6	14.6	9.9	0.3	11.4	0.0	4.7
L198	2	5.5	28.9	39.0	22.8	0.2	0.2	0.0	2.6
L199	2	4.3	45.9	28.8	15.5	0.2	0.9	0.0	2.3
L201	2	46.9	12.0	0.7	0.9	0.8	23.9	0.1	14.5
L203	3	26.3	23.1	1.7	4.4	1.1	30.3	0.2	12.8
L204	4	17.9	24.6	0.7	2.2	1.8	34.6	0.0	18.2
L205	2.5	36.8	4.6	0.5	1.2	2.6	38.2	0.2	15.6
L206	8	3.4	55.7	26.3	13.2	0.2	0.0	0.0	0.0
L207	3	15.6	15.2	18.3	10.2	0.5	33.8	0.3	5.7
L211	2	2.5	52.1	33.2	15.5	0.4	0.0	0.0	0.1
L212	2	34.2	21.7	0.5	1.3	0.8	27.7	0.2	13.4
L214	2	25.0	29.7	2.6	2.7	0.8	25.7	0.3	12.9
L215	8	1.0	55.5	27.6	14.6	0.3	0.1	0.0	0.1
L216	2	16.6	44.7	2.5	3.7	0.6	24.1	0.1	7.0
L219	2	3.1	50.5	6.2	7.2	0.3	24.5	0.1	7.2
L220	2	3.7	66.7	6.1	3.7	0.2	17.7	0.0	1.0
L221	2.5	35.0	17.4	10.4	6.3	0.3	23.4	0.4	6.5
L223	4	37.8	15.4	0.5	1.1	1.0	27.6	0.0	16.6
L225	3	35.2	18.3	1.2	1.9	1.1	26.8	0.1	15.1
L226	2	18.7	40.5	1.2	2.3	0.8	25.7	0.0	10.8
L228	3	25.2	30.0	2.0	4.6	0.8	26.3	0.1	10.6
L229	3	36.8	14.2	1.1	2.0	1.0	29.5	0.0	14.9
L331	4	40.2	18.5	1.2	2.0	2.2	25.2	0.3	10.1
L332	3.5	51.6	4.0	0.2	0.6	0.6	26.2	0.2	16.4
L333	3	33.5	20.2	0.7	1.8	1.1	26.8	0.3	15.6
L334	4	48.2	4.5	0.3	0.6	1.7	26.2	0.3	18.1
L335	2	33.2	25.1	1.2	2.5	0.7	24.7	0.0	12.3
L336	2	5.0	58.2	4.9	10.0	0.6	9.7	0.0	11.1
L337	2	22.0	48.6	2.4	3.2	0.3	13.8	0.1	9.2
L339	3	42.9	7.3	0.7	1.4	1.1	34.5	0.5	11.4
L340	4	45.3	2.1	0.2	1.8	1.3	25.8	0.0	23.3
L341	2	51.1	8.2	0.3	0.7	0.6	23.3	0.2	15.5
L342	2	20.1	36.2	0.8	2.2	0.8	26.1	0.1	13.4
L343	2	27.5	32.8	0.9	1.4	0.8	23.6	0.1	12.7
L345	3	39.5	13.5	0.3	1.1	0.8	28.2	0.4	16.2
L346	2	36.4	18.4	1.1	1.9	0.9	26.4	0.1	14.6
L348	7	37.6	10.4	11.5	6.2	0.4	29.2	0.2	4.4

TABLE 13 : SEM COMPOSITIONAL ANALYSIS OF INCLUSIONS IN STEEL 4

NMI STEEL4	SIZE µm	O	FE	Mn	S	Si	Al	Mg	Ca
R2	15.0	4.0	49.9	25.5	14.5	0.3	4.1	0.4	0.1
R3	2	6.9	21.0	41.6	23.8	0.2	2.3	2.4	0.1
R4	2	3.9	79.3	1.4	0.0	7.7	6.3	0.4	0.1
R6	5	25.8	34.6	14.3	7.6	0.3	10.4	4.9	0.2
R7	5	31.7	15.1	16.9	6.7	0.3	19.8	8.8	0.1
R12	6	1.2	42.6	31.9	17.4	0.4	0.1	0.3	0.1
R14	6	2.7	63.6	18.2	11.7	0.6	0.2	0.4	0.1
R15	1	3.3	76.7	13.3	8.2	0.5	0.3	0.5	0.1
R17	5	0.2	66.7	18.9	8.5	0.3	0.1	0.0	0.1
R19	4	11.3	20.3	32.4	19.2	0.3	8.7	5.9	0.3
R20	2	22.2	35.3	21.9	11.3	0.1	4.4	3.1	0.5
R22	2.5	2.4	30.7	35.5	21.3	0.4	6.4	5.2	0.5
R23	3	1.6	42.8	27.8	17.7	0.3	3.6	2.9	0.4
R24	3	7.3	34.2	38.6	17.1	0.1	0.2	0.6	0.3
R30	3	5.4	33.6	35.0	19.0	0.2	2.0	2.0	0.1
R31	2	7.8	65.8	13.5	7.7	0.4	0.3	0.1	0.2
R32	3	18.0	38.5	21.2	12.2	0.2	3.3	3.4	0.9
R33	4	1.4	38.9	21.3	16.0	0.3	10.8	8.2	1.0
R36	4	3.0	77.9	6.5	6.1	0.5	3.9	4.5	0.5
R37	2	33.5	33.2	11.5	6.1	0.1	8.8	5.1	0.8
R39	4	6.2	50.6	23.1	12.3	0.5	0.4	0.8	0.3
R40	2	6.5	61.8	17.5	9.2	0.5	0.2	0.1	0.0
R41	5	15.0	5.0	38.5	26.1	0.4	6.8	6.5	0.6
R44	4	8.8	33.1	19.3	13.9	0.3	13.7	9.5	0.8
R46	4	8.5	49.8	23.2	11.5	0.2	4.1	1.2	0.0
R47	3	0.2	47.6	20.8	17.6	0.2	3.1	7.4	0.8
R51	2	17.5	29.3	14.2	11.3	0.2	16.2	10.1	0.4
R52	8	24.4	34.4	17.5	7.1	0.1	9.9	4.9	0.3
R54	3.5	29.8	8.6	25.8	14.7	0.2	12.1	7.3	0.2
R55	2	12.8	51.3	13.7	10.6	0.2	3.9	4.9	0.9
R56	6	10.5	26.2	29.7	16.1	0.1	10.1	5.7	0.3
R58	4	5.9	8.0	50.5	28.9	0.2	2.9	1.4	0.1
R61	8	2.3	62.4	14.8	10.0	0.1	3.9	3.7	0.7
R62	3	3.8	54.8	23.5	13.0	0.1	1.0	1.3	0.2
R64	3	12.8	38.6	21.0	12.6	0.3	7.1	5.6	0.2
R65	2.5	15.1	27.9	20.4	12.6	0.2	14.1	8.6	0.4
R67	1.5	16.9	33.7	22.0	15.3	0.1	3.6	5.3	0.9
R69	2	3.7	56.9	22.5	13.1	0.4	0.1	0.7	0.1
R71	3	0.2	46.7	31.5	18.5	0.3	0.1	0.5	0.1
R350	2	13.5	52.3	34.4	19.1	0.5	1.8	1.5	0.3
R351	2	11.9	16.0	31.6	21.9	0.3	8.9	7.0	0.8
R352	2	3.5	44.4	11.2	6.5	0.2	22.1	10.8	0.4
R354	2	8.0	67.6	11.9	7.2	0.3	0.5	0.3	0.0
R355	4	11.1	32.9	28.9	17.4	0.3	4.7	3.7	0.2
R356	3	1.9	63.2	15.0	9.3	0.3	5.1	2.3	0.0
R357	2	17.3	22.6	27.9	17.6	0.1	7.6	5.2	0.1
R359	10	13.5	34.7	17.1	7.6	0.2	17.3	8.2	0.1
R360	3	12.4	35.3	15.1	10.4	0.3	17.1	7.7	0.2
R361	3	0.0	55.7	24.5	15.1	0.3	0.2	0.5	0.2
R363	2	12.4	47.0	5.1	4.4	0.2	14.3	16.2	0.2

TABLE 14 : SEM COMPOSITIONAL ANALYSIS OF INCLUSIONS IN STEEL 5.

NMI STEEL5	SIZE μm	O	FE	Mn	S	Si	Al	Mg	Ca
B101	2	15.5	30.7	8.2	3.5	0.1	41.5	0.0	0.0
B103	4	17.6	25.3	15.2	5.7	0.2	35.0	0.1	0.1
B105	6	14.3	69.8	25.7	12.4	0.2	0.0	0.2	0.1
B107	10	2.5	50.1	31.0	14.1	0.2	0.0	0.0	0.0
B108	6	0.4	66.1	22.2	10.4	0.2	0.0	0.0	0.0
B109	2	0.9	69.7	18.5	11.1	0.3	0.0	0.0	0.0
B110	12	2.0	45.3	34.2	17.0	0.1	0.0	0.2	0.0
B112	16	0.8	43.9	35.5	18.0	0.2	0.0	0.1	0.0
B113	16	3.7	40.0	35.6	16.9	0.3	0.2	0.0	0.0
B114	6	2.1	76.7	14.9	8.9	0.3	0.0	0.0	0.0
B115	4	1.2	71.2	18.7	9.9	0.2	0.1	0.1	0.0
B117	3	30.6	24.8	12.8	6.0	0.1	25.3	0.0	0.1
B118	7	1.7	61.1	24.9	14.9	0.2	0.1	0.0	0.0
B119	8	0.5	65.7	21.8	10.4	0.2	0.0	0.1	0.0
B120	8	1.7	56.7	27.1	12.9	0.1	0.0	0.2	0.1
B122	2	2.7	72.1	17.9	10.8	0.3	0.1	0.1	0.0
B123	6	2.1	77.9	14.4	8.2	0.3	0.0	0.0	0.0
B124	16	1.6	70.2	16.8	7.4	0.3	0.1	0.1	0.0
B125	2	12.3	37.9	25.4	14.4	0.2	8.8	0.0	0.1
B127	3	3.3	76.4	14.9	8.9	0.3	0.0	0.1	0.1
B130	8	3.0	33.4	41.2	20.2	0.2	0.0	0.0	0.0
B131	20	0.5	63.2	24.2	10.7	0.3	0.0	0.0	0.0
B132	17	6.3	45.1	33.8	13.4	0.3	0.1	0.0	0.0
B133	16	6.3	21.3	48.1	22.5	0.1	0.0	0.0	0.0
B134	5	3.0	38.2	38.7	18.7	0.3	0.1	0.1	0.0
B136	3	18.0	28.1	11.9	6.2	0.1	35.0	0.1	0.0
B137	6	4.3	44.2	33.9	16.0	0.2	0.0	0.0	0.0
B138	10	1.0	80.3	11.6	7.1	0.2	0.1	0.0	0.0
B140	2	25.4	36.6	1.8	1.1	0.2	35.0	0.1	0.0
B141	4	2.6	55.7	26.7	13.5	0.2	0.0	0.1	0.0
B142	8	0.2	82.3	10.0	5.8	0.4	0.1	0.0	0.1
B143	4	2.3	53.6	28.3	14.4	0.2	0.0	0.0	0.0
B146	4	50.1	16.2	0.3	0.0	0.1	33.0	0.1	0.0
B147	6	2.7	47.5	32.9	14.4	0.2	0.1	0.1	0.1
B148	6	0.2	83.0	7.8	3.9	0.4	0.0	0.1	0.1
B149	6	0.2	67.8	20.5	8.9	0.4	0.1	0.3	0.0
B150	10	1.3	68.1	18.8	10.3	0.4	0.0	0.1	0.0
B151	20	1.0	40.8	37.5	18.9	0.2	0.0	0.1	0.0
B155	8	1.2	62.0	22.1	12.1	0.3	0.0	0.1	0.0
B156	6	3.5	36.5	41.7	16.8	0.4	0.1	0.1	0.0
B157	3	1.1	71.9	17.6	9.7	0.3	0.0	0.1	0.1
B158	2	3.3	51.8	30.6	13.1	0.2	0.0	0.0	0.0
B159	2	4.6	50.0	30.8	12.7	0.3	0.0	0.0	0.0
B161	4	3.8	57.9	24.8	12.2	0.3	0.0	0.0	0.1
B162	2	3.0	61.9	22.9	10.2	0.2	0.2	0.1	0.1
B163	4	0.9	80.3	12.1	6.8	0.4	0.0	0.2	0.0
B164	2	1.5	65.9	21.8	9.4	0.3	0.0	0.0	0.0
B165	4	2.9	57.7	26.5	11.5	0.1	0.0	0.3	0.0
B166	10	4.0	48.2	32.3	14.3	0.2	0.2	0.1	0.0
B167	16	3.6	47.0	32.1	15.3	0.3	0.1	0.0	0.1

TABLE 15. Charpy V Notch Properties Of The Steels.

STEEL	ORIENTATION	UPPER SHELF ENERGY (J)	TRANSITION TEMPERATURE (°C)	ANISOTROPY RATIO $USE_L \cdot USE_T$
1	LONGITUDINAL	230	-68	1.25
	TRANSVERSE	184	-66	
2	LONGITUDINAL	206	-70	1.29
	TRANSVERSE	160	-68	
3	LONGITUDINAL	142	-22	1.65
	TRANSVERSE	86	-24	
4	LONGITUDINAL	190	-60	1.32
	TRANSVERSE	144	-52	
5	LONGITUDINAL	140	-46	2.06
	TRANSVERSE	68	-48	

TABLE 16. MEAN RELATIVE PLASTICITY INDICES FOR THE CONTROLLED ROLLED AND ISOTHERMALLY ROLLED STEELS

MEAN RELATIVE PLASTICITY INDEX					
	STEEL 1	STEEL 2	STEEL 3	STEEL 4	STEEL 5
ISOTHERMALLY ROLLED AT 800 °C	- -	- -	0.31	0.38	0.79
ISOTHERMALLY ROLLED AT 1000 °C	- -	- -	0.24	0.31	0.61
ISOTHERMALLY ROLLED AT 1200 °C	- -	- -	0.31	0.28	0.38
CONTROLLED ROLLED	0.17	0.16	0.33	0.26	0.50

TABLE 17 RATIO'D SEM ANALYSIS OF INCLUSIONS IN STEEL 1

SIZE	SHAPE CATEGORY	Mn	S	Al	Mn/S RATIO
16	4	58.2	26.2		2.221
1	2	4.4	1.51	28.9	2.914
1	2	46.1	25	18.3	1.844
4	4	10.2	3.9	35.5	2.615
1	2	6.1	2.7	47.9	2.259
3	4	53.4	30		1.780
2	4	53.4	31.2		1.712
1	2	8.3	4.4	44.2	1.886
2	2	8.2	4	91.2	2.050
1	3	4.4	1.9	56.8	2.316
1	2	15.6	4.2	34.2	3.714
1	2	9.3	3.9	66.4	2.385
10	4	60.9	25.7		2.370
6	4	59.7	26.1	3.0	2.287
1	2	4.6	1.5	29.3	3.067
2	4	49.6	25.5	13.3	1.945
2	4	40.4	21.3	4.7	1.897
1	2	9.8	4	43.1	2.450
1	2	28.4	15.4	25.9	1.844
2	3	12.7	6	62.0	2.117
4	4	49.3	28.2	10.5	1.748
4	4	59	31.3		1.885
3	4	13.6	5.2	48.3	2.615
2	4	64.5	37.9		1.702
2	3			53.8	
2	2			53.4	
3	2			39.9	
1	1			80.9	
2	4			71.4	
5	4			76.7	
2	2			74.7	
2	4			42.1	
1	2			57.1	
2	4			81	
2	2			33.7	
1	2			34.3	
2	4			56.9	
2	2			59.6	
1	2			39.3	
2	2			37.7	
1	2			66.2	
2	4			57.8	
1	1			44.6	
1	2			35.5	
3	4			45.8	
2	2			35.9	
1	1			63.7	
2	2			72.1	
1	2			57.7	

TABLE 18. RATIO'D SEM ANALYSIS OF INCLUSIONS IN STEEL 2.

SIZE	SHAPE CATEGORY	Mn	S	Ca	Al	Mn/S RATIO
2	1	1.6	20.9	19.4	47	0.077
1	1	20.3	25.9	19	57.1	0.784
1	1	9.1	21.2	11.1	34.8	0.429
2	1	12.1	13.4	17.1	36.6	0.903
5	3	52.1	29.6	6.4	3.2	1.760
2	1	2.9	3.7	10.1	36.7	0.784
1	1	31.1	28.4	14.9	17.6	1.095
2	1	10.9	26.3	31.4	15.2	0.414
1	1	22.7	12.8	6.5	31.7	1.773
2	1	3.9	9.6	14.2	49.7	0.406
2	1	1.6	6.3	14.9	36.5	0.254
3	1	2.8	13.5	19.4	33.5	0.207
2	1	4.8	8.2	13.8	40.8	0.585
2	1	15	21.6	19.1	11.8	0.694
4	4	56.3	30.4			1.852
1	1	33.2	17.9		18.4	1.855
4	3	41.6	27.7	6	20.9	1.502
2	2		3.9	17.5	22.5	
2	1		1.4	14.9	34	
3	1	1.9	11.9	26.7	29.6	0.160
1	1	33.7	28.2	16.6	17.5	1.195
2	1	41.4	28.1	15.2		1.473
2	1	32.1	27.5	17.9	9.1	1.167
2	2	57.9	33.5	2.8	1.9	1.728
2	1	1.8	1.7	5.2	50.8	1.059
1	1	9.4	15.6	17.5	28.5	0.603
1	1	15.7	24.4	25.6	4.3	0.643
3	1	6.1	13.2	18.5	23.2	0.462
2	1	2.8	3.7	4.8	52.7	0.757
3	1	11.2	17.2	20.8	30.1	0.651
3	1	4.6	16.2	20	18.1	0.284
3	1	7.9	17	20.3	33.1	0.465
2	1	2.8	9.2	14.1	42.4	0.304
2	1	17.5	20.8	16.7	12.9	0.841
2	1	27	39.9	31.3	4.8	0.677
2	1	49.8	27.2	7.9	18	1.831
20	4	47.1	29.9			1.575
2	1	27.6	25.6	14.4	21.9	1.078
8	4	67.6	39.3			1.720
2	1	19.2	24.1	17.1	29.2	0.797
2	1	30.2	38.5	25.7		0.784
7	4	51.7	24.8		5.5	2.085
2	1	18.2	25.8	24.5	19.1	0.705
2	1	9.8	33.8	38	9.2	0.290
2	2	7.8	5.9	3.4	53.5	1.322
1	1	7.3	11.4	13	35.3	0.640
1	1	19.2	18.7	13.6	22.2	1.027
3	1	5.6	16.5	21.7	26.6	0.339
5	4	55.9	30		5.4	1.863
1	2	46	25.3	4.6	13.1	1.818

TABLE 19 RATIO'D SEM ANALYSIS OF INCLUSIONS IN STEEL 3.

SIZE	SHAPE CATEGORY	Mn	S	Ca	Al	Mn/S RATIO
2	1	1.6	3.1	18.4	32.4	0.516
2	1	20.3	15.1	9.5	15.1	1.344
2	1	9.1	5.8	9	37.8	1.569
2	1	7.5	5.3	9.5	32.6	1.415
1	1	12.6	8.4	9.3	19.6	1.500
2	1	2.3	5.8	17.2	9.2	0.397
3	1	1.6	3	18.8	37.8	0.533
2	1	2.6	3.8	19.9	37.4	0.684
2	1	5.1	4.4	7.2	55.9	1.159
2	1	19.8	16.5	8.5	45.6	1.200
4	4	48.8	26.2			1.863
2	3	54.9	32.1	3.7		1.710
2	2	53.2	28.7	4.3		1.854
12	4	60.3	33.2			1.816
12	4	46.2	22.6			2.044
2	1	32.9	22.3	10.6	25.7	1.475
3	1	2.2	5.7	16.6	39.4	0.386
4	1			24.1	45.9	
3	1			16.4	40.0	
8	4	59.4	29.8			1.993
3	3	21.6	12	6.7	39.9	1.800
2	4	69.3	32.4			2.139
2	1	3.7	3.8	18.3	36.6	0.974
8	4	62	32.8			1.890
2	1	4.5	6.7	12.7	43.6	0.672
7	4	12.8	6.9	4.9	32.6	1.855
2	1	1.3	2.3	17.9	32.4	0.565
2	1	1.6	3.3	16.4	33.0	0.485
2	1	11.7	23.9	26.6	23.2	0.490
2	4	4.7	6.2	17.9	26.8	0.758
4	3	1.5	2.5	12.4	30.9	0.600
2	1	2	3.9	18.2	43.2	0.513
3	1	1.5	2.3	18.5	32.8	0.652
2	1	12.5	14.5	14.5	49.5	0.862
2	2	18.3	11.1	3	53.2	1.649
3	2	12.6	7.6	7.9	28.3	1.658
3	1	2.9	6.6	15.1	37.6	0.439
3	1	1.3	2.3	17.4	34.4	0.565
2	1		1.7	17.1	35.4	
2	1			16.5	27.2	
3	1		1.3	18.7	32.6	
4	1		1.8	23.8	26.4	
2	1			16.9	25.4	
2	1		3.9	21	40.9	
2	1		2.1	18.9	35.1	
3	1		1.5	12.3	37.2	
4	1			19	27.4	
4	1			17.1	27.3	
3	2		2.3	19.5	33.6	
4	2		1.3	19.6	32.6	

TABLE 20 RATIO'D SEM ANALYSIS OF INCLUSIONS IN STEEL 4

SIZE	SHAPE CATEGORY	Mn	S	Mg	Al	Mn/S RATIO
3	3	52.7	28.6	3	3	1.843
2	1	52.7	30.1	3	2.9	1.751
2	1	39.5	22.5			1.756
2	1	45.8	24.1			1.900
2	1	20.1	16	14.3	22.9	1.256
2	1	28.1	21.8	10.1	8	1.289
3	1	28.3	17.5	11.9	19.6	1.617
2	1	33.2	23.1	7.8	5.4	1.437
2	1	20.1	11.7	19.4	39.7	1.718
2	1	9.6	8.3	30.6	27	1.157
15	4	50.9	28.9		8.2	1.761
1	2	57.1	35.2		30.4	1.622
4	2	40.7	24.1	7.4	10.9	1.689
2	2	33.8	17.5	4.8	6.8	1.931
3	2	51.2	30.7	7.5	9.2	1.668
3	2	48.6	30.9	5.1	6.3	1.573
2	2	17.2	9.1	7.6	13.2	1.890
5	2	40.5	27.5	6.8	7.2	1.473
2	2	72.1	40	3.1	3.8	1.803
2	2	37.6	26.1	8.3	10.6	1.441
3	3	58.7	26			2.258
4	3	34.9	26.2	13.4	17.7	1.332
4	3	28.8	20.8	14.2	20.5	1.385
3	3	39.7	33.6	14.1	5.9	1.182
4	3	28.2	16.1	8	13.2	1.752
4	3	54.9	31.4	1.5	3.2	1.748
3	3	34.2	20.5	9.1	11.6	1.668
2	3	52.2	30.4			1.717
3	3	59.1	34.7			1.703
2	3	36	22.7	6.7	9.8	1.586
5	4	21.9	11.6	7.5	15.9	1.888
5	4	19.9	7.9	10.4	23.3	2.519
6	4	55.6	30.3			1.835
6	4	50	32.1			1.558
5	4	56.8	25.5			2.227
3	4	34.5	19.8	5.5	5.4	1.742
4	4	29.4	27.6	20.4	17.6	1.065
4	4	46.8	24.9			1.880
4	4	46.2	22.9	2.4	8.2	2.017
8	4	26.7	10.8	7.5	15.1	2.472
6	4	40.2	21.8	7	13.7	1.844
8	4	39.4	26.6	9.8	10.4	1.481
3	4	52	28.8	2.9	2.2	1.806
2	4	36.7	22.2			1.653
4	4	43.1	25.9	5.5	7	1.664
3	4	40.8	25.3	6.3	13.9	1.613
10	4	26.2	11.6	12.6	26.5	2.259
3	4	23.3	16.1	11.9	26.4	1.447
3	4	55.3	34.1			1.622

TABLE 21 RATIO'D SEM ANALYSIS OF INCLUSIONS IN STEEL 5.

SIZE	SHAPE CATEGORY	Mn	S	Al	Mn/S RATIO
8	4	56.5	32.8		1.723
2	2	11.8	5.1	59.9	2.314
4	2	20.3	7.6	46.9	2.671
4	4	61	31		1.968
4	4	60.3	30.5		1.977
2	3	2.8	1.7	55.2	1.647
10	4	58.9	36		1.636
6	4	60.8	28.7		2.118
3	3	16.6	8.6	48.7	1.930
5	4	62.6	30.3		2.066
16	4	61.1	28.6		2.136
17	4	61.6	24.4		2.525
20	4	65.8	29.1		2.261
8	4	61.9	30.3		2.043
16	4	56.4	24.8		2.274
2	3	40.9	23.2	14.2	1.763
3	3	63.1	37.7		1.674
7	4	64	36.2		1.768
8	4	63.6	30.3		2.099
8	4	62.6	29.8		2.101
2	3	64.2	38.7		1.659
6	4	65.1	37.1		1.755
3	4	17	8	33.6	2.125
4	4	64.9	34.4		1.887
6	4	63.9	38.2		1.673
16	4	59.3	28.2		2.103
10	4	62.1	28.3		2.194
6	4	65.5	30.7		2.134
6	4	62.7	27.4		2.288
6	4	45.9	22.9		2.004
6	4	63.7	27.6		2.308
10	4	58.9	32.3		1.824
20	4	63.3	31.9		1.984
8	4	58.2	31.8		1.830
6	4	65.7	26.5		2.479
3	4	62.6	34.5		1.814
2	4	63.5	27.2		2.335
2	4	61.6	25.4		2.425
4	4	58.9	29		2.031
2	4	60.1	26.8		2.243
4	4	61.4	34.5		1.780
2	4	63.9	27.6		2.315
4	4	62.6	27.2		2.301
10	4	62.4	27.6		2.261
16	4	60.6	28.9		2.097
6	4	85.1	41.1		2.071
2	2	61.1	36.6		1.669
12	4	62.5	31.1		2.010

TABLE 22. HIC TEST RESULTS.

STEEL	CRACK LENGTH RATIO (CLR)% $\left[\frac{\sum a}{W} 100\ \%\right]$	CRACK THICKNESS RATIO (CTR)% $\left[\frac{\sum b}{T} 100\ \%\right]$	CRACK SENSITIVITY RATIO (CSR)% $\left[\frac{\sum a\ b}{W\ T} 100\ \%\right]$
1	0 0 0 0	0 0 0 0	0 0 0 0
2	15 17 20 0	2 8 6 0	<1 1 1 0
3	43 5 18 38	12 <1 3 7	4 <1 <1 3
4	50 22 12 11	8 6 5 2	4 1 1 <1
5	64 60 58 60	31 28 21 34	20 17 12 21
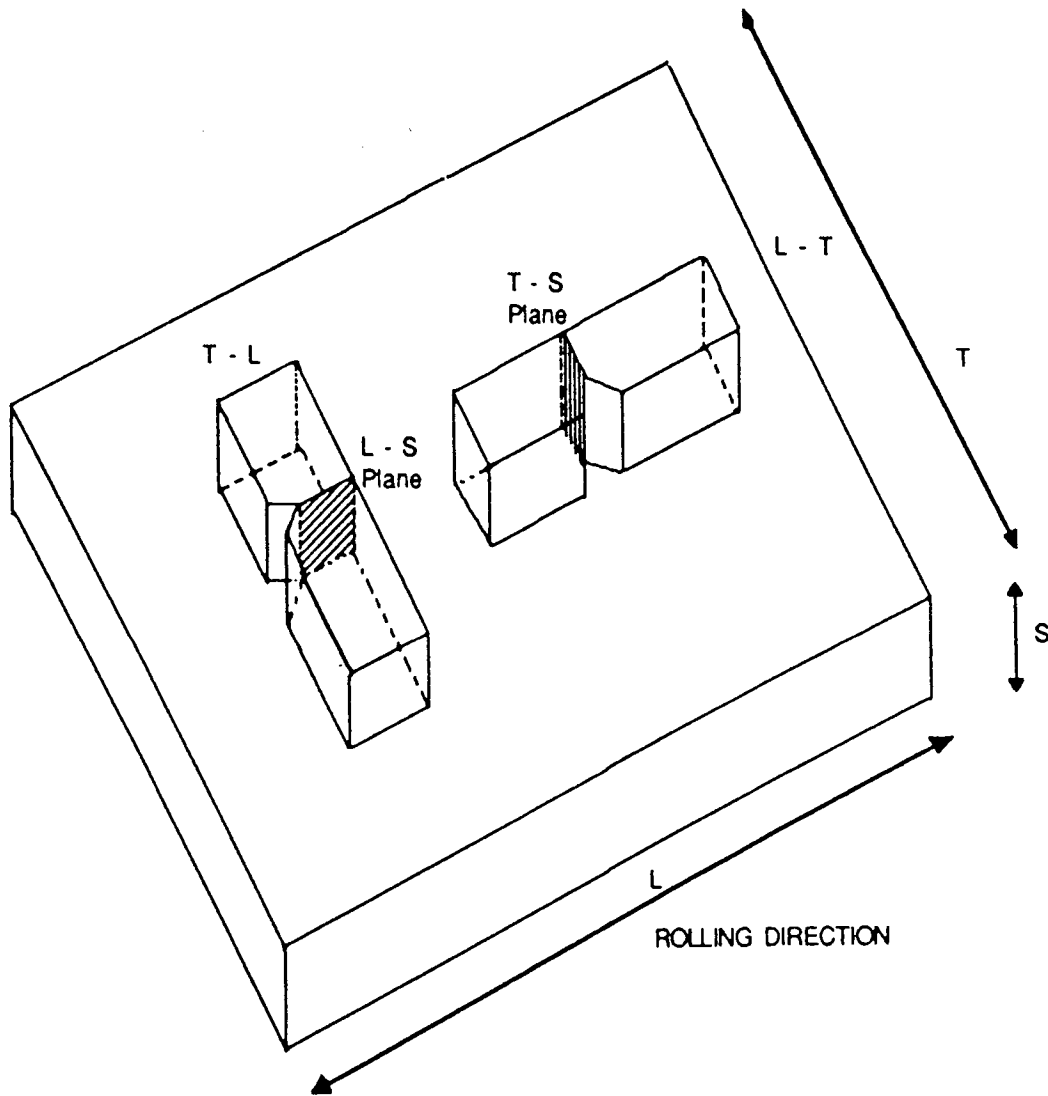
FIGURE 18. SPECIMEN ORIENTATION AND PLANES OF EXAMINATION
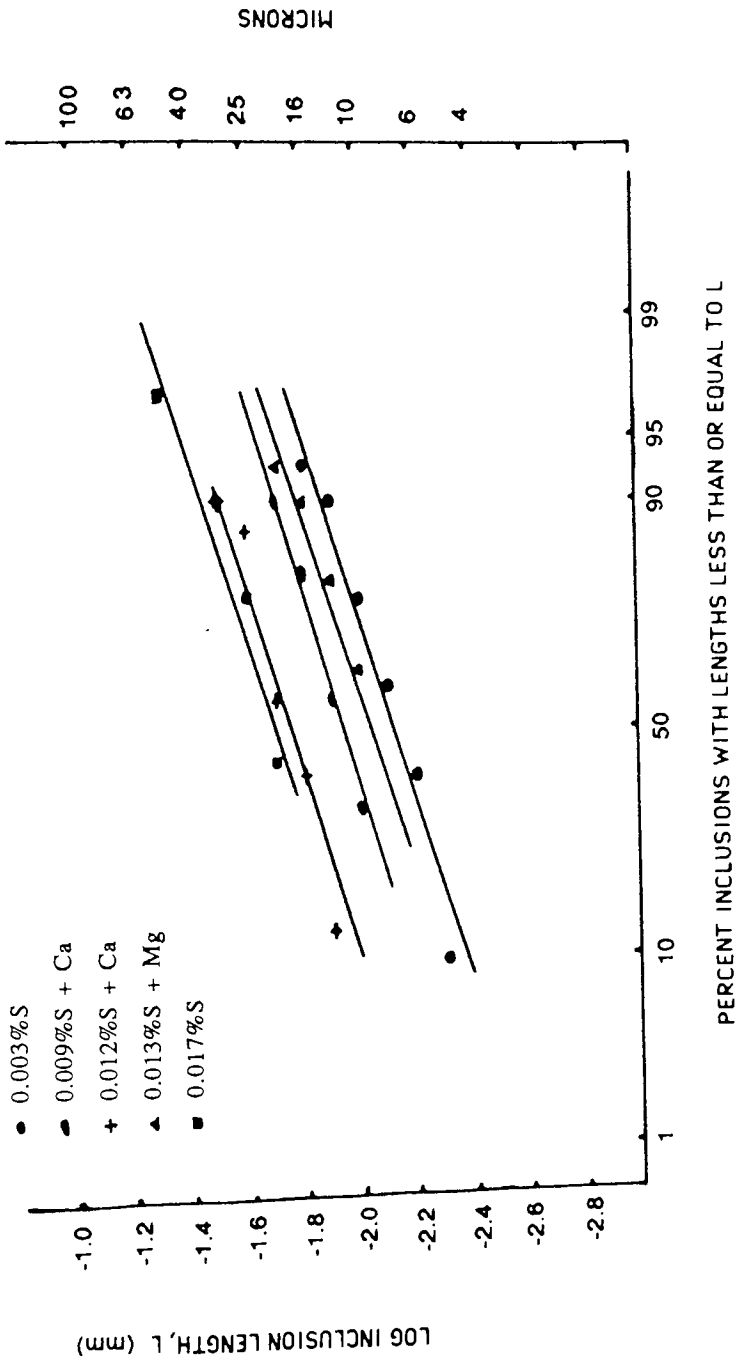
FIGURE.19 INCLUSION LENGTH DISTRIBUTIONS FOR STEELS 1-5
FROM THE PHOTOGRAPHIC ASSESSMENT DATA

FIGURE 20 : SHAPE CATEGORISATION OF INCLUSIONS IN STEEL 1
ANALYSED ON THE SEM.

FIGURE 21 : SHAPE CATEGORISATION OF INCLUSIONS IN STEEL 2
ANALYSED ON THE SEM
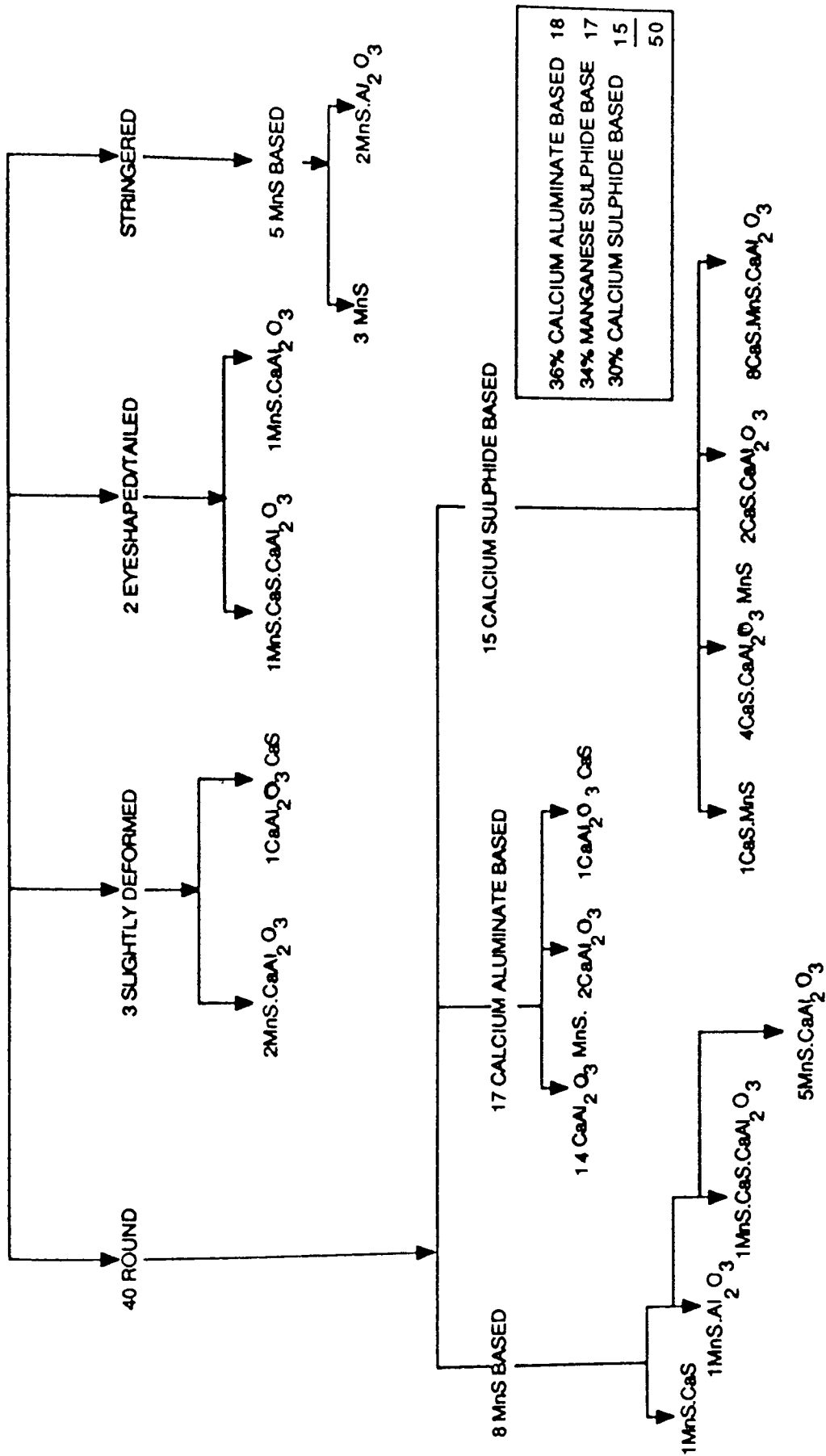
FIGURE 22 : SHAPE CATEGORISATION OF INCLUSIONS IN STEEL 3
ANALYSED ON THE SEM

SHAPE CATEGORY

76% CALCIUM ALUMINATE BASED	38
20% MANGANESE SULPHIDE BASED	10
2% CALCIUM SULPHIDE BASED	1
2% ALUMINA BASED	1
	50
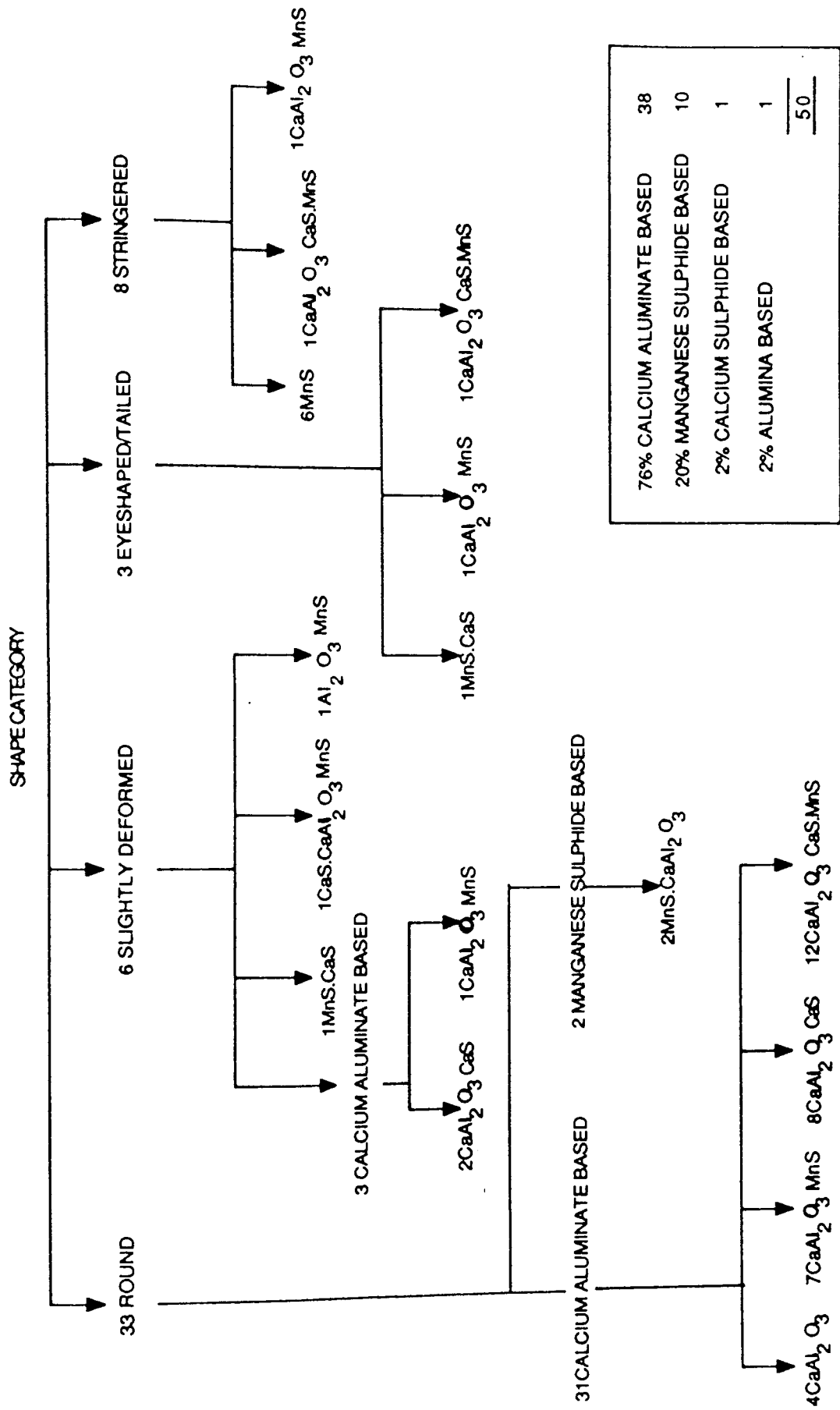
FIGURE 23 : SHAPE CATEGORISATION OF INCLUSIONS IN STEEL 4 ANALYSED ON THE SEM

SHAPE CATEGORY

9 ROUND   10 SLIGHTLY DEFORMED   11 EYESHAPED/TAILED   20 STRINGERED

4MnS.MgO.Al$_2$O$_3$ 3MgO.Al$_2$O$_3$ MnS   2MnS

1SiO$_2$ Al$_2$O$_3$ MnO   8MnS.MgO.Al$_2$O$_3$ 1MnS

8MnS.MgO.Al$_2$O$_3$ 3MnS

6MnS   1MnS.Al$_2$O$_3$ 10MnS.MgO.Al$_2$O$_3$ 3MgO.Al$_2$O$_3$ MnS

86% MANGANESE SULPHIDE BASED   43
12% MAGNESIA-ALUMINA BASED   6
2% OXIDE BASED   1
                                 50

159
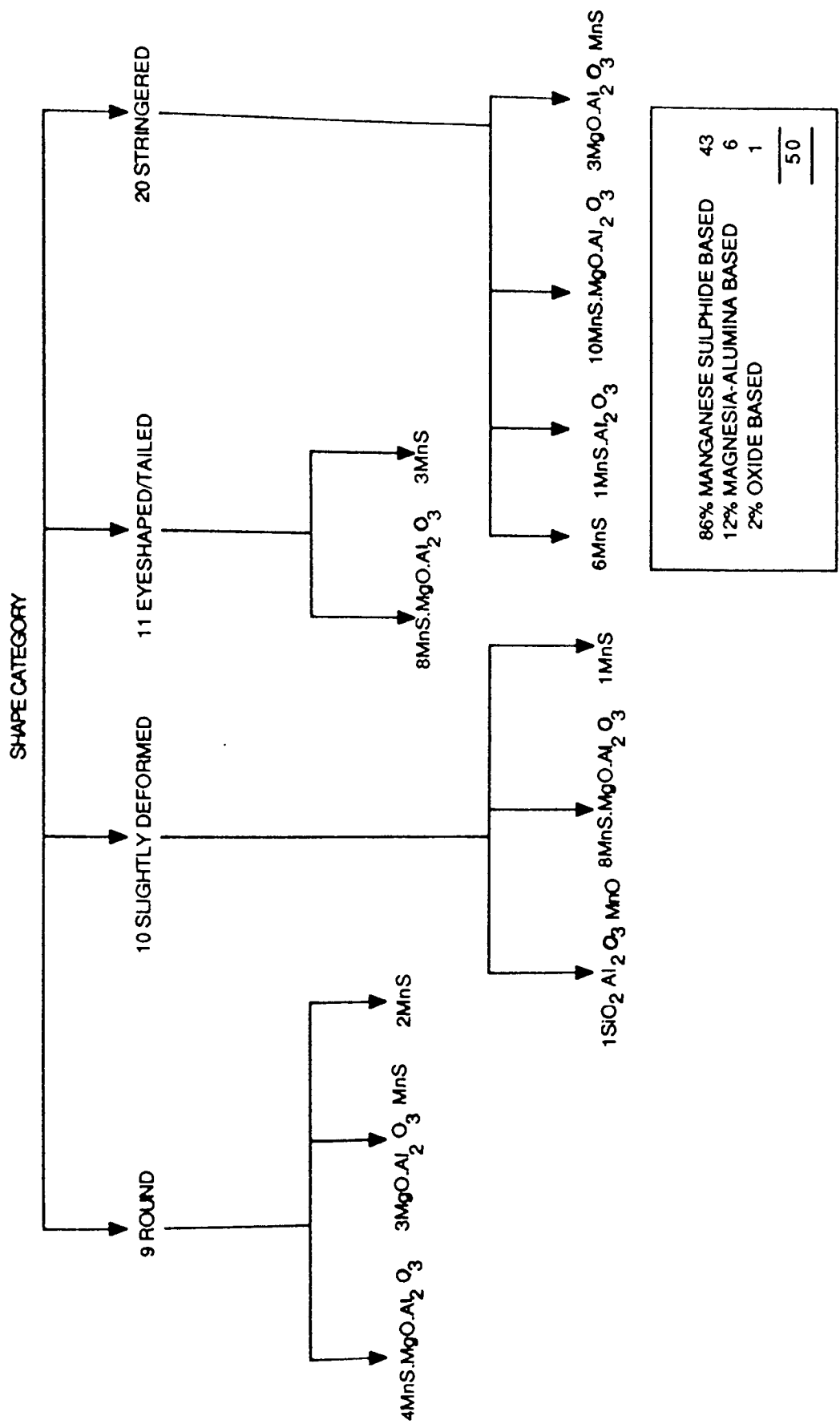
FIGURE 24 : SHAPE CATEGORISATION OF INCLUSIONS IN STEEL 5
ANALYSED ON THE SEM

SHAPE CATEGORY

0 ROUND

4 SLIGHTLY DEFORMED

2Al$_2$O$_3$ MnS   1Al$_2$O$_3$ 1MnS

5 EYESHAPED/TAILED

2Al$_2$O$_3$ MnS   1MnS. Al$_2$O$_3$ 2MnS

41 STRINGERED

1Al$_2$O$_3$ MnS   40 MnS

88% MANGANESE SULPHIDE BASED INCLUSIONS   44

12% ALUMINA BASED INCLUSIONS   6

50

FIGURE 26 Transverse ductile brittle transition
temperature curves
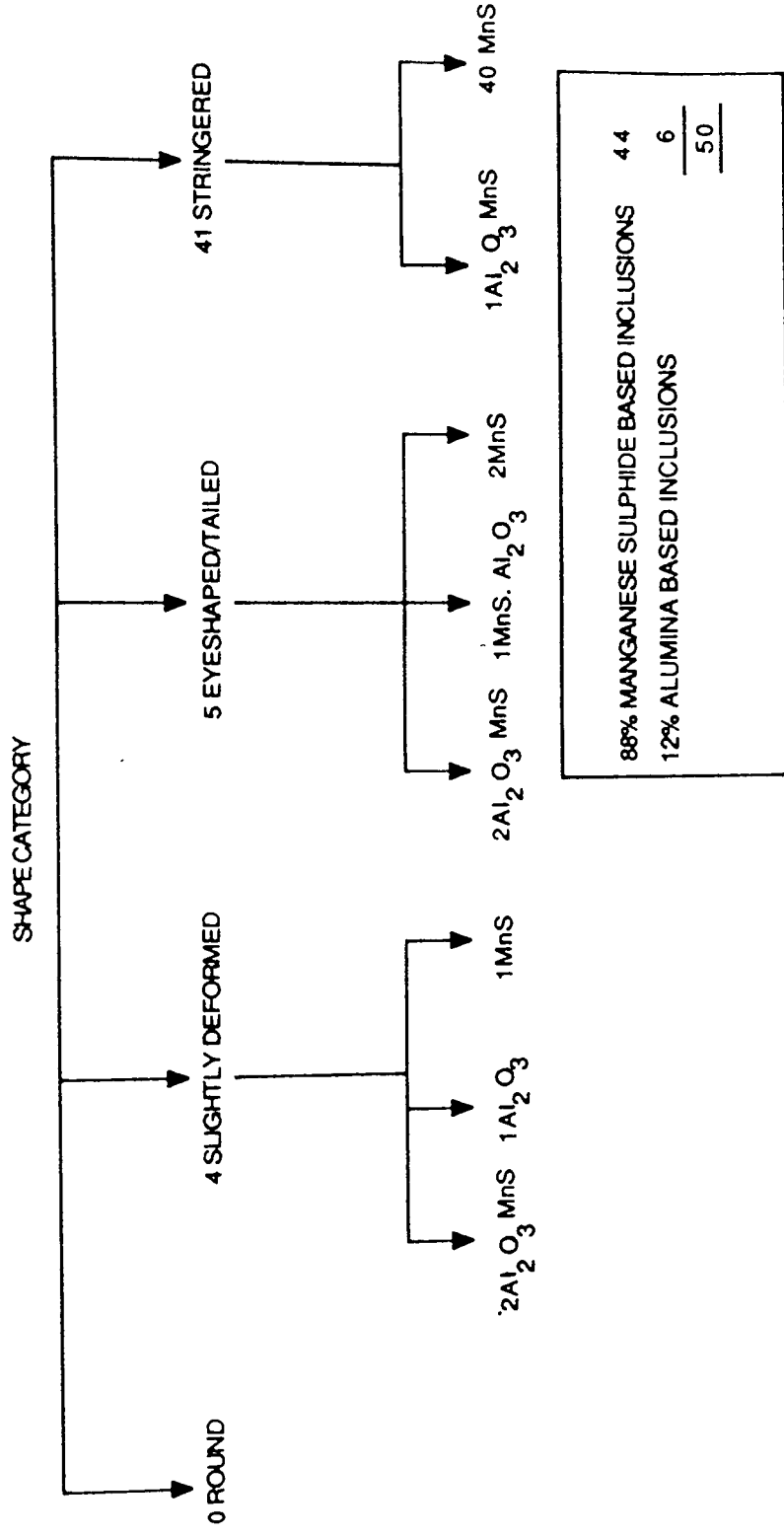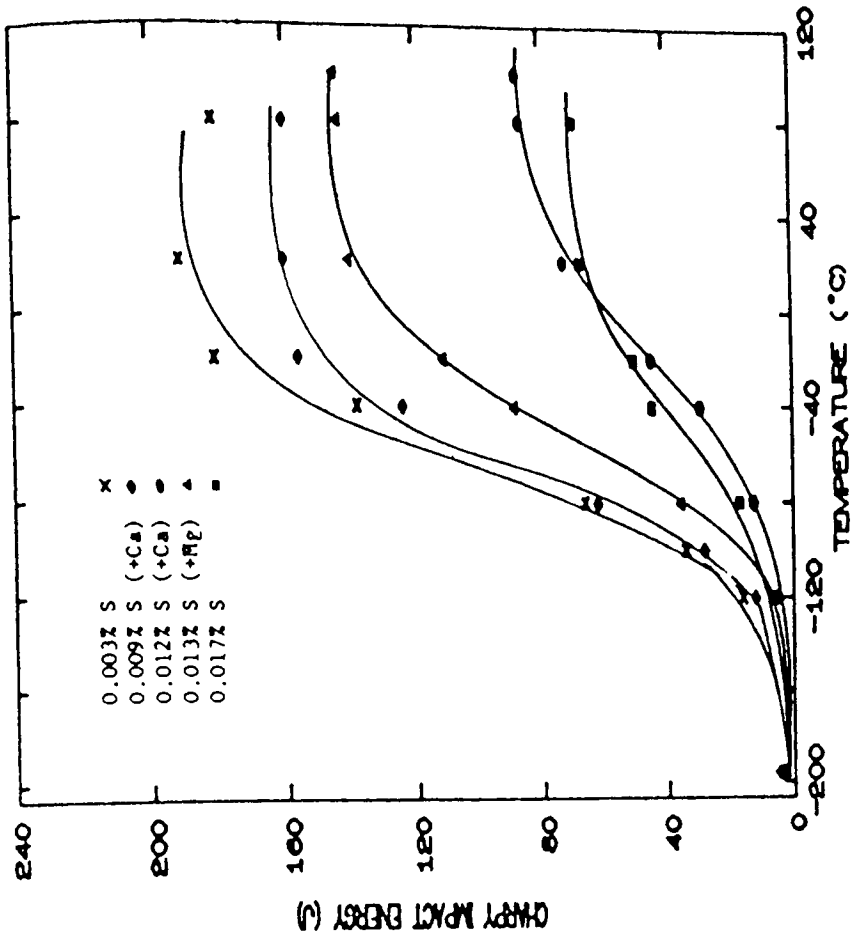
FIGURE 25 Longitudinal ductile brittle transition
temperature curves
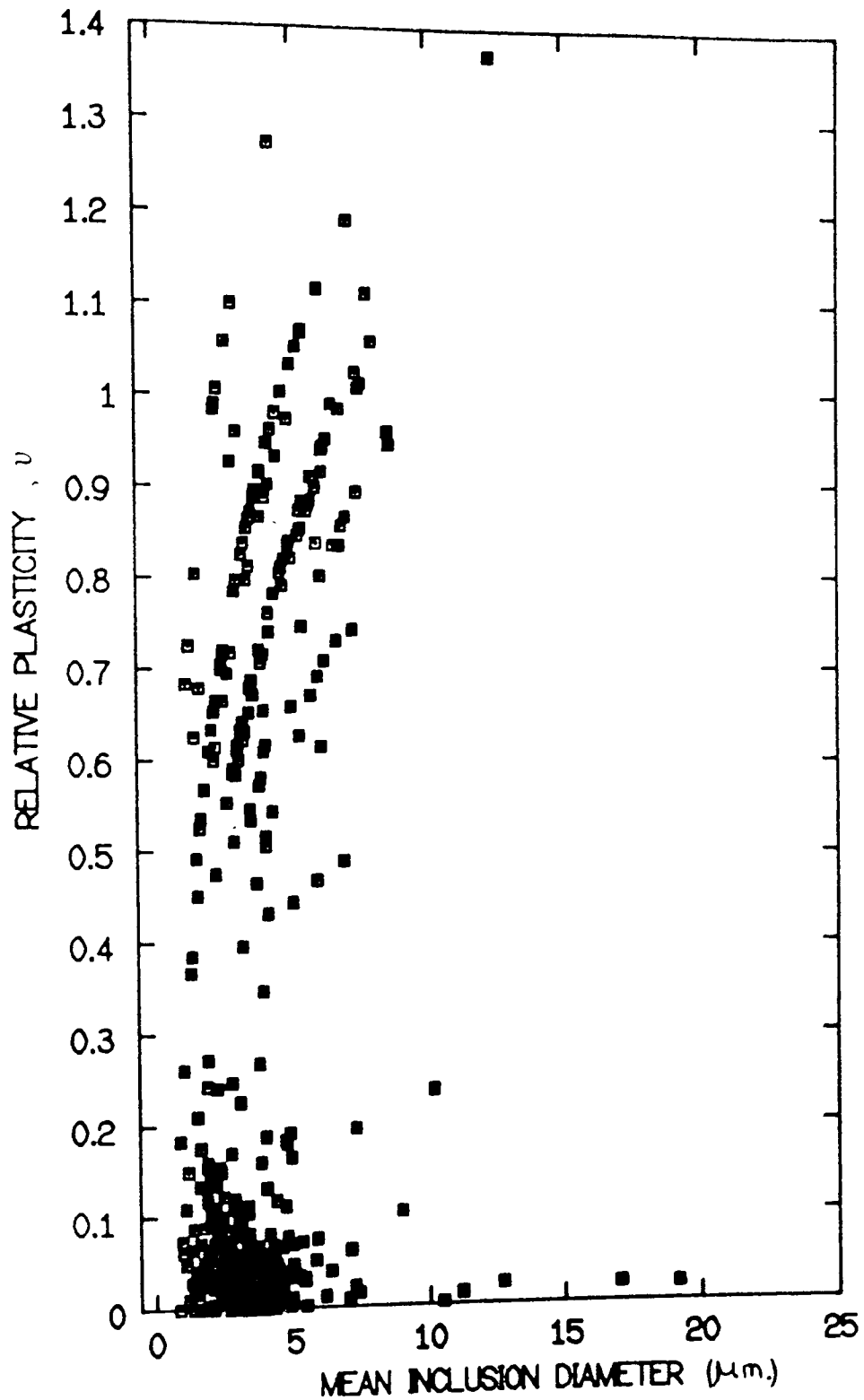
FIGURE 27 RELATIVE PLASTICITY OF THE INCLUSIONS IN THE 0.012% SULPHUR CALCIUM TREATED STEEL ROLLED AT 800°C
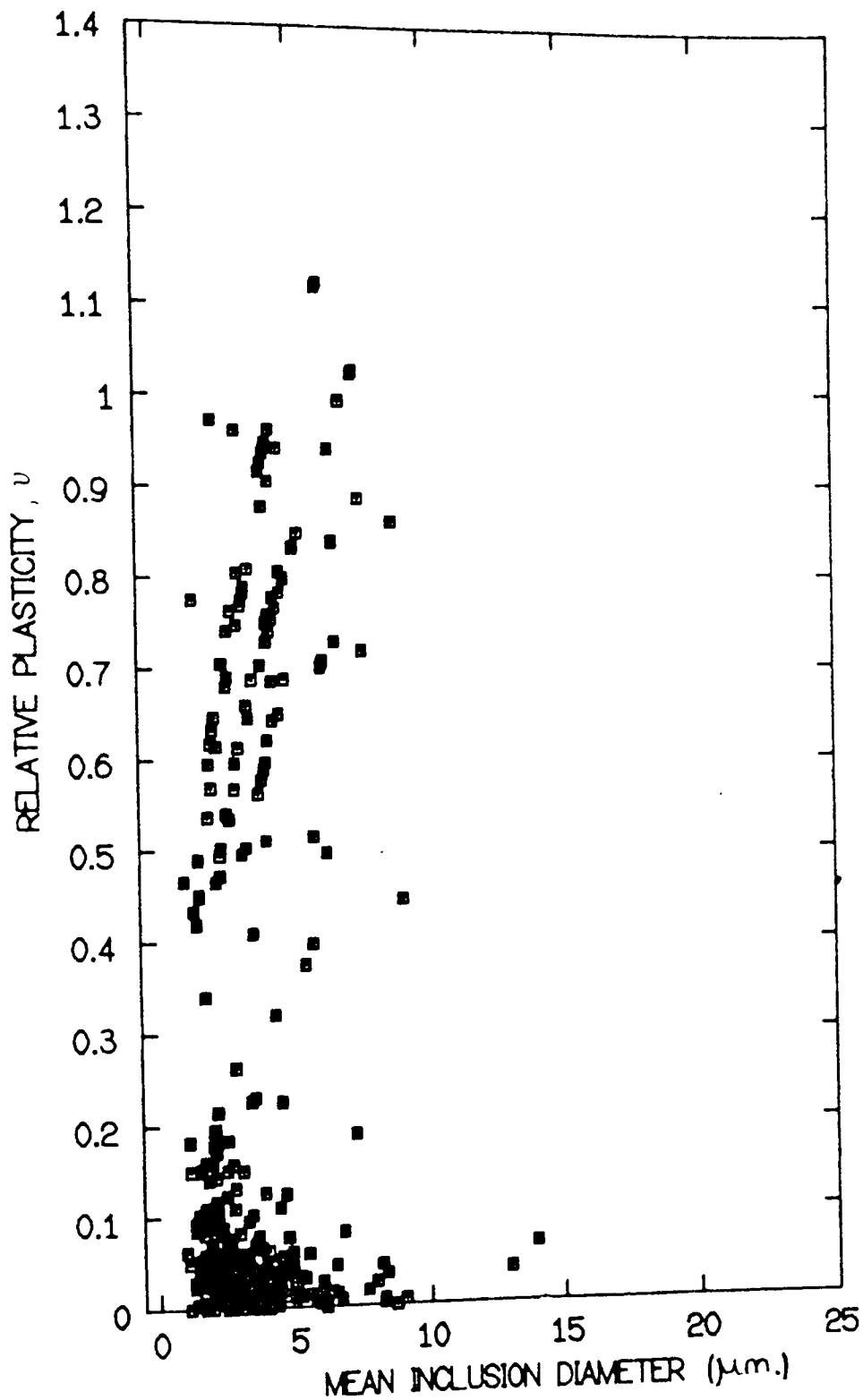
FIGURE 28 RELATIVE PLASTICITY OF THE INCLUSIONS IN THE 0.012% SULPHUR
CALCIUM TREATED STEEL ROLLED AT 1000°C
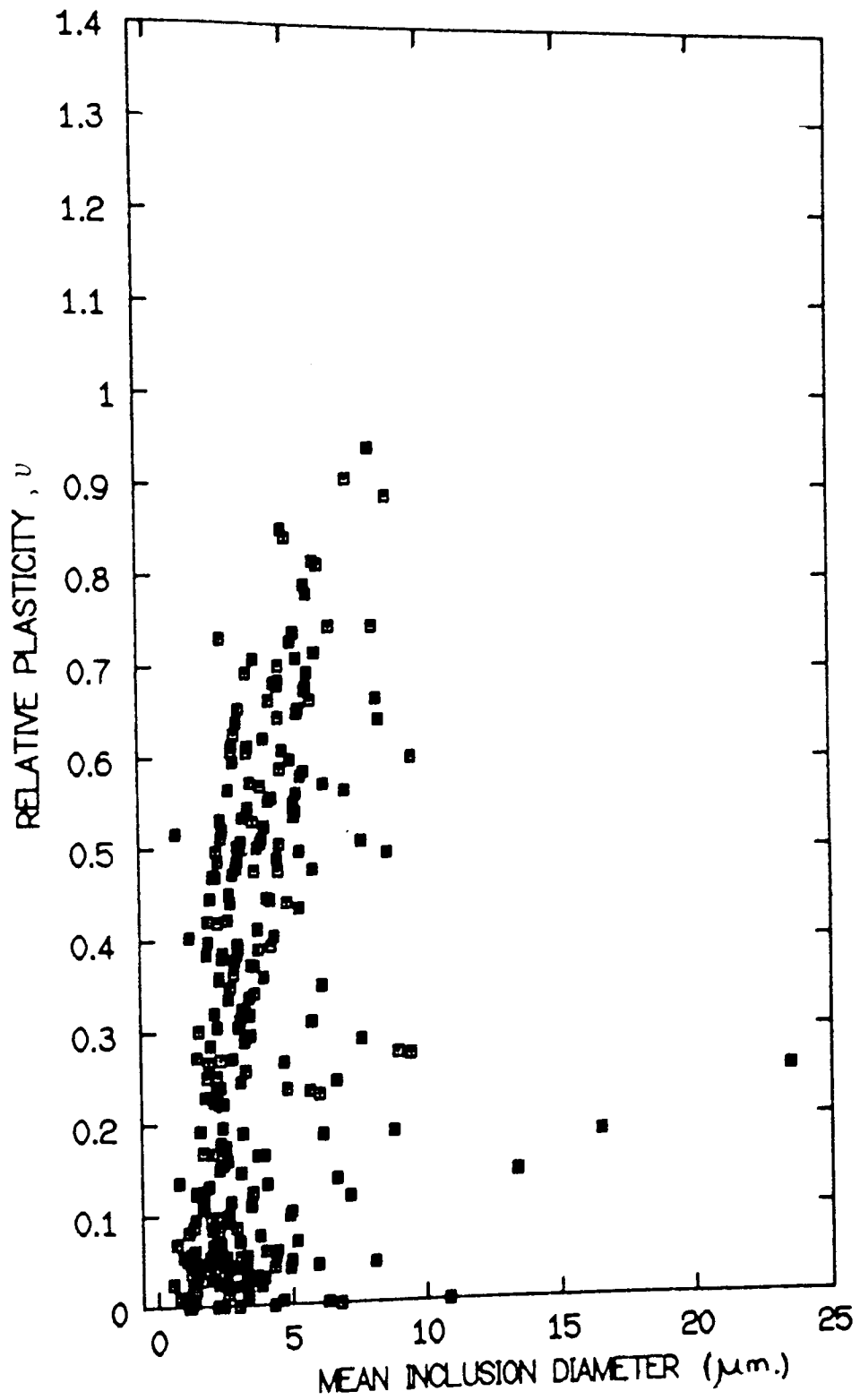
FIGURE 29 RELATIVE PLASTICITY OF THE INCLUSIONS IN THE 0.012% SULPHUR CALCIUM TREATED STEEL ROLLED AT 1200°C
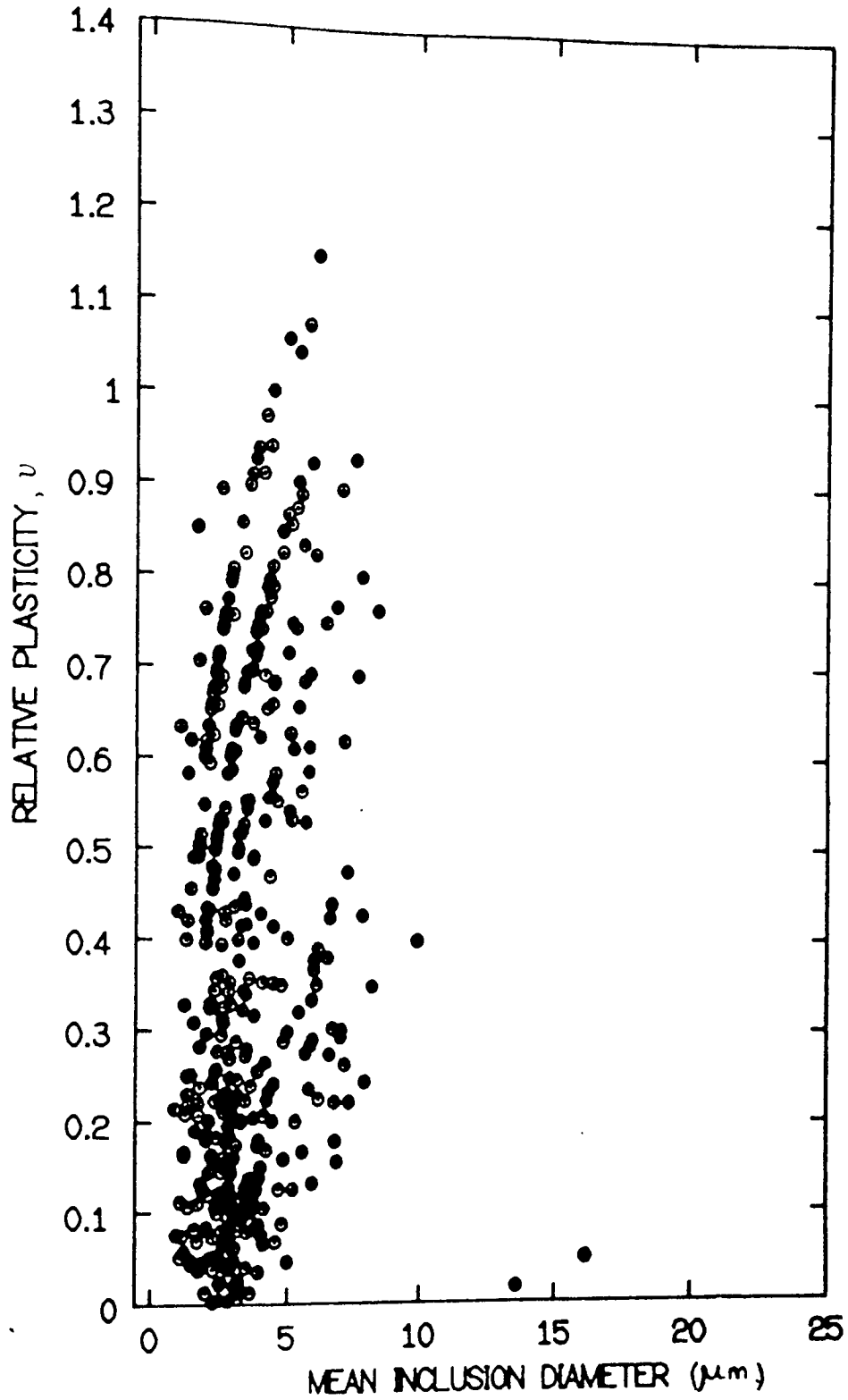
FIGURE 30 RELATIVE PLASTICITY OF THE INCLUSIONS IN THE 0.013% SULPHUR MAGNESIUM TREATED STEEL ROLLED AT 800°C
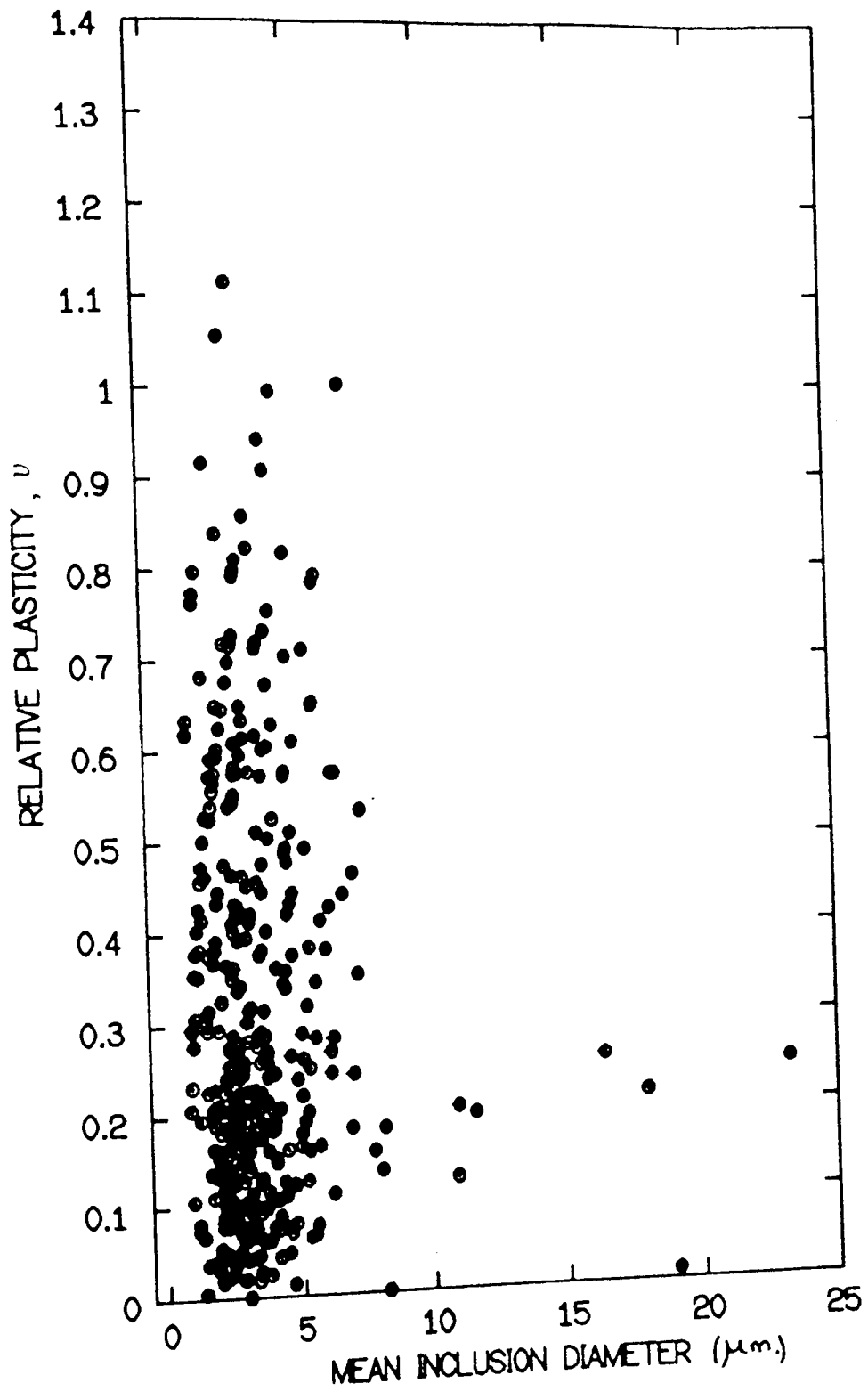
FIGURE 31   RELATIVE PLASTICITY OF THE INCLUSIONS IN THE 0.013% SULPHUR MAGNESIUM TREATED STEEL ROLLED AT 1000°C
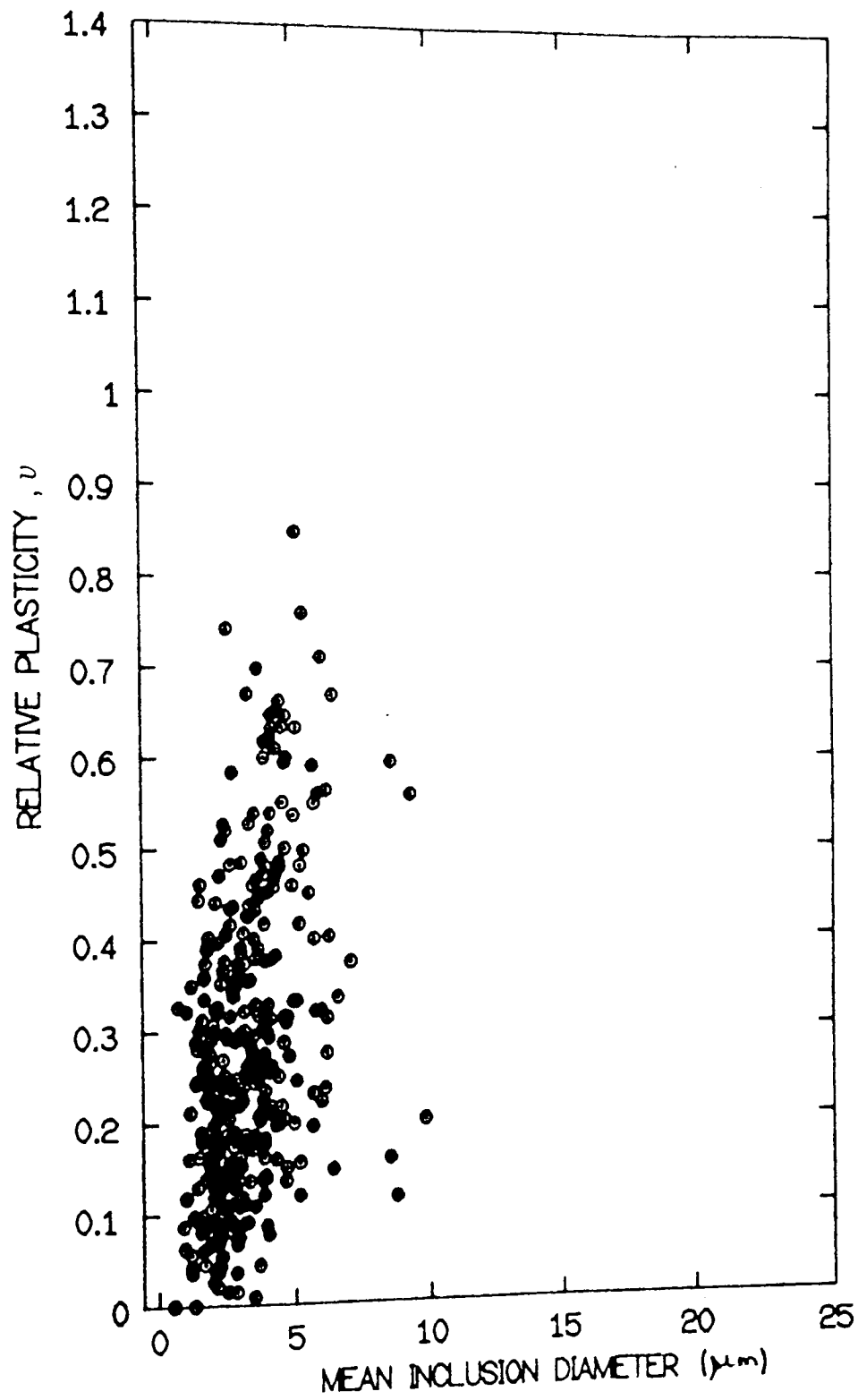
FIGURE 32 RELATIVE PLASTICITY OF THE INCLUSIONS IN THE 0.013% SULPHUR
MAGNESIUM TREATED STEEL ROLLED AT 1200°C
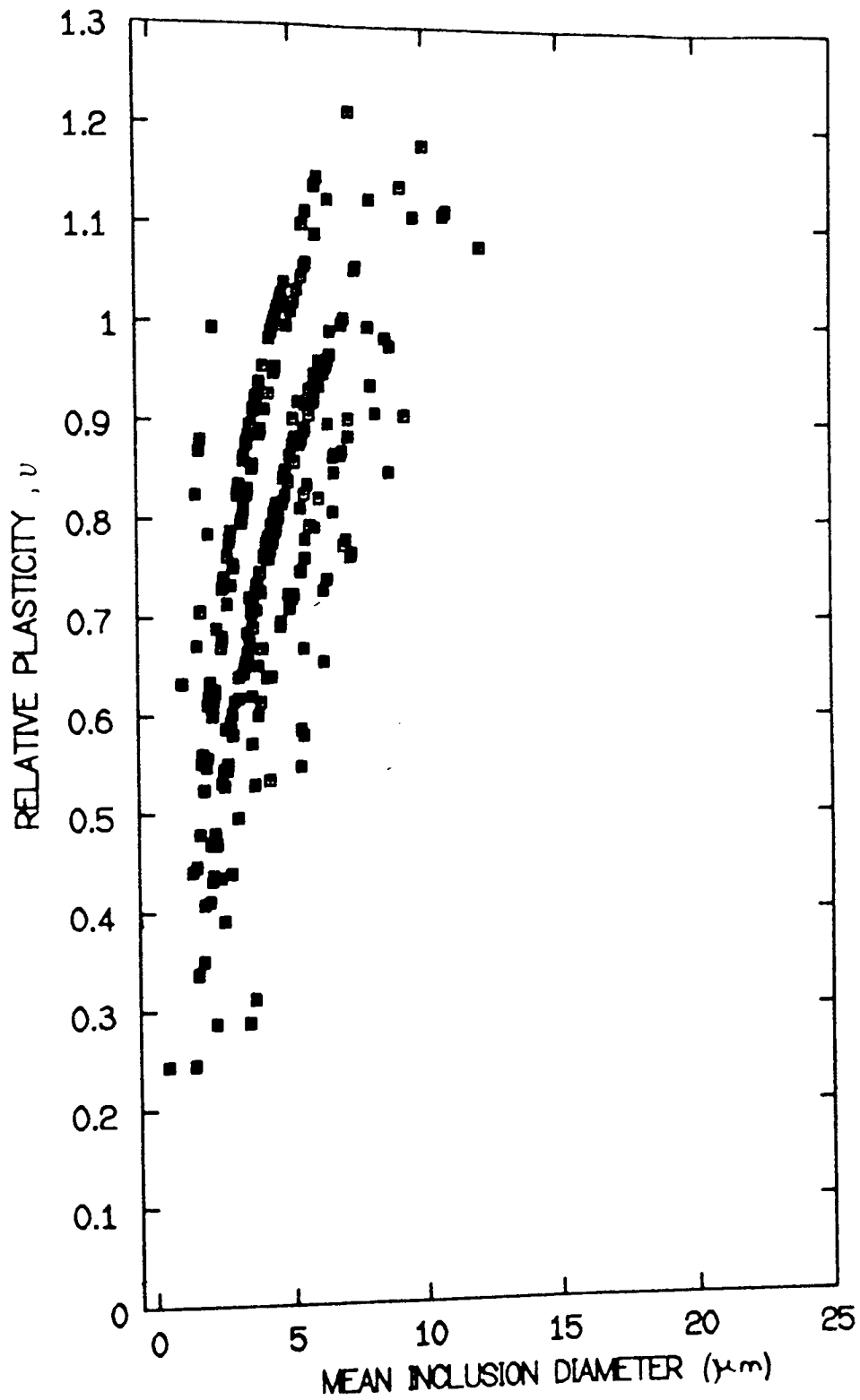
FIGURE 33 RELATIVE PLASTICITY OF THE INCLUSIONS IN THE 0.017% SULPHUR
UNTREATED STEEL ROLLED AT 800°C
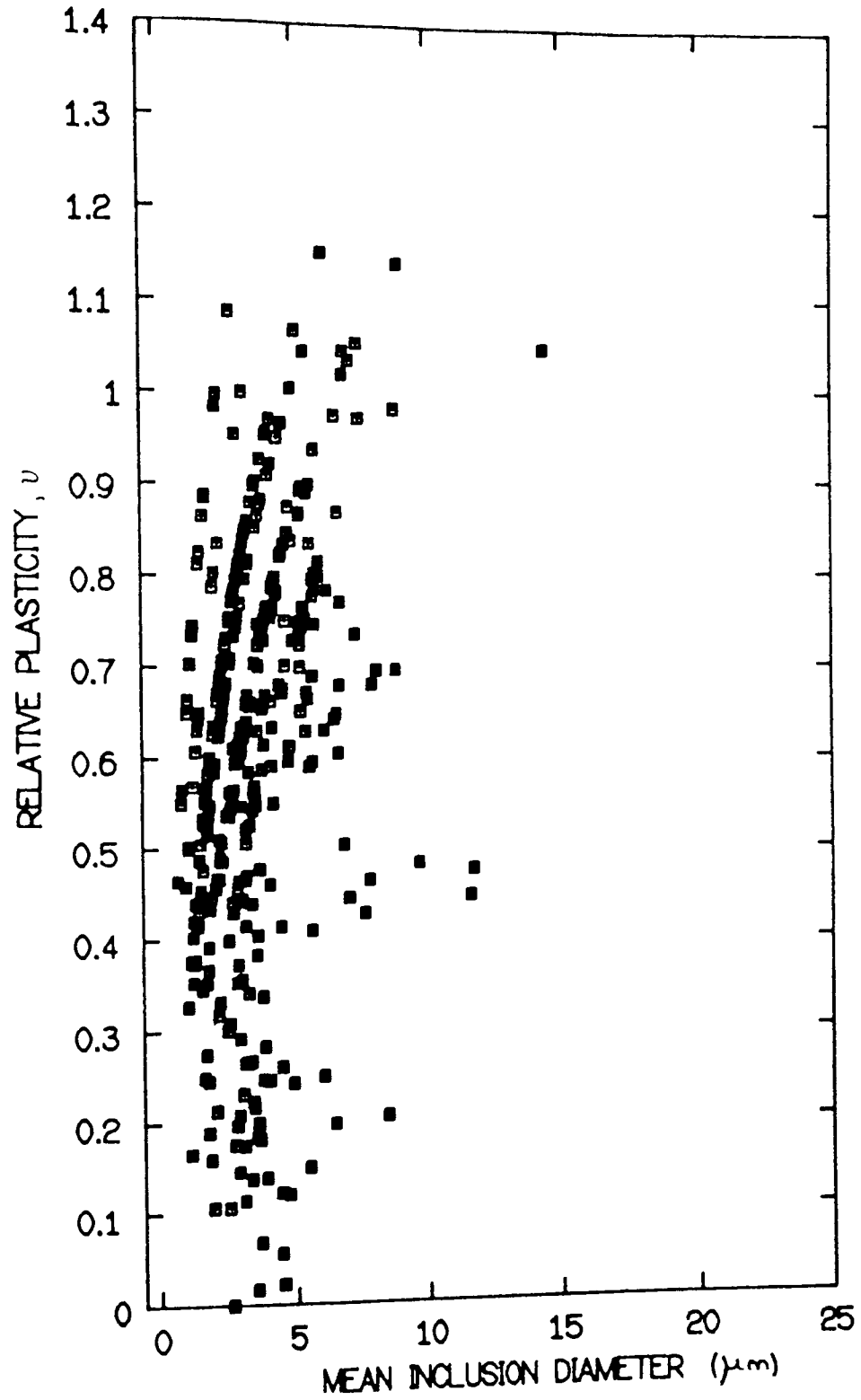
FIGURE 34 RELATIVE PLASTICITY OF THE INCLUSIONS IN THE 0.017% SULPHUR
UNTREATED STEEL ROLLED AT 1000°C
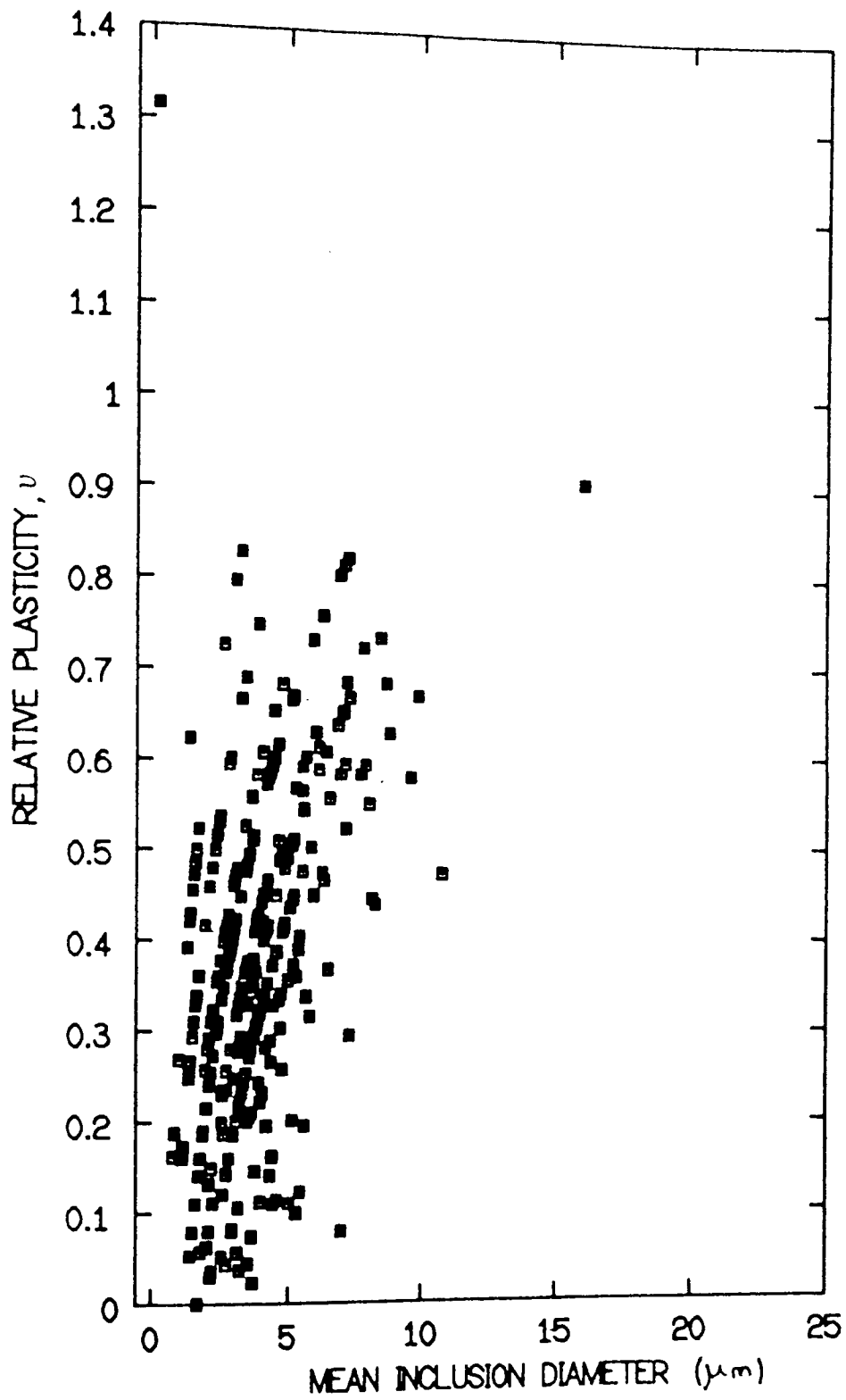
FIGURE 35 RELATIVE PLASTICITY OF THE INCLUSIONS IN THE 0.017% SULPHUR UNTREATED STEEL ROLLED AT 1200°C
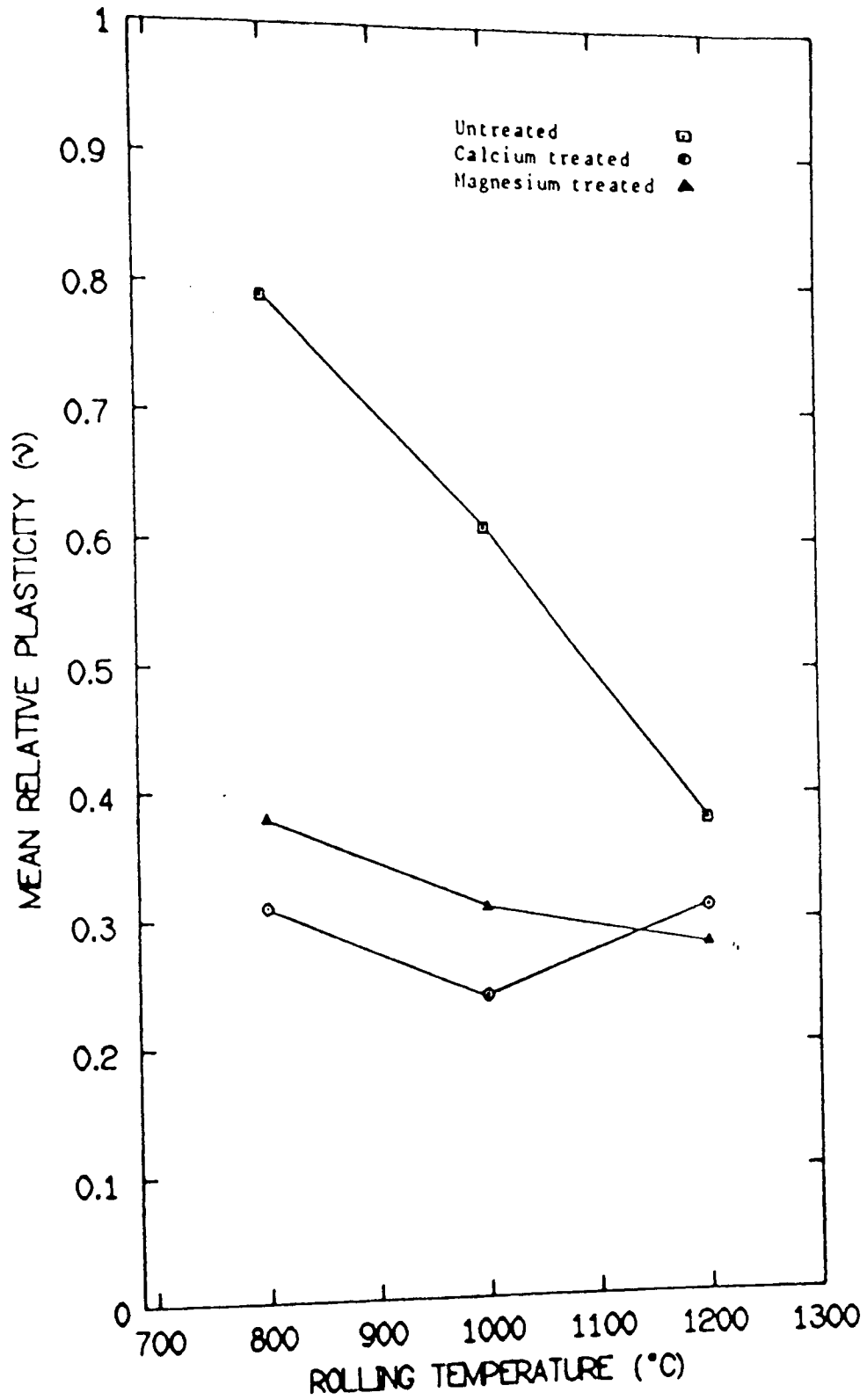
FIGURE 36   Mean relative plasticity versus rolling
temperature
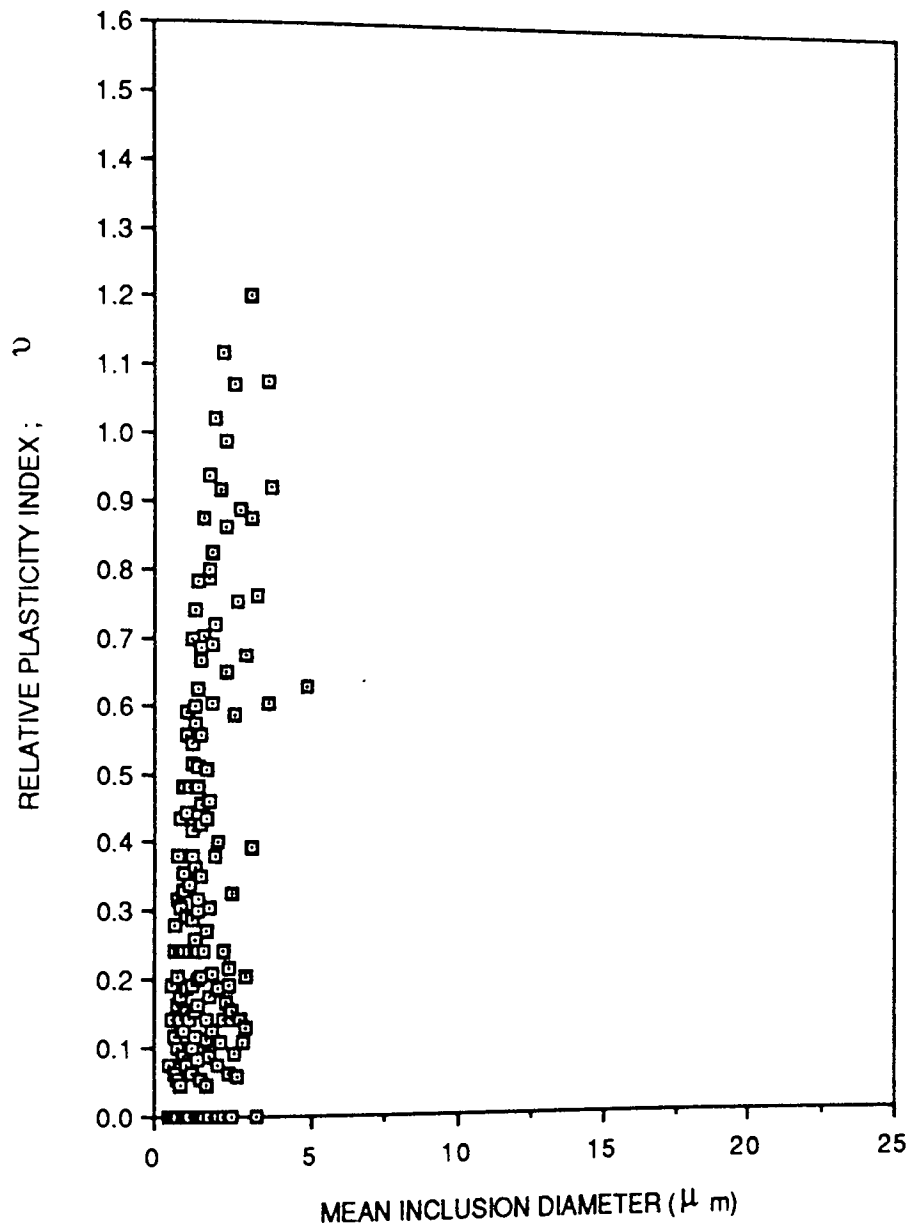
FIGURE 37. RELATIVE PLASTICITY INDEX VERSUS SIZE FOR STEEL 1.
(CONTROLLED ROLLED)
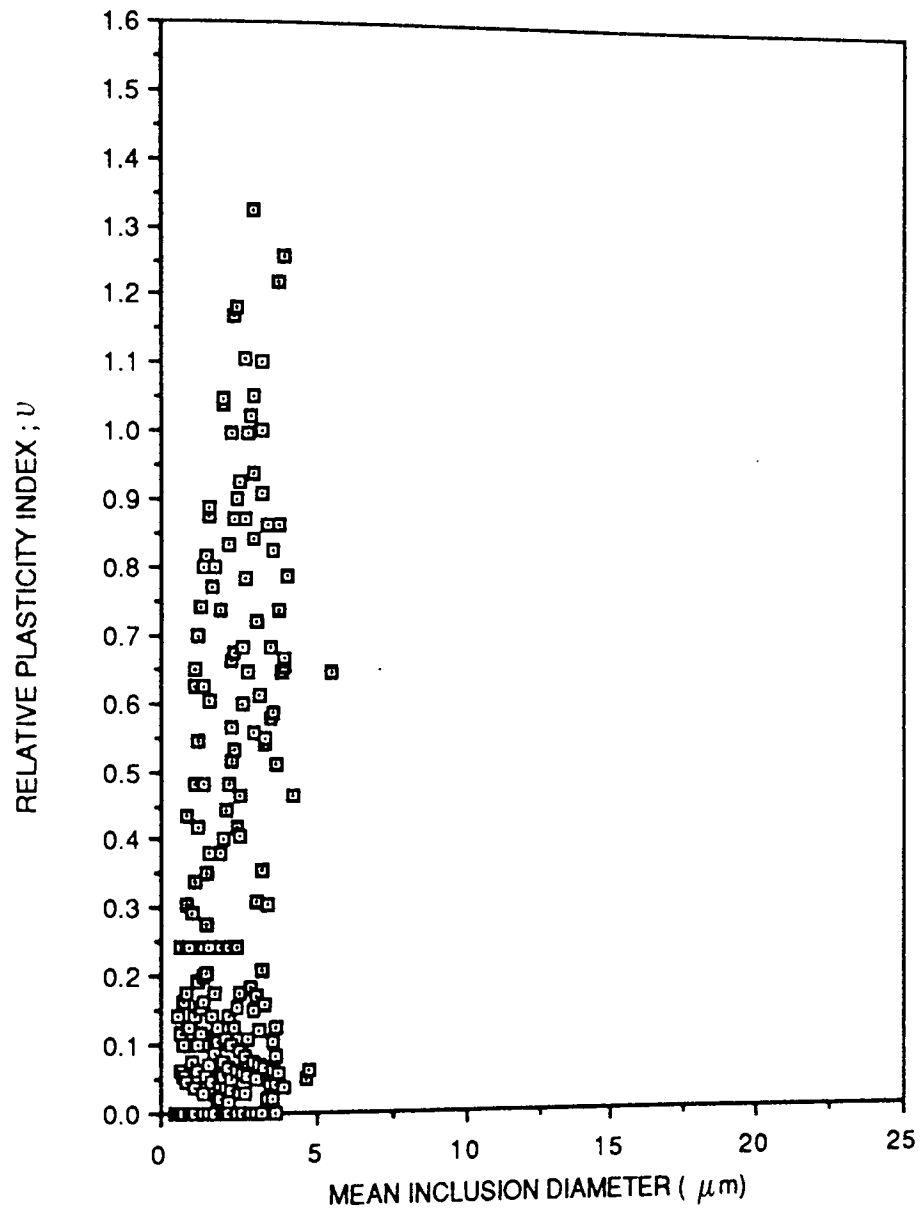
FIGURE 38. RELATIVE PLASTICITY INDEX VERSUS SIZE FOR STEEL 2.
(CONTROLLED ROLLED)
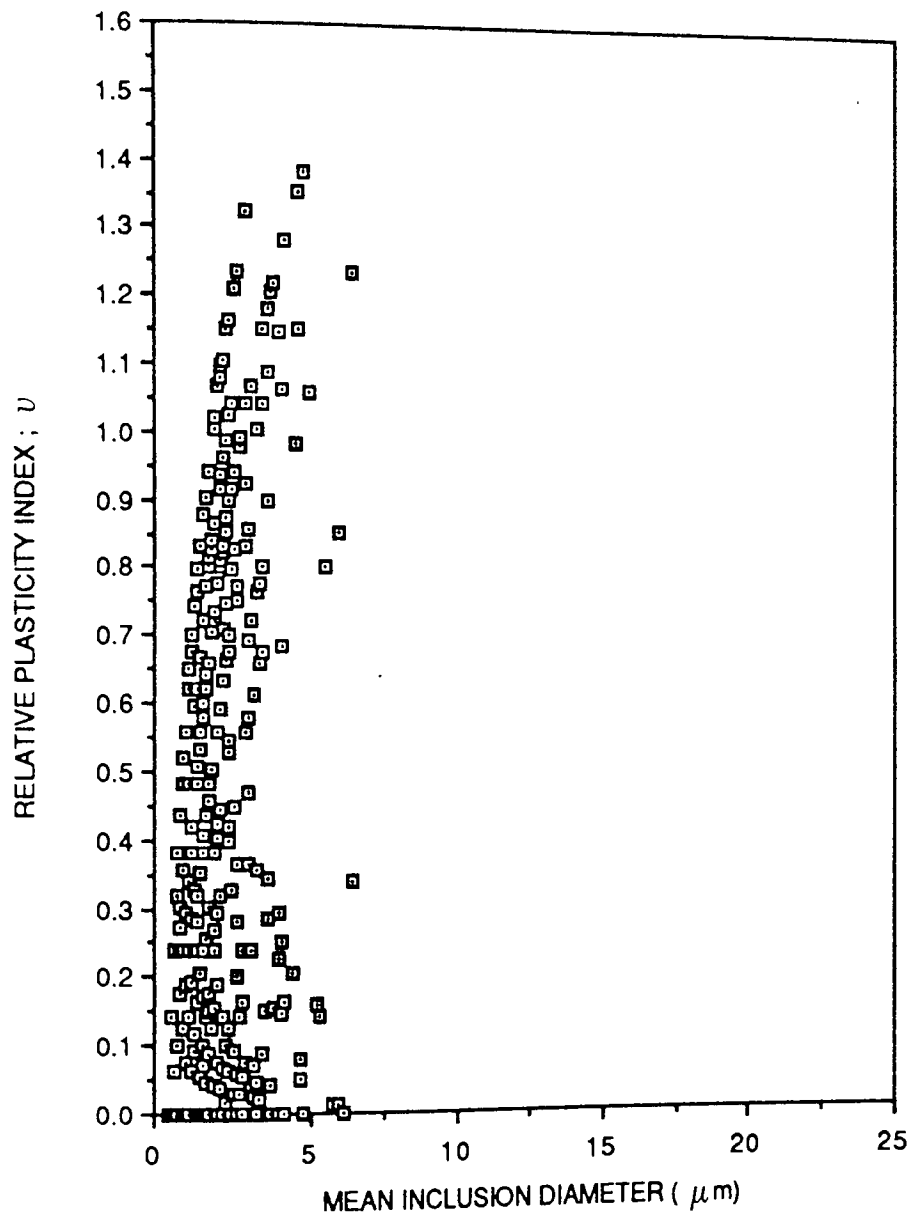
FIGURE 39. RELATIVE PLASTICITY INDEX VERSUS SIZE FOR STEEL 3.
(CONTROLLED ROLLED)
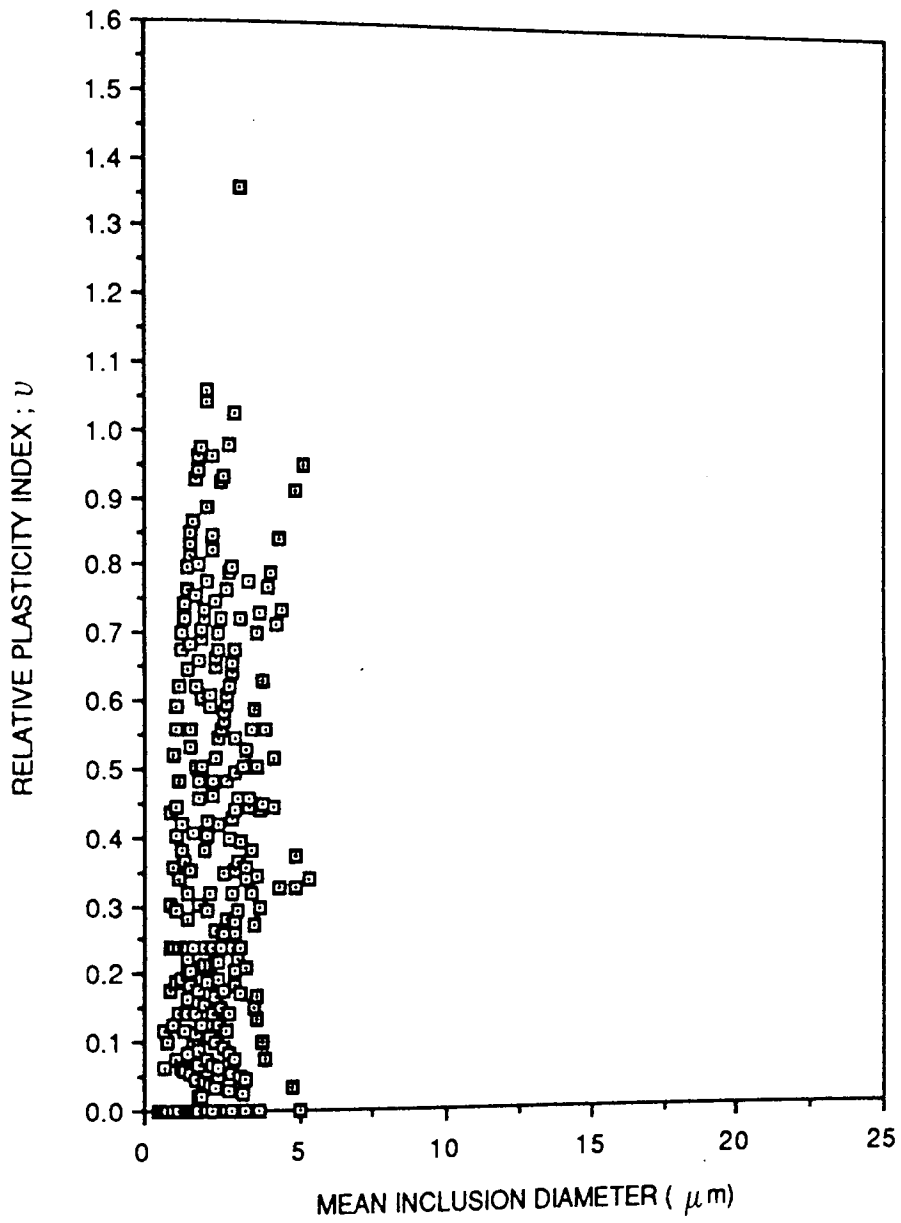
FIGURE 40. RELATIVE PLASTICITY INDEX VERSUS SIZE FOR STEEL 4
(CONTROLLED ROLLED)
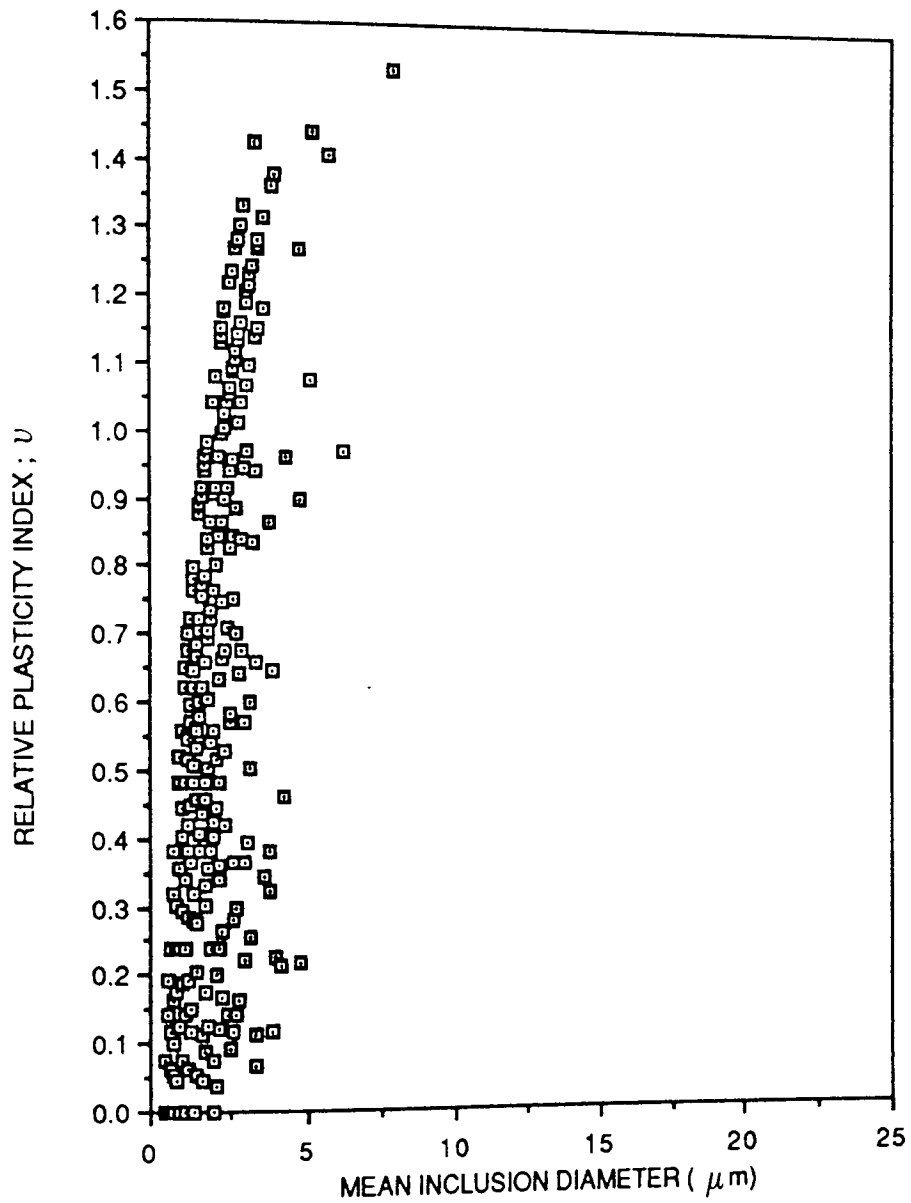
FIGURE 41. RELATIVE PLASTICITY INDEX VERSUS SIZE FOR STEEL 5
(CONTROLLED ROLLED)
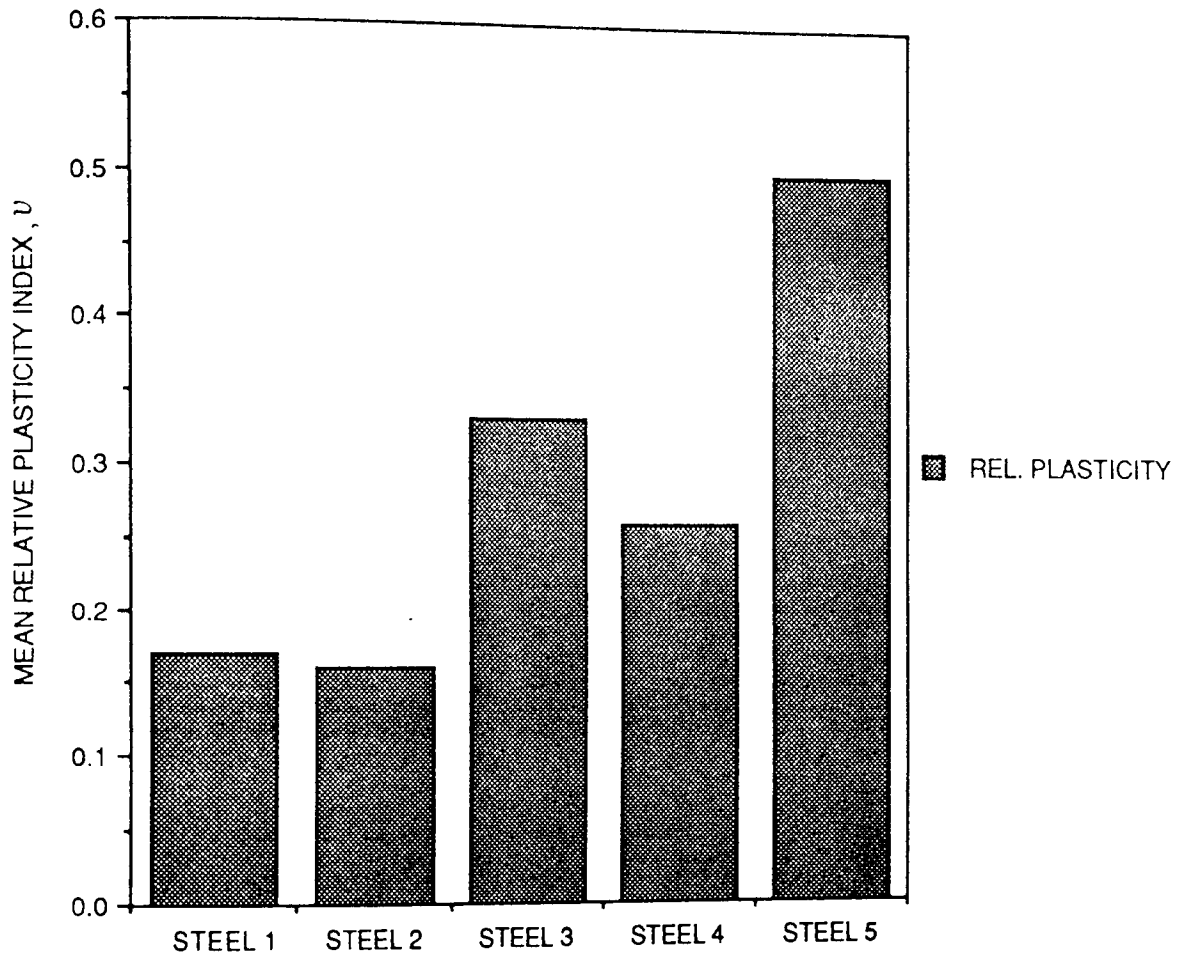
FIGURE 42. MEAN RELATIVE PLASTICITY INDICES FOR STEELS 1- 5 (CONTROLLED ROLLED)
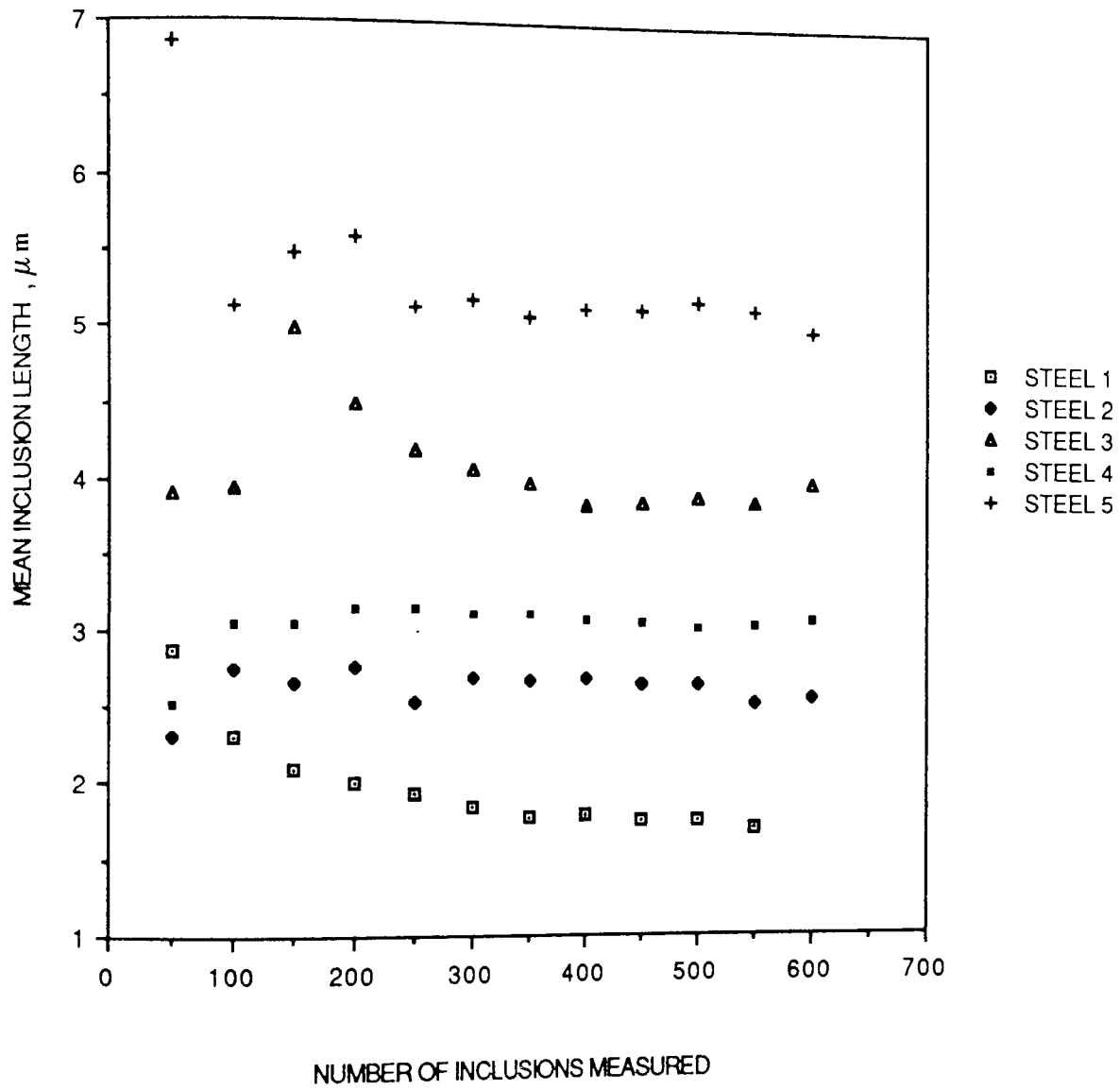
FIGURE 43. MEAN INCLUSION LENGTH VERSUS NUMBER OF INCLUSIONS MEASURED FOR STEELS 1-5.
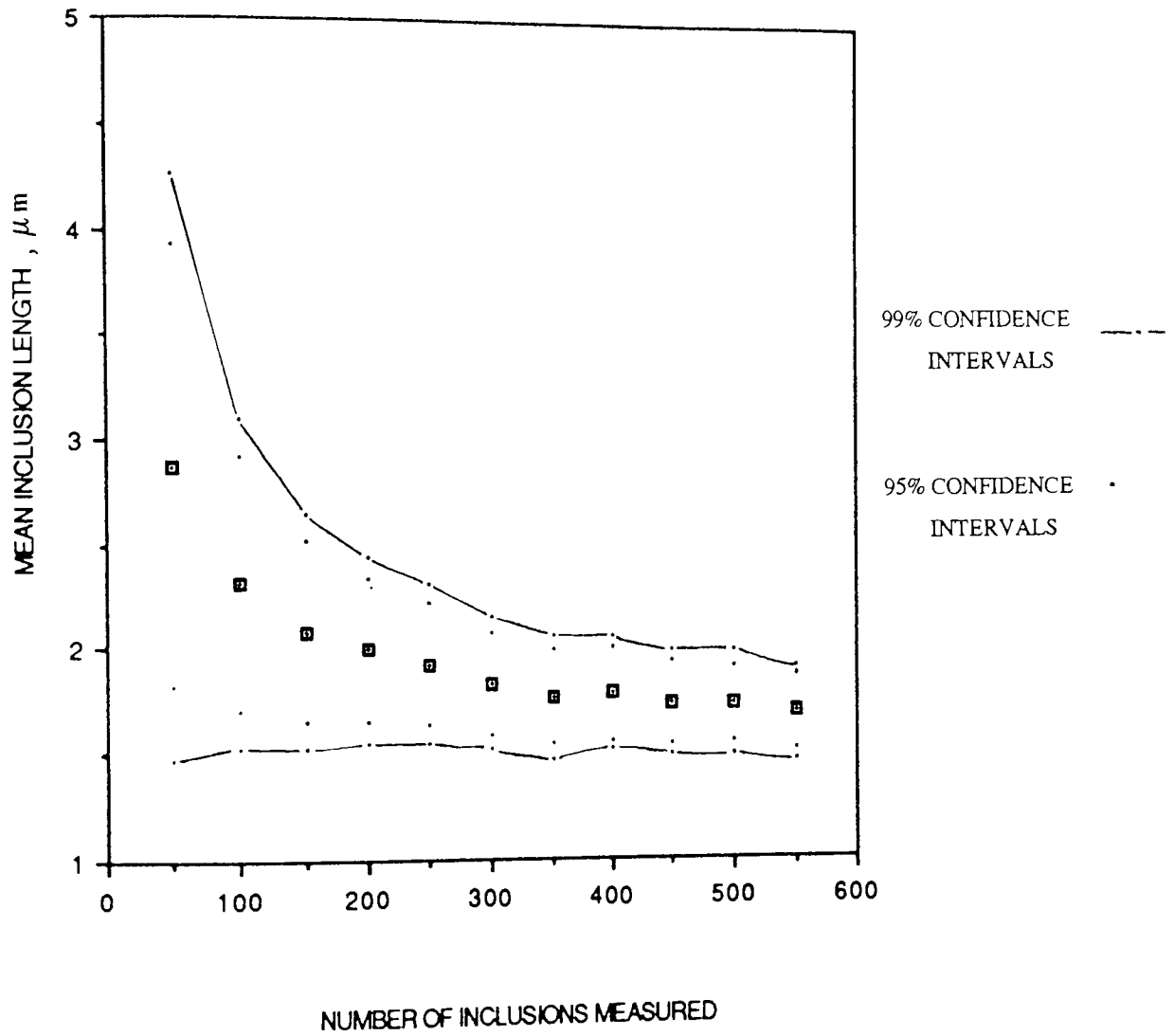
FIGURE 44. MEAN INCLUSION LENGTH VERSUS NUMBER OF INCLUSIONS MEASURED FOR STEEL 1
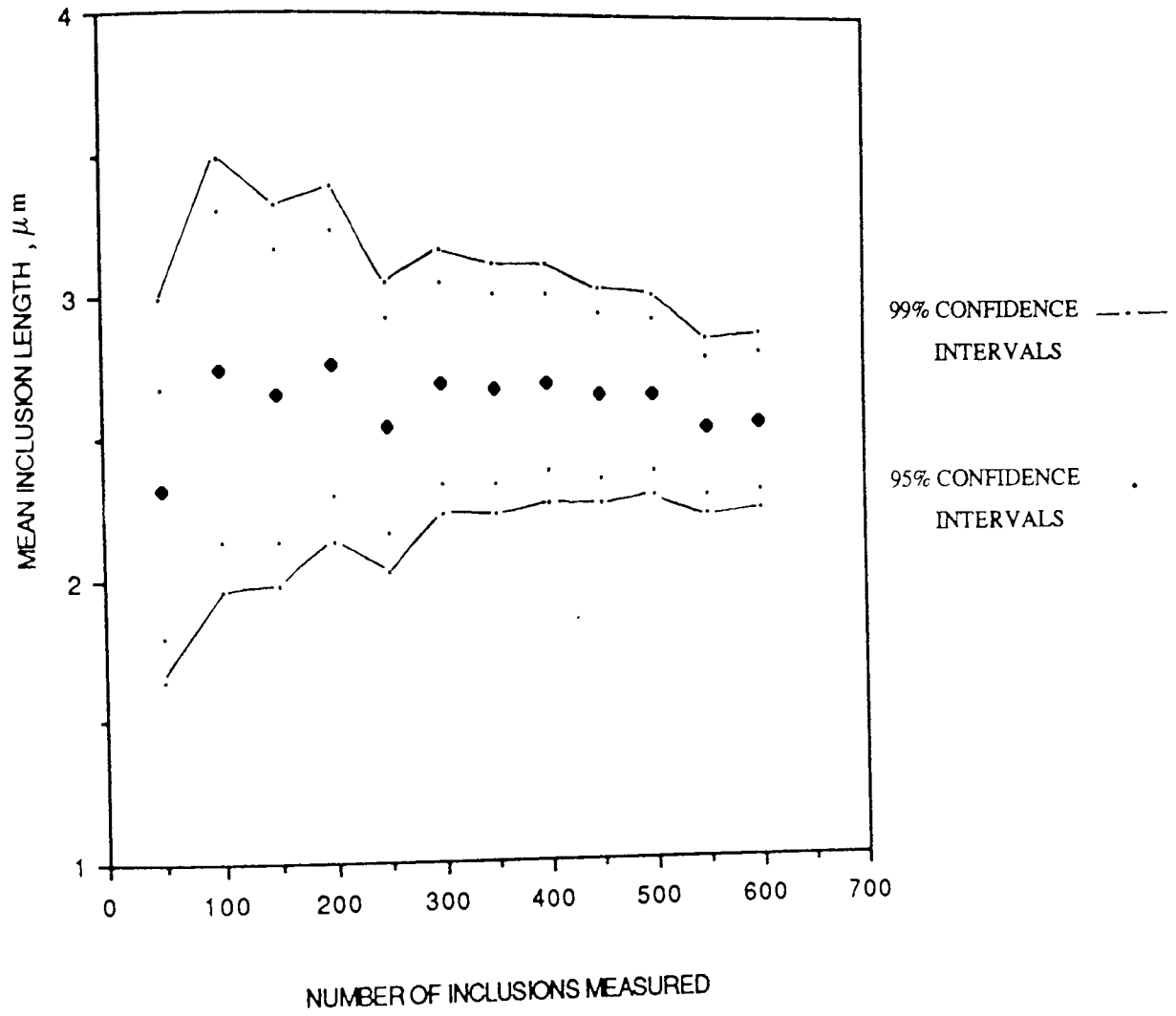
FIGURE 45. MEAN INCLUSION LENGTH VERSUS NUMBER OF INCLUSIONS MEASURED FOR STEEL 2.
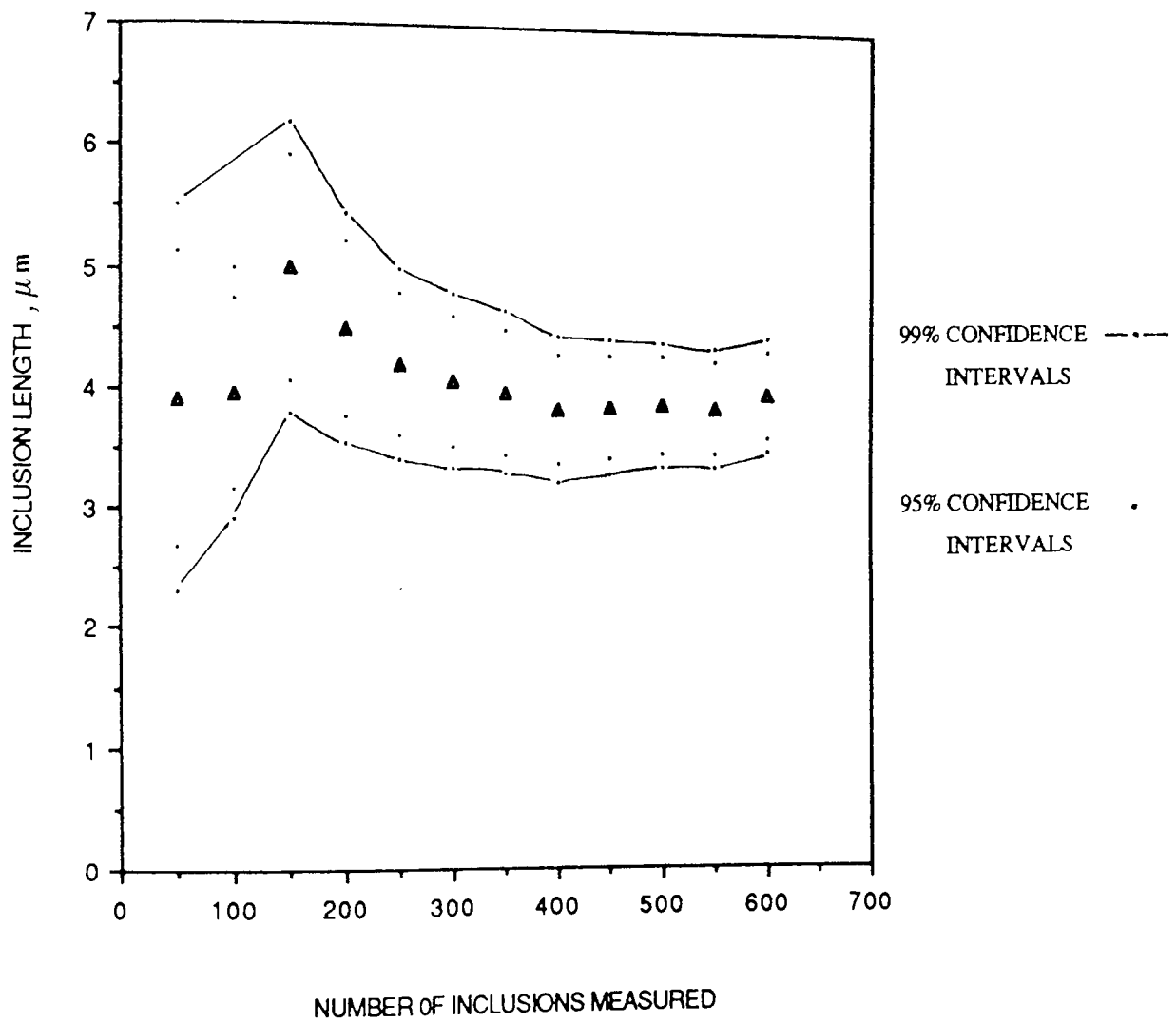
FIGURE 46. MEAN INCLUSION LENGTH VERSUS NUMBER OF INCLUSIONS MEASURED IN STEEL 3.
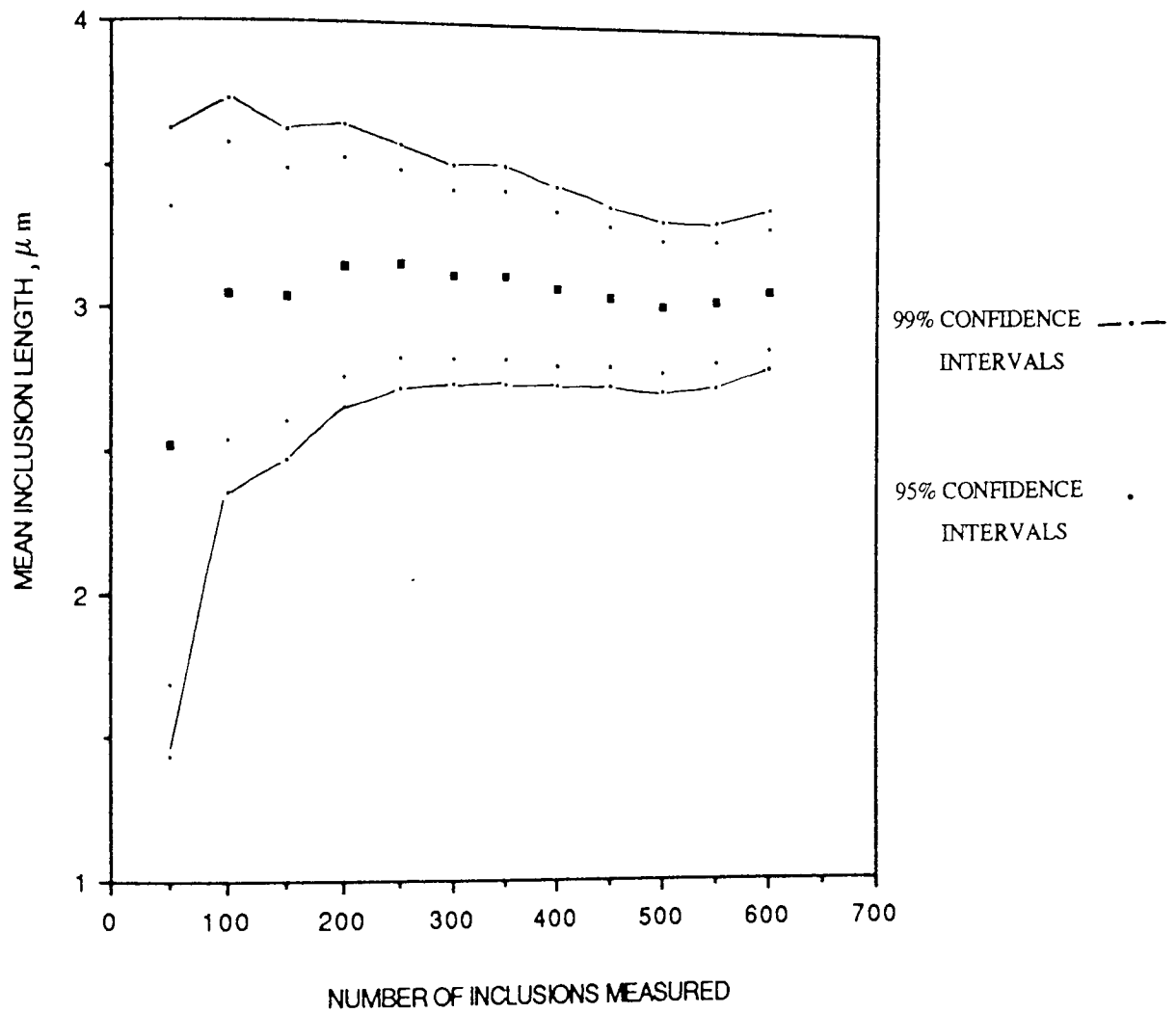
FIGURE 47. MEAN INCLUSION LENGTH VERSUS NUMBER OF INCLUSIONS MEASURED IN STEEL 4.
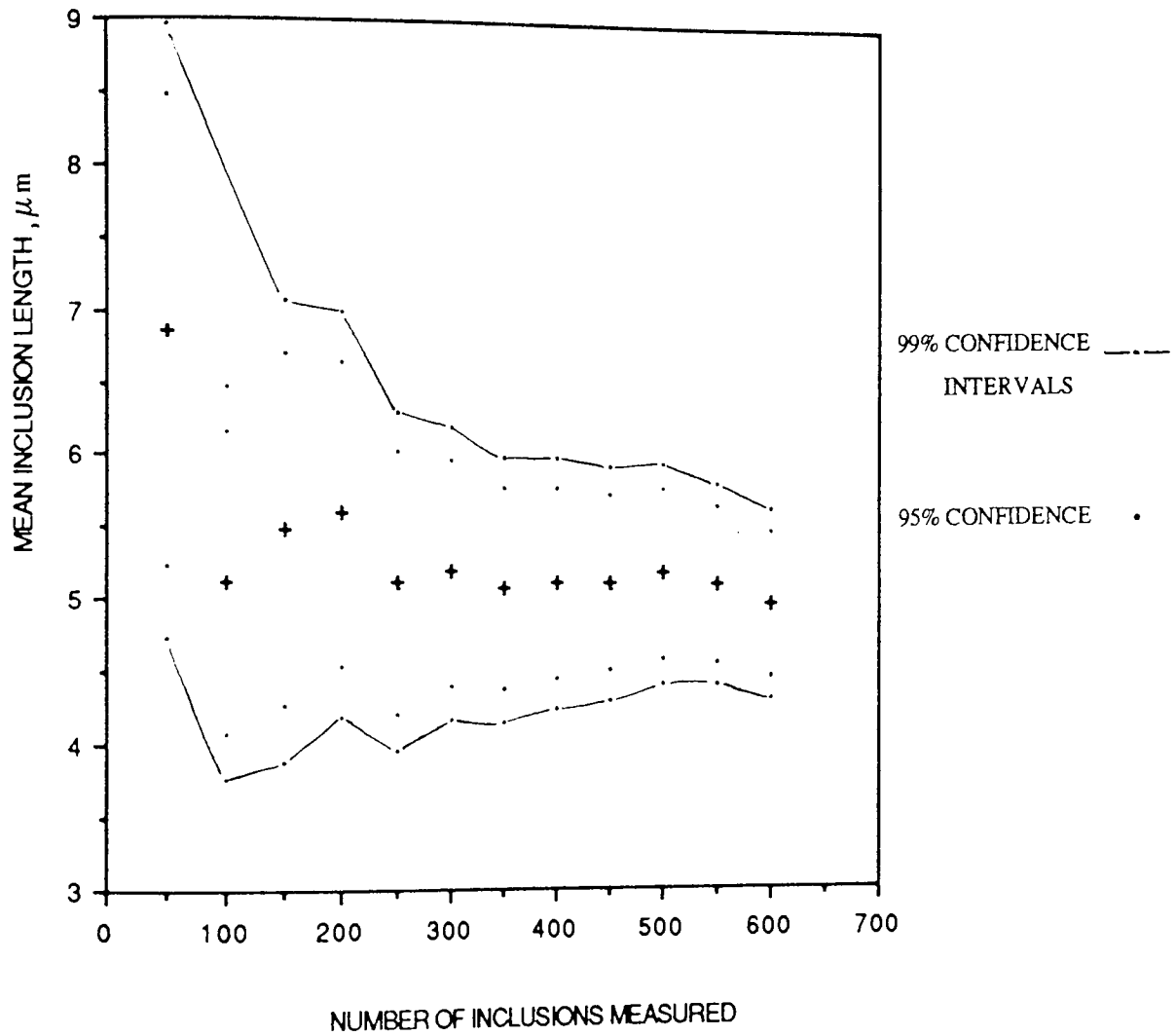
FIGURE 48. MEAN INCLUSION LENGTH VERSUS NUMBER OF INCLUSIONS MEASURED FOR STEEL 5.
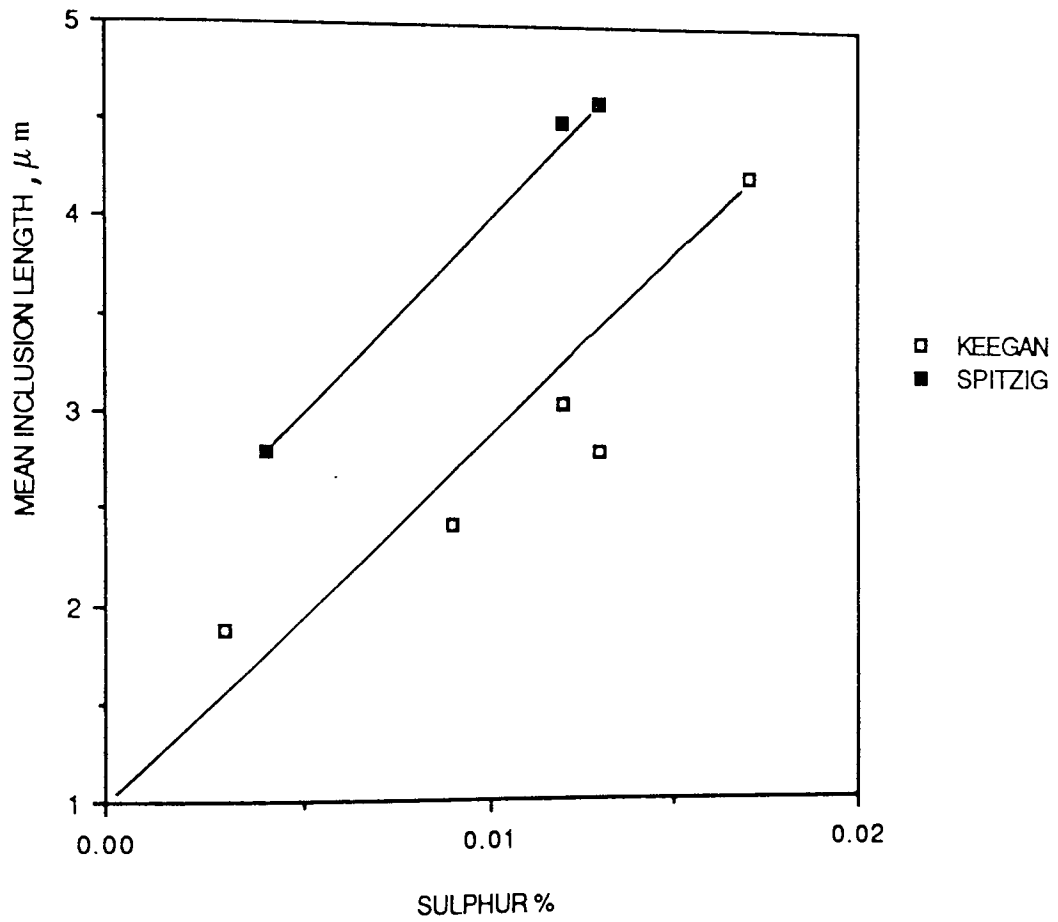
FIGURE 49. MEAN INCLUSION LENGTH VERSUS SULPHUR CONTENT
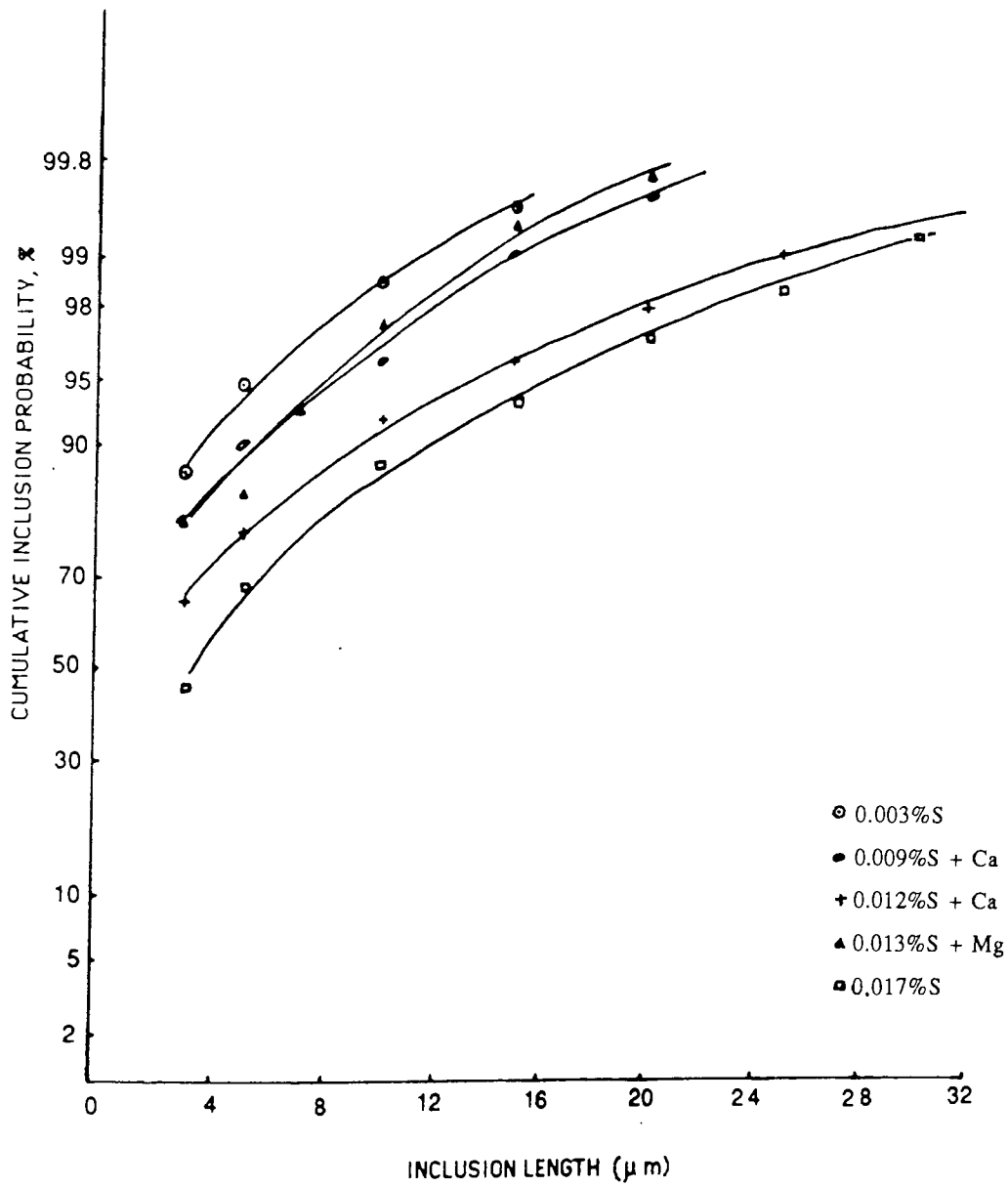
FIGURE 50. CUMULATIVE INCLUSION LENGTH DISTRIBUTION FOR STEELS 1-5
FROM THE PHOTOGRAPHIC ASSESSMENT DATA
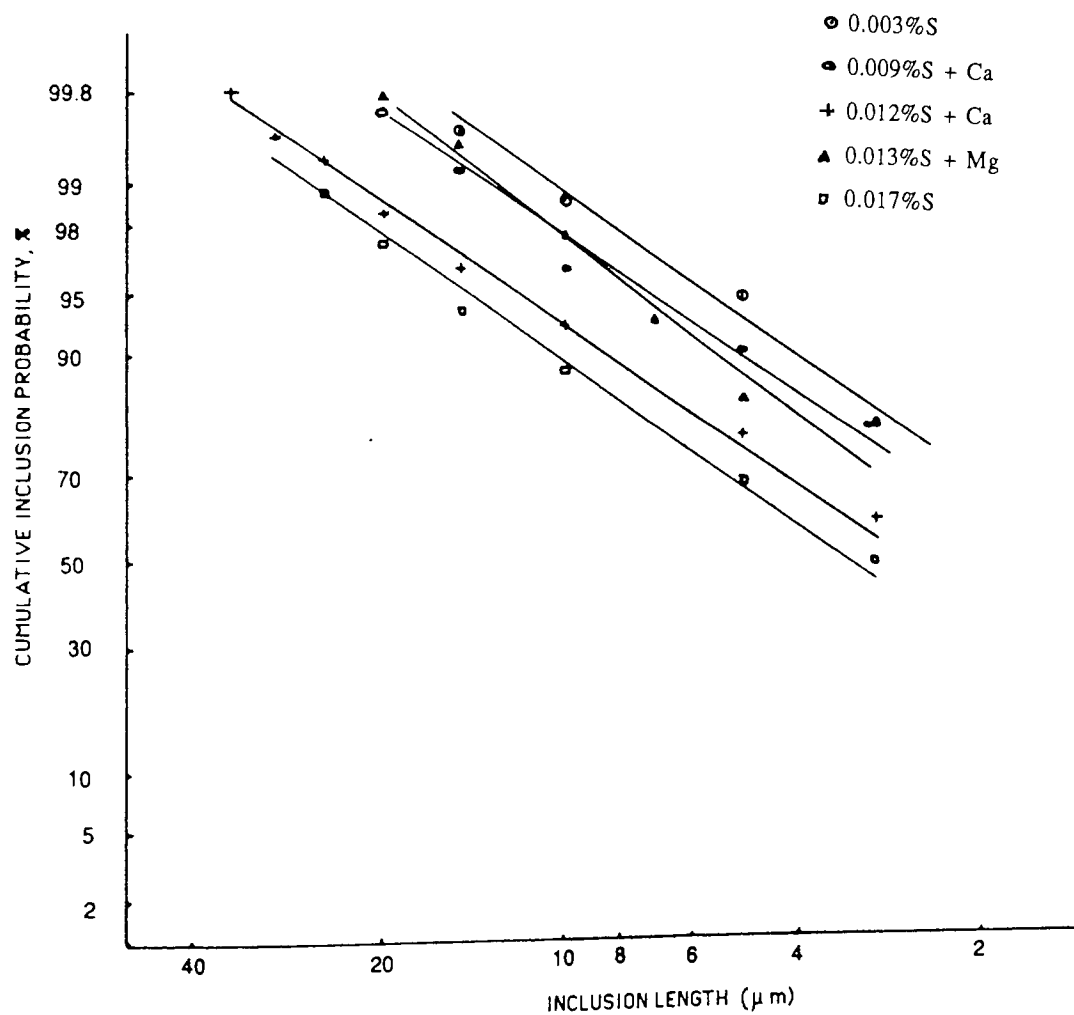
FIGURE 51. CUMULATIVE INCLUSION LENGTH DISTRIBUTION FOR STEELS 1-5
FROM THE PHOTOGRAPHIC ASSESSMENT DATA
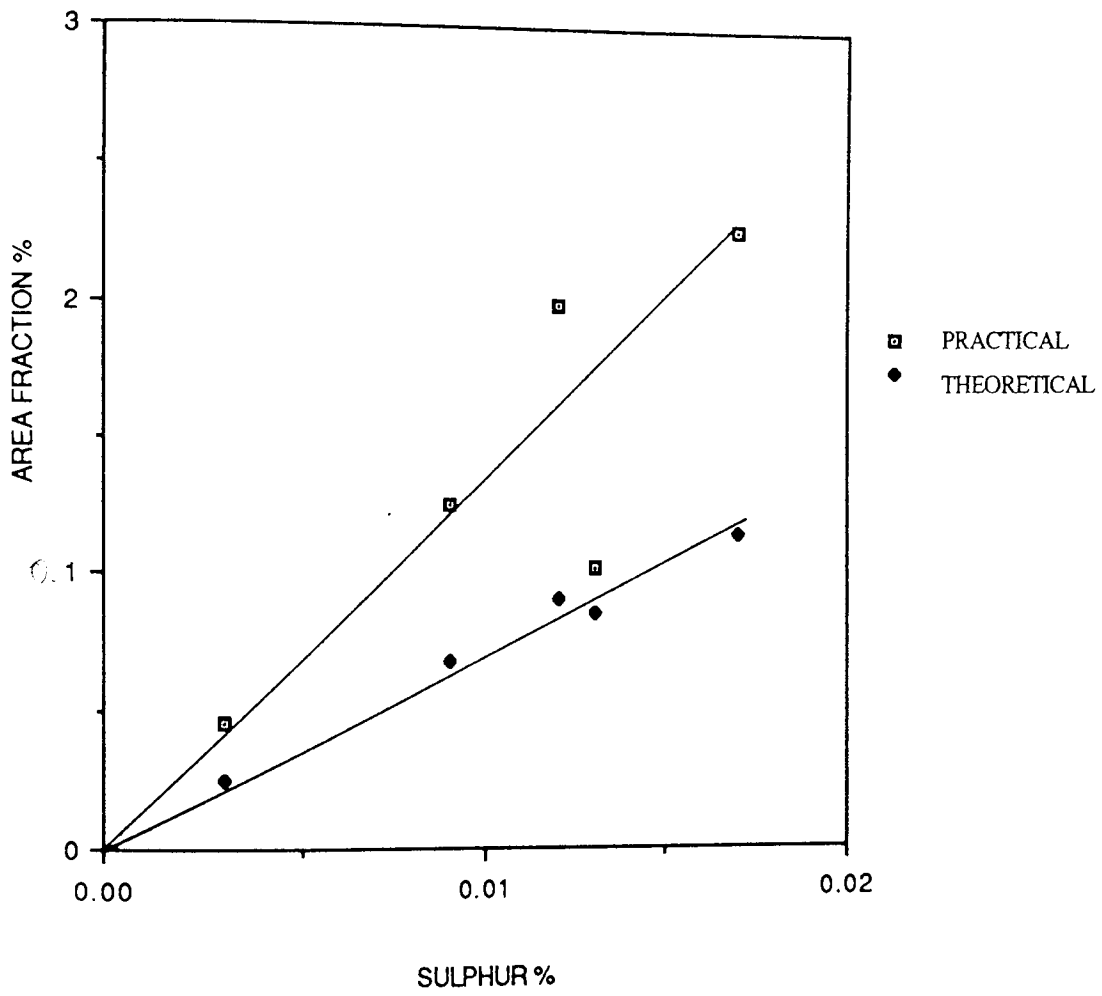
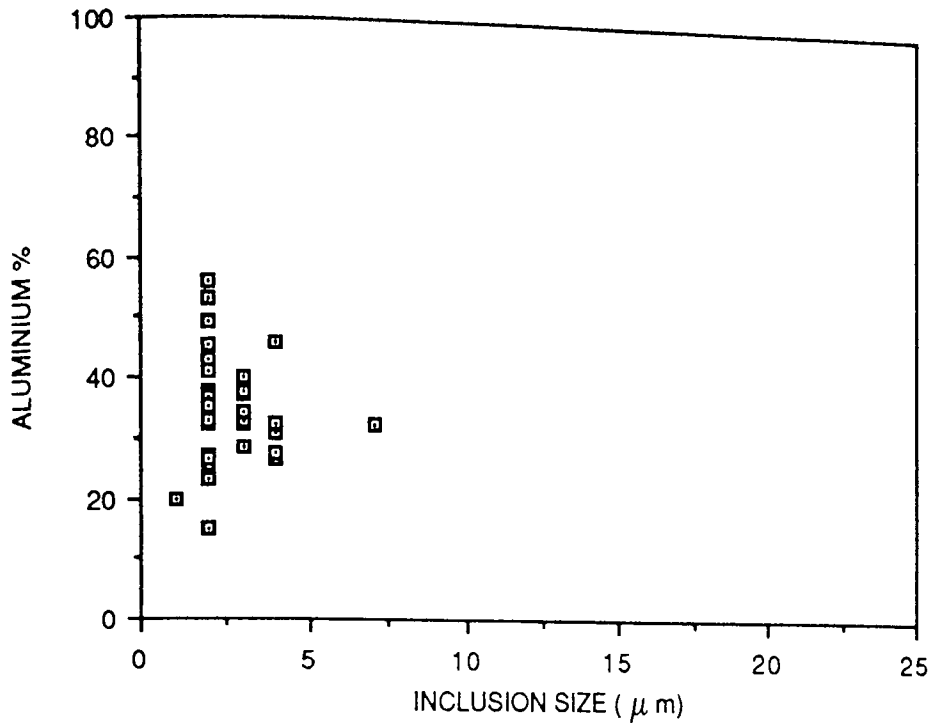FIGURE 52. INCLUSION AREA FRACTION VERSUS STEEL SULPHUR CONTENT
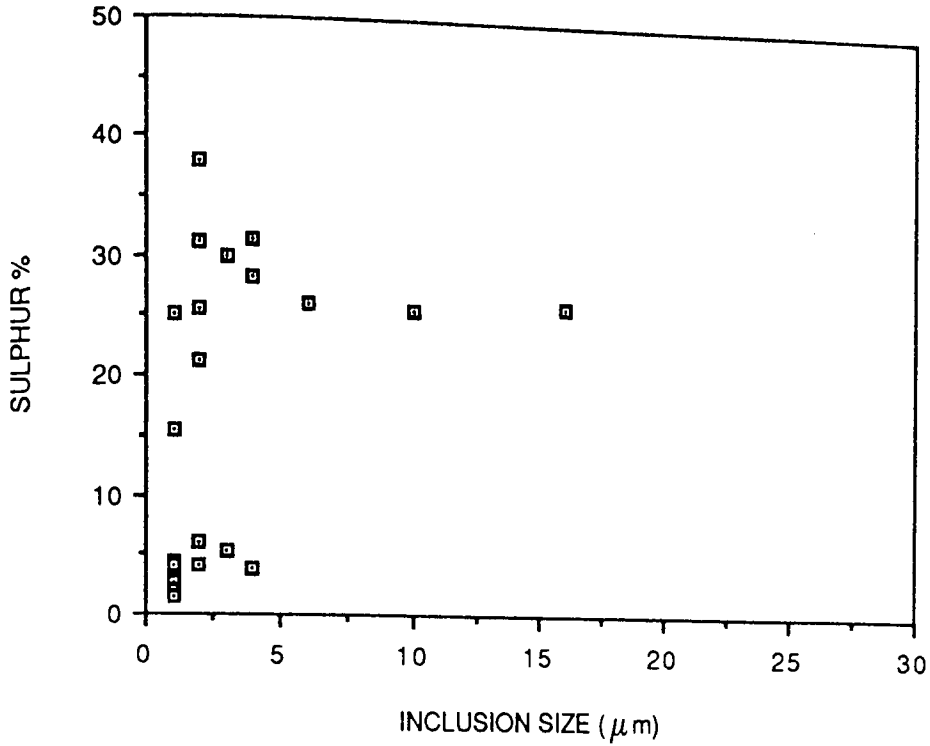
FIGURE 53. INCLUSION SIZE VERSUS SULPHUR CONTENT FOR STEEL 1.
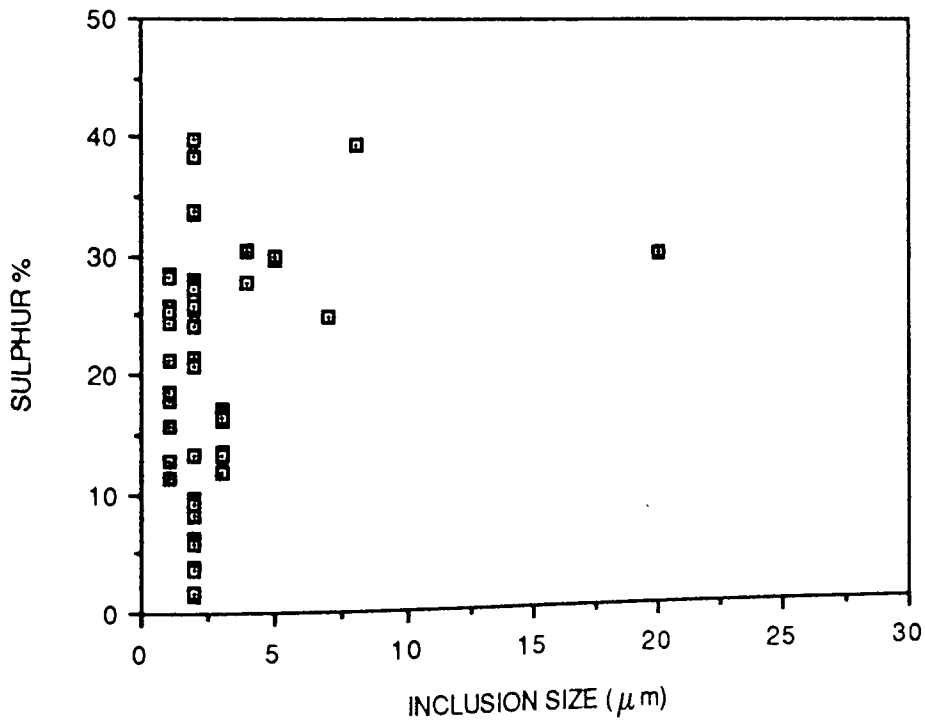
FIGURE 54. INCLUSION SIZE VERSUS SULPHUR CONTENT FOR STEEL 2.
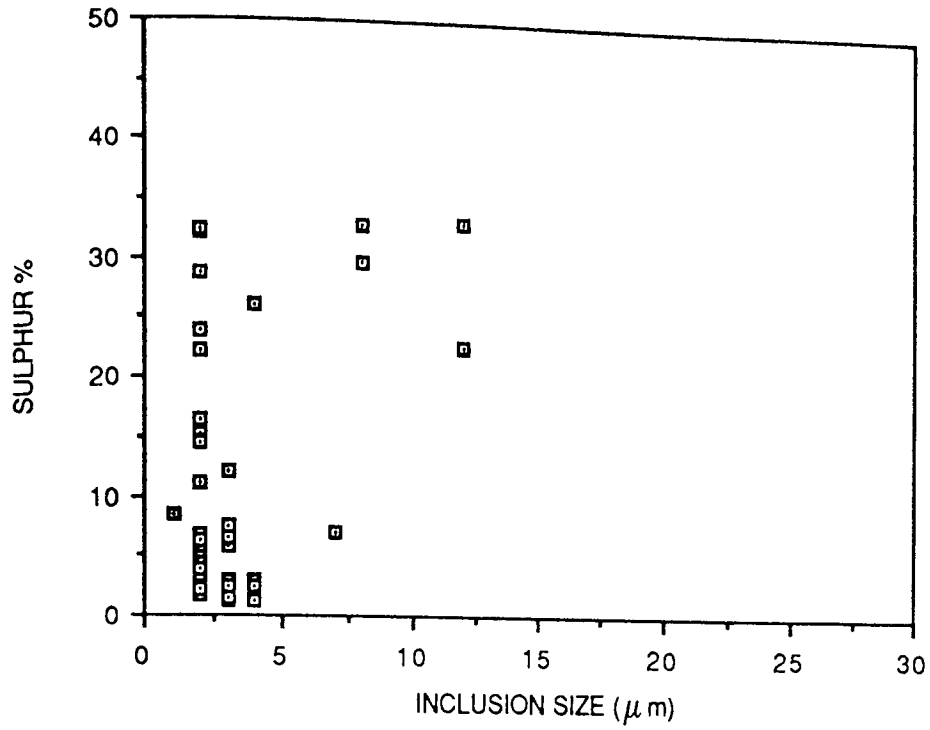
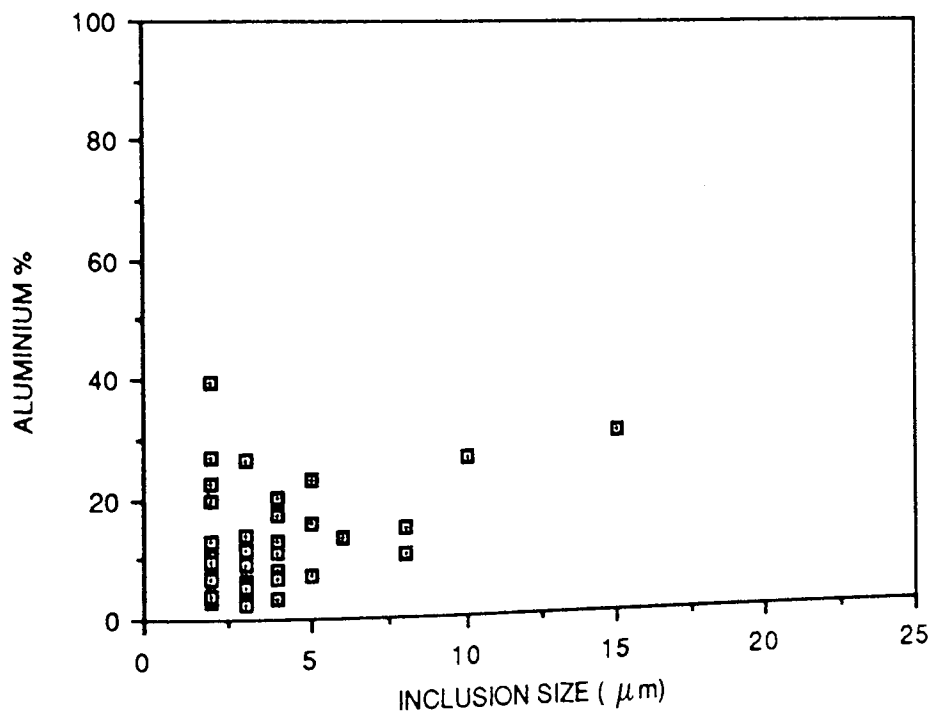FIGURE 55. INCLUSION SIZE VERSUS SULPHUR CONTENT FOR STEEL 3.
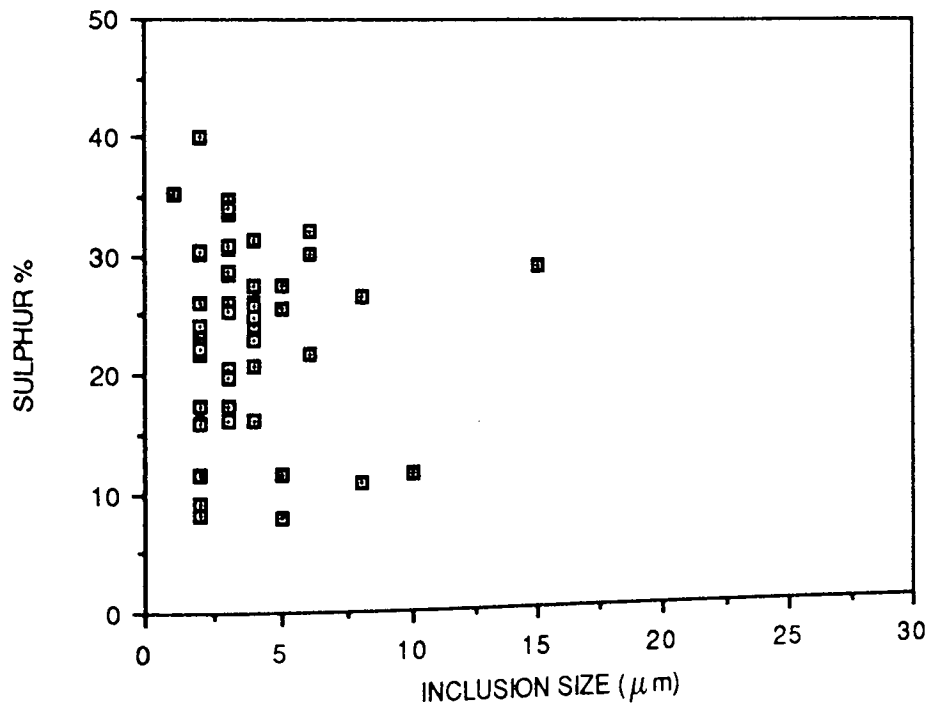
FIGURE 56. INCLUSION SIZE VERSUS SULPHUR CONTENT FOR STEEL 4.

FIGURE 57. INCLUSION SIZE VERSUS SULPHUR CONTENT FOR STEEL 5.

SHAPE	CATEGORY
1	ROUND
2	S. DEFORMED
3	EYESHAPED/TAILED
4	STRINGERED

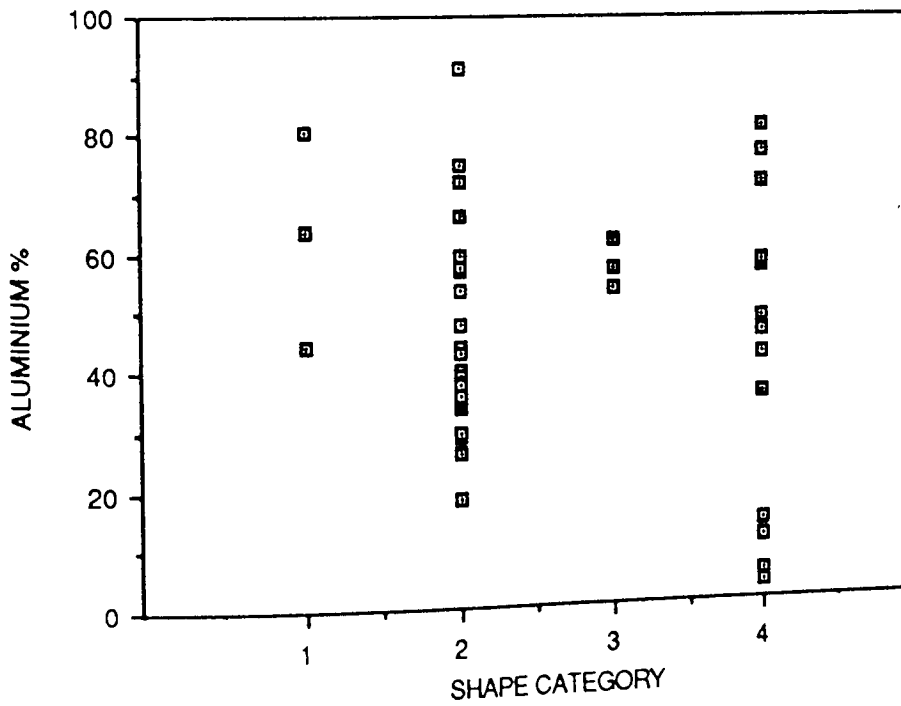FIGURE 58. INCLUSION SHAPE VERSUS SULPHUR CONTENT FOR STEEL 1.
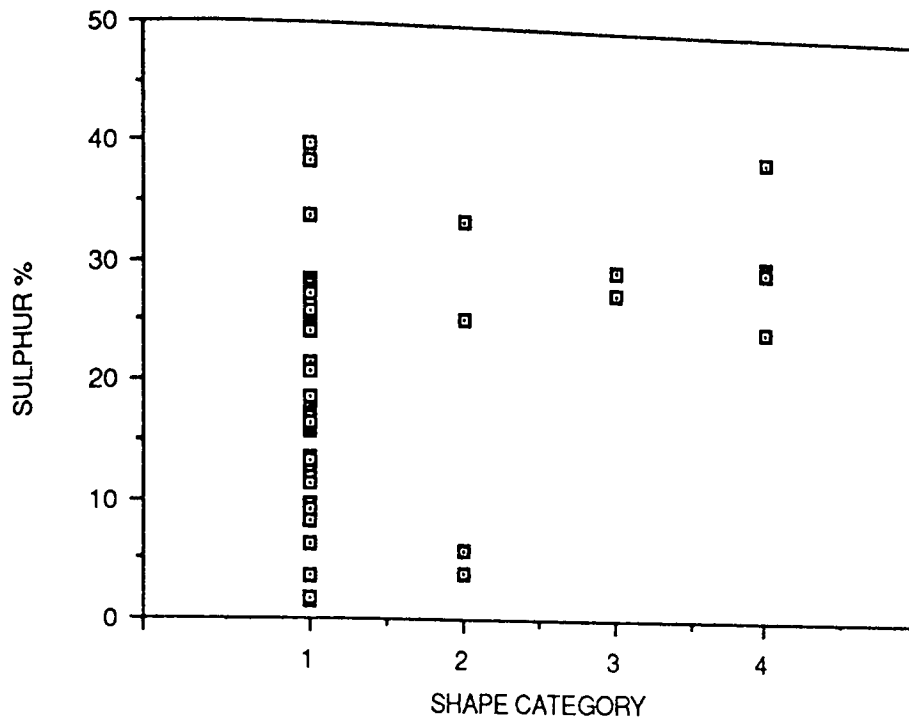
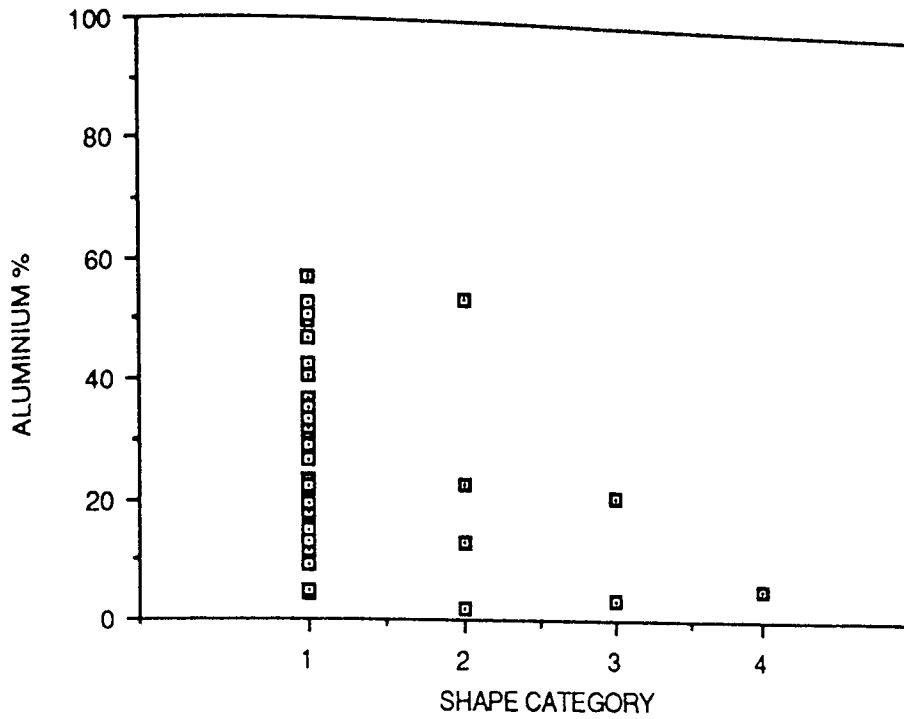FIGURE 59. INCLUSION SHAPE VERSUS SULPHUR CONTENT FOR STEEL 2.
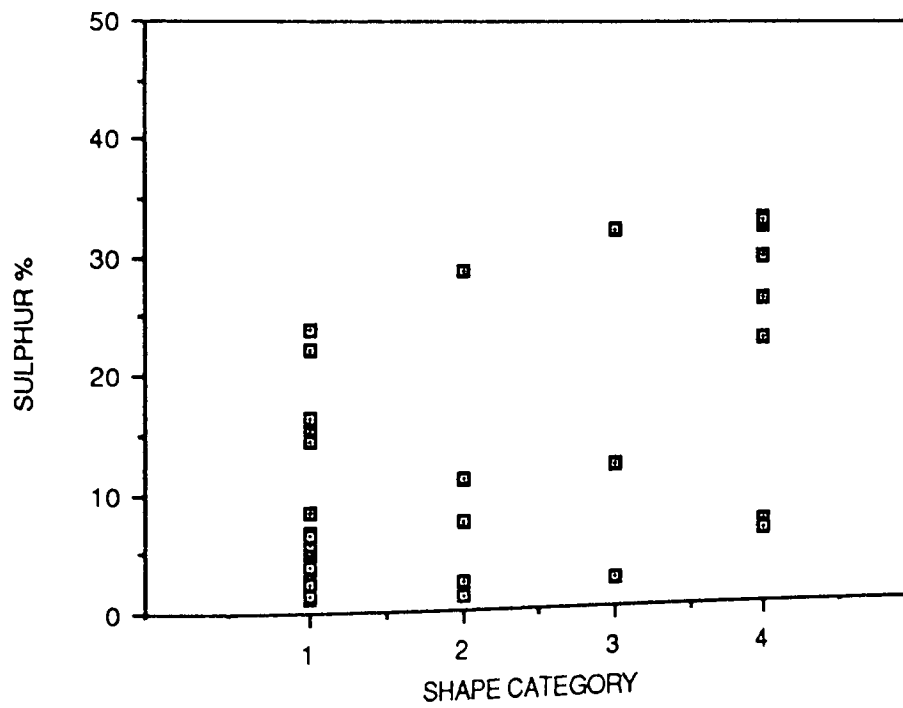
FIGURE 60. INCLUSION SHAPE VERSUS SULPHUR CONTENT FOR STEEL 3.
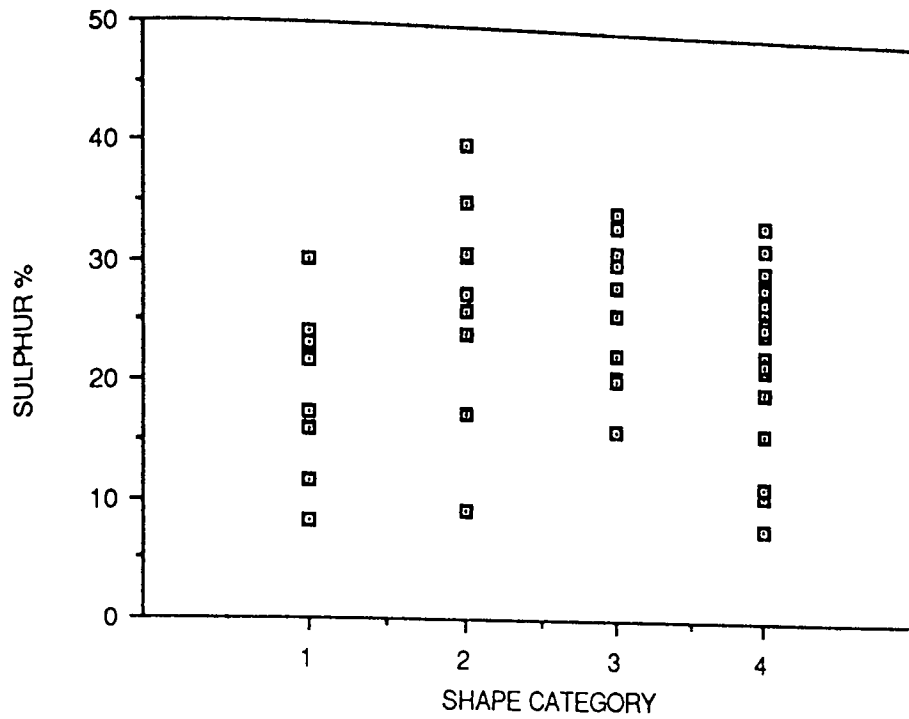
FIGURE 61. INCLUSION SHAPE VERSUS SULPHUR CONTENT FOR STEEL 4.
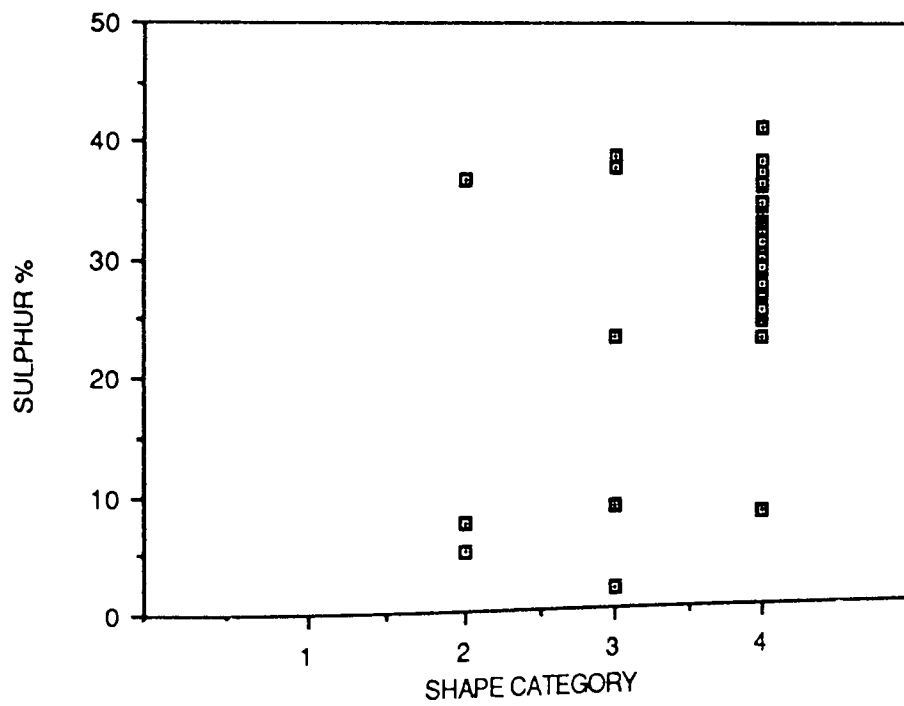
FIGURE 62. INCLUSION SHAPE VERSUS SULPHUR CONTENT FOR STEEL 5.
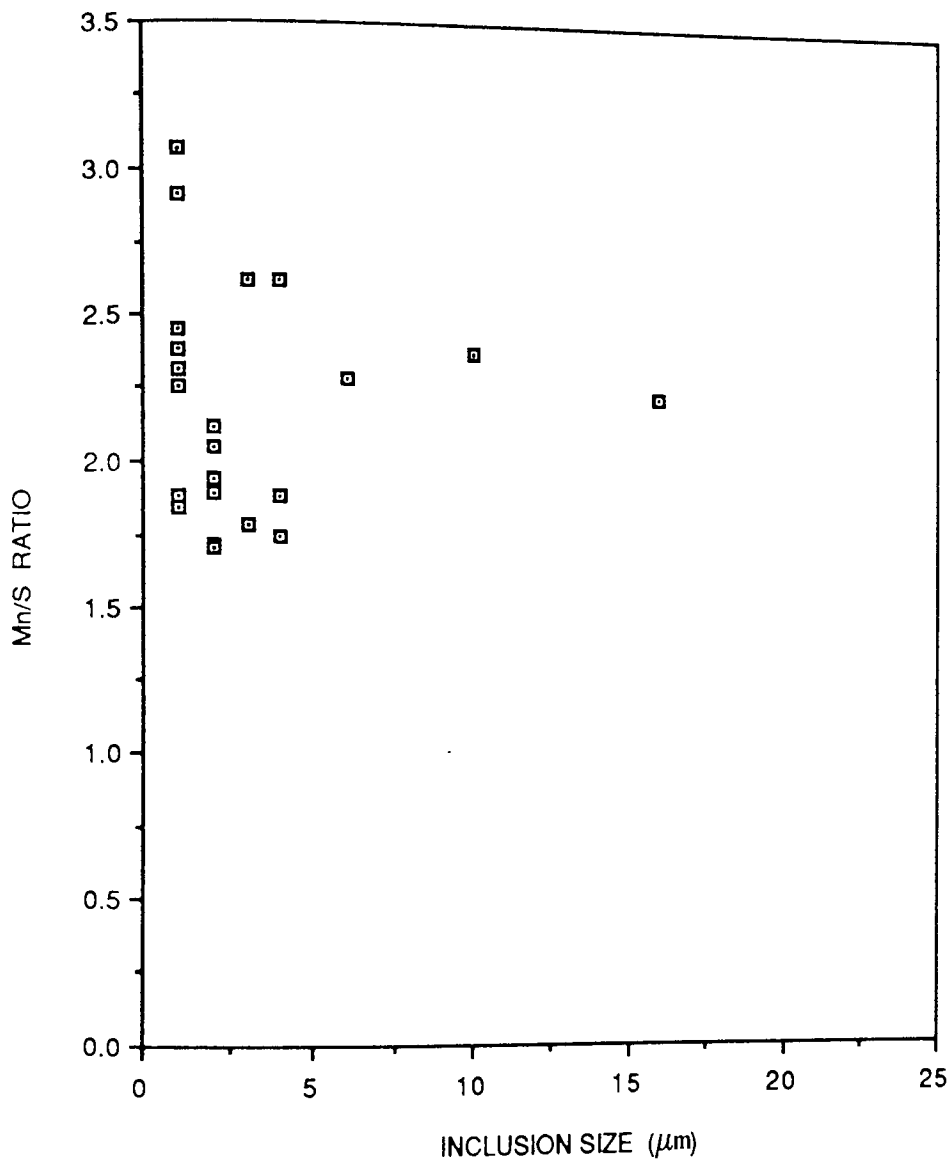
FIGURE 63. Mn/S RATIO VERSUS SIZE FOR THE INCLUSIONS IN STEEL 1.
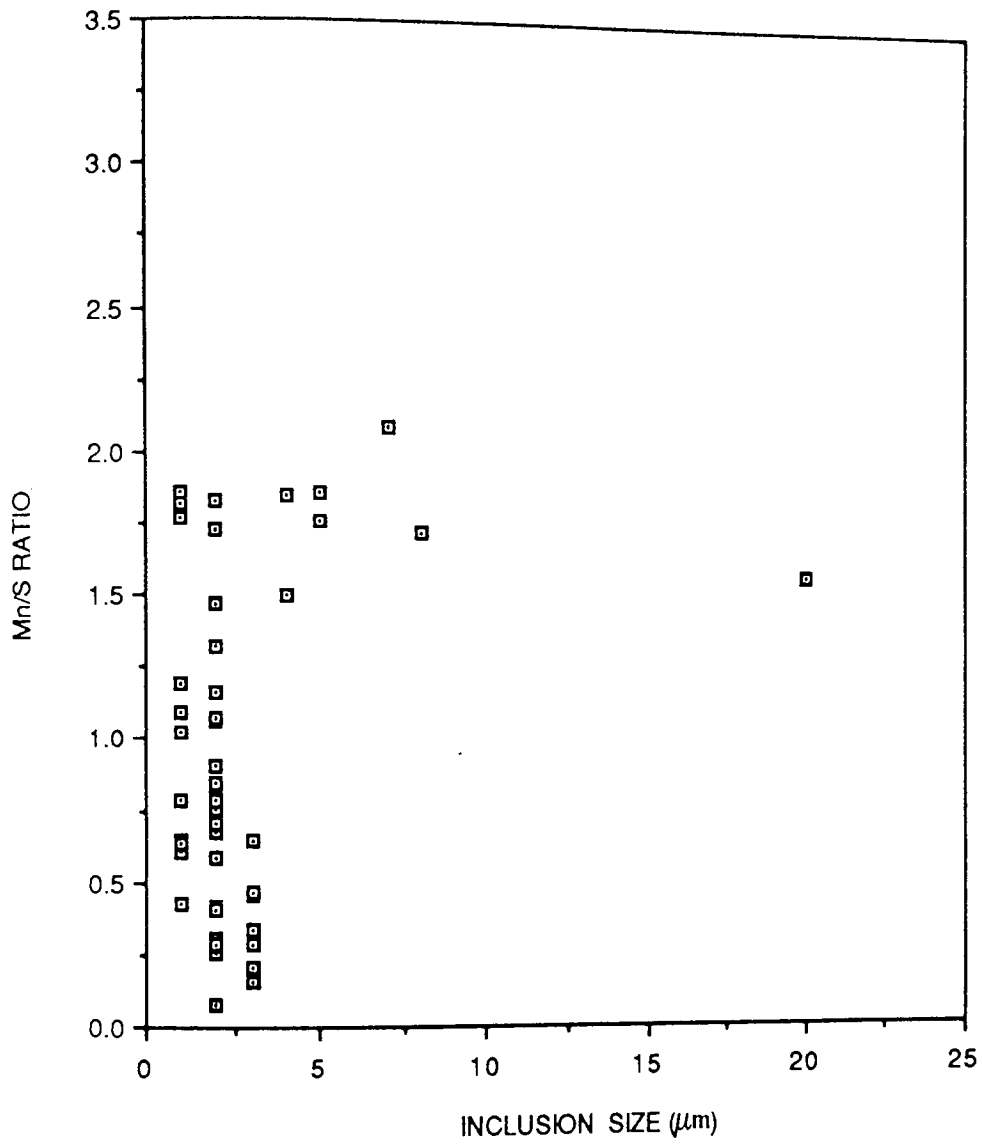
FIGURE 64. Mn/S RATIO VERSUS SIZE FOR THE INCLUSIONS IN STEEL 2.
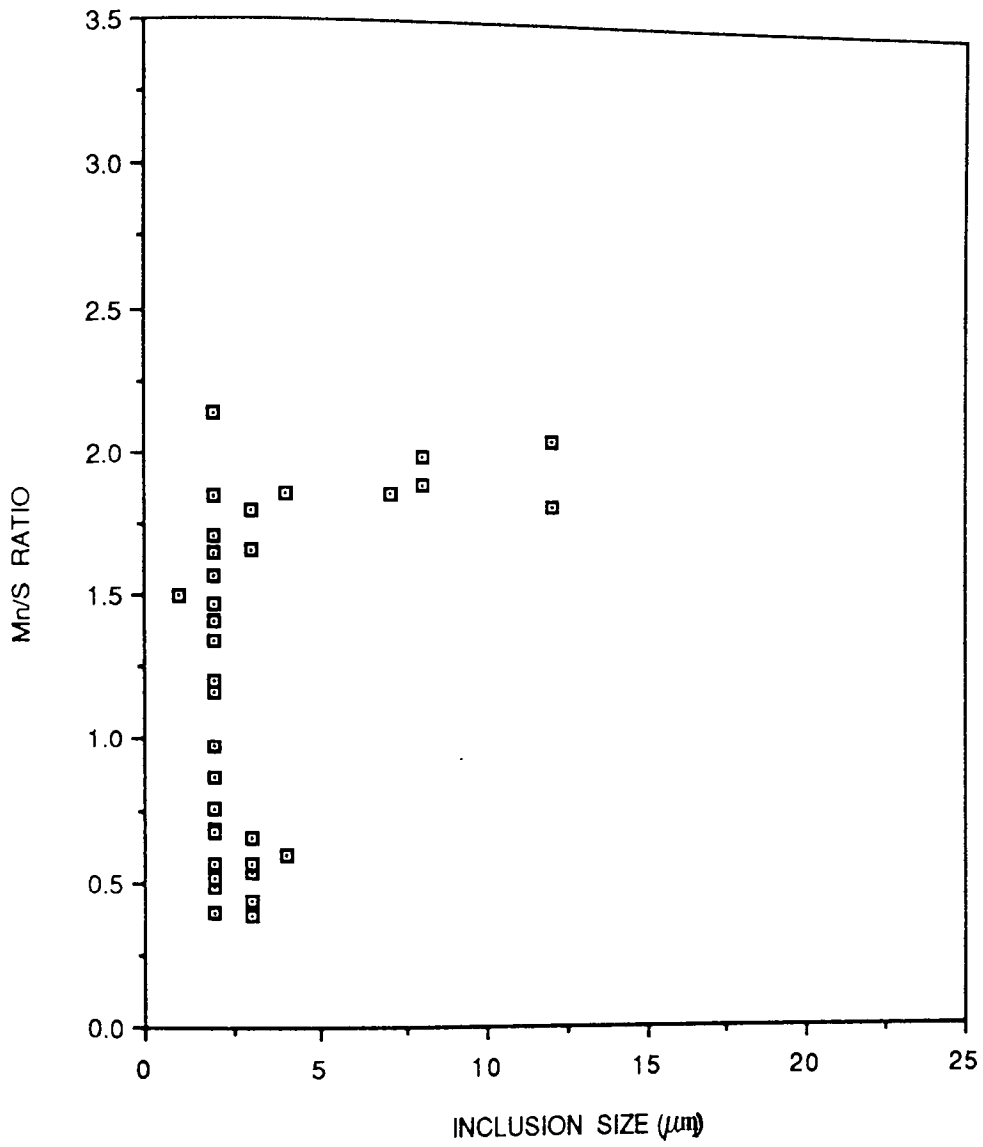
FIGURE 65. Mn/S RATIO FOR THE INCLUSIONS IN STEEL 3.
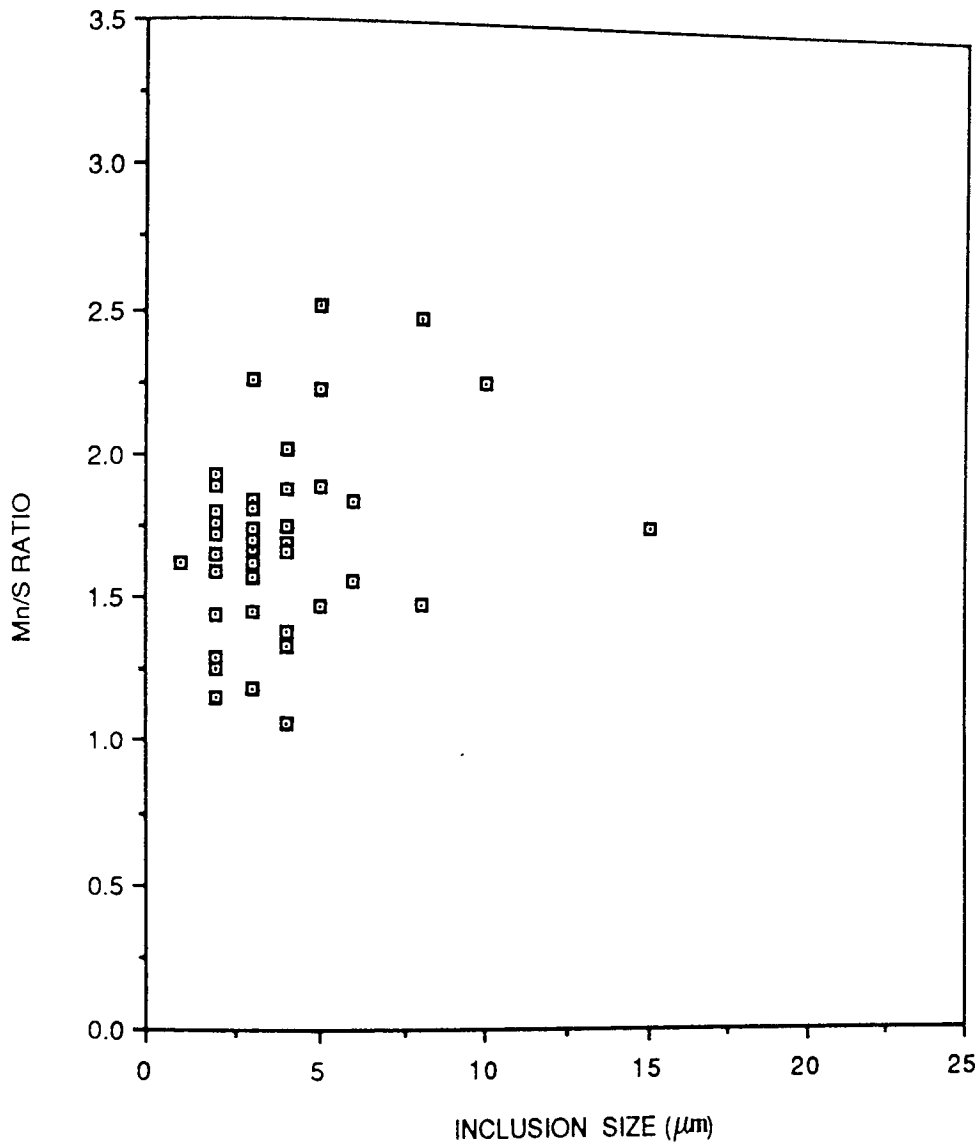
FIGURE 66. Mn/S RATIO VERSUS SIZE FOR THE INCLUSIONS IN STEEL 4.
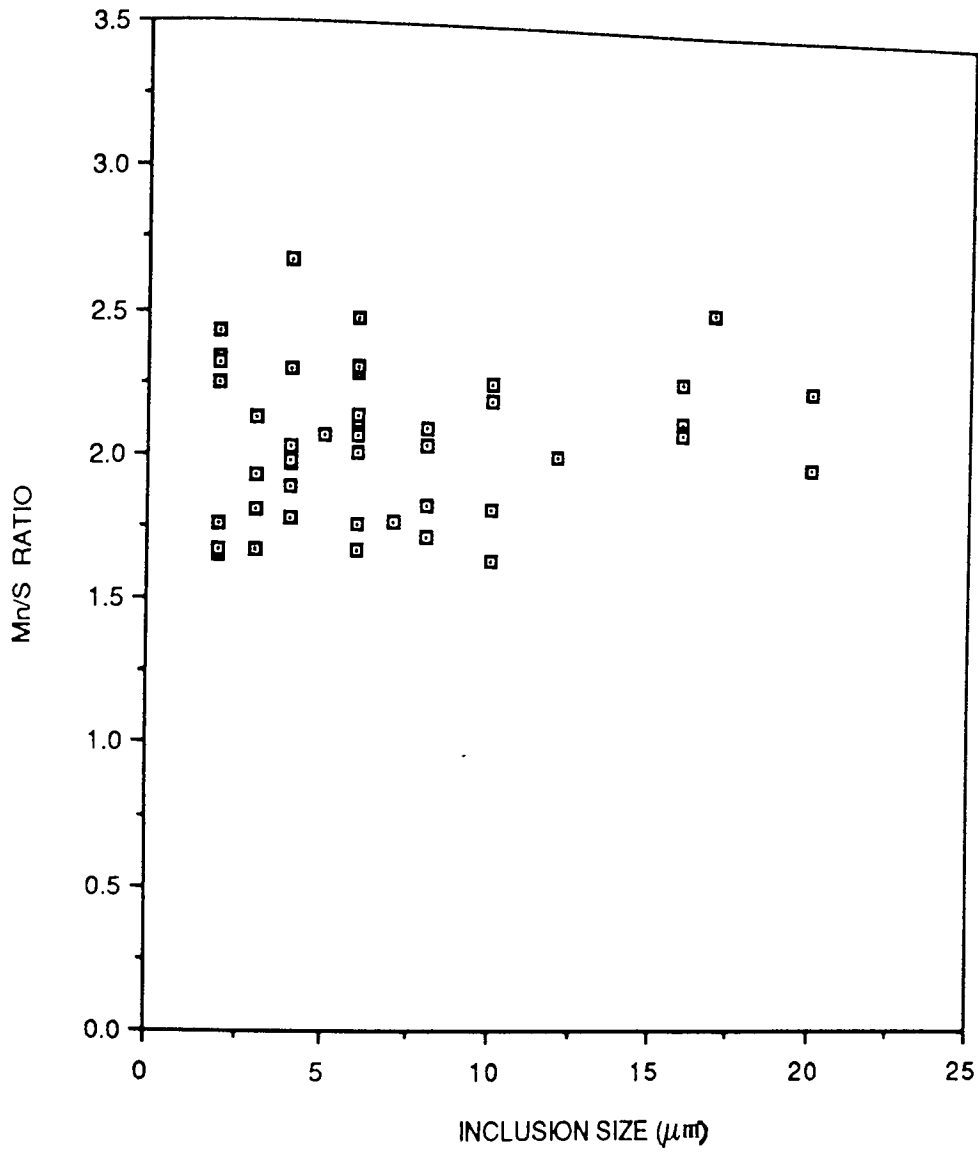
FIGURE 67. Mn/S RATIO VERSUS SIZE FOR THE INCLUSIONS IN STEEL 5.
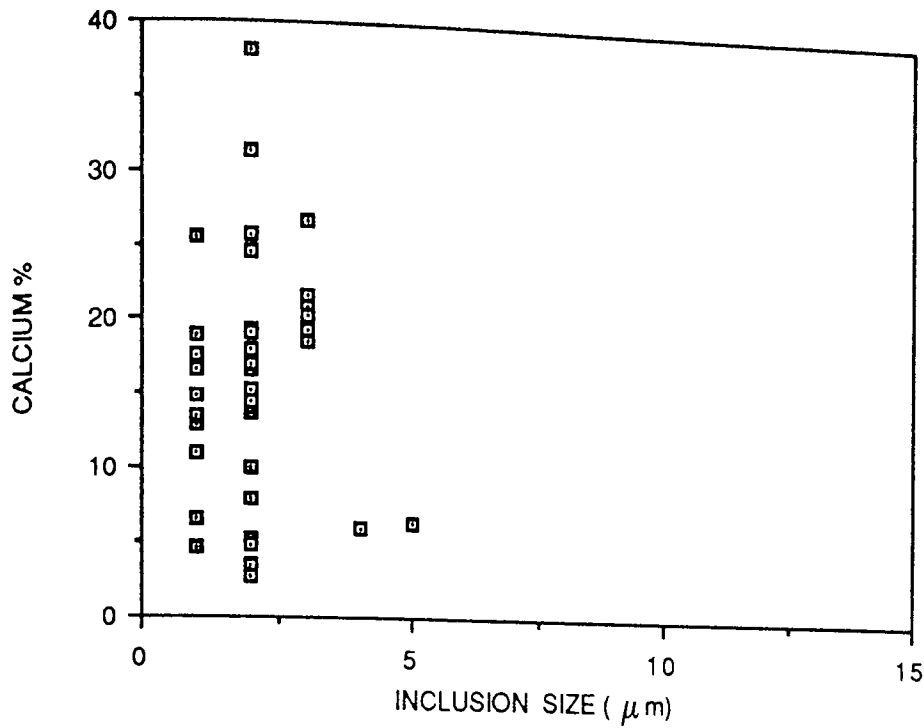
FIGURE 68. INCLUSION SIZE VERSUS CALCIUM CONTENT FOR STEEL 2.
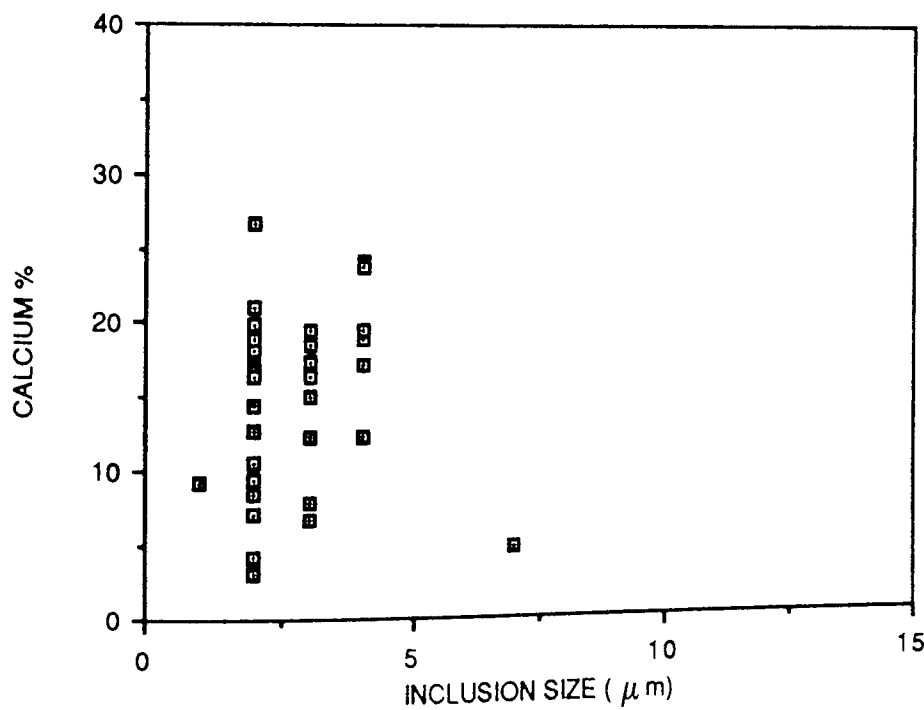
FIGURE 69. INCLUSION SIZE VERSUS CALCIUM CONTENT FOR STEEL 3.
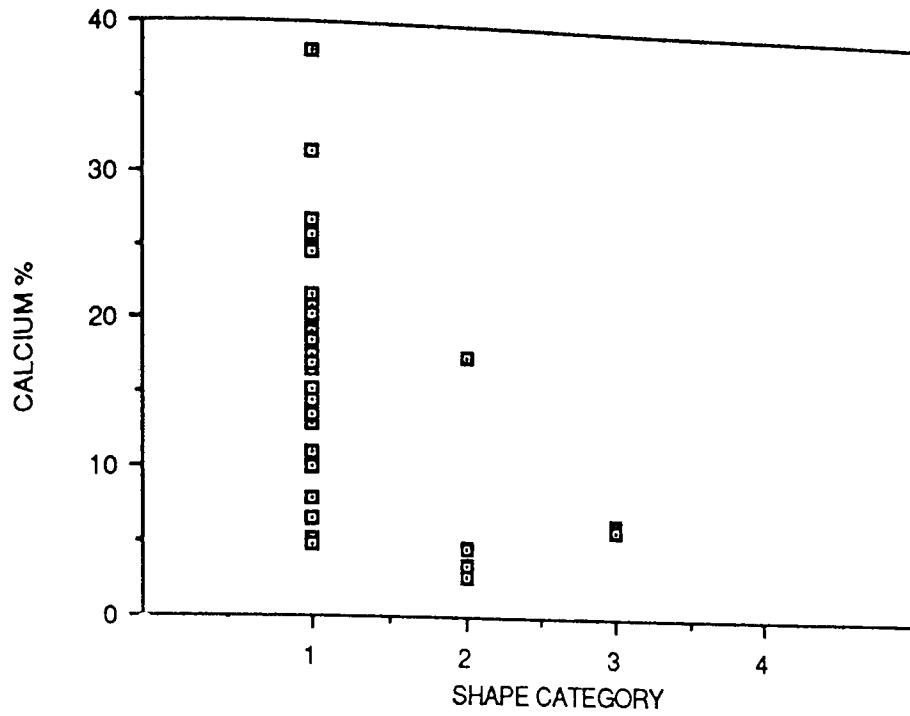
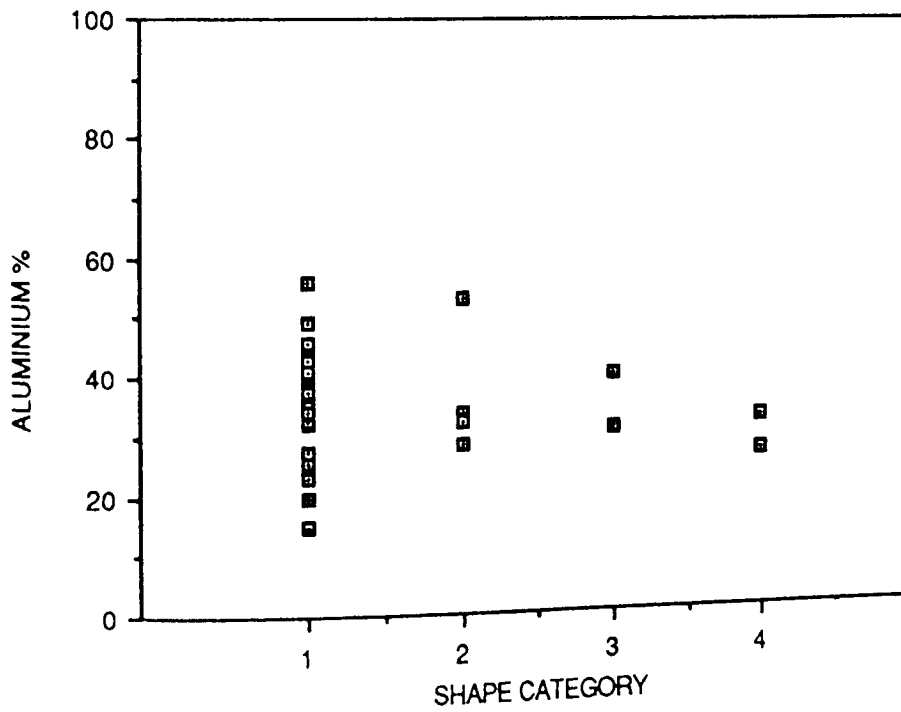FIGURE 70. INCLUSION SHAPE VERSUS CALCIUM CONTENT FOR STEEL 2.
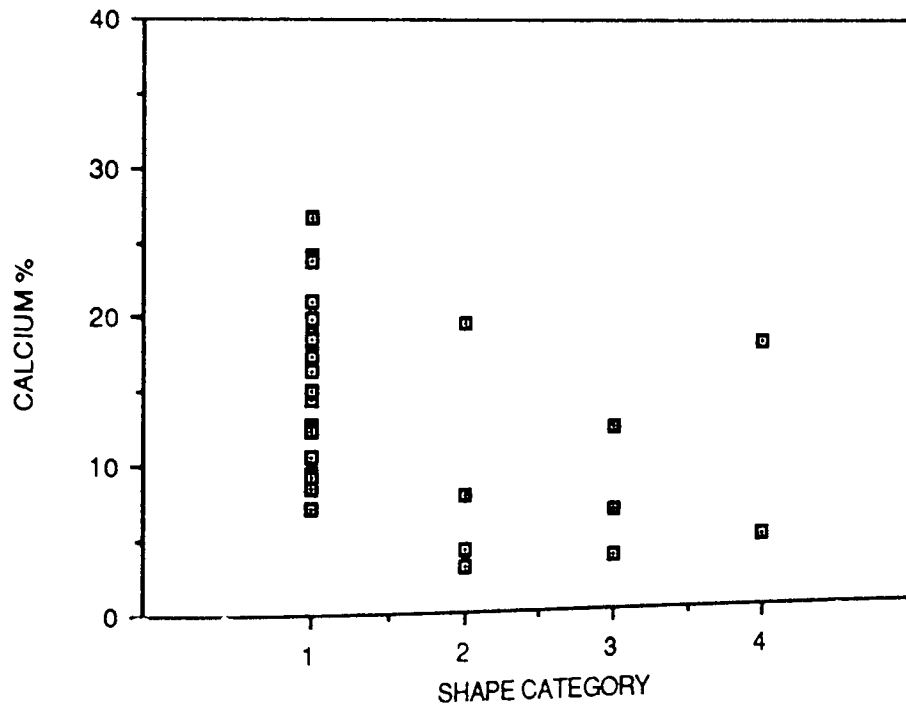
FIGURE 71. INCLUSION SHAPE VERSUS CALCIUM CONTENT FOR STEEL 3.
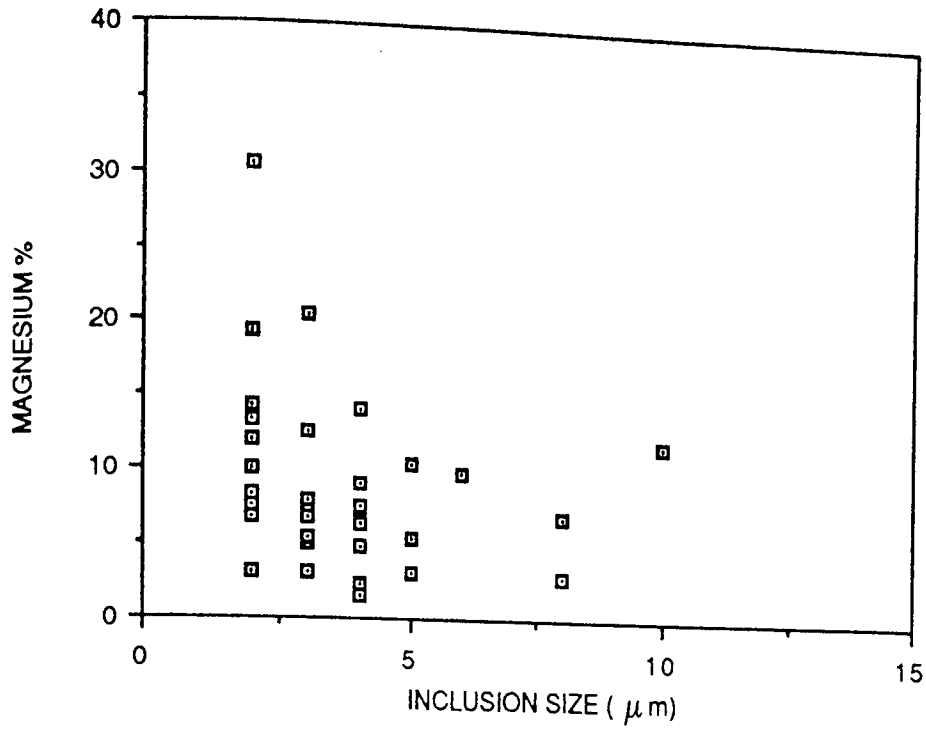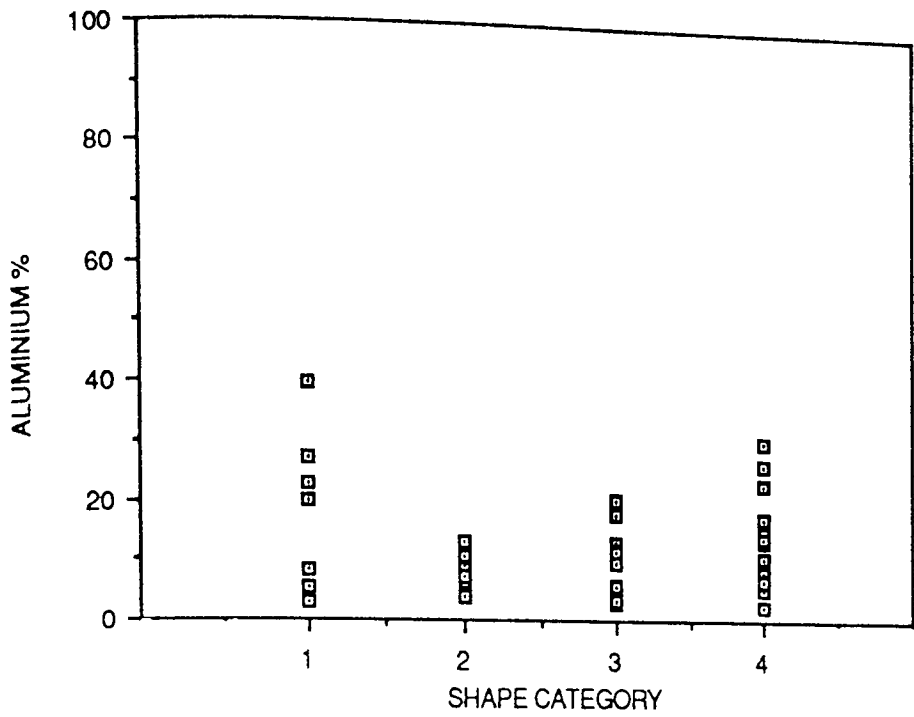
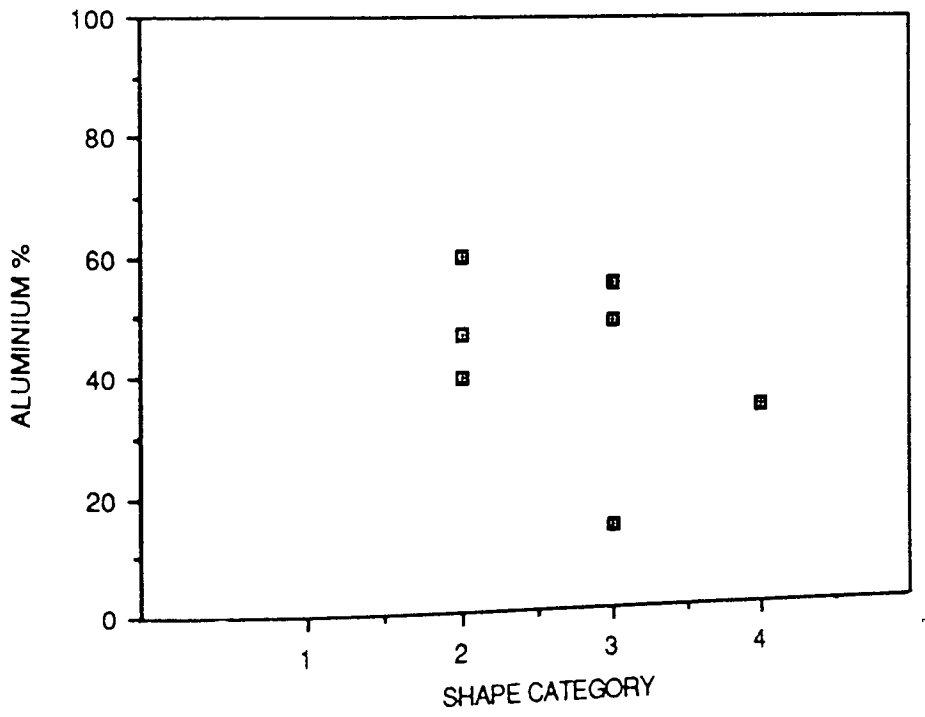FIGURE 72. INCLUSION SIZE VERSUS MAGNESIUM CONTENT FOR STEEL 4.
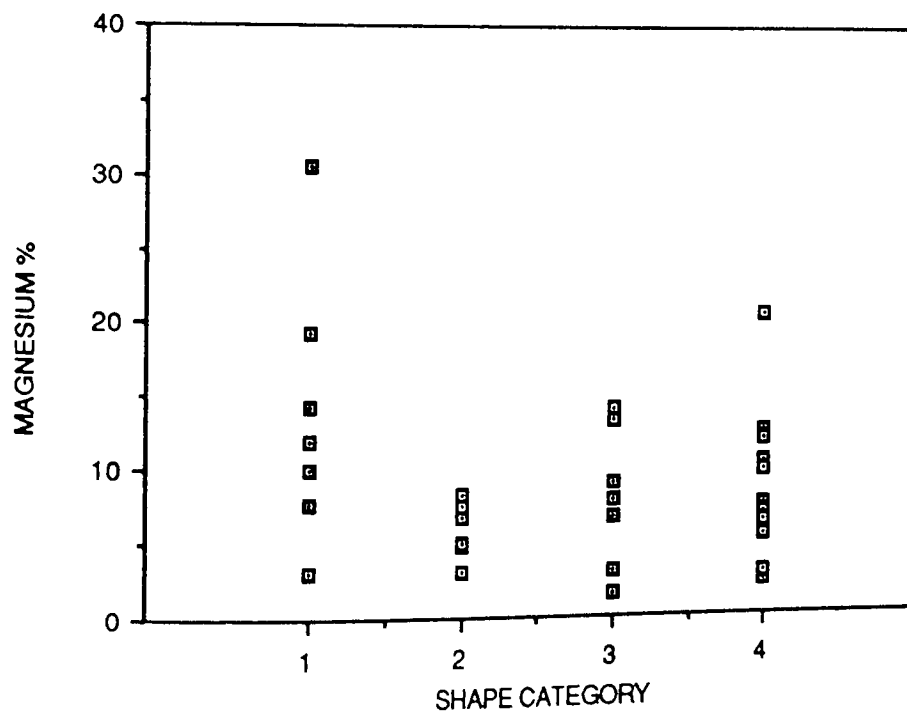
FIGURE 73. INCLUSION SHAPE VERSUS MAGNESIUM CONTENT FOR STEEL 4.
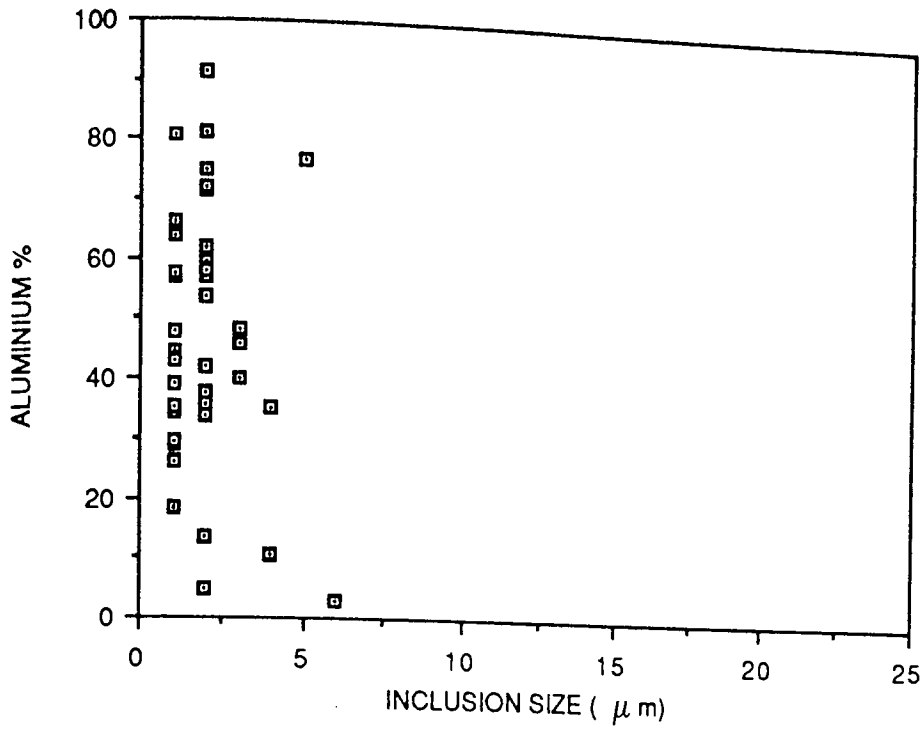
FIGURE 74. INCLUSION SIZE VERSUS ALUMINIUM CONTENT FOR STEEL 1.
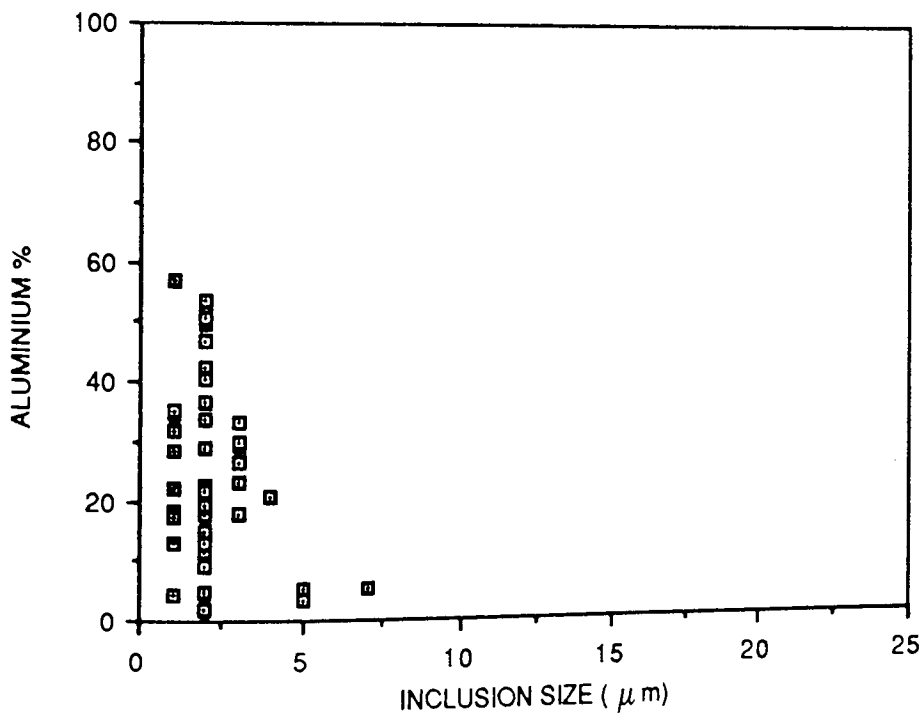
FIGURE 75. INCLUSION SIZE VERSUS ALUMINIUM CONTENT FOR STEEL 2.

FIGURE 76. INCLUSION SIZE VERSUS ALUMINIUM CONTENT FOR STEEL 3.

FIGURE 77. INCLUSION SIZE VERSUS ALUMINIUM CONTENT FOR STEEL 4.
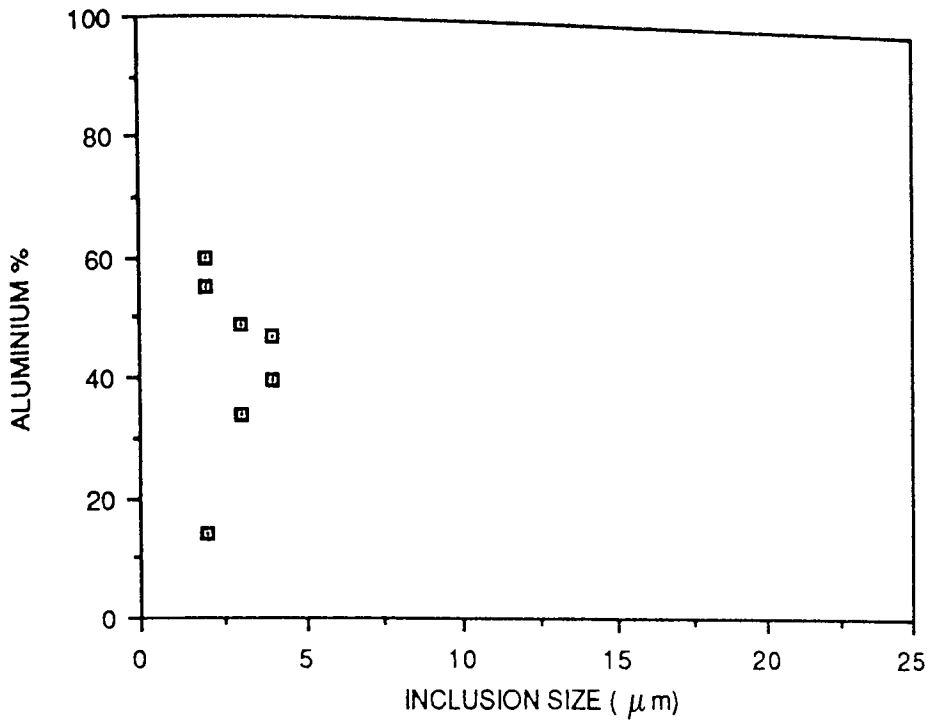
FIGURE 78. INCLUSION SIZE VERSUS ALUMINIUM CONTENT FOR STEEL 5.

FIGURE 79. INCLUSION SHAPE VERSUS ALUMINIUM CONTENT FOR STEEL 1.

FIGURE 80. INCLUSION SHAPE VERSUS ALUMINIUM CONTENT FOR STEEL 2.

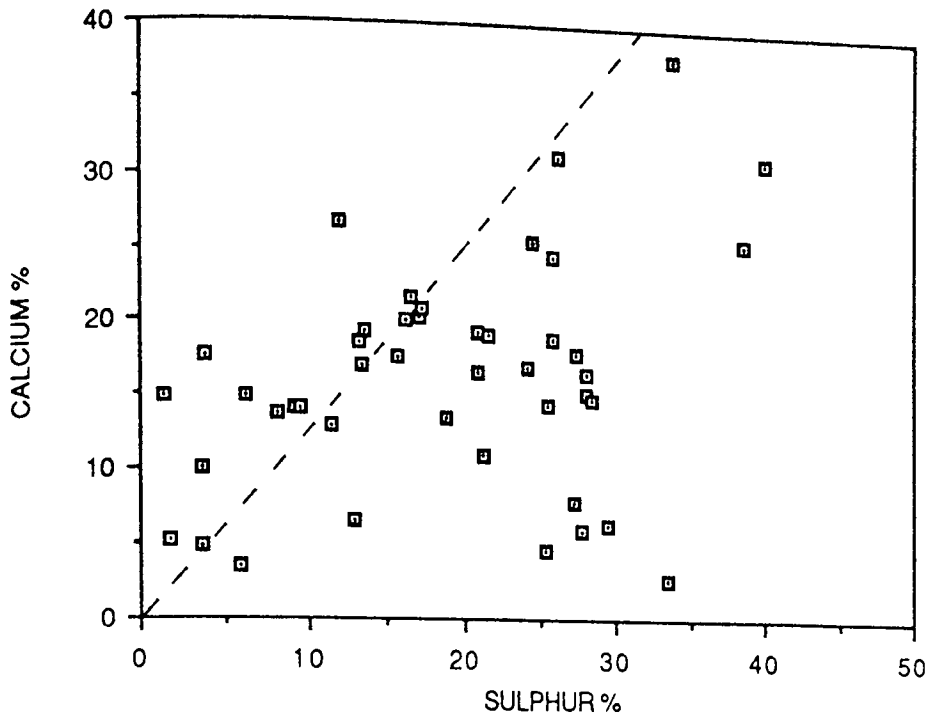FIGURE 81. INCLUSION SHAPE VERSUS ALUMINIUM CONTENT FOR STEEL 3.

FIGURE 82. INCLUSION SHAPE VERSUS ALUMINIUM CONTENT FOR STEEL 4.

FIGURE 83. INCLUSION SHAPE VERSUS ALUMINIUM CONTENT FOR STEEL 5.

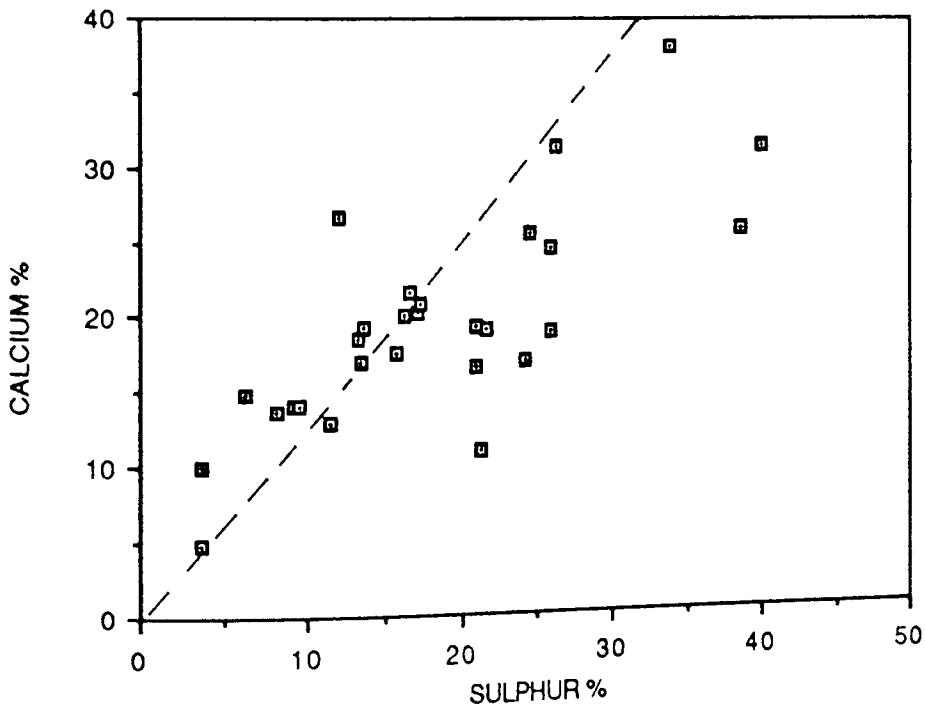FIGURE 84. CALCIUM VERSUS SULPHUR CONTENT FOR THE INCLUSIONS IN STEEL 2.

FIGURE 85. CALCIUM VERSUS SULPHUR CONTENT FOR THE INCLUSIONS IN STEEL 2.
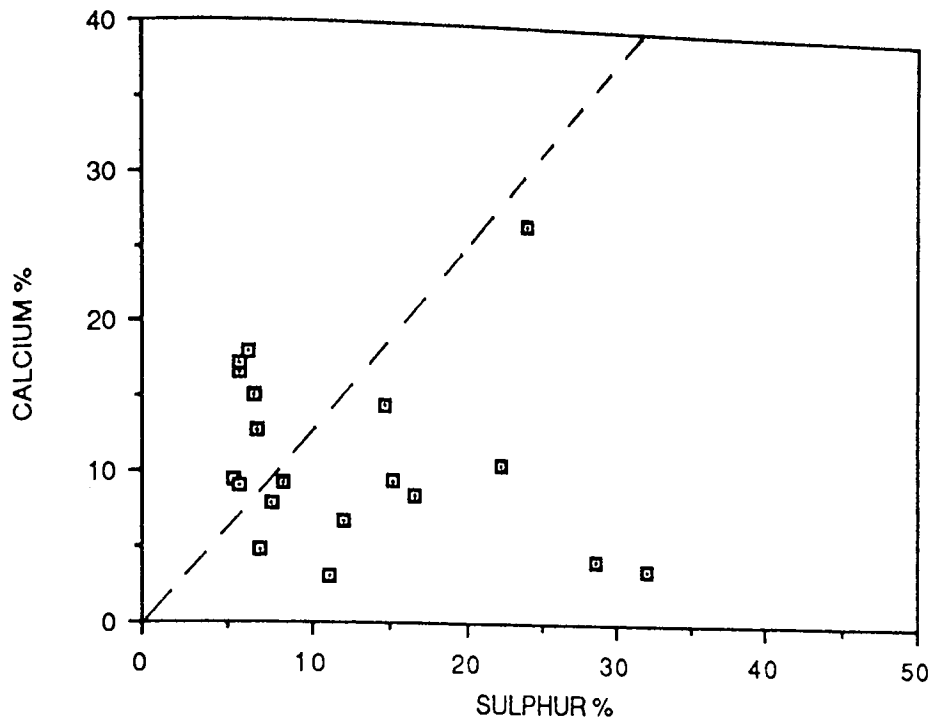
FIGURE 86. CALCIUM VERSUS SULPHUR CONTENT FOR THE INCLUSIONS IN STEEL 2.

FIGURE 87. CALCIUM VERSUS SULPHUR CONTENT FOR THE INCLUSIONS IN STEEL 3.

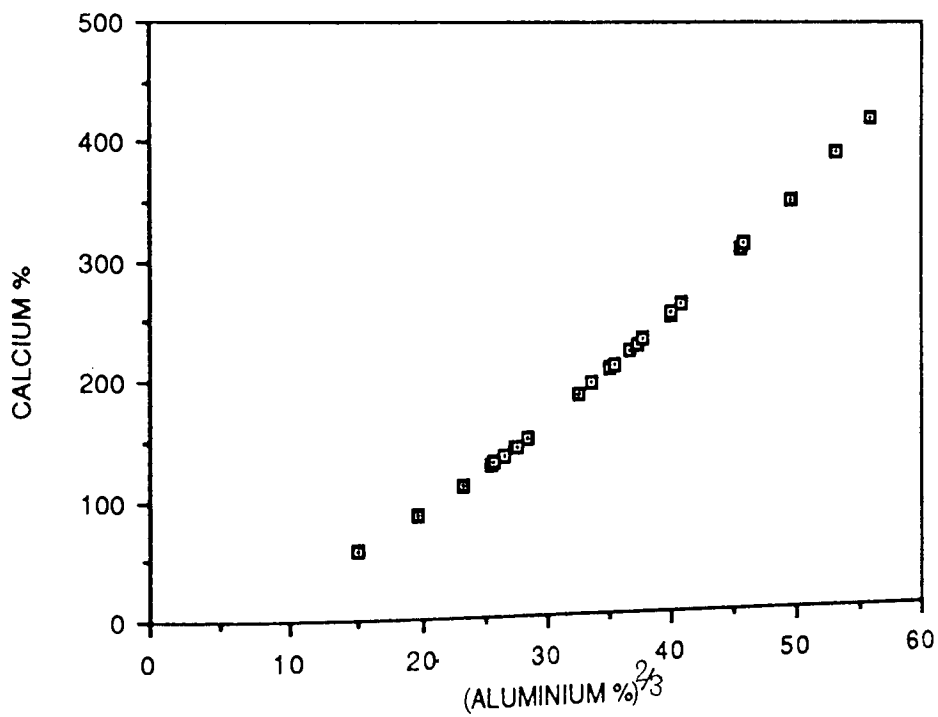FIGURE 88. CALCIUM VERSUS SULPHUR CONTENT FOR THE INCLUSIONS IN STEEL 3.

FIGURE 89. CALCIUM VERSUS ALUMINIUM FOR THE INCLUSIONS IN STEEL 3
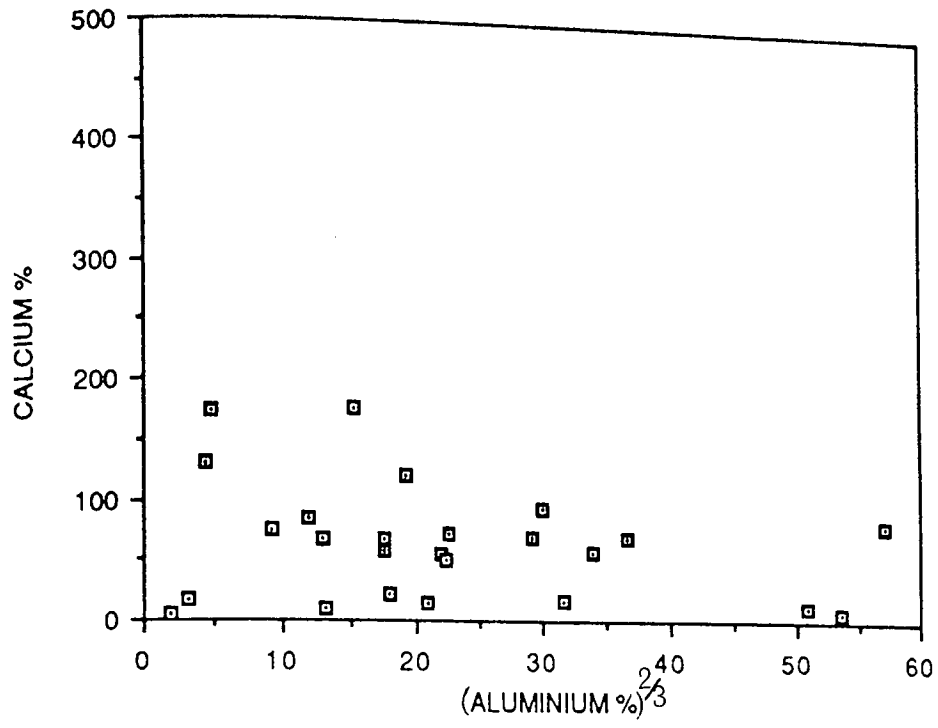
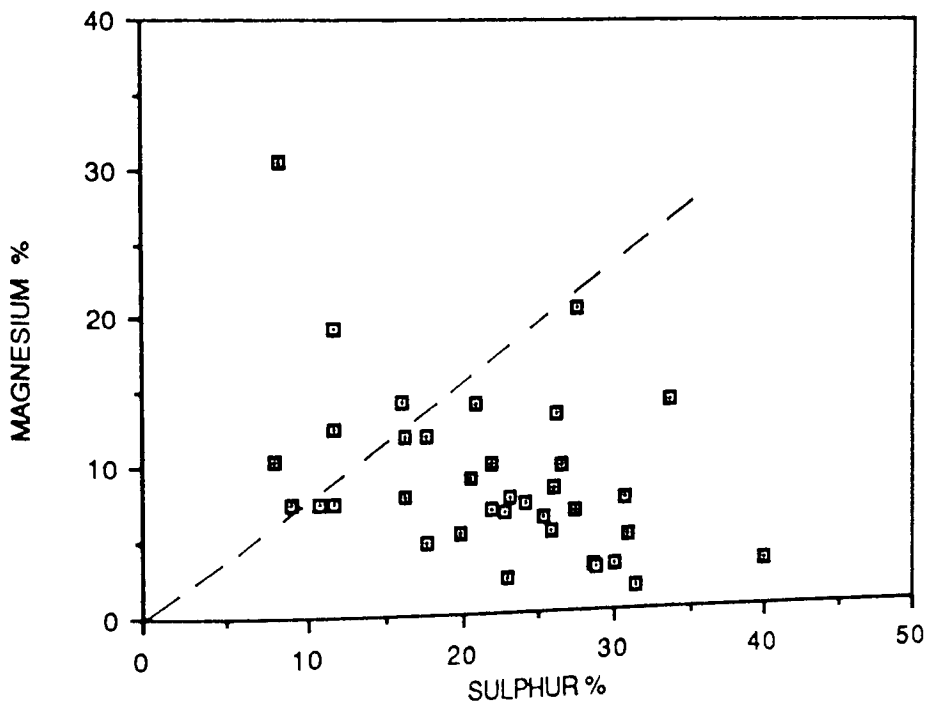FIGURE 90. CALCIUM VERSUS ALUMINIUM FOR THE INCLUSIONS IN STEEL 2.

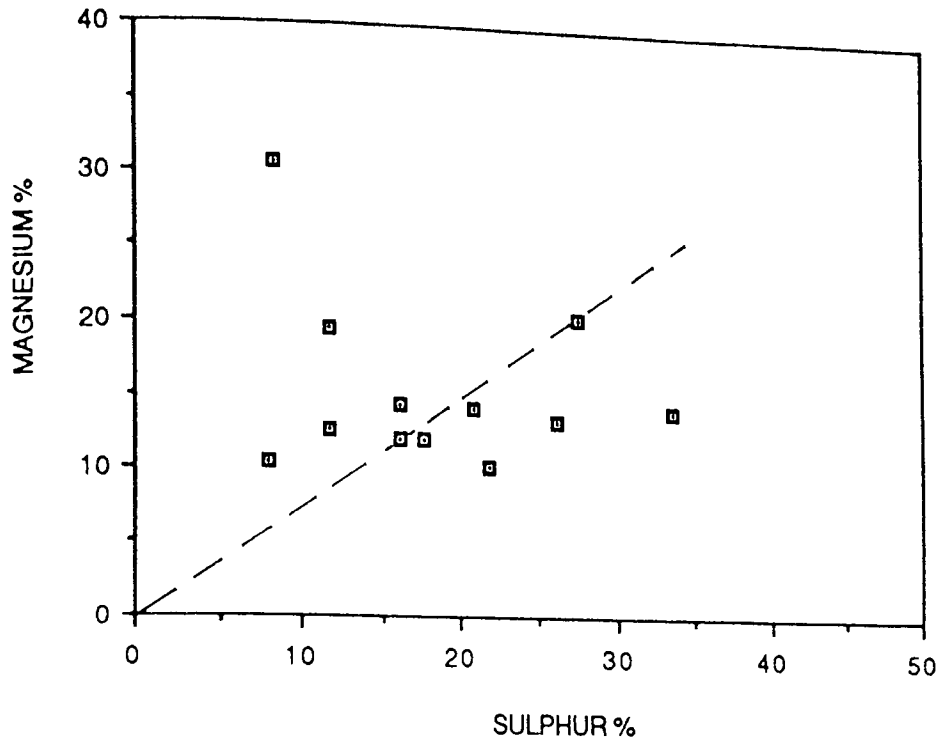FIGURE 91. MAGNESIUM VERSUS SULPHUR CONTENT FOR THE INCLUSIONS IN STEEL 4.

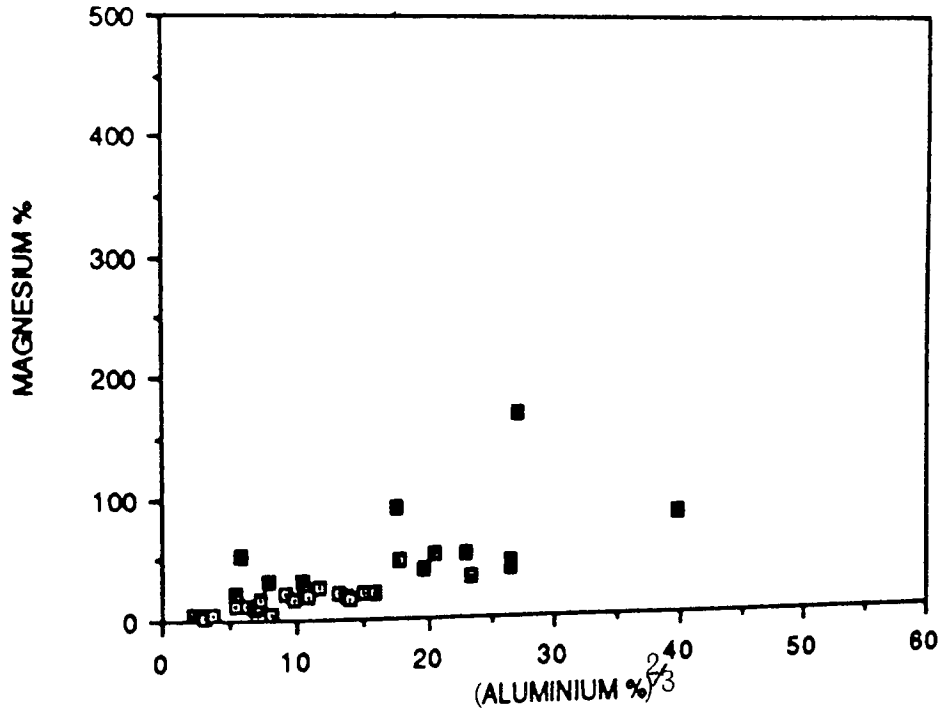FIGURE 92. MAGNESIUM VERSUS SULPHUR CONTENT FOR THE INCLUSIONS IN STEEL 4

FIGURE 93. MAGNESIUM VERSUS ALUMINIUM CONTENT FOR THE INCLUSIONS IN STEEL 4.

FIGURE 94. MANGANESE VERSUS SULPHUR CONTENT FOR THE INCLUSIONS IN STEELS 1-5.
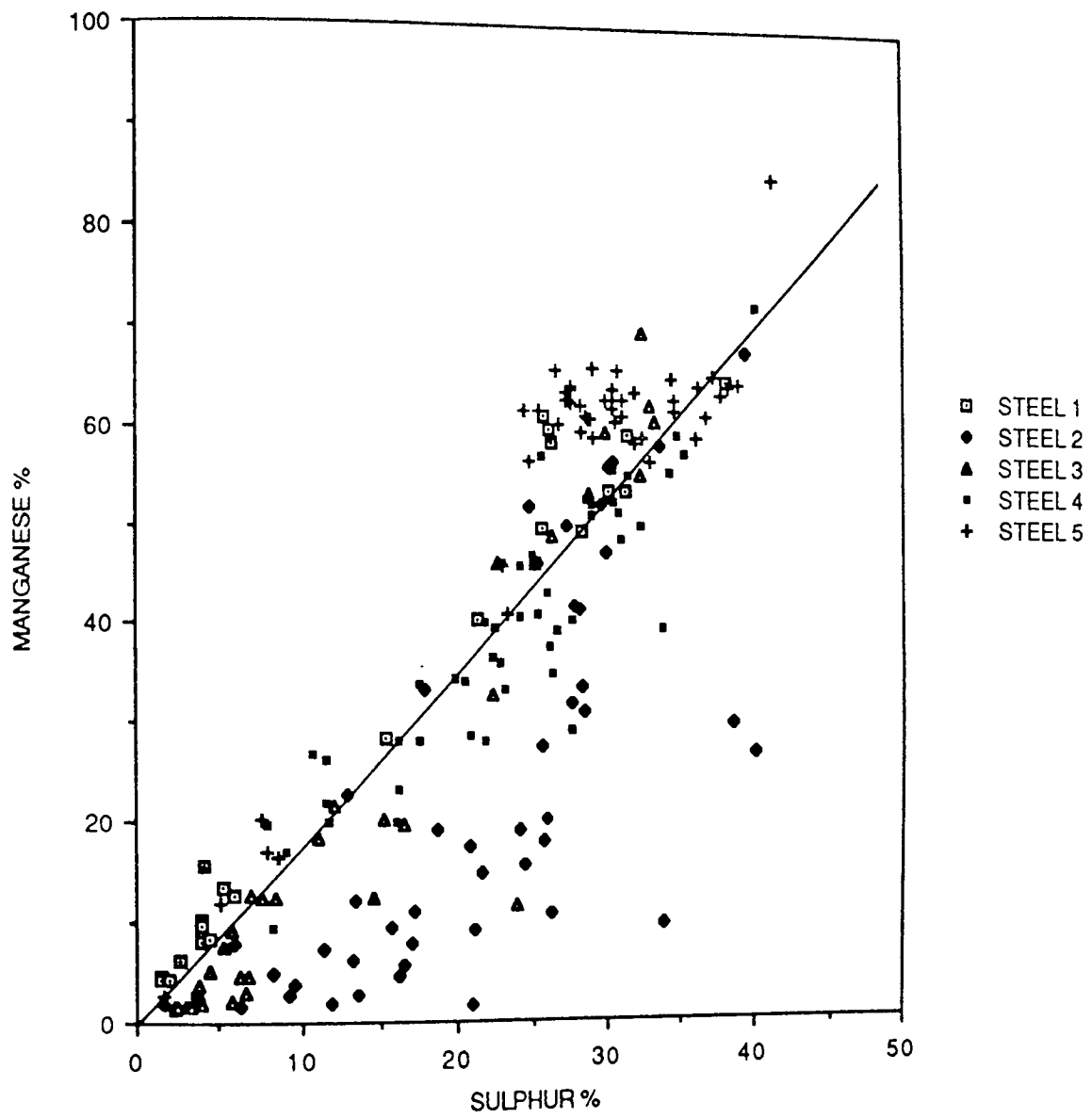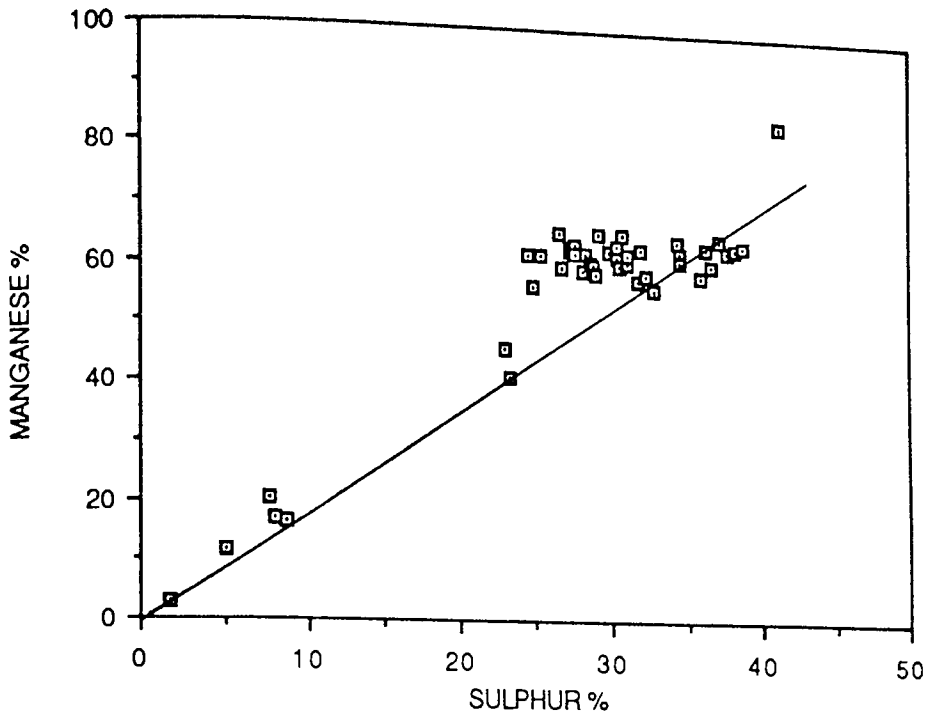
FIGURE 95. MANGANESE VERSUS SULPHUR CONTENT FOR THE INCLUSIONS IN STEEL 5.
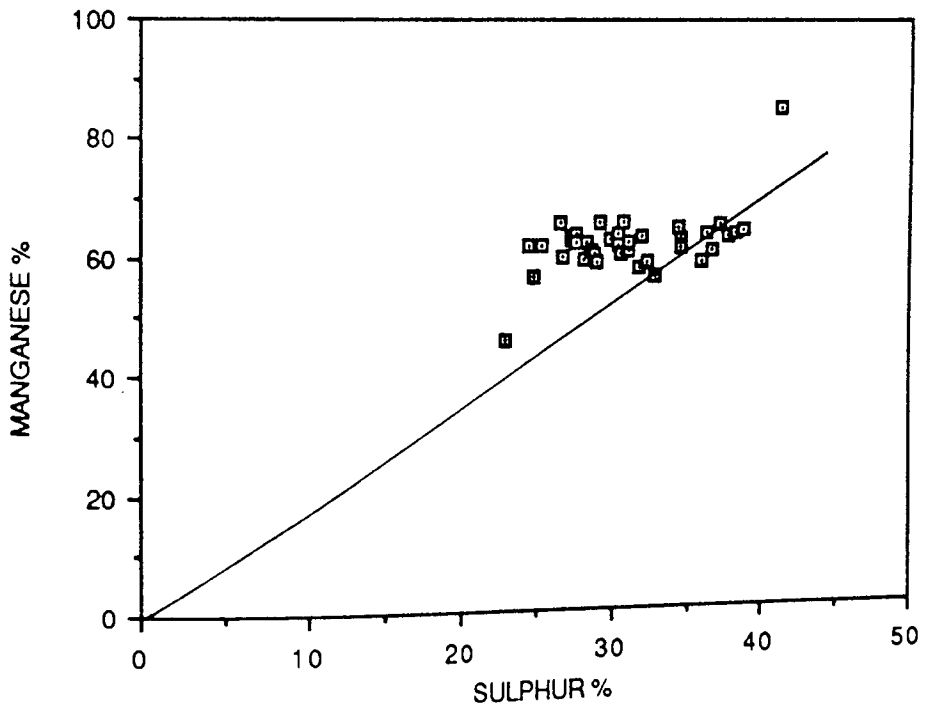
FIGURE 96. MANGANESE VERSUS SULPHUR CONTENT FOR THE INCLUSIONS IN STEEL 5.
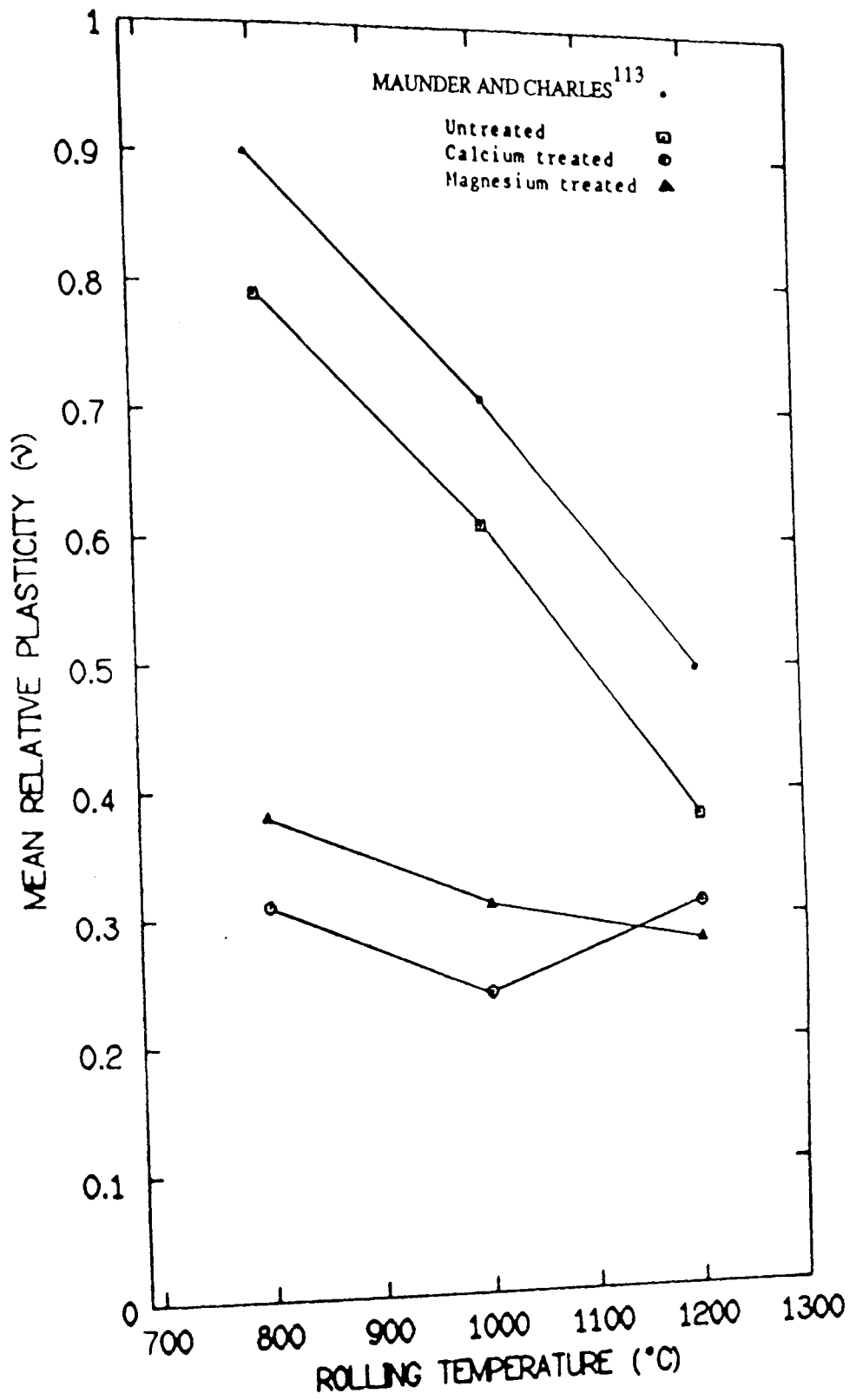
FIGURE 97 Mean relative plasticity versus rolling temperature
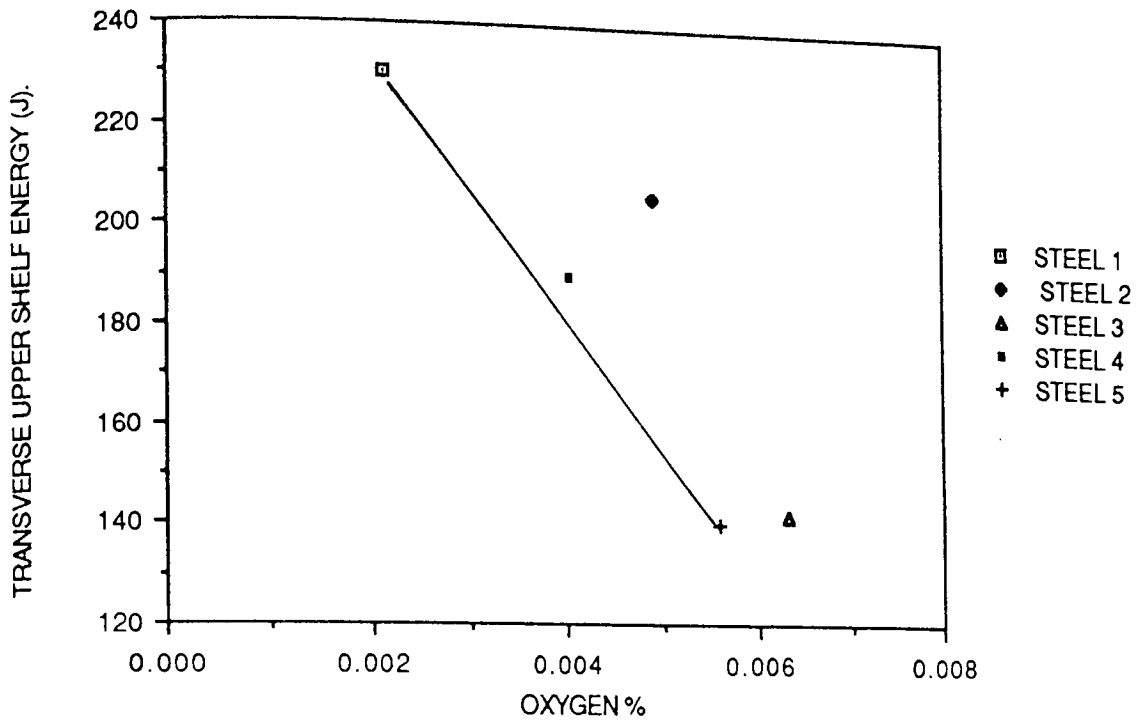
FIGURE 98. TRANSVERSE UPPER SHELF ENERGY VERSUS OXYGEN CONTENT FOR STEELS 1-5.
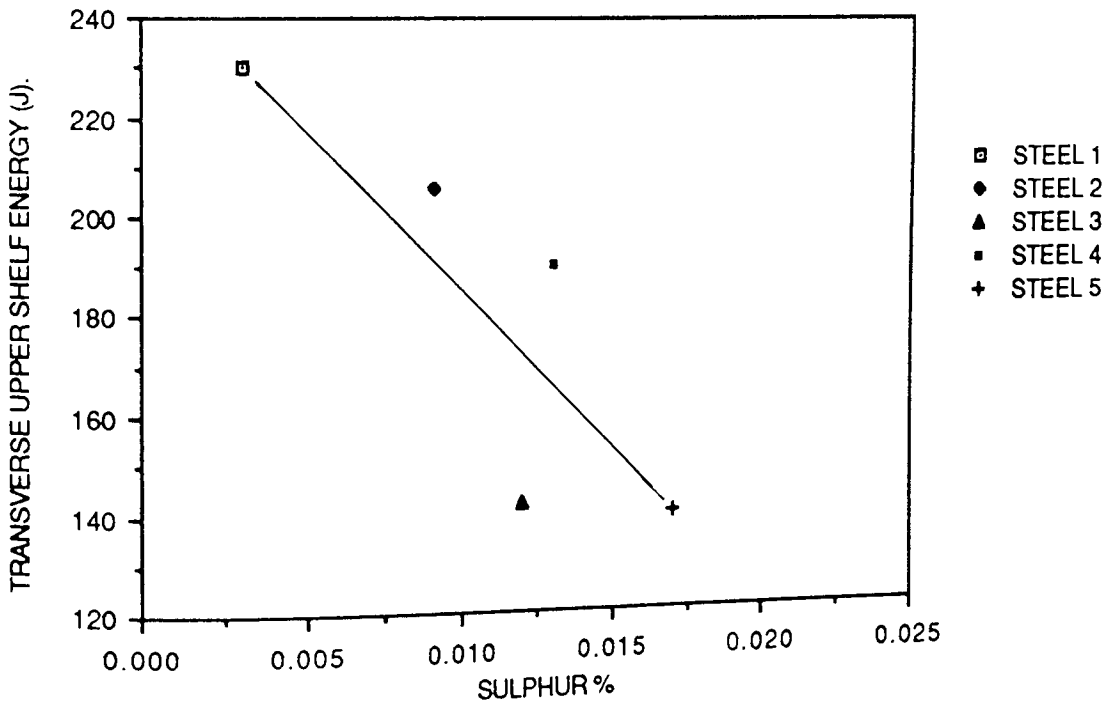
FIGURE 99. TRANSVERSE UPPER SHELF ENERGY VERSUS SULPHUR CONTENT FOR STEELS 1-5.
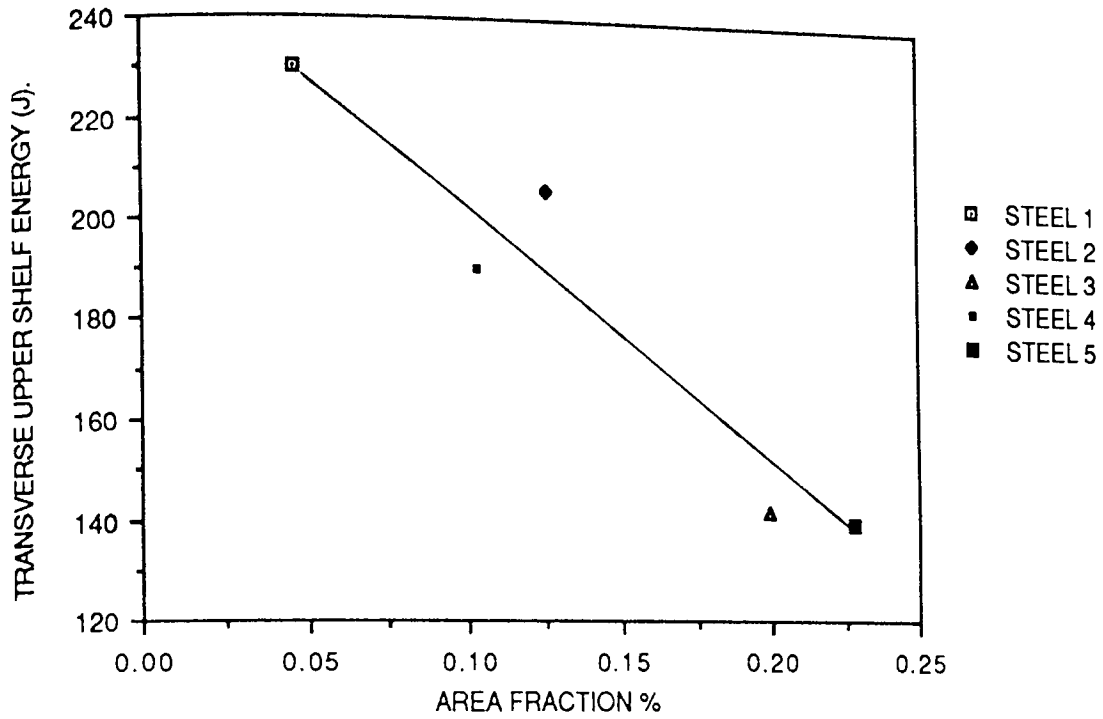
FIGURE 100. TRANSVERSE UPPER SHELF ENERGY VERSUS INCLUSION AREA FRACTION FOR STEELS 1-5.
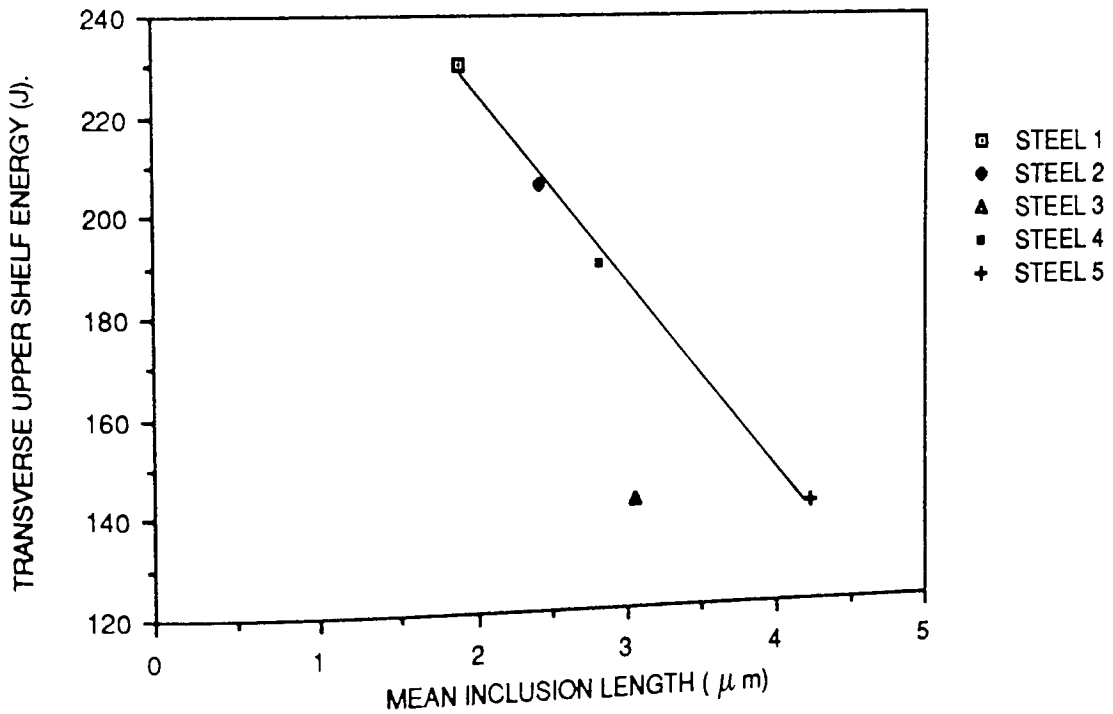
FIGURE 101. TRANSVERSE UPPER SHELF ENERGY VERSUS MEAN INCLUSION LENGTH FOR STEELS 1-5.
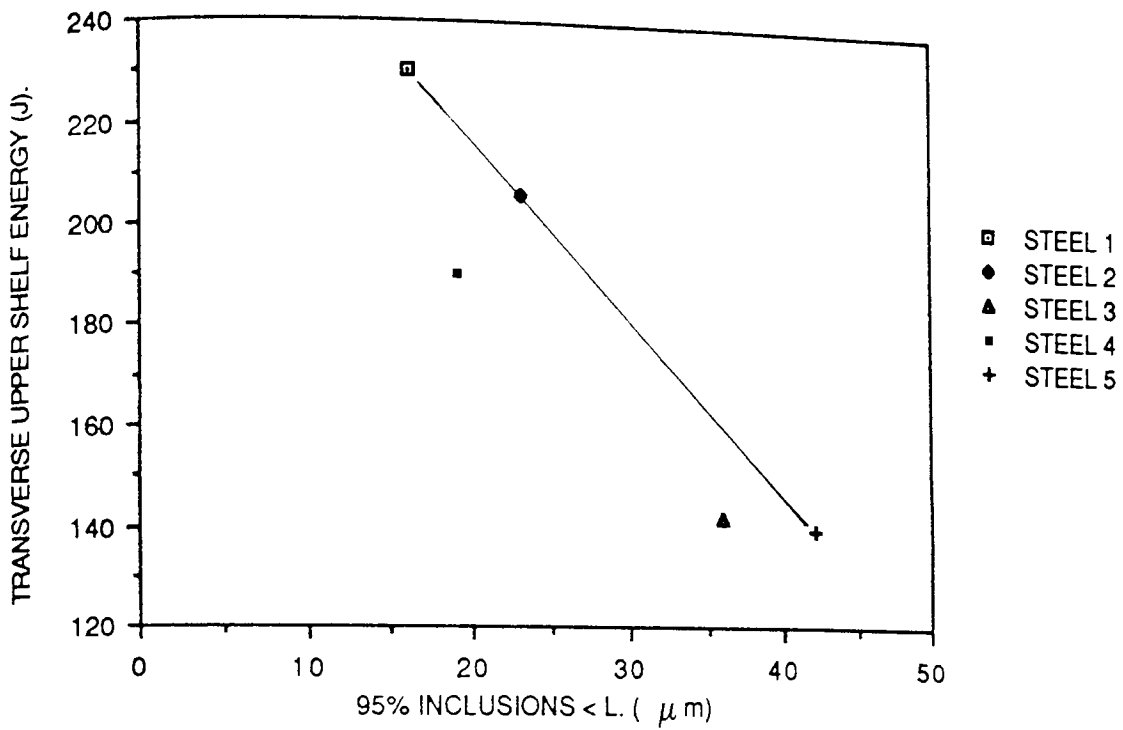
FIGURE 102. TRANSVERSE UPPER SHELF ENERGY VERSUS INCLUSION LENGTH DISTRIBUTION FOR STEELS 1-5
(Thirty Largest Inclusions)
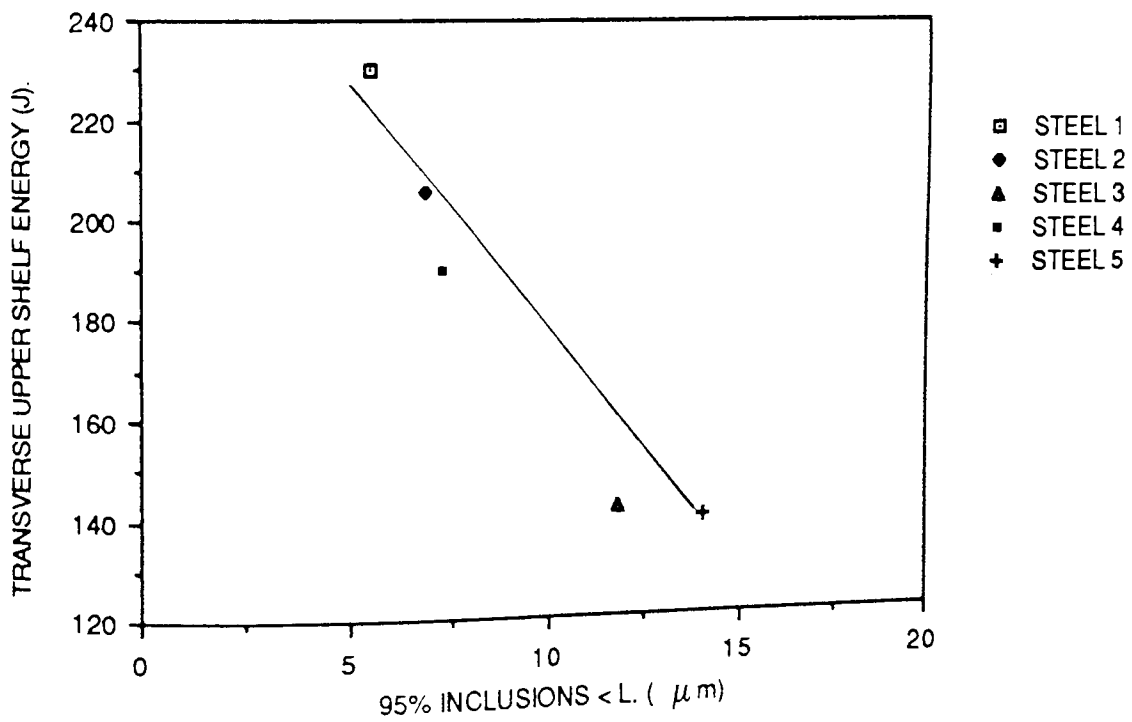
FIGURE 103. TRANSVERSE UPPER SHELF ENERGY VERSUS INCLUSION LENGTH DISTRIBUTION FOR STEELS 1-5
(Photographic Analysis)

Figure 104.   Hydrogen induced 'stepwise' crack found in steel 5.
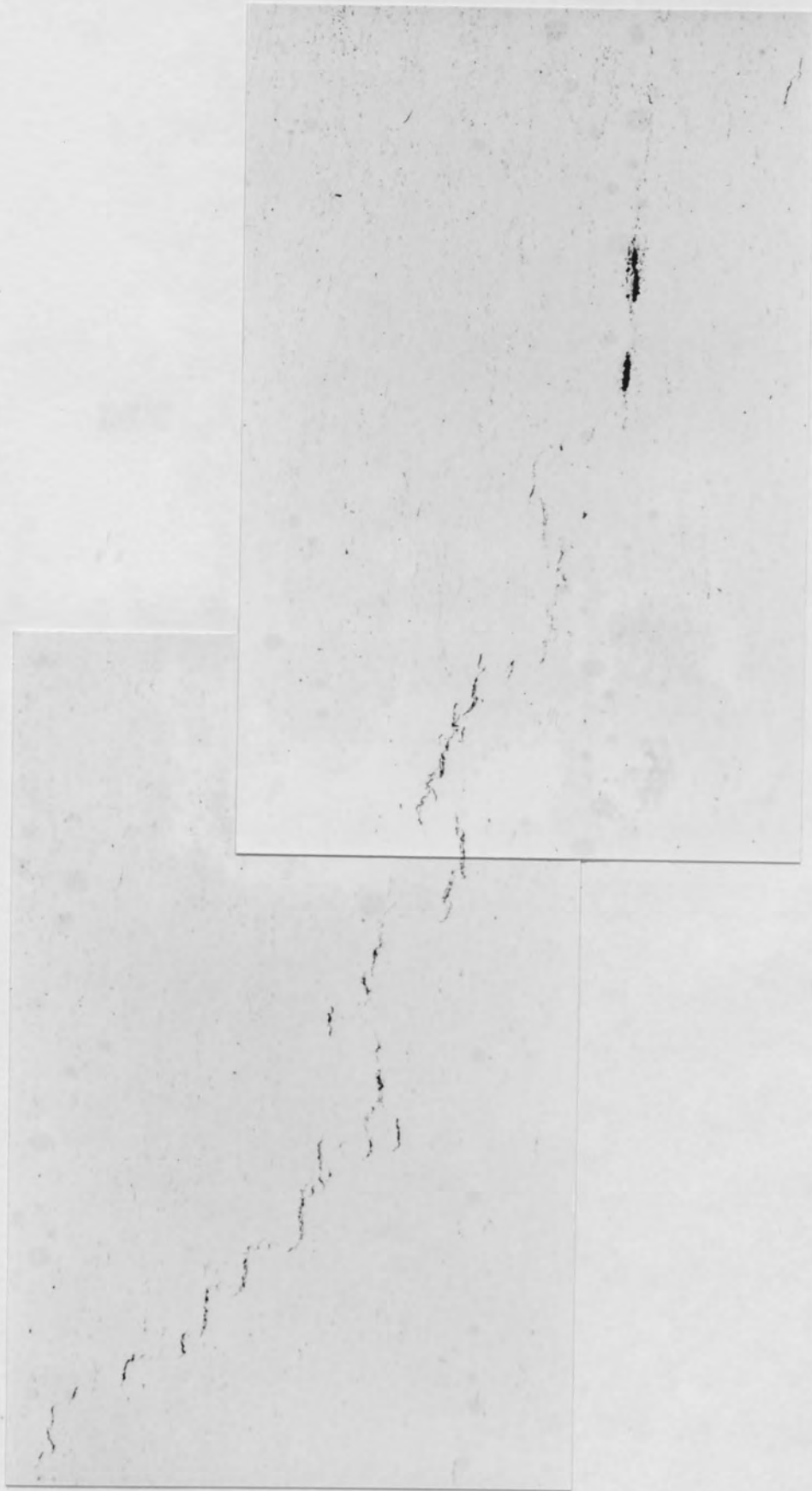
Figure 105.   Elongated inclusions associated with hydrogen induced cracking.

APPENDIX '1'.

CONTROLLED ROLLED SEQUENCE.

INGOT THICKNESS	NUMBER OF PASSES.	TEMPERATURE.
		1160^0C
76 mm.		
	4 EQUAL	
46 mm.		HOLD TO 900^0C
	2 EQUAL	
37 mm.		840^0C
	4 EQUAL	
18 mm.		FINISH ROLL 820^0C

TOTAL REDUCTION
76 %

APPENDIX '2'.

1. $\underline{\text{Sulphur at 0.003\% all converted to manganese sulphide}}$ = 0.003 x 88/32

$$= 0.00825\%$$

Assuming the density of MnS = 4.0 g/cc. this equals 0.00206 cc by volume.

If the density of steel is taken to be 7.8 g/cc , 99.99175 weight % occupies a

volume of 12.81946 cc. $\underline{\text{The volume \% MnS is therefore 0.016\%.}}$

$\underline{\text{Oxygen at 21 p.p.m. all converted to alumina}}$ = 0.0021 x 102/48 = 0.00446%

assuming the density of alumina to be 4.0 g/cc this equals 0.00112 cc by volume.

99.99554 weight % steel occupies a volume of 12.81994 cc.

$\underline{\text{The volume\% Al}_2\text{O}_3 \text{ is therefore 0.009\%.}}$

$\underline{\text{The total volume\% of inclusions in steel 1 is therefore 0.025\%}}$

2. Similarly, $\underline{\text{sulphur at 0.009\%}}$ = 0.009 x 88/32 = 0.02475 weight %

$$= 0.00619 \text{ cc by volume.}$$

99.97525 weight % steel occupies a volume of 12.81734 cc

$\underline{\text{The volume \% manganese sulphide is therefore 0.048\%}}$.

Oxygen at 49 p.p.m. all converted to alumina = 0.0049 x 102/48 = 0.01041%

99.98959 weight % steel occupies a volume of 12.81918 cc.

$\underline{\text{The volume \% alumina is therefore 0.020\%}}$

$\underline{\text{The total volume \% of inclusions in steel 2 is therefore 0.068\%.}}$

3. Further, Sulphur at 0.012% = 0.064 volume % MnS

63 p.p.m. Oxygen can be converted to 0.027 volume % Al_2O_3.

The total volume % of inclusions in steel 3 is therefore 0.091%.

4. Sulphur at 0.013% = 0.069 volume % MnS.

40 p.p.m. Oxygen can be converted to 0.017 volume % Al_2O_3.

The total volume % of inclusions in steel 4 is therefore 0.086%.

5. Sulphur at 0.017% = 0.091 volume % MnS.

56 p.p.m. Oxygen can be converted to 0.024 volume % Al_2O_3.

The total volume % of inclusions in steel 5 is therefore 0.115%

APPENDIX '3'.

Relationships between Calcium, Magnesium and Sulphur in Steels.

It is aimed to examine the equilibria between calcium and magnesium, and manganese sulphide to discover if the alkaline earths will reduce manganese sulphide. All calculations will be made for 1600°C (1873K)

From Pehlke [34]

$$Mg_{(v)} + \underline{S}_\% \longrightarrow MgS_{(S)} \qquad K_{1873K} = 4.12 \times 10^2$$

$$\Delta G^\circ_{1873} = -93800 \text{ Joules.}$$

$$Ca_{(v)} + \underline{S}_\% \longrightarrow CaS_{(S)} \qquad K_{1873K} = 9.3 \times 10^6$$

$$\Delta G^\circ_{1873} = -250000 \text{ J.}$$
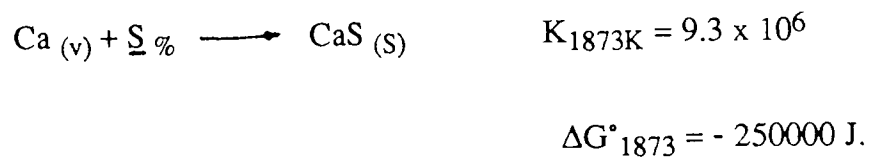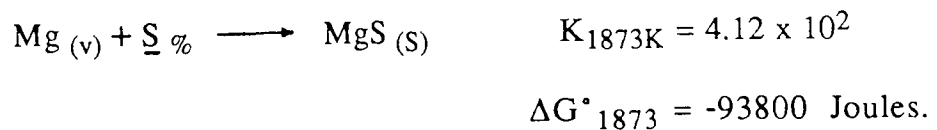
where the standard states are 1 weight percent of sulphur in iron , pure calcium and magnesium vapours at 1 atmosphere pressure and the sulphides are pure solids.

From Elliott and Gleiser [163]

$$Mn_{(L)} + 1/2 \, S_2 \longrightarrow MnS_{(L)} \qquad \Delta G^\circ = -140000 \text{ J.}$$
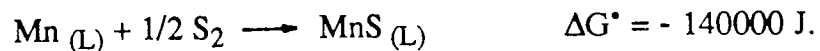
From Bodsworth and Bell [164]

$$Mn_L \longrightarrow \underline{Mn}_\% \qquad \Delta G^\circ = -71500 \text{ J.}$$

$$\underline{Mn}_\% + 1/2 \, S_2 \longrightarrow MnS_{(L)} \qquad = -68500 \text{ J.}$$

$$1/2 \, S_2 \longrightarrow \underline{S}_\% \qquad = -91300 \text{ J.}$$

$$\underline{Mn}_\% + \underline{S}_\% \longrightarrow MnS_{(L)} \qquad = +22800 \text{ J.}$$

$$Mg_{(v)} + \underline{S}_{\%} \longrightarrow MgS_{(S)} \qquad \Delta G^{\bullet} = -93800 \text{ J.}$$

$$MnS_{(L)} + Mg_{(v)} \longrightarrow MgS_{(S)} + \underline{Mn}_{\%} \qquad = -116600 \text{ J.}$$

$$K_{1873} = 1.79 \times 10^3$$

$$Ca_{(v)} + \underline{S}_{\%} \longrightarrow CaS_{(S)} \qquad = -250000 \text{ J.}$$

$$MnS_{(L)} + Ca_{(v)} \longrightarrow CaS_{(S)} + \underline{Mn}_{\%} \qquad = -272800 \text{ J.}$$
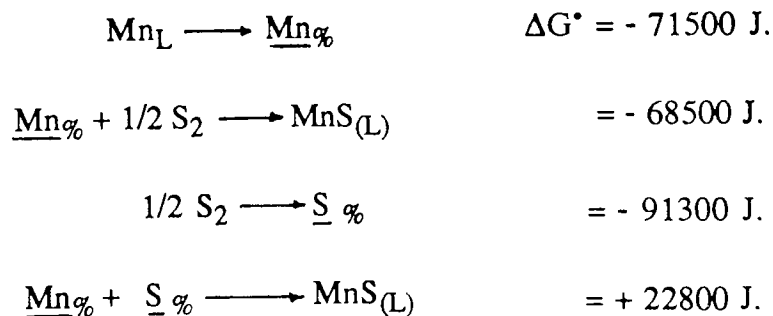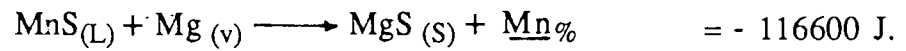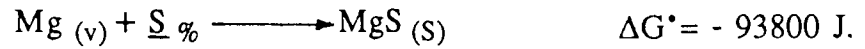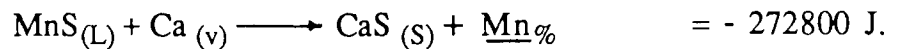
$$K_{1873} = 4.1 \times 10^7$$

Assuming $\underline{Mn}_{\%} = 1.3\%$, $P_{Ca_v} = P_{Mg_v} = 1$ atmosphere at top of melt

$$a_{MgS}/a_{MnS} = 1.38 \times 10^3 \qquad a_{CaS}/a_{MnS} = 3.15 \times 10^7$$

If ideal solutions are assumed in the Non-metallic inclusions ie. Raoult's law applies then

$$a_{MeS} = N_{MeS} \text{ and thus :}$$

$$N_{MgS}/N_{MnS} = 1380 \qquad N_{CaS}/N_{MnS} = 3.15 \times 10^7$$

The calculations show that MnS can be reduced by magnesium or calcium, with the latter reducing the sulphur content of the steel to $10^{-7}\%$ and magnesium to 0.0024% (in contrast to 1.3% Mn reducing the sulphur to 0.1% approximately).

These are equilibrium values for the reactions at 1600°C but they will be controlled under practical conditions by kinetics.

It has been shown that the solubilities of calcium and magnesium in steel at 1600°C are only 0.016 and 0.023% respectively [56], but in this work the total calcium and magnesium contents were 46 and 40 p.p.m. respectively. Therefore, equilibrium was not achieved in

these melts.- the final calcium and magnesium contents not only represent these elements in solution but also their presence in the inclusions. Again, the interaction with the inclusions was only possible via the soluble elements or by direct contact between the oxides/sulphides and very rapidly ascending vapour bubbles. Further, to progress the interaction between oxides/sulphides and dissolved alkaline earths there must be continuous transport of all the species to and from the interface which may be fast in liquid metal at 1600°C but is unlikely to be so rapid in an oxide/sulphide inclusion. Although violent turbulence is present during injection it will only aid transport within the metal and be of less importance in the liquid oxide/sulphide particles. Consequently, the thermodynamic calculations can only indicate that calcium is more likely to reduce manganese sulphide than magnesium but cannot show how far the manganese is removed in either case although some manganese sulphide should be reduced by both alkaline earths.

REFERENCES

1. B.L.Jones and D.L.Johnson, "The metallurgical design of major pipelines", 'Steels for linepipe and pipeline fittings', Proceedings of International Conference, October 21-23rd. 1981, The Metals Society, London, Book 285, pp 14-21.

2. H.N.Lander and J.L.Mihelich, "Production experiences with Mo-Nb linepipe steels", 'Molybdenum containing steels for gas and oil industry applications- a state of the art review', Climax molybdenum Company, 1976.

3. Y.Nara,T. Kyogoku,T.Yamura and I.Takeuchi,"The production of linepipe in Japan",'Steels for linepipe and pipeline fittings', Proceedings of International Conference, October 21-23rd. 1981, The Metals Society, London, Book 285, pp 201-208.

4. T.Patten, "The first twenty years of oil and gas development offshore UK.- an Engineer reflects", Proceedings of the Institute of Mechanical Engineers, Vol.199, A3, 1985, pp. 151-176.

5. E.Shelton, A.B.Rothwell and R.I.Coote,"Steel requirements for current and future Canadian gas pipeline systems", 'Steels for linepipe and pipeline fittings', Proceedings of International Conference, October 21-23rd. 1981, The Metals Society, London, Book 285, pp.5-13.

6. A.Coolen, F.Caron and J.LeClerc,"Developments by USINOR to meet new pipeline requirements", 'Steels for linepipe and pipeline fittings', Proceedings of International Conference, October 21-23rd. 1981, The Metals Society, London, Book 285, pp.209-213

7. C.D.Desforges,W.E.Duckworth and T.F.J.N.Ryan, "Manganese in ferrous metallurgy", The Manganese Centre, 1976, pp 51-60.

8. C.E. Sims and F.B.Dahle,"Effect of aluminium on the properties of medium carbon cast steel", Transactions of the American Foundrymen's Association, 46, 1938, pp 65-132

9. H.Fredriksson and M.Hillert, "Eutectic and monotectic formation of manganese sulphide in steel and cast iron", J.I.S.I., 209, 1971, pp. 109-113.

10   T.J.Baker and J.A.Charles,"Morphology of manganese sulphide in steel", J.I.S.I., 210, 1972, pp. 702-706.

11.   H.Fredriksson and M.Hillert, "On the formation of manganese sulphide inclusions in steel", Scandinavian Journal of Metallurgy, 2, 1973, pp. 125-145.

12.   T.J.Baker, "Use of SEM in studying sulphide morphology on fracture surfaces", 'Sulfide inclusions in steel', Proceedings of an International Symposium, 7-8th Nov.1974, A.M.S., Port Chester, New York , pp 135-158.

13.   E.T.Turkdogan and R.A.Grange, "Microsegregation in Steel", J.I.S.I., 208, 1970, pp. 482-494.

14.   E.T.Turkdogan, "Ladle deoxidation, desulphurisation, and inclusions in steel − fundamentals and observations in practice", 'Clean Steel', Proceedings of an International Conference, 1-3rd June 1981, Balatonfured, Hungary, The Metals Society, Book 281, pp 75-121.

15.   H.B.Bell, " Equilibrium between FeO-MnO-MgO-SiO_2 slags and molten iron at 1550^0C", J.I.S.I., 201, 1963, pp. 116-121.

16.   P.H.Lindon and J.C.Billington, " Deoxidation of steel with Ca-Si-Al and Mg-Si-Al alloys", J.I.S.I., 207, 1969, pp. 340-347.

17.   E.T.Turkdogan, "Deoxidation of steel", J.I.S.I., 210, 1972, pp. 21-36.

18.   R.J.Frueman, "Thermodynamics and kinetics of reaction involving elements in ladle metallurgy", Iron and Steelmaker, March 1983, pp. 33-37.

19.   S.Ekerot, " The behaviour of silicate inclusions in steel during hot working", Scandinavian Journal of Metallurgy, 3, 1974, pp.29-34

20.   E.Grethen and L.Philippe, "Kinetics of deoxidation reactions", International Conference on the 'Production and application of clean steels', Balatonfured, Hungary, June 1970, The Iron and Steel Institute, London, pp.29-34.

21.   W.O.Philbrook, "Oxygen reactions with liquid steel ", International Metals Reviews, 22,1977, pp 187-201.

22. L.E.K.Holappa, "Ladle injection metallurgy", International Metals Reviews, 27, No.2, 1982, pp 73-85.

23. K.Torssell and M.Olette, " Influence de la deformation d'amas sur l'elimination des inclusions d'alumine provenant de la desoxydation du fer liquide par l'aluminium", Revue De.Metallurgie, 66, 1969, pp. 813-821.

24. B.C.Allen and W.D.Kingery, " Surface Tension and contact angles in some liquid metal-solid ceramic systems at elevated temperatures", Trans. A.I.M.E., 215, 1959, pp 30-36

25. P.Kozakevitch and M.Olette, "Role of surface phenomena in the mechanism of removal of solid inclusions", International Conference on the 'Production and application of clean steels', Balatonfured, Hungary, June 1970, The Iron and Steel Institute, London, pp.42-49.

26. V.E.Plockinger and M.Wahlster, Stahl Und Eisen, 80,1960, pp.656-669.

27. P.V.Ribould and C.Gatellier, "New products : what should be done in Secondary Steelmaking ?", 'Secondary Steelmaking for product improvement', Proceedings of an International Conference, London, 23-24th Oct. 1984, The Metals Society, pp 73-80.

28. V.H.Knuppel, K.Broztmann and N.W.Forster, Stahl Und Eisen, 85, 1965, pp 675-688.

29. Y.Miyashita, K.Nishikawa, Japanese - USSR joint symposium on the Physical Chemistry of Metallurgical Processes, pp101

30. N.Lindskog and H.Sandberg, "Studies on the deoxidation mechanisms in a stirred steel bath using radioactive isotopes", Scandinavian Journal of Metallurgy, 2, 1973, pp 71-78.

31. E.T.Turkdogan, "Nucleation, growth and flotation of oxide inclusions in liquid steel", J.I.S.I., 204, 1966, pp 914-919.

32. B.Tivelius and T.Sohlgren and J.Wayne,"Secondary Steelmaking by the ASEA/SKF and the TN process: a comparison", Steelmaking Proceedings, Vol 61,Chicago 16-20th April 1978, AIMMPE, pp 154-173.

33. A.G.Shalimov and L.F.Kosoi, "Non-metallic inclusions in steel treated with synthetic slag and pulverised silicocalcium", 'Clean Steel', Proceedings of an International Conference, 1-3rd June 1981, Balatonfured, Hungary, The Metals Society, Book 281, pp 232-240

34 R.D.Pehlke and T.Fuwa, "Control of sulphur in liquid iron and steel", International Metals Reviews, 30, No.3, 1985, pp 125-140.

35. M.G.Frohberg, M.L.Kapoor and A.Nilas, " Desulphurisation", Proceedings of an International Conference on the 'Chemical Metallurgy of Iron and Steel", 1973, London, The Iron and Steel Institute, pp 139-143.

36. B.Ohman and T.Lehner, "Ladle refining of steel", Scaninject II, Proceedings of the Conference on injection, 12-13th June, 1980, Lulea, Sweden pp 2:1-2:30.

37. C.W.Finkl and A.L.Lehman, "Ladle steelmaking : a new era", 'Secondary Steelmaking for product improvement', Proceedings of an International Conference, London, 23-24th Oct. 1984, The Metals Society, pp 225-230.

38. P.Stubbs, "Ladle Metallurgy - a personal overview", 40th. Electric Steel Conf. Proc. Kansas City, USA, 7-10th Dec.1982, ISS/AIME, pp 303-311.

39. O.B.Herrera, R.C.Sussman, J.S.Smith and G.M.Taylor, "Results of ladle desulphurisation of plate steels at ARMCO",40th. Electric Steel Conf. Proc. Kansas City, USA, 7-10th Dec.1982, ISS/AIME, pp 161-i67.

40. A.Ishii, M.Tate, T.Ebisawa and K.Kawakami,"The ladle refining process for alloyed oil country tubular goods steels at Nippon Kokan KK" 40th. Electric Steel Conf. Proc. Kansas City, USA, 7-10th Dec.1982, ISS/AIME, pp 121-128.

41. K.Taguchi and K.Tachibana and Y.Ogura, "Application of Secondary Steelmaking to seemless production in NKK", 'Secondary Steelmaking for product improvement', Proceedings of an InternationalConference, London, 23-24th Oct.1984, The Metals Society, pp 145-152

42. I.G.Davies and P.C.Morgan, "Secondary Steelmaking developments on Engineering steels at Stocksbridge works", 'Secondary Steelmaking for product improvement', Proceedings of an InternationalConference, London, 23-24th Oct. 1984, The Metals Society.,pp 153-164.

43. M.Brunner and G.Carlsson, "Refining of steel in the ladle", 'Clean Steel', Proceedings of an International Conference, 1-3rd June 1981, Balatonfured,Hungary, The Metals Society, Book 281, pp 256-260.

44. T.Hamre and R.D.O'Hara," Control of sulphur using the T.N. process", 40th. Electric Steel Conf. Proc. Kansas City, USA, 7-10th Dec.1982, ISS/AIME, pp 129-131.

45. H.P.Haastert, H.Richter, H.Taxhet and J.Wolf, "The use of various desulphurising agents and their effects on steel cleanness and service properties", 'Clean Steel', Proceedings of an International Conference, 1-3rd June 1981, Balatonfured,Hungary, The Metals Society, Book 281, pp 281-289.

46. V.Caruso, A.Coperchini, A.Giaccone, J.M.Dixmier, J.M.Henry and J.L.Margot, "Recent applications of cored wire in continuous casting", Scaninject III, June 15-17th, 1983, Lulea, Sweden. pp 34:1-34:27.

47. D.W.P.Lynch and J.W.Robison, "Calcium wire ladle treatment - cleanliness and ductility improvement of foundry steel",40th. Electric Steel Conf. Proc. Kansas City, USA, 7-10th Dec.1982, ISS/AIME, pp 303-311.

48. T.Lehner, "Reactor models for powder injection", paper 11, Scaninject, International Conference on Injection Metallurgy, June 9-10th, 1977, Lulea, Sweden.

49. D.Sponseller and R.A.Flinn,"The solubility of calcium in liquid iron and third element interaction effects", Trans. AIME, 230, 1964, pp 876-888.

50. W.G.Wilson, "Results from various methods of adding rare earths",Proceedings of the A.I.M.E. Electric furnace steel conference, 31, 1973, pp 154-161.

51. K.Sanbongi, "Controlling sulphide shape with rare earths or calcium during the processing of molten steel", Trans. I.S.I.J., 19, 1979, pp 1-10.

52. T.Emi, O.Haida, T.Sakuraya and K.Sanbongi, "Mechanism of sulphides precipitation during solidification of calcium and rare earth treated ingots", Steelmaking Proc., 61, Chicago III, 16-20th April 1978, AIMMPE, pp 574-584.

53. T.Sakuraya, T.Emi, Y.Habu, A.Ejima and K.Sanbongi, "Mechanism and removal of the accumulation in the sedimental zone of inclusions precipitating during solidification of large ingots", Tetsu-to-Hagane, I.S.I.J., 62,1976, 1653.

54. Y.Habu, T.Emi and H.Kitaoka, Tetsu-to-Hagane, I.S.I.J., 62, 1971, 971.

55. T.Emi, O.Haida, T.Sakuraya and K.Sanbongi, "Treating fully deoxidised RH degassed HSLA steel melts with rare earths or calcium for stringent shape control", Third Germany - Japan Seminar , Dusseldorf, 27-28th April, 1978.

56. M.Olette and C.Gatellier, "Effect of additions of calcium, magnesium or rare earth elements on the cleanness of steels", 'Clean Steel', Proceedings of an International Conference, 1-3rd June 1981, Balatonfured,Hungary, The Metals Society, Book 281, pp 165-185.

57. L.Luyckx, J.R.Bell, A.Mclean and M.Korchynsky,"Sulphide shape control in HSLA steels", Metallurgical Transactions, 1, 1970, pp 3341-3350.

58. W.J.M.Henderson and J.A.Chapman,"The use of Rare earth metals in the production of high quality plate steels", Proceedings of the A.I.M.E. Electric furnace steel conference, 31, 1973, pp 162-166.

59. P.E.Waudby," Rare earth additions to steel", International Metals Reviews, 23, 1973, pp74-101.

60. M.Ishiguro, M.Ito and T.Osuga, "Effects of rare earth elements on the properties of high quality ingots", Trans. I.S.I.J., 16, 1976, pp 359-367.

61. D.C.Hilty and J.W.Farrell,"Steel flow through nozzles the influence of deoxidisers", Proceedings of the A.I.M.E. Electric furnace steel conference, 29, 1971, pp31-45.

62. W.O.Philbrook, "Oxygen reactions with liquid steel", International Metals Reviews, 22,1977, pp 187-201

63. J.J.Debarbadillo, "Reactivity of magnesium and calcium in liquid steel", 'Sulfide inclusions in steel', Proceedings of an International Symposium, 7-8th Nov.1974, A.M.S., Port Chester, New York , pp 70-100.

64. O.P.Watts, "Iron and Calcium", Journal American Chemistry Society, 28, 1906, pp 1152-1155.

65. H.Goldschmidt,"Calcium Silicide for the purification of metals : particularly steel", Electrochemical. Met.Ind., 6,1908, p 244.

66. W.Crafts, J.J.Egan and W.D.Foreng,"Formation of inclusions in steel castings", Trans.A.I.M.E., 140, 1940, pp 233-262.

67. E.Kucharski and C.G.Mickelson, "Role of calcium-titanium-silicon deoxidiser in production of steel castings", Proceedings of the A.I.M.E. Electric furnace steel conference, 25, 1967, pp 34-38.

68. A.Y.Shulte, A.P.Grechanyi, Y.D.Capin, B.M.Blagikh, V.V.Lunev, I.P.Volchok, I.B.Kharaz, Y.N.Kalenikhin, S.I.Gladkii and P.A.Mikhailov,"Improving the reliability of steel castings for use at low temperatures", Russian Castings Production, May 1968, pp 146-148

69. D.C.Hilty and V.T.Popp, "Improving the influence of calcium on inclusion control", Proceedings of the A.I.M.E. Electric furnace steel conference, 1969, pp.52-56.

70. C.Gatellier and M.Olette, "Complex deoxidation - a tool to modify composition and the rate of removal of inclusions.", Scaninject II, International Conference on Injection Metallurgy, June 12-13th, 1980, Lulea, Sweden, pp 8:1-8:26.

71. T.Ototani, "Desoxydation par le calcium et desulfuration par l'aluminium des bains de fer ou d'alliages ferreux dans un creuset de chaux",Tetsu-to-Hagane, I.S.I.J., 61,1975, pp 2167-2181.

72. T.E.Gammal and Rui-ming Ni, "The refining of steel with calcium and its effect on inclusion morphology", Scaninject III, Refining of Iron and Steel by powder injection part II, 15-17th June 1983, Lulea, Sweden, pp46:1-46:15.

73. G.M.Faulring, J.W.Farrell and D.C.Hilty, "Steel flow through nozzles: influence of calcium", Iron and Steelmaker, February 1980, pp 14-19.

74. H.Nashiwa, A.Mori, 6th.Japanese - USSR Symposium on Physical and Chemical Metallurgical processes, I.S.I.J., 81, 1977,

75. R.J.Freuhan, "Thermodynamics and kinetics of reaction involving elements in ladle metallurgy", Iron and Steelmaker, March 1983, pp. 33-37.

76. T.Kawawa, R.Imai, Tetsu-to-Hagane, I.S.I.J., 62, 1976, p1653.

77. K.Narita, A.Tomita, Tetsu-to-Hagane, I.S.I.J., 64, 1978, .S161.

78. K.Tahtinen, R.Vainola and R.Sandholm,"Ladle injection a way to continuously cast Al-killed steels for billets at Ovako", Scaninject II, International Conference on Injection Metallurgy, June 12-13th, 1980, Lulea, Sweden, paper 14.

79. C.H.Leung and L.H.Van Vlack, "Solution and precipitation hardening in (Ca,Mn) sulphides and selenides", Met.Trans.A, Vol 12A, June 1981, pp 987-991.

80. M.Abe, "Tonnage production specification requirements for strip steels", 'Secondary Steelmaking for product improvement', Proceedings of an International Conference, London, 23 - 24th Oct. 1984, The Metals Society, pp 27-34

81. D.J.Price, "Secondary Steelmaking at BSC Scunthorpe Works in production of low alloy high strength formable strip", 'Secondary Steelmaking for product improvement', Proceedings of an International Conference, London, 23-24th Oct. 1984, The Metals Society,

82. C.Wasberg,"The status of magnesium as a desulphuriser and refining agent in Iron and Steel", Steel Times, June 1985, pp 288-291.

83. N.A.Voronova,"Desulphurisation of hot metal by magnesium", Proceedings of the 34th Annual World Magnesium Conference, Dayton, Ohio, International Magnesium Association, 1977, pp 44-52.

84. R.I.L.Guthrie, "Technical considerations in the use of magnesium for desulphurising iron and steel", Proceedings of the 40th Annual World Magnesium Conference, Toronto, Canada, 1983, pp 70-76.

85. A.M.Smillie and R.A.Huber,"Operating Experience at Youngstown steel with injected salt-coated magnesium granules for external desulphurisation of hot metal." Proc.A.I.M.E. Steelmaking Conference, Detroit Mich. USA, 25-28th March 1979,pp 12-24.

86. G.A.Irons and R.I.L.Guthrie,"The kinetics of molten iron desulphurisation using magnesium vapour", Metallurgical Trans.B, Vol 12B, Dec 1981, pp 755-767.

87. G.A.Irons and R.I.L.Guthrie,"Kinetic aspects of magnesium desulphurisation of blast furnace iron", Ironmaking and Steelmaking, No. 3, 1981, pp 114-121.

88. P.Ritakallio,"Desulphurisation and nitrogenization as examples for powder injection", Scaninject II, International Conference on Injection Metallurgy, June 12-13th, 1980, Lulea, Sweden, pp 13:1-13:29.

89. R.Hultgren, P.D.Desai, D.T.Hawkins, M.Gleiser, K.K.Kelly and D.D.Wagman,"Selected values of the thermodynamic properties of binary alloys", American Society for Metals, Metals Park, Ohio, 1973.

90. S.K.Saxena, "Refining reactions of magnesium in steel at steelmaking temperatures", International Symposium on the Physical Chemistry of Iron and Steelmaking, Toronto, Canada, 1982, pp 17-22.

91. S.K.Saxena," The potential of magnesium as a refining agent in steel", Proceedings of the 40th Annual World Magnesium Conference, Toronto, Canada, 1983, pp 70-76.

92. R.Kiessling, "Clean steel - a debatable concept", 'Clean Steel', Proceedings of an International Conference, 1-3rd June 1981, Balatonfured,Hungary, The Metals Society, Book 281, pp 1-9

93. A.M.Sage, "A review of the physical metallurgy of HSLA linepipe and pipe fitting steels", 'Steels for linepipe and pipeline fittings', Proceedings of International Conference, October 21-23rd. 1981, The Metals Society, London, Book 285, pp. 39-50.

94. H.Nakasugi, H.Matsuda and H.Tamehiro,"Ultra low carbon bainitic steel for linepipes",'Steels for linepipe and pipeline fittings', Proceedings of International Conference, October 21-23rd. 1981, The Metals Society, London, Book 285, pp.90-95.

95. R.C.Cochrane and W.B.Morrison,"Transformation characteristics of some linepipe steels containing Nb, V and Mo and their relationship to processing and microstructure", 'Steels for linepipe and pipeline fittings', Proceedings of International Conference, October 21-23rd. 1981, The Metals Society, London, Book 285, pp 70-78.

96. T.Takeuchi, T.Suzuki, T.Hashimoto and T.Yokoi, International Conference on 'Steel Rolling', Tokyo, Sept - Oct 1980, I.S.I.J., paper 77

97. G.K.Platts, A.D.Vassiliou and F.B.Pickering,"Developments in microalloyed HSLA steels - An overview", The Metallurgist and Materials Technologist, Sept.1984, pp 447-454

98. Y.Nara, T.Tyogoku, T.Yamura and I.Takeuchi, "Production Of Linepipe in Japan", Metals Technology, 10, August 1983, pp 322-329.

99. T.Gladman and R.F.Dewsnap,"The effects of alloying additions on the properties of controlled rolled vanadium - niobium steels", 'Steels for linepipe and pipeline fittings', Proceedings of International Conference, October 21-23rd. 1981, The Metals Society, London, Book 285, pp 61-69.

100. W.S.Owen and M.J.Crooks," Recrystallisation of austenite and separation of ferrite during and after the hot rolling of some microalloyed steels", 'Steels for linepipe and pipeline fittings', Proceedings of International Conference, October 21-23rd. 1981, The Metals Society, London, Book 285, pp 104-112.

101. G.Gorges, W.Recknagel and F.O.Koch,"Quality assurance in the production of HSLA steel for spiral welded, large diameter linepipe", Steels for linepipe and pipeline fittings', Proceedings of International Conference, October 21-23rd. 1981, The Metals Society, London, Book 285, pp 224-229.

102. A.M.Sage,"Physical metallurgy of HSLA linepipe and pipe fitting steels", Metals Technology, 10,June 1983, pp 224-233.

103. A.M.Sage,"Effect of rolling schedules on structure and properties of 0.45% vanadium weldable steel for X70 pipelines", Metals Technology, March 1981, pp 94-102.

104. A.P.Coldren and T.G.Oakwood,"A new economical X70 linepipe steel", Journal of Metals, April 1983, pp 28-33.

105. R.J.Gray, W.R.Irving and R.Baker,"Steelmaking, casting and rolling of pipeline steels in BSC", Ironmaking and Steelmaking, 10, No.4, 1983, pp 185-192

106. D.Brooksbank and K.W.Andrews,"Thermal expansion of some inclusions found in steels and their relation to tessellated stresses ", J.I.S.I., 206, 1968, pp 595-599.

107. D.Brooksbank and K.W.Andrews,"Tessellated stresses associated with some inclusions in steel", J.I.S.I., 207, 1969, pp 474-483

108. D.Brooksbank,"Thermal expansion of calcium aluminate inclusions and relation to tessellated stresses", J.I.S.I., 208, 1970, pp 495-499.

109. K.W.Andrews and D.Brooksbank,"Stresses associated with inclusions in steel - a photoelastic analogue and the effects of inclusions in proximity", J.I.S.I., 210, 1972, pp 765-776.

110. D.Brooksbank and K.W.Andrews,"Stress fields around inclusions and their relation to mechanical properties", International Conference on the 'Production and application of clean steels', Balatonfured, Hungary, June 1970, The Iron and Steel Institute, London, pp.186-198.

111. R.Kiessling and H.Nordberg,"Influence of inclusions on mechanical properties of steel", International Conference on the 'Production and application of clean steels', Balatonfured, Hungary, June 1970, The Iron and Steel Institute, London, pp.179-185.

112. S.Rudnik,"Discontinuities in hot rolled steel caused by non-metallic inclusions", J.I.S.I., 204, 1966, pp 374-376.

113. P.J.Maunder and J.Charles,"Behaviour of non-metallic inclusions in a 0.2% carbon steel ingot during hot rolling", J.I.S.I., 206, 1968, pp 705-715.

114. T.Malkiewicz and S.Rudnik,"Deformation of non-metallic inclusions during rolling of steel", J.I.S.I., 201, 1963, pp 33-38.

115. R.Kiessling,'Non-metallic inclusions in steel (part III) , Iron and Steel Institute Publication 115, The Iron and Steel Institute, London, 1968.

116. M.Atkinson,"The influence of non-metallic inclusions on the fatigue properties of ultra high tensile steels", J.I.S.I., 195, 1960, pp 64-75.

117. D.V.Edmonds and C.J.Beevers,"The effect of inclusions on the stress distribution in solids", J. Material Science, 3, 1968, pp 457-463

118. R.Tricot,"Relative detrimental effect of inclusions on service properties of bearing steels", International Conference on the 'Production and application of clean steels', Balatonfured, Hungary, June 1970, The Iron and Steel Institute, London, pp.199-204.

119. H.F.Fischmeister, E.Navara and K.E.Easterling,"Effects of alloying additions on structural stability and cohesion between phases in oxide/metal composites", Metal Science Journal, 6, 1972, pp 211-215.

120. W.C.Leslie, "Inclusions and mechanical properties", Mechanical Working and Steel Processing, Proc. Int. Conf., Iron and Steel Society of AIME, Warrendale, USA, 1982, pp 3-50.

121. R.Lagneborg,"The influence of impurities on the mechanical properties of steel", Swedish Symposium on non-metallic inclusions in steel, Uddeholm Research Foundation, 1981, pp 285-353.

122. T.Gladman,"Cavitation at sulphides during deformation", 'Sulfide inclusions in steel', Proceedings of an International Symposium, 7-8th Nov.1974, A.M.S., Port Chester, New York , pp 273-285.

123. A.D.Wilson,"Through thickness tension testing of steel", ASTM, STP, 794.

124. J.F.Knott, "The toughness of steel", Trans I.S.I.J., 21, 1981, pp 305-317.

125. R.Iricibar, G.Leroy and J.D.Embury, "Relationship of strain hardening and damage in ductile fracture", Metal Science, 14, Aug./Sept. 1980, pp 337-343.

126. R.P.Oates and R.D.Stout, "A quantitative weldability test for susceptibility to lamellar tearing", The Welding Journal, 52, No.11, Nov 1973, pp 481-491.

127. D.C.Ludwigson, ASTM, STP, 794, 1981.

128. J.Kaufmann, A.W.Pense and R.D.Stout, "An evaluation of factors significant to lamellar tearing", The Welding Journal, 60, No.3, March 1981, pp 33-40.

129. C.G.Interrante, "Basic aspects of the problems of hydrogen in steels", 'Hydrogen in Steel', American Society for Metals, Metals Park, Ohio, 1982, pp 3-17.

130. E.M.Moore and J.J.Warga, "Factors influencing the hydrogen cracking sensitivity of pipeline steels", Materials Performance, June 1976, pp 17-23.

131. A.Brown and C.L.Jones, "Hydrogen induced cracking in pipeline steels", Corrosion -NACE , 40, No.7, July 1984, pp 330-336.

132. P.E.Timmins,"Assessing hydrogen damage in sour service lines and vessels is key to plant inspection", Technology, Nov 5, 1984, Oil and Gas Journal, pp 103-105.

133. T.Taira, Y.Kobayashi, K.Matsumoto and K.Tsukada, "Resistance of line pipe steels to wet sour gas", Corrosion -NACE, 40, No.9, Sept. 1984, pp 478-486.

134. S.L.I.Chan, M.Martinez-Madrid and J.A.Charles, "Effect of grain size and second phase particles on the hydrogen occlusivity of iron and steels", Int. Conf. on Metallic Corrosion, Toronto, Canada, 3-7th June 1984, pp 237-245.

135. T.V.Venkatasubramanian and T.J.Baker, "Role of manganese sulphide inclusions in hydrogen assisted cracking of steel exposed to H_2S saturated salt solution", Materials Science, 18, May 1984, pp 241-247.

136. T.Taira and Y.Kobayashi, "Development of linepipe for sour gas service", 'Steels for linepipe and pipeline fittings', Proceedings of International Conference, October 21-23rd. 1981, The Metals Society, London, Book 285, pp 170-180.

137. E.Myoshi, T.Tanaka, F.Terasaki and A.Ikeda, "Hydrogen induced cracking of steels under wet hydrogen sulphide environment", Journal of Engineering for Industry, Nov.1976, pp 1221-1230.

138. "General Discussion", 'Clean Steel 3', International Conference, Balatonfured, Hungary, June 2-5th 1986.

139. J.P.Motte and J.Cordier, "In depth powder injection in liquid iron and steel", Scaninject II, International Conference on Injection Metallurgy, June 12-13th, 1980, Lulea, Sweden, pp 12:1-12:15.

140. N.Keegan, "Injection of volatile material into molten steel", Steel Times International, Dec. 1985, pp 48-50.

141. "Test method : Evaluation of pipeline steels for resistance to stepwise cracking", NACE STD. TM - 02 - 84, Materials performance, May 1984, pp 9-16.

142. P.S.Mitchell and R.R.Barr,"Manufacture of high quality SAW linepipe at British Steel Corporation", Iron and Steel International, Feb 1984,.pp 9-13.

143. T.Eumura, H.Nashiwa, T.Ikeda, A.Mori and M.Tokuda,"Development and effect of calcium adding technology into molten steel", 59th National Open Hearth and Basic Oxygen Steel Conference, 28-31st March 1976, St. Louis, USA, pp 457-478.

144. D.Broek.," Some contributions of electron fractography to the theory of fracture", International Metal Reviews, 19, 1974, pp 135-182.

145. I.Kozasu and J.Tanaka,"Effects of sulphide inclusions on notch toughness and ductility of structural steels", 'Sulfide inclusions in steel', Proceedings of an International Symposium, 7-8th Nov.1974, A.M.S., Port Chester, New York , pp 286-308.

146. A.J.DeArdo and E.C.Hanbury,"Influence of elongated inclusions on the mechanical properties of high strength steel plate", 'Sulfide inclusions in steel', Proceedings of an International Symposium, 7-8th Nov.1974, A.M.S., Port Chester, New York , pp 309-337

147. A.J.DeArdo, G.A.Ratz and W.D.Wilson, Steelmaking Proceedings, vol 63, 1980, pp 162.

148. W.A.Spitzig and R.J.Sober, "Influence of Sulphide Inclusions and pearlite content on the mechanical properties of hot rolled carbon steels", Met. Trans. A., 12A, Feb.1981,pp 281-291

149. W.A.Spitzig ,"Effects of sulphide inclusion morphology and pearlite banding on anistropy of mechanical properties in normalized C-Mn steels", Met.Trans.A., 14A, Feb 1983, pp 271-283

150. W.A.Spitzig, R.J.Sober, N.J.Panseri and R.J.Lee,"SEM-based automatic image analysis of sulphide inclusions in hot rolled carbon steels", Metallography, 16, 1983, pp 171-198

151. F.B.Pickering,"Some effects of mechanical working on the deformation of non-metallic inclusions", J.I.S.I. II, 1958, pp 148-159

152. G.Wardle,"The deformation characteristics of deoxidation products in hot rolled steel", PhD Thesis, 1979, The University of Aston in Birmingham

153. J.C.B.Asanti,"Hot deformation characteristics of oxide/sulphide inclusions in low carbon steels", PhD Thesis, 1980, The University of Aston in Birmingham

154. K.B.Gove and J.A.Charles,"Further aspects of inclusion deformation", Metals Technology, Sept. 1974, 1, 9, pp 425-431.

155. R.A.Grange,"Effect of microstructural banding in steel", Met. Trans., 2, 1971, pp 417-426.

156. H.W.Paxton,"The metallurgy of steels for large diameter line pipe", 'Alloys for the eighties', Climax Molybdenum Company, Greenwich, CN, 1980, pp 185-212.

157. H. de Boer, H.Rellermeyer and R.Simon,"Impact of ladle metallurgy on product quality", Scaninject III, Refining of Iron and Steel by powder injection part II, 15-17th June 1983, Lulea, Sweden, pp 39:1-39:27.

158. G.J.Bieffer,"The stepwise cracking of linepipe steels in sour environments", Materials Performance, June 1982, pp 19-24.

159. D.P. Hill,"Influence of Non metallic inclusions upon the properties of linepipe steels", PhD Thesis, 1986, The University of Aston in Birmingham.

160. C.O.Emineke,"The effect of alloying elements on the properties of pipeline steels", PhD Thesis, 1986, The University of Aston in Birmingham.

161. G.Herbsleb, R.K.Popperling and W.Schwenk,"Occurence and prevention of Hydrogen Induced stepwise cracking and stress corrosion cracking of low alloy pipeline steels", NACE National Conference, Chicago, 1980, paper 9.

162. B.E.Wilde, C.D.Kim and E.H.Phelps,"Some observations on the role of inclusions in the hydrogen induced blister cracking of linepipe steels in sulphide environments", NACE National Conference, Chicago, 1980, paper 7.

163. Elliott and M. Gleiser, 'Thermochemistry for steelmaking', Vol 1, Addison Wesley, Pergamon, 1960, p 248.

164. C.Bodsworth and H.B.Bell,'Physical chemistry of iron and steel manufacture', Longman, 1972, p 461.